TRANSPORTATION RESEARCH RECORD

515

Formerly issued as Highway Research Record

Characteristics of and Factors Influencing Bituminous Materials and Mixtures

14 reports prepared for the 53rd Annual Meeting of the Highway Research Board

TRB

TRANSPORTATION RESEARCH BOARD

NATIONAL RESEARCH COUNCIL

Washington, D. C., 1974

PB 240 257

Transportation Research Record 515
Price $6.80
Edited for TRB by Marianne Cox Wilburn

subject areas
31 bituminous materials and mixes
40 maintenance, general

These papers report research work of the authors that was done at institutions named by the authors. The papers were offered to the Transportation Research Board of the National Research Council for publication and are published here in the interest of the dissemination of information from research, one of the major functions of the Transportation Research Board.

Before publication, each paper was reviewed by members of the TRB committee named as its sponsor and accepted as objective, useful, and suitable for publication by the National Research Council. The members of the review committee were chosen for recognized scholarly competence and with due consideration for the balance of disciplines appropriate to the subject concerned.

Responsibility for the publication of these reports rests with the sponsoring committee. However, the opinions and conclusions expressed in the reports are those of the individual authors and not necessarily those of the sponsoring committee, the Transportation Research Board, or the National Research Council.

Each report is reviewed and processed according to the procedures established and monitored by the Report Review Committee of the National Academy of Sciences. Distribution of the report is approved by the President of the Academy upon satisfactory completion of the review process.

The National Research Council is the principal operating agency of the National Academy of Sciences and the National Academy of Engineering, serving government and other organizations. The Transportation Research Board evolved from the 54-year-old Highway Research Board. The TRB incorporates all former HRB activities but also performs additional functions under a broader scope involving all modes of transportation and the interactions of transportation with society.

LIBRARY OF CONGRESS CATALOGING IN PUBLICATION DATA

National Research Council. Highway Research Board.
Characteristics of and factors influencing bituminous materials and mixtures.

(Transportation research record; 515)
1. Bituminous materials—Addresses, essays, lectures. I. National Research Council. Transportation Research Board. II. Title. III. Series.
TE7.H5 no. 515 [TE221] 380.5'08s [625.8'5] 75-4756
ISBN 0-309-02359-9

CONTENTS

FOREWORD

The reports presented in this RECORD are concerned with bituminous mixture characteristics related to: (a) the effects of water on tensile strength, resilient modulus, and retention of a bituminous coating, and (b) physical behavior under laboratory and field evaluation procedures. These papers should be of interest to the researcher and the practicing bituminous paving engineer.

In the first group of reports, Jimenez discusses a laboratory test for evaluating the water susceptibility of asphalt concrete. Standard-sized specimens were subjected to cyclic pore water pressures at 50 C and then tested for tensile strength at 25 C by a double punch method. A comparison of strengths for control specimens indicated that the new test procedure responded as expected to different mixture variables.

Lottman et al. describe a test procedure for predicting moisture damage in paving mixtures. The damage in laboratory specimens and field cores is established by the loss of tensile strength and E-modulus as determined by the split cyclinder test. (Loss is caused by water saturation or temperature cycling of the saturated specimen.) Comparisons of results obtained for laboratory-prepared specimens and pavement cores are presented.

Schmidt's work is concerned with the variations in resilient modulus (M_R) of asphalt mixture caused by differences of temperature, moisture content, and freeze-thaw cycles. The M_R is obtained through a repeated loading split cylinder setup. The author suggests that for hot asphalt mixtures the highest M_R below 255 K is estimated to be 3.4×10^{10} N/m^2, which decreases curvilinearly to 296 K and continues to decrease linearly to 333 K if the relationship is plotted as log M_R versus $1/K$.

Evaluation of asphalt stripping by a gas-producing chemical reaction is presented by Ford, Manke, and O'Bannon. The stripping of 1-size asphalt coated aggregates was obtained quantitatively through the measurement of gas pressure developed in a sealed container when hydrochloric acid was made to react with carbonaceous stones or when hydrofluoric acid was made to react with siliceous aggregates. Eleven aggregates are evaluated and compared for stripping by the new surface reaction procedure and by 2 qualitative ratings after static and dynamic immersion in water.

Load-deformation curves for asphalt concrete loaded by a split cylinder method are used by Ruth and Potts to calculate energy expended on the test specimens. Tests of laboratory specimens and road cores indicated that the strain energy corresponding to the fracture load decreases as the asphalt viscosity increases and that neither asphalt content nor specimen density has any appreciable influence on the energy to cause fracture.

The final report of the first group is by Petersen, Ensley, and Barbour. It is concerned with interactions at the asphalt-aggregate interface. The paper summarizes the developmental work in 3 new methods related to understanding the aggregate surface-asphalt chemistry. These procedures involve inverse gas-liquid chromatography, selective chemical reactivity, and heats of immersion of aggregate in asphalt.

Bin storage of asphalt concrete is discussed by Zdeb and Brown with particular reference to changes in asphalt consistency and aggregate gradation. They found that storage of up to 48 hours of fine-graded mixtures in an inert gas atmosphere had no appreciable effect on recovered asphalt viscosity. The same was true for fine-graded mixtures stored for 24 hours in a normal atmosphere. However, 2 types of coarse-graded asphalt concrete showed significant increase in asphalt viscosity after 18 hours of storage in a normal atmosphere.

The paper by Beecroft, Jenkins, and Wilson presents the analysis and recommendations developed after a 10-year study of asphalt concrete pavements. One of the most important characteristics related to good performance is the control of density of all layers.

An evaluation of asphalt concrete containing a synthetic rubber is reported by Vega, Battiato, and La Bella. The report presents data on rheological behavior to show improvements in high temperature, creep stiffness, and fatigue life resulting from the use of the SBR rubber.

Methods for predicting moduli and fatigue equations for bituminous paving mixtures are presented by Francken and Verstraeten. From a study of many mixtures and bending tests, it is concluded that these can be calculated from the volumes of aggregate, bitumen, and air and the binder's penetration value and asphaltene content.

Alexander shows that highway materials (soils, asphalt, and portland cement mixtures) should be classified by using a systems approach. He states that all of these are aggregate-binder composites and that their rheological behavior can be described graphically.

Mix-design criteria for gap-graded bituminous mixtures are presented by Marais. Because they meet certain requirements for the Marshall procedure, air permeability and tensile strength will produce mixtures that are satisfactory for resistance to distortion, toughness, fatigue, and durability.

The abridgment of a report by Lee attests to the capability of producing high-quality asphalt concrete with gap-graded aggregates.

Paterson presents an abbreviation of the significant findings of a study related to particle orientation resulting from the compaction of asphalt concrete. Particle orientation is considered the principal cause for differences in the physical properties between laboratory and field-compacted mixtures.

—R. A. Jimenez

TESTING FOR DEBONDING OF ASPHALT FROM AGGREGATES

R. A. Jimenez, Arizona Transportation and Traffic Institute, University of Arizona

This paper presents the development of new apparatus and procedure for the measurement of stripping susceptibility of asphaltic concrete. In the new method a regular Hveem specimen [4-in. diameter by 2½-in. height (101.6-mm diameter by 63.4-mm height)] was water saturated at 122 F (50.0 C). Then the specimen was subjected to repeated pore water pressure. The effect of the exposure on tensile strength was expressed as retained strength determined with a double punch procedure. The work showed that the method responded to variations in type of aggregate, cleanliness of aggregate, and asphalt content in a direction dictated by experience. Comparative results with the immersion compression test are presented.

•THE PHENOMENON of stripping has resulted in complete failure of a pavement within 2 weeks after opening to traffic and failure by loss of surface fines over a period of 2 years. To minimize the expense and inconvenience that result from rebuilding and resurfacing a damaged pavement, one has to expend much effort to define, measure, and predict the occurrence of asphalt stripping. The aim of this investigation was to develop an improved method for determining the susceptibility to stripping of asphalt concrete mixtures.

FACTORS CONTRIBUTING TO STRIPPING

Early failure of asphalt pavement surfaces generally has been attributed to stripping because cracking from structural failure is not expected in the very early life of a highway. All stripping failures have been associated with the presence of water (1). Stripping or debonding implies a surface-to-surface separation; however, Schmidt (2) and others suggest that they are not necessarily adhesion failures but may be attributed to cohesion deficiency. It is not our intent to define or describe the mechanisms of the stripping failure but to list the factors that reportedly contribute to stripping occurrence. These are

1. Water,
2. Traffic,
3. Cool temperatures,
4. Low asphalt content,
5. Low asphalt viscosity,
6. High air void content,
7. Cleanliness of fine aggregate,
8. Coating on aggregate,
9. Composition of aggregate, and
10. Surface texture of aggregate.

The generalized mechanism of stripping is the rupture or displacement or both of the asphalt films that bind the aggregate in asphaltic concrete, which results in loss of tensile and abrasion resistance to traffic loads. The stresses that cause failure of the asphalt film are assumed to be water pressure and erosion caused by traffic or thermal cycles or both (3) on wet pavements.

Publication of this paper sponsored by Bituminous Section.

TEST PROCEDURES

Unconfined Compression

The best known procedure for determining the susceptibility to stripping of asphaltic concrete is the immersion compression test (ASTM D1075-54, AASHO T165-55). This procedure uses a numerical index for the complete and compacted design mixture to measure the loss of cohesion resulting from the action of water. Specimens are compacted by double-plunger action at a pressure of 3,000 psi (20.7 MN/m^2). The exposed specimens generally are soaked for 24 hours in a water bath held at 140 F (60.0 C). Testing is performed under unconfined compression at a deformation rate of 0.20 in./min (8.3×10^{-6} m/s) for a specimen 4 in (101.6 mm) high at a temperature of 77 F (25.0 C). The index of retained strength is obtained by dividing the strength of the exposed specimens into that of the control or dry specimens. Requirements on the value of the retained strength for acceptable mixtures vary from 55 to 75 percent.

Marshall Compression

The Marshall test method has been used to determine resistance to stripping in much the same manner as the immersion compression test. Research done by Gallaway and Jimenez (4) showed that for certain aggregate-asphalt mixtures the results obtained by this procedure can be misleading.

Confined Compression

The loss of strength or stiffness of asphaltic concrete because of the action of water and repeated stressing has been determined by Majidzadeh and Stander (5). In these works, triaxial compression with a repeated deviator stress was used.

Split Cylinder Test

The most recent method for measuring stripping susceptibility of asphaltic concrete is based on the split cylinder test proposed by Lottman (6). A "retained strength" index is obtained from measurements of indirect tensile strength for specimens (or cores) 4 in. (101.6 mm) in diameter. Exposure is achieved by 12 freeze-thaw cycles of 0 to 120 to 0 F (-17.8 to 48.9 to -17.8 C) of water-saturated specimens. Strength testing is done at 55 F (12.8 C) with a deformation rate of 0.065 in./min (0.3×10^{-6} m/s).

These test procedures led us to conclude that there must be a simpler method to determine the susceptibility of asphaltic concrete to stripping or debonding.

NEW TEST DESCRIPTION

Loss of cover material of asphaltic surfaces occurs during or soon after a cold rain on a trafficked pavement. The combination of water, lower temperature, and traffic stresses are the most critical at this time and cause raveling. Complete disintegration or cracking of the asphaltic layer that is caused by debonding of the asphalt from the aggregate is not a surface phenomenon as is raveling; therefore, more time is required for failures to manifest themselves. Visual examinations and research into these failures indicated that stripping or debonding was caused by the action of water.

The new debonding susceptibility test has 4 basic concepts.

1. Specimen size is to be approximately 4 in. (101.6 mm) in diameter by 2½ in. (63.5 mm) in height. However, field cores 3 to 4 in. (75 to 100 mm) in diameter and 2 to 4 in. (50 to 100 mm) in height can be tested.
2. Specimen is to be saturated because pore water pressure is to be used in the exposure portion of the test. It is believed that pore water pressure develops in the field.
3. The exposure of the specimen should be to only repeated pore water pressure at 122 F (50.0 C). The use of only pore water pressure simplifies the loading of different sized specimens. The temperature of 122 F (50.0 C) is near the value found by Jimenez (7) for saturated pavements in southern Arizona; this temperature reduces asphalt viscosity and thus resistance to debonding. The use of a 122 F (50.0 C) temperature rather

than a "cold rain" temperature was based on the thought that the loss of surface material in raveling was due to a brittle failure rather than an adhesive failure that related directly to stripping or debonding.

4. The strength test should be a simple, repeatable tension test. The test temperature for strength should be 77 F (25.0 C).

Strength Test

The effects of stripping or debonding asphalt from the aggregate of asphaltic concrete should be most easily detected by tension testing. Because a direct tension test is not practical, some simple indirect tension test such as the cohesiometer, Marshall, split cylinder, or double punch test was considered. Prior experiences with the cohesiometer and Marshall tests were not particularly good and thus were not used. The work of Lottman (6) and others suggested the split cylinder procedure. However, the work reported by Fang and Chen (8) with the double punch test appeared most promising.

In the double punch test, a cylindrical specimen is centrally loaded on both the top and bottom surfaces with cylindrical steel punches. The penetration of the cones that develop between the punches serves to split the specimen along the weakest radial plane. Preliminary work with the split cylinder and double punch tests was carried out with 2 mixtures of asphaltic concrete compacted by vibratory kneading compaction (10). The split cylinder specimens were loaded through steel bars with a width of 1 in. (25.4 mm); the double punch test used punches 1 in. (25.4 mm) in diameter. Table 1 gives the repeatability of the 2 test methods and the relationship between the stresses obtained for 2 aggregate gradations. The specimens were compacted by vibratory kneading and were tested in triplicate (14). The data indicated that the double punch test had better repeatability than the split cylinder and that the stresses obtained by the 2 procedures were identical to each other because the value of the slope coefficient was almost 1.

Observations of these 2 test methods indicated that the double punch test was simple in operation and that stress analysis did not have to be corrected for flattening of the load surface as it would have in the split cylinder test.

Specimen Size

Other preliminary work with the double punch test was concerned with the size of specimen and punch diameter. Specimens were compacted by vibratory kneading and tested in triplicate at 77 F (25.0 C) with a deformation rate of 1 in./min (25.4 mm/s) (15). Specimen diameter size varied from 2 to 4 to 6 in. (50.8 to 101.6 to 152.5 mm) and height size from 2 to 4 to 8 in. (50.8 to 101.6 to 203.2 mm); punch diameters were from $\frac{3}{8}$ to $\frac{5}{8}$ to 1 in. (9.5 to 15.9 to 25.4 mm). The results of this testing are given in Table 2. The data indicated the following:

1. For constant specimen height, the tensile stress decreased as the ratio of specimen diameter to punch diameter (D/d) increased; and
2. For constant specimen height and D/d ratio, the tensile strength decreased as specimen diameter decreased.

Specimen Saturation

A review of the literature indicated that vacuum saturation of asphaltic concrete specimens is a rather simple and effective means of filling the voids with water. A limited investigation was done to determine the duration and amount of vacuum needed to saturate a specimen. Work was centered on a mixture with good resistance to the action of water and specimens compacted with the California kneading compactor. A submerged specimen could be saturated fully with distilled water with a vacuum of 20 in. of mercury (67.6×10^3 N/m^2), held for 5 min at this pressure, and then 5 min at atmospheric pressure for a blotting effect. The temperature of the water was that of the laboratory—about 75 F (24.0 C).

Double punch tensile tests performed on control and vacuum-saturated specimens indicated no adverse effect or loss of strength caused by the vacuum-saturation procedure. However, later work with a more water-susceptible mixture and with vacuum

Table 1. Tensile stress by indirect methods.

Deformation (in./min)	Test Temperature (deg F)	Split Cylinder[a] Stress (psi)	Split Cylinder[a] Coefficient of Variation (percent)	Double Punch Stress (psi)	Double Punch Coefficient of Variation (percent)
Dense-Graded Aggregate					
0.05	75	40.8	13.5	49.9	11.8
0.50	75	105.9	13.6	93.4	14.2
1.00	75	113.9	10.6	116.4	2.4
0.065	55	120.2	13.7	—	—
Gap-Graded Aggregate					
0.05	75	70.9	14.5	65.0	10.8
0.50	75	140.5	5.0	133.2	5.0
1.00	75	176.5	10.0	161.9	2.1
0.065	55	167.6	14.7	—	—

Note: 1 in./min. = 41.5 x 10^{-6} m/s. 1°C = $\frac{5}{9}$ (°F - 32). 1 psi = 6.89 x 10^3 N/m^2.

[a]For dense-graded aggregate, $S_{S.C.} = 1.14\ S_{D.P.} - 12.2$ and $r^2 = 0.94$. For gap-graded aggregate, $S_{S.C.} = 1.07\ S_{D.P.} + 0.8$ and $r^2 = 0.98$.

Table 2. Effects of specimen and double punch size on tensile strength.

Specimen Size (in.)	Punch Diameter (in.)	Tensile Strength (psi)	Sample Standard Deviation	Coefficient of Variation (percent)
6 by 2	1	145	11.4	7.9
4 by 2	1	150	5.6	3.7
2 by 2	1	284	22.2	7.9
6 by 2	$\frac{5}{8}$	82	4.5	5.6
4 by 2	$\frac{5}{8}$	74	2.1	2.8
2 by 2	$\frac{5}{8}$	130	15.0	11.6
4 by 2	$\frac{3}{8}$	47	1.7	3.7
2 by 2	$\frac{3}{8}$	52	12.5	24.1
4 by 4	$\frac{5}{8}$	42	0.6	1.4
4 by 8	$\frac{5}{8}$	22[a]		
4 by 8	1	40[a]		

Note: 1 in. = 25.4 mm. 1 psi = 6.89 x 10^3 N/m^2. 1°C = $\frac{5}{9}$ (°F - 32).

[a]Not a tensile failure.

Figure 1. Disassembled saturation and stressing chamber.

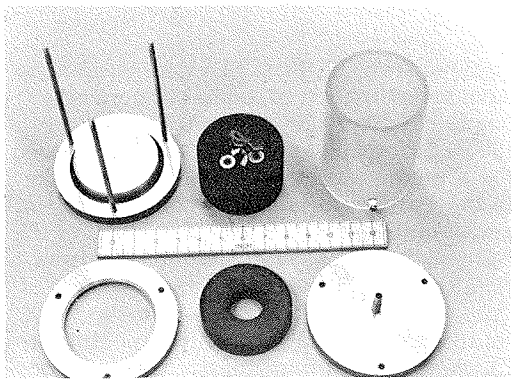

Figure 2. Water bath and saturation setup.

saturation at 122 F (50.0 C) indicated that this combination of exposure can cause a loss of tensile strength of as much as 20 percent of the dry specimen.

Specimen Stressing

The desire to simulate traffic loading conditions that cause debonding resulted in using repeated pore water pressure for specimen exposure. This stressing or conditioning followed the vacuum saturation of the specimen at 122 F (50.0 C). The saturation chamber containing a submerged specimen was fitted with a rubber-like annulus that was submerged but not in contact with the specimen. A sinusoidal loading was applied to the annulus that caused a hydraulic pressure varying from 5 to 30 psi (34.5×10^3 to 217.0×10^3 N/m^2) at a rate of 580 times/min. Because the saturation chamber was clear plastic, the muddying of water and surging of loose sand particles could be observed as the stressing of a specimen continued. Repeated pore water pressure and surging of sand particles within the saturated specimen approached the stressing that a rain-soaked pavement receives from moving traffic loads.

DEBONDING TEST PROCEDURE

Because hot, water-saturated pavements may be most susceptible to debonding failure when subjected to dynamic loading (traffic), a duplication of the physical state of such pavements was attempted in the laboratory by both saturating and stressing the specimen. Given a 2½- by 4-in. (63.5- by 101.6-mm) cylindrical asphaltic concrete specimen, the following basic procedure should be used to determine its resistance to debonding: (a) saturate specimen; (b) subject it to cyclic stressing; and (c) test it for strength.

Saturate Specimen

Previous testing has shown that the following procedure will yield a high degree of saturation (99 to 100 percent) in a short time. Research has shown that, during the summer months in the desert Southwest, temperatures in saturated asphaltic concrete pavements seldom fall below 122 F (50.0 C). Water in a bath used for saturating specimens was maintained at 122 F (50.0 C) to a depth of approximately 8 in. (200 mm); distilled water was preferred. The following step-by-step procedure to full saturation should be used:

1. Place specimen in the plexiglass saturation-stressing chamber (Fig. 1);
2. Place chamber in hot-water bath, cover specimen with about 2 in. (50 mm) of hot water, and secure lid on chamber (Fig. 2);
3. Allow specimen to stand in hot water for approximately 15 min;
4. With spigot at base of chamber closed, connect vacuum hose to top of chamber and apply vacuum pressure (20 in. of mercury) (67.6×10^3 N/m^2) for 5 min; and
5. Release vacuum and let specimen stand an additional 30 min in hot-water bath to bring specimen to bath temperature.

Cyclic Stressing

This method was the result of previous work and was designed so that the specimen would not be loaded directly. Loading was accomplished through a layer of water ¼ to ½ in. (6 to 13 mm) deep between the rubber annulus and the top of the specimen. A cyclic load operating at 580 rpm was used to generate pressures within the water-saturated specimen ranging from 5 to 30 psi (34.5×10^3 to 217.0×10^3 N/m^2)—a range comparable to that expected in saturated pavements under traffic. The following stress procedure should be used:

1. With the chamber (and specimen) still in the hot-water bath, remove the vacuum-tight lid, replace it with a stress-ring lid, and secure this lid tightly by hand by turning the wing nuts;
2. Place the Flexane rubber annulus that is 1 in. (25 mm) thick into the chamber (under the water in the chamber) and carefully release all entrapped air from beneath the annulus;

3. Adjust the annulus until it is perpendicular to the cylindrical axis of the chamber and push it slowly down until approximately ¼ to ½ in. (6 to 13 mm) of water remains between its bottom surface and the specimen's top surface;
4. Remove the chamber from the hot-water bath and quickly place it in proper position on the vibratory kneading compactor table;
5. Lower the loading apparatus carefully until the foot 4 in. (101.6 mm) in diameter makes contact with top of annulus. Then continue lowering crossbar until annulus and water support the weight of the loader;
6. Set timer to the time required to obtain the desired number of load repetitions and activate the electric motor; and
7. After stressing time has elapsed, raise loader, remove chamber from compactor, remove stressing ring lid and annulus, and remove specimen from chamber and place it in a 77 F (25.0 C) water bath for a minimum of 45 min.

Figure 3 shows repeated pore water pressure stressing.

Strength Test

After stressing and cooling, the tensile strength of the specimen was determined by the double punch test, which consists of loading with two steel rods (punches) 1 in. (25.4 mm) in diameter centered on both top and bottom surfaces of the cylindrical specimen.

If the specimen is to be tested while it is fully saturated, it should be taken directly from the 77 F (25.0 C) water bath and tested immediately. If a lesser degree of saturation is required, the specimen should be removed from the water and allowed to dry for a time before testing. When the specimen has reached the desired state of saturation, the following test procedure should be used:

1. Center specimen on bottom punch by using wooden centering blocks;
2. Lower the test machine head until the upper punch just touches the upper surface of the specimen; and
3. Set head speed to 1.0 in./min (41.5×10^{-6} m/s) and begin loading.

Figure 4 shows a specimen being tested.

Maximum load registered by the testing machine was considered the failure load. Tensile strength was calculated by using the following equation:

$$\sigma_t = \frac{P}{\pi(1.2bH - a^2)}$$

where

σ_t = tensile stress, in pounds per square inch;
P = maximum load, in pounds;
a = radius of punch, in inches;
b = radius of specimen, in inches; and
H = height of specimen, in inches.

MATERIALS FOR PROCEDURAL APPRAISAL

Aggregates

Three general aggregate blends were selected to represent best, average, and worst.

1. The limestone aggregate was selected as representative of the best aggregates because it resists debonding well.
2. The Tucson aggregate was selected as representative of average aggregates from dry washes and pits because it is typical of the aggregate used for asphaltic concrete in the Tucson area.
3. The Holbrook aggregate was selected as representative of the worst aggregates because it is most susceptible to debonding.

Aggregate characteristics are given in Table 3. There was an inconsistency between sand equivalent value and performance; limestone aggregate had a lower (worse) sand

Figure 3. Repeated pore water stressing.

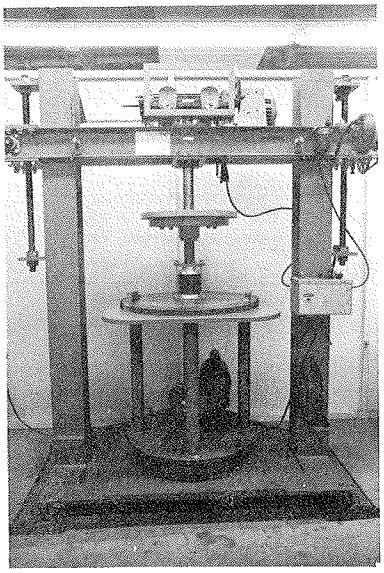

Figure 4. Double punch test.

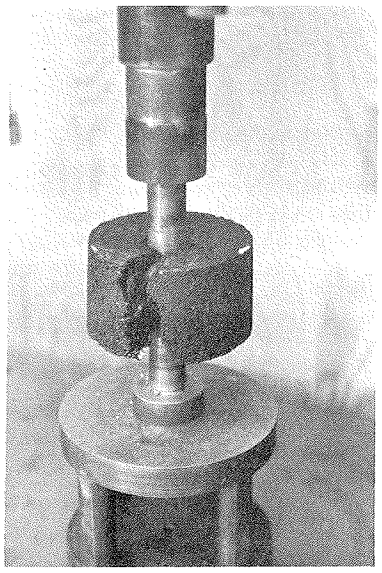

Table 3. Gradation and SE values of aggregate combinations.

	Percent Passing							
	Tucson		Limestone		Holbrook No. 1		Holbrook No. 2	
Item	Wet	Washed	Wet	Washed	Wet	Washed	Wet	Washed
Gradation, sieve size								
3/4 in.	100	100	100	100	100	100	100	100
1/2 in.	99	99	75	74	87	87	85	85
3/8 in.	93	93	70	69	73	73	75	74
No. 4	64	62	59	57	56	56	48	46
No. 8	44	40	45	43	53	52	43	41
No. 16	35	31	32	29	45	44	32	30
No. 30	26	21	22	19	31	30	28	26
No. 50	17	12	15	11	13	12	14	11
No. 100	11	5	11	7	3	2	6	3
No. 200	7	1	5	1	1	0	4	1
Sand equivalent	31	91	38	85	59	89	—	—

Table 4. Component analysis and consistency of original and reconstituted asphalts.

	Percent of Component							
Asphalt	A	N	A_1	A_2	P	CRR[a]	Viscosity at 140 F (poise)	Penetration Grade at 77 F
RH	15.81	42.56	13.22	19.81	8.59	1.96	2,829	45
RO	18.30	33.20	16.38	21.89	10.23	1.54	1,908	67
Original	16.25	29.79	20.79	20.68	12.51	1.52	1,895	65
RL	23.75[b]	26.43	12.33	22.93	14.57	1.03	803	122

Note: 1°C = 5/9 (°F · 32). 1 poise = 0.1 Pa·S.

[a]This is expressed as $(N + A_1)/(P + A_2)$. [b]Extra asphaltene was added to increase viscosity.

equivalent (SE) value than did the Holbrook aggregate, which has a record of poor performance. However, the SE value by itself cannot be used to predict performance, specifically, the stripping of asphaltic concrete.

Asphalt

The asphalt used in most of this study had a penetration grade of 60-70, which meets specification 705(C) of the Arizona Highway Department (10).

A portion of the study was concerned with the effect of an asphalt's chemical reactivity ratio (CRR) on a paving mixture's resistance to stripping. The CRR is a ratio of sums of components obtained from the Rostler-White (11) component analysis. The composition of the reconstituted asphalts and values of CRR are given in Table 4.

RESULTS OF VARIOUS TESTING PROGRAMS

The new test developed to detect the stripping susceptibility of asphaltic concrete was investigated for its response to mixture and specimen variations such as asphalt content, type of aggregate, aggregate cleanliness, asphalt composition, and specimen exposures. All specimens were prepared according to a standard procedure. Before mixing, aggregates were heated to 300 ± 10 F (149 ± 6 C); the asphalt was heated to 285 ± 5 F (141 ± 3 C). All compaction was done at an initial mixture temperature of 250 ± 2 F (121 ± 1 C). For the double punch specimen the mixture was compacted with the California kneading compactor by following the general procedure of the Arizona Highway Department (12). The specimens evaluated by the immersion compression method were compacted and tested according to AASHO T167-60 and T165-55 (13).

Tucson Aggregate

Dry Storage Time—Because the mixture was not aged before compacting or testing, it was necessary to investigate the effects of variable storage or shelf time on the dry and wet double punch strength of an asphaltic mixture. The basic Tucson aggregate (SE 31) with asphalt contents (AC) of 5.5 and 6.0 percent was compacted and the specimens stored in air at 77 F (25.0 C) from 2 to 84 days. The results of these tests are given in Table 5; wet specimens were saturated and stressed for 5,800 repetitions at 122 F (50.0 C) before they were tested at 77 F (25.0 C). A presentation also is shown in Figure 5. The discussion of the results will be based only on strength values.

The curves of Figure 5 indicated that within the range-of-time variable storage time had no great effect on dry strength. However, it had an effect on wet strength; it increased to an optimum value at 7 days and then it decreased. The maximum strength at 7 days might have been caused by the lower void content, but, because saturation was not much different from the value at 84 days, some other factor must have made a greater contribution to the loss in wet strength. Aging of the asphalt and changes in its resistance to the repeated pore water pressure might have been primarily responsible for the change in strength. But, regardless of the actual cause, dry storage time must be kept constant in any comparative strength measurements.

Variable Saturation—Degree of specimen saturation should not affect the tensile strength of asphaltic concrete and, therefore, this variable should not have to be investigated. But, because the variable saturation is obtained after pore pressure stressing, there might be a healing effect caused by drying down from full saturation. The Tucson aggregate specimens were saturated and subjected to pore water pressure stressing. To minimize the effects of storage from stressing to testing, we kept the specimens for high saturation in a 77 F (25.0 C) water bath for 3 days; the specimens for medium saturation were allowed to dry for 3 days in a desiccator at 77 F (25.0 C); the specimens for low saturation were subjected to a vacuum of 10 in. of mercury (33.8×10^3 N/m^2) on 1 flat surface with laboratory air flowing through parallel to the geometric axis for 10 min. Then the specimens were stored for 3 days in a desiccator at 77 F (25.0 C).

The results of this testing are given in Table 6, and a plot is shown in Figure 6. The relationship between degree of saturation and tensile strength after exposure was some-

Table 5. Effect of variable storage time on tensile strength of Tucson aggregate.

Time	Density (pcf)	Voids (percent)	Saturation (percent)	Failure Stress (psi)		Retained Strength (percent)
				Wet	Dry	
2 days						
AC 5.0 percent	141.0	6.7	128	65	145	45
AC 6.0 percent	143.0	3.8	114	118	149	79
7 days						
AC 5.0 percent	144.0	4.9	118	125	165	76
AC 6.0 percent	145.0	2.6	121	145	164	88
42 days						
AC 5.0 percent	140.0	7.5	128	55	143	38
AC 6.0 percent	143.5	3.7	125	98	162	61
84 days						
AC 5.0 percent	139.5	7.9	119	48	146	33
AC 6.0 percent	142.5	4.8	114	82	141	58

Note: 1 pcf = 16.0 kg/m^3. 1 psi = 6.89 x 10^3 N/m^2.

Figure 5. Effect of variable storage time on tensile strength of Tucson aggregate.

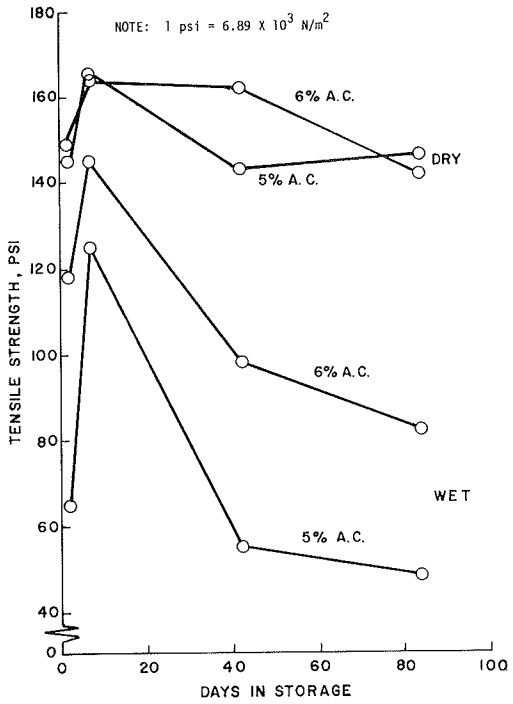

Table 6. Effect of variable saturation on tensile strength after pore water stressing of Tucson aggregate.

Level of Saturation	Density (pcf)	Voids (percent)	Saturation (percent)	Wet Tensile Strength (psi)
Low				
AC 5.0 percent	138.5	8.7	66	22
AC 5.5 percent	139.0	7.4	64	35
Medium				
AC 5.0 percent	138.0	9.0	73	23
AC 5.5 percent	139.0	7.5	91	27
High				
AC 5.0 percent	138.5	8.6	160	16
AC 5.5 percent	139.0	7.7	158	28
Dry				
AC 5.0 percent	138.5	8.5	0	92
AC 5.5 percent	139.5	7.3	0	119

Note: 1 pcf = 16.0 kg/m^3. 1 psi = 6.89 x 10^3 N/m^2

what linear with strength decreasing with increases in degree of saturation. Perhaps of greater interest is the finding that the degree of saturation exceeded 100 percent. This is attributed to the increase of permeable voids in the mineral aggregate from application of the 5,800 repetitions of the fluctuating pore water pressure and to an increase in gross volume and a satisfying aggregate absorption after asphalt film rupture. The amount of water in the specimen divided by the original air void content yielded the degree of saturation. The 2 important findings of this phase were that the void space, through the exposure condition of the test, could be increased and that the period of time from taking the specimen out of the water bath, blotting, weighing, and testing was not a critical one.

Pore Water Pressure Repetitions—The effect of the number of stress repetitions on the wet strength of the Tucson aggregate was established by using 2 asphalt contents and a saturation and stressing temperature of 77 F (25.0 C). The data given in Table 7 show a strength decrease with a loading time increase. The plot shown in Figure 7 shows the strength-number relationship to be linear. Saturation, stressing, and testing took place at 77 F (25.0 C). Future work should include the temperature of 122 F (50.0 C).

Variable Specimen Diameter and Height—Mechanical properties of laboratory prepared specimens are different from those of the same mixture in service. In addition, samples taken from in-service pavements are not of the same dimensions as laboratory-prepared specimens and this difference yields added effects in comparing the properties of specimens. This work attempted to establish geometrical effects on the new method of evaluation for stripping susceptibility. The variables were asphalt content, specimen height, and specimen diameter; because of unforeseen circumstances, the storage time of compacted specimens was an uncontrolled variable. The data for this testing are given in Table 8. The specimens were formed by vibratory kneading compaction. Wet specimens were saturated at 122 F (50.0 C) before they were tested at 77 F (25.0 C). The most acceptable comparison that could be made was that of retained strengths between the specimens 4 and 3.15 in. (80.2 and 101.6 mm) in diameter and it is shown in Figure 8. The retained strengths for specimens of these 2 diameters were essentially the same.

Mixture Variables—The effects of asphalt content and aggregate cleanliness as shown by the SE value on the retained strength according to the new method were determined for the Tucson aggregate. These same variables were used for evaluation by the immersion compression test.

Table 9 gives the results of this testing with AC ranging from 5.0 to 6.0 percent and SE values varying from 31 to 91. The intermediate SE value of 55 was obtained by blending the wet and washed Tucson aggregates having SE values of 31 and 91 respectively. In analyzing the data, one must recognize that the gradation of the 3 blends was not constant. In the double punch method, wet specimens were stressed for 5,800 repetitions at 122 F (50.0 C) before they were tested at 77 F (25.0 C).

A review of the data given in Table 9 shows that the double punch specimens formed by the California kneading compactor had higher densities than those compacted according to the immersion compression method. In general, as the AC and SE values increased, the retained strength increased for both methods of testing.

From the data of Table 9, the degree of saturation of specimens subjected to the repeated pore pressure stressing can be greater than 100 percent.

In Figure 9, the curves show the effects of AC and SE values on the wet and dry strengths obtained by the new method. Generally, the dry strength decreased as the SE value increased. This behavior could be due to the loss of filler material in the blend. Specimen density also decreased with increases of SE value. The same figure shows that the wet strength increased with SE value.

The data plotted in Figure 10 show that according to the new method the retained tensile strength increased as the SE value increased. The point established by a SE value of 91 for the mixture with an AC of 6.0 percent appears to be out of line; however, one must recall that for all 3 values of SE there was a slight variation in filler content.

Figure 11 shows a graphical comparison for retained strengths obtained by the new method and the immersion compression procedure. The plot shows that the new method yields higher values of retained strength than those obtained by the immersion com-

Figure 6. Effect of variable saturation on tensile strength after pore water stressing of Tucson aggregate.

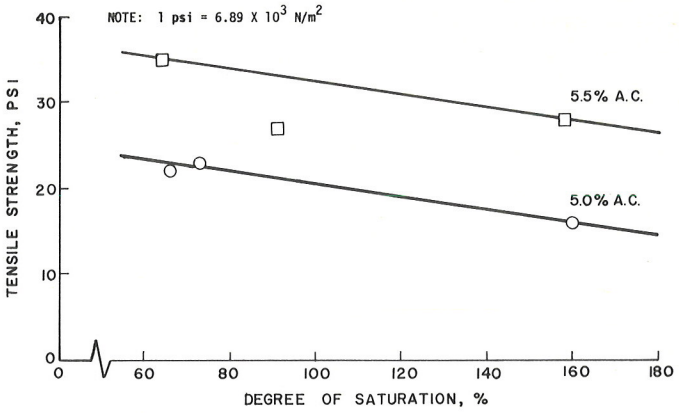

Table 7. Effect of pore water pressure repetitions on tensile strength of Tucson aggregate.

Stress Applications	Density (pcf)	Voids (percent)	Saturation (percent)	Wet Tensile Strength (psi)
0				
AC 5.0 percent	141.0	7.0	95	78
AC 5.5 percent	142.0	5.8	93	106
5,800				
AC 5.0 percent	141.0	7.0	95	68
AC 5.5 percent	142.0	5.8	93	104
13,200				
AC 5.0 percent	141.0	7.0	98	55
AC 5.5 percent	142.0	5.8	95	90

Note: 1 pcf = 16.0 kg/m³. 1 psi = 6.89 x 10³ N/m².

Figure 7. Effect of stress duration on tensile strength of Tucson aggregate.

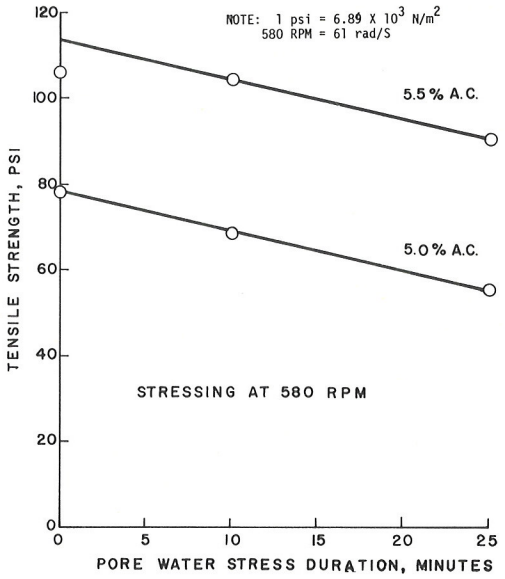

Table 8. Effect of variable specimen diameter and height on tensile strength of Tucson aggregate.

Specimen Size (in.)	Density (pcf)	Voids (percent)	Failure Stress (psi)		Retained Strength (percent)
			Wet	Dry	
3.15 by 2					
AC 5.0 percent	142.0	6.2	164	322	51
AC 5.5 percent	144.0	4.4	134	264	51
AC 6.0 percent	144.5	3.0	211	274	77
3.15 by 4					
AC 5.0 percent	143.0	5.5	89	161	55
AC 5.5 percent	144.5	3.8	159	196	81
AC 6.0 percent	146.5	1.6	130	132	99
4.0 by 2					
AC 5.0 percent	143.5	5.1	137	219	63
AC 5.5 percent	144.5	3.9	105	201	52
AC 6.0 percent	145.5	2.3	200	250	80
4.0 by 4					
AC 5.0 percent	142.0	6.1	70	148	47
AC 5.5 percent	147.5	1.9	136	160	85
AC 6.0 percent	144.5	2.9	77	142	54

Note: 1 pcf = 16.0 kg/m^3. 1 psi = 6.89 x 10^3 N/m^2.

Figure 8. Relationship between the retained strength of 4-in.- and 3.15-in.-diameter specimens with variable AC.

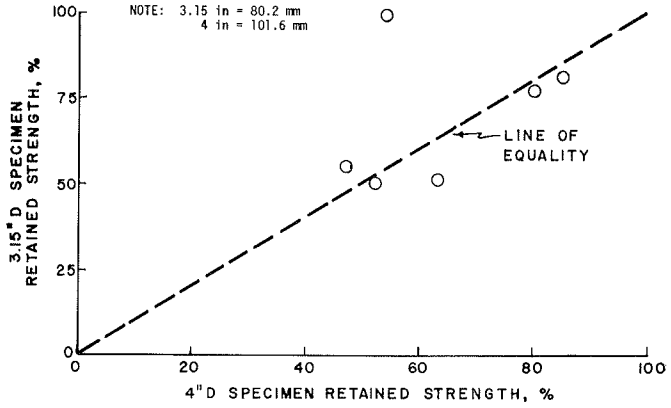

Table 9. Effect of AC and SE value on wet and dry strengths of Tucson aggregate.

Value	Density (pcf)	Voids (percent)	Saturation (percent)	Failure Stress (psi)		Retained Strength (percent)
				Wet	Dry	
Double Punch Method						
Sand equivalent 31						
AC 5.0 percent	141.0	6.8	107	43	124	35
AC 5.5 percent	141.5	5.7	128	58	118	49
AC 6.0 percent	144.0	3.6	116	76	104	73
Sand equivalent 55						
AC 5.0 percent	140.0	7.6	116	61	113	54
AC 5.5 percent	141.0	6.1	110	83	105	79
AC 6.0 percent	144.0	3.7	117	123	135	91
Sand equivalent 91						
AC 5.0 percent	140.5	7.2	106	72	85	85
AC 5.5 percent	139.5	7.2	105	73	79	92
AC 6.0 percent	142.0	4.8	99	85	110	77
Immersion Compression Method						
Sand equivalent 31						
AC 5.0 percent	137.5	9.2	99	170	553	31
AC 5.5 percent	138.5	7.9	88	192	421	46
AC 6.0 percent	139.5	6.5	72	275	502	55
Sand equivalent 55						
AC 5.0 percent	135.0	10.4	102	159	346	46
AC 5.5 percent	136.0	9.1	107	217	346	63
AC 6.0 percent	137.0	7.1	86	257	406	63
Sand equivalent 91						
AC 5.0 percent	135.5	10.5	92	162	307	53
AC 5.5 percent	134.5	10.5	92	200	341	59
AC 6.0 percent	135.5	9.2	74	282	438	64

Note: 1 pcf = 16.0 kg/m^3. 1 psi = 6.89 x 10^3 N/m^2.

Figure 9. Relationship between SE value and tensile strength as affected by AC for the Tucson aggregate.

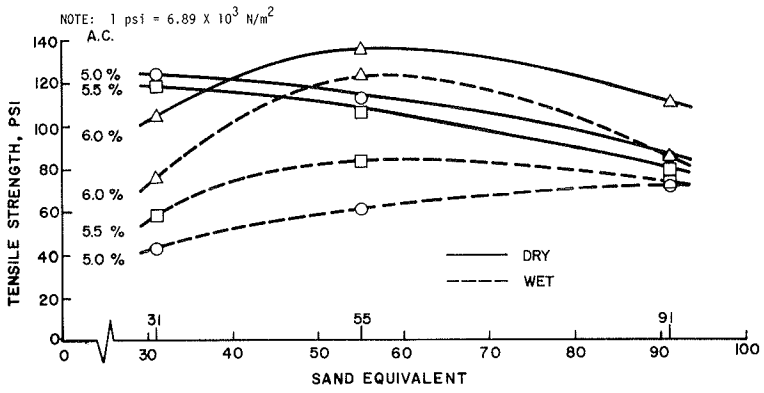

Figure 10. Relationship between SE value and retained tensile strength for the Tucson aggregate.

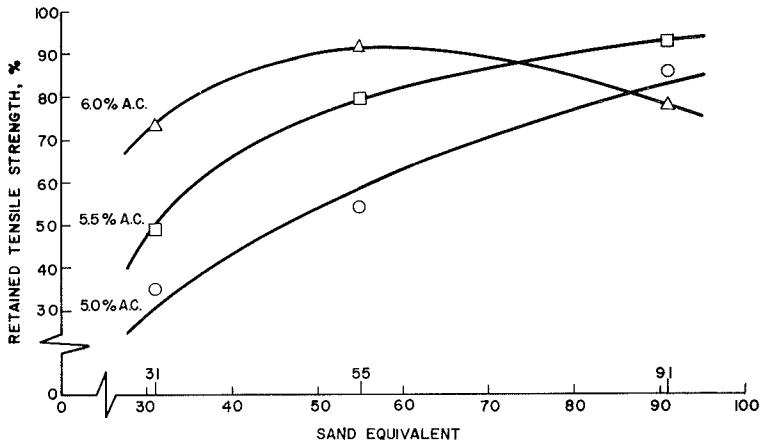

Figure 11. Relationship between retained strengths obtained by the double punch method and the immersion compression method for the Tucson aggregate.

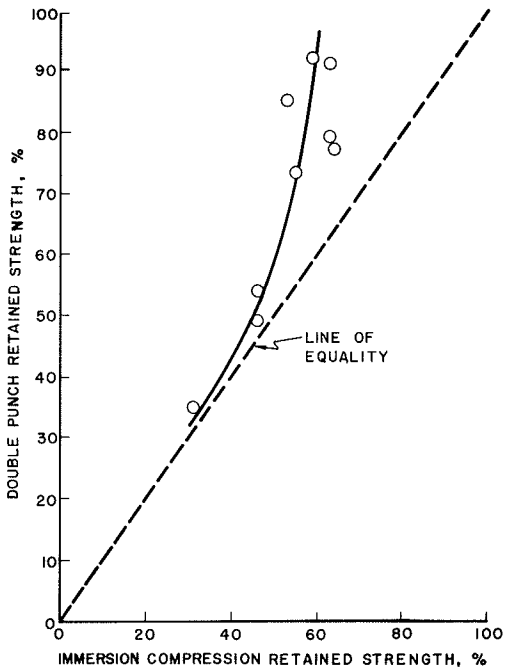

pression procedure. Because the slope of the curve is greater than 1, the new procedure was more sensitive to the variables than was the immersion compression method. Higher value does not mean better value.

Limestone Aggregate

The evaluation of this blend included SE value and testing method variables. Table 10 gives the specimen characteristics for mixtures evaluated by the new and immersion compression methods. In the double punch method wet specimens were stressed for 5,800 repetitions at 122 F (50.0 C) before they were tested at 77 F (25.0 C). The values of particular interest are for the degree of saturation and retained strength. It is apparent that the exposure conditions of both methods resulted in significant saturation of the specimens. The aggregate blend had been presented as having a good performance record. The data of Table 10 indicate that the new method, for SE values of 38 and 85, yielded retained strengths of 66 and 78 percent respectively. The immersion compression test yielded retained strengths of 36 and 53 percent respectively.

Holbrook Aggregate (No. 1)

Because it was known that the complete aggregate blend as it came from the pit contained some clay, an elaborate procedure of separating, soaking, elutriating, boiling, and elutriating again was used to cleanse the aggregate of the deleterious clay. Table 11 gives specimen characteristics for the stripping resistance of asphaltic concrete made with this aggregate. In the double punch method, wet specimens were stressed for 5,800 repetitions at 122 F (50.0 C) before they were tested at 77 F (25.0 C). Of particular interest are the relatively high values for degree of saturation for both types of specimen; it appears that aggregate characteristics rather than exposure conditions are responsible for the degree of saturation for the immersion compression and double punch specimens.

The change in SE value from 59 to 89 did not cause a significant change in retained strength according to either method. Because an appreciable change in gradation was not caused by the cleansing of the aggregate, the poor resistance to stripping seemed to be due to aggregate surface texture and composition of the aggregate.

Asphalt Composition

Asphalt composition may contribute to the stripping susceptibility of an asphaltic mixture. To investigate this, we decided to separate the basic asphalt into its Rostler-White components and then recombine it to obtain a range of CRR values from low to high. These reconstituted asphalts were then used with a second Holbrook aggregate blend. These materials have been described earlier in Tables 3 and 4. Because the main effects were to be related to asphalt composition, voids and saturation measurements were not made for the specimens tested by the new procedure.

The effects of asphalt composition on the wet and dry strength obtained by the new procedure can be seen from the data given in Table 12. In the double punch method, wet specimens were stressed for 5,800 repetitions at 122 F (50.0 C) before they were tested at 77 F (25.0 C). The compositional differences of the asphalts are presented by CRR. These data indicate that the CRR did affect the wet and dry strength separately but there was no significant difference in retained strength for the various CRRs. A graphical representation of the results for a blend with an AC of 5.5 percent is shown in Figure 12. Generally, the wet and dry strengths increased as CRR and viscosity at 140 F (60.0 C) increased.

DISCUSSION AND CONCLUSIONS

Testing Procedure

The general testing procedure appeared to be adequate for laboratory evaluation of asphaltic mixtures. The conditions set for saturation, stressing, and strength testing were reasonable for time, temperature, and repeatability. Of particular interest are

Table 10. Effect of SE value on wet and dry strengths of limestone aggregate.

Item	Sand Equivalent Values[a]	
	38	85
Double Punch Method		
Density, pcf	141.5	139.0
Voids, percent	4.0	5.8
Saturation, percent	158	142
Failure stress, psi		
Wet	96	107
Dry	144	137
Retained strength, percent	66	78
Immersion Compression Method		
Density, pcf	139.5	137.0
Voids, percent	6.6	8.1
Saturation, percent	135	133
Failure stress, psi		
Wet	222	199
Dry	620	379
Retained strength, percent	36	53

Note: 1 pcf = 16.0 kg/m^3. 1 psi = 6.89 x 10^3 N/m^2.

[a]Asphalt content was 5.5 percent.

Table 11. Effect of SE value on wet and dry strengths of Holbrook aggregate No. 1.

Item	Sand Equivalent Values[a]	
	59	89
Double Punch Method		
Density, pcf	144.0	142.0
Voids, percent	2.3	4.0
Saturation, percent	281	212
Failure stress, psi		
Wet	59	54
Dry	89	95
Retained strength, percent	65	57
Immersion Compression Method		
Density, pcf	138.5	136.5
Voids, percent	6.5	8.5
Saturation, percent	154	144
Failure stress, psi		
Wet	110	94
Dry	274	161
Retained strength, percent	40	58

Note: 1 pcf = 16.0 kg/m^3. 1 psi = 6.89 x 10^3 N/m^2.

[a]Asphalt content was 5.5 percent.

Table 12. Effect of CRR on wet and dry strengths of Holbrook aggregate No. 2.

Value	Density (pcf)	Failure Stress (psi)		Retained Strength (percent)
		Wet	Dry	
CRR 1.52[a]				
AC 5.0 percent	148.0	97	143	68
AC 5.5 percent	147.0	92	125	73
AC 6.0 percent	147.0	99	109	91
CRR 1.54[b]				
AC 5.0 percent	147.5	143	180	79
AC 5.5 percent	146.5	148	180	83
AC 6.0 percent	147.0	138	173	80
CRR 1.96[b]				
AC 5.0 percent	146.0	133	190	70
AC 5.5 percent	147.0	176	199	88
AC 6.0 percent	147.0	193	199	97
CRR 1.03[b]				
AC 5.0 percent	146.0	62	83	75
AC 5.5 percent	147.5	80	93	86
AC 6.0 percent	147.0	89	85	107

Note: 1 pcf = 16.0 kg/m^3. 1 psi = 6.89 x 10^3 N/m^2.

[a]Original. [b]Reconstituted.

Figure 12. Effect of CRR on tensile strength of Holbrook aggregate No. 2 with an AC of 5.5 percent.

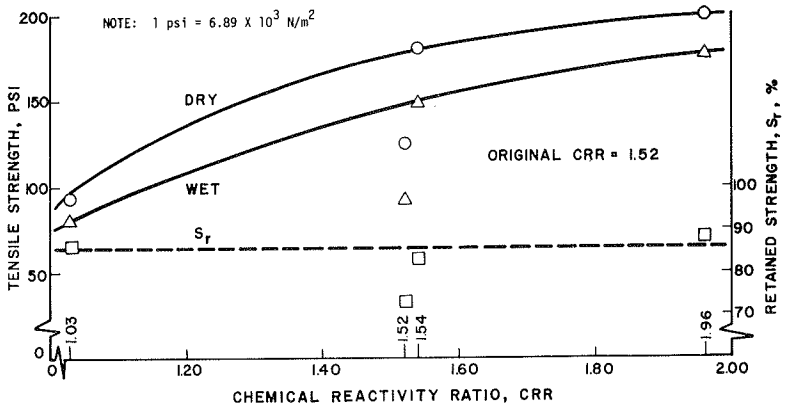

the measurements for degree of saturation and the method for applying the repetitive loads for the exposure of the wet specimens.

There appeared to be some relationship between degree of saturation of different aggregate mixtures and their resistance to stripping. It was difficult to accept that in-service paving mixtures dilate under the action of water or pore water pressure; nevertheless, it was apparent that water-caused permeable volume changes would indicate a water-susceptible mixture.

The repetitive pore water pressure given the specimens was effected through a unique device. The device may not have been important but the rate of loading was in that pore pressure surging and sand particle erosion were affected by cycling rate.

The double punch test was found to be simple and repeatable; however, it suffered, as did most others, from effects on strength caused by specimen geometry. As such the test will require that specimen size be standardized, even though the data presented showed that retained strength may not have been affected by specimen geometry.

Comparison between the double punch and immersion compression wet and dry strengths only indicated that the 2 tests rated the mixtures in essentially the same order. In general, the new method yielded higher values of retained strength.

Material Variables

The data obtained with the new procedure indicated that the resistance to stripping was improved with increases in AC and SE values. But this was expected based on prior experience.

Selection of the limestone and Holbrook aggregates for the study was based on good performance for the limestone and poor for the Holbrook. The service record for the Tucson aggregate was considered to have been acceptable for the region. For the natural aggregates 5.5 percent AC seemed to have been the design amount for the limestone and Tucson aggregates, but it was 0.5 percent high for the Holbrook No. 1 aggregate. For these conditions, the double punch test rated the limestone mixture as the best and the Tucson aggregate as the worst; the immersion compression test rated the Tucson aggregate as the best and the limestone as the worst for retained strength. The terms best and worst are relative and are not meant to be related to acceptable and rejectable.

The effect of CRR on retained strength according to the new method was surprising. The data showed that the higher the CRR value, the greater the viscosity. Our general experience has been that higher retained strengths are obtained with the immersion compression method for mixtures having asphalt with higher viscosity. In this case, retained strength according to the new method was independent of viscosity or CRR value.

An interesting finding in the asphalt composition study was the greatly improved value of retained strength obtained for the Holbrook aggregate. The gradation for Holbrook No. 2 was improved, and greater amounts of asphalt were used to obtain the improved values of wet, dry, and retained strength.

CONCLUSIONS

Careful examination of the data together with experience in evaluating durability of asphaltic concrete leads to the following conclusions:

1. The new procedure for evaluating the stripping susceptibility of asphaltic concrete is simple and repeatable;
2. The responses to test and material variables generally follow established trends;
3. At present, one must fix specimen and punch sizes for comparison of different mixtures to eliminate geometrical effects; and
4. As with any new mixture evaluation procedure, the new procedure must be field tested.

The new procedure to evaluate the debonding susceptibility of asphaltic concrete was based on the following:

1. The way to determine the presence of debonding is with a tension test;
2. The action that causes debonding in the field should be simulated in the laboratory; and
3. The procedure should be capable of testing a pavement core without remolding.

Because these considerations are incorporated in the new procedure and because the work presented has indicated acceptable responses for material variables, repeatability, and simplicity, we recommend that the debonding test procedure be used to evaluate standard Hveem specimens prepared for the routine testing of asphaltic concrete by the Arizona Highway Department. To aid in establishing required minimum strength and/or retained strength, one should sample in-service mixtures on a continuing basis to compare with results obtained from laboratory-prepared specimens.

ACKNOWLEDGMENT

I would like to recognize the contributions of personnel from the Materials and Test Section of the Arizona Highway Department, who obtained the aggregates, and also those who separated and recombined the asphalt for the CRR variation study. Don Stout and Elmer Green were particularly helpful. The contents of this report reflect the views of the author, who is responsible for the facts and the accuracy of the data presented herein. The contents do not necessarily reflect the official views or policies of the Arizona Highway Department or the Federal Highway Administration.

REFERENCES

1. Effects of Water and Moisture on Bituminous Mixes. Questionnaire of Highway Research Board, 1965.
2. Schmidt, R. J. Discussion of Symposium—Pavement Cracking. Proc. AAPT, 1966.
3. Lottman, R. P., and Johnson, D. L. The Moisture Mechanism That Causes Asphalt Stripping in Asphaltic Pavement Mixtures. Res. Proj. 45-302 (R-47DH), Univ. of Idaho, 1969.
4. Gallaway, B. M., and Jimenez, R. A. Interim Report on a Study of Laboratory Method to Determine Susceptibility to Raveling of Bituminous Mixtures. National Asphalt Paving Association, QIP 65, 1963.
5. Majidzadeh, K., and Stander, R. R. Effect of Water on Behavior of Sand-Asphalt Mixtures Under Repeated Loading. Highway Research Record 273, 1969, pp. 99-109.
6. Lottman, R. P. The Moisture Mechanism That Causes Asphalt Stripping in Asphaltic Pavement Mixtures. Res. Proj. 45-302 (IDH-R-47), Univ. of Idaho, 1971.
7. Jimenez, R. A. Frictional Characteristics of Pavement Surface. Rept. to Arizona Highway Department, 1970.
8. Fang, H. Y., and Chen, W. F. New Method for Determination of Tensile Strength of Soils. Highway Research Record 345, 1971, pp. 62-68.
9. Jimenez, R. A. Fatigue Testing of Asphaltic Concrete Slabs. STP 508, ASTM, 1971.
10. Standard Specifications for Road and Bridge Construction. Arizona Highway Department, 1969.
11. Rostler, F. S., and White, R. M. Composition and Changes in Composition of Highway Asphalt, 85-100 Penetration Grade. Proc. AAPT, 1962.
12. Materials Testing Manual. Arizona Highway Department, 1969.
13. Standard Specifications for Highway Materials and Methods of Sampling and Testing, Part 2. AASHTO, 1970.
14. Turner, R. E. C.E. 290 Report—Indirect Tensile Testing by the Split Cylinder and Double Punch Methods. Univ. of Arizona, 1971.
15. Winzerling, A. W. C.E. 290 Report—Evaluation of Double Punch Test for Asphaltic Concrete. Univ. of Arizona, 1972.

A LABORATORY TEST SYSTEM FOR PREDICTION OF ASPHALT CONCRETE MOISTURE DAMAGE

Robert P. Lottman, R. P. Chen, K. S. Kumar, and L. W. Wolf, University of Idaho

Representative results are described and shown for a practical laboratory test system developed to predict moisture damage in asphalt concrete pavements or to monitor the rate of moisture damage in existing pavements. Moisture-damage predictions are based on the results of tensile strength and tensile E-moduli tests performed on laboratory-fabricated specimens that have undergone freeze-soak and thermal-cycle accelerated moisture conditionings. These test results are compared to similar mechanical tests on pavement cores. The conventional laboratory specimens were made to duplicate pavements that were sampled throughout the United States and that had various levels of moisture damage. Implications of using the test system for predictability of moisture damage are discussed.

•THIS paper summarizes some of the findings of a laboratory system developed to predict moisture damage in asphalt concrete pavements. It also discusses the implications of these findings. Details of the laboratory methods, procedures, and data are in a report by Lottman (1).

MOISTURE DAMAGE AND TESTS FOR PREDICTION

Definition of Moisture Damage and Its Effects

For the purpose of this paper, moisture damage can be defined as the following:

1. Disintegration or deterioration of the intrinsic property of the asphalt concrete layer by entry of moisture that can be measured by the asphalt concrete's loss of mechanical properties, and
2. Loss of pavement serviceability because of increased deflections and higher tensile stresses and strains, which lead to pavement cracking and surface rutting.

Disintegration may take the form of stripping, softening, or swelling, which are often accompanied by loss of stiffness modulus, tensile or compressive strength or both, and aggregate retention properties and by a gain of strain at failure and void space.

Many times both disintegration and loss of serviceability occur simultaneously. However, it is possible to have a disintegrating pavement layer that is caused by moisture damage without pavement performance criteria being affected significantly. In either case, though, the pavement will have to be repaired by using overlays or penetrant additives. Moisture damage can exist in several forms; therefore, a program should be developed to avoid mix problems before pavements are constructed.

Kinds of Moisture-Damage Tests

Moisture-damage tests are applied to 2 different physical forms of asphalt concrete. In the first form, asphalt concrete is in a loose state; only a portion of the aggregate (coated with asphalt) is subjected to static or ultrasonic action in water. The amount of coating that comes off is related to the amount of stripping. Those working in

Publication of this paper sponsored by Committee on Effects of Natural Elements and Chemicals on Bitumen-Aggregate Combinations.

fundamental research use this form because "free" conditions of thermodynamics and other scientific approaches can be applied. However, the effects of the amount of coating or coating that comes off eventually have to be measured in the product as compacted asphalt concrete subject to moisture intrusion after field compaction.

The second form, the compacted form, appears to be the favorite of those working with mechanical properties and machines. In certain cases, mechanical properties can be incorporated into pavement layered design theories for performance prediction; in other cases, the mechanical units and related mechanics are not suitable for inclusion. Immersion compression, surface abrasion, Marshall immersion, and tensile split are the tests that use compacted asphalt concrete specimens in dry and wet conditions.

MOISTURE-DAMAGE TEST SYSTEM USED IN THIS STUDY

Comparative Scheme

Pavements were sampled at various locations around the United States. Highway departments sent cores 4 in. (10.16 cm) in diameter, mix materials (aggregate and "equivalent" asphalt representing the pavement), and mix design data (including field sampling data) for pavements that fell into 1 of the following categories:

1. An approximately 5-year-old pavement that shows distress caused by moisture damage, and
2. An approximately 5-year-old pavement that does not show distress caused by moisture damage.

Ten different pavement samples were received for category 1 and 3 for category 2. The locations of many of the samples were selected by severity of climatic temperature according to freezing indexes.

The procedure mechanically and visually tested the cores and compared their data to data from laboratory-fabricated specimens that duplicated the core mixes as closely as possible. The laboratory-fabricated specimens, 4-in. (10.16-cm) in diameter by 2.5-in. (6.35-cm) in thickness made in a kneading compactor, were subjected to specified accelerated moisture conditionings. A comparison of mechanical and visual data between cores and laboratory specimens would show that accelerated moisture conditions are predictive of pavement moisture damage. Therefore, it would be advantageous to use these moisture-damage predictive tests in the laboratory.

Core and Specimen Moisture Conditionings

Pavement cores were tested in a vacuum-saturated condition and in a dry condition (constant weight in desiccator). After testing, core interiors were examined visually by eye and photograph, sometimes by using microphotographs, to observe the level of moisture damage.

Laboratory-fabricated specimens were tested in groups representing the following conditions:

1. Dry, vacuum saturation only;
2. Vacuum saturation followed by 15 hours of 0 F (255.4 K) air freeze followed by 24 hours of 140 F (333.2 K) water bath soak; and
3. Vacuum saturation followed by eighteen 8-hour cycles of 0 to 120 to 0 F (255.4 to 322.0 to 255.4 K) in an air bath.

Specimen interiors were examined visually and by photograph.

Mechanical and visual test data were used to compare core damage to laboratory-fabricated specimen damage.

Mechanical Tests

Tensile split (indirect tension) tests produced tensile strength data and tensile E-modulus data simultaneously. Rates of vertical (compression) deformation and test temperatures were 0.065 in./min. at 55 F (0.165 cm/min. at 285.9 K) and 0.150 in./min.

at 73 F (0.381 cm/min. at 295.9 K). Test times were from 1 to 2 min. per test specimen. A flat loading block was used that did not confine the test specimen during the tensile split test.

Tensile strengths were determined by using the conventional tensile split formula for round test specimens modified for the flattening of the ends of the test specimens at maximum load.

The E-modulus test incorporated a specimen riding device that measured tensile displacement over the test specimen's cross section. These displacements were monitored simultaneously in 5- or 10-second periods with the different loads on the specimens. E-moduli were calculated from these data by extrapolation of the "E-data" to zero test time. Data were recorded easily by 2 operators, 1 working the compression test machine and 1 working an ordinary strain indicator. Figure 1 shows a typical test setup.

A minimum of 4 cores or 4 laboratory specimens per pavement were tested for each of the several moisture conditions and for each of the 2 test temperatures. The test data for the 4 specimens were averaged, and the averages were compared.

REPRESENTATIVE RESULTS AND LABORATORY IMPLICATIONS

Test Results of Pavement Cores

Representative test results of several pavement cores are shown in Figures 2 and 3. The data show tensile strengths and tensile E-moduli for cores in dry and vacuum-saturated conditions. The 55 F (285.9 K) test results are shown; similar trends were obtained at 73 F (295.9 K).

Tensile strengths have a wide range for the pavements shown, and should have some influence, by magnitude only, on the cracking susceptibility of the pavement when asphalt concrete thicknesses are taken into account. Dry tensile strengths are usually higher than saturated tensile strengths. Similar results are observed by using E-moduli.

Tensile tests on dry cores do not show the degree of moisture damage in the cores. There are cores from each of the moisture damage or performance levels shown in Figures 2 and 3 whose test results in the dry condition vary and do not relate to the actual moisture damage level.

Changes (usually relative decreases) of strength and modulus from dry to saturated conditions are much more important to evaluate the extent of moisture damage. For

Figure 1. Tensile split test setup with E-modulus jig.

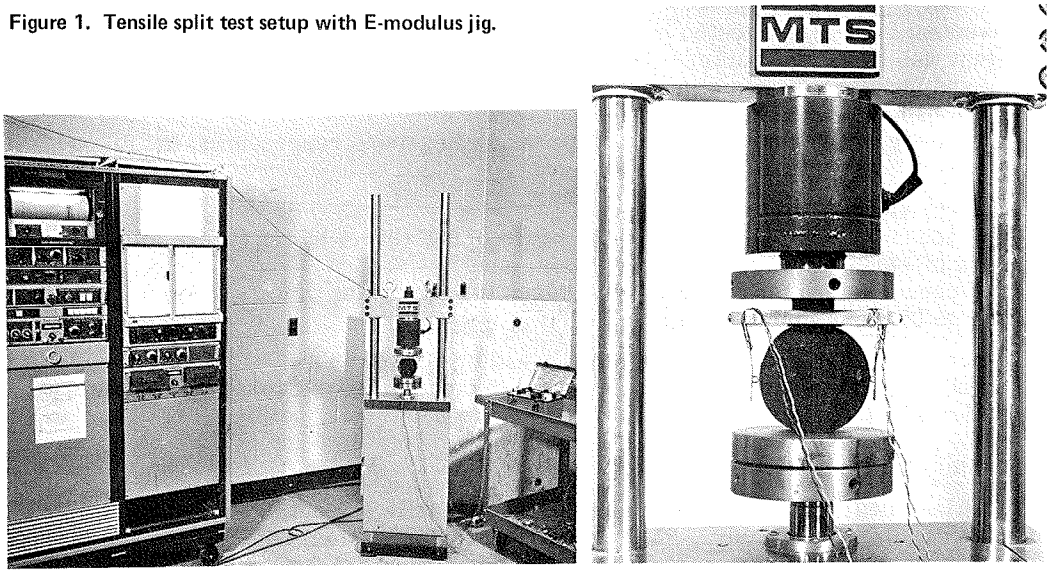

Figure 2. Pavement core tensile strengths.

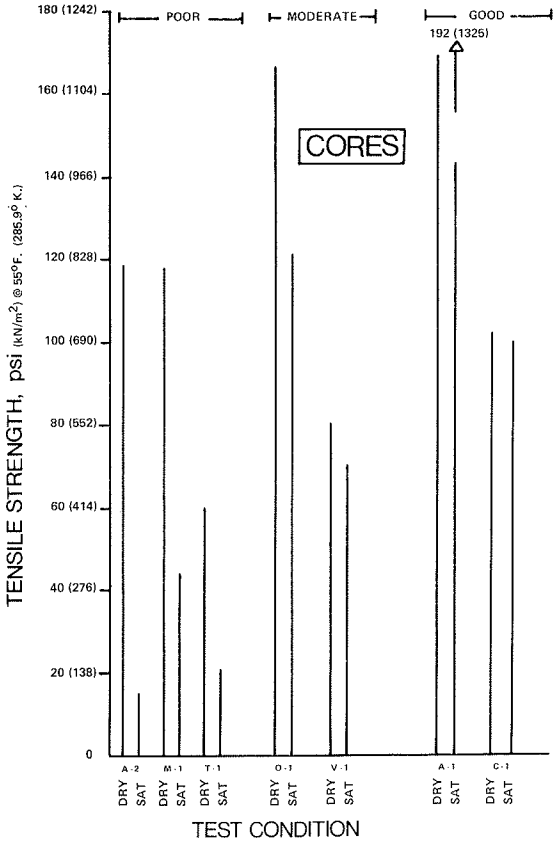

Figure 3. Pavement core E-moduli.

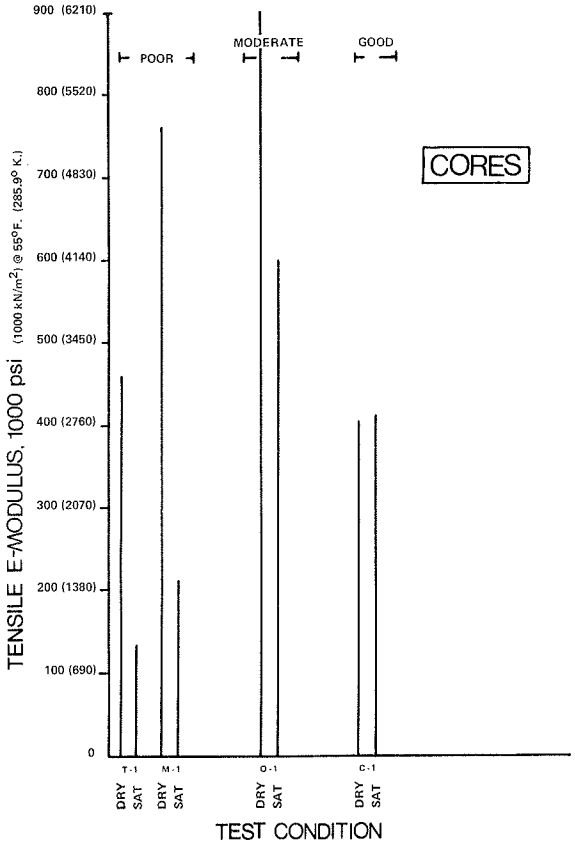

example, test results of cores in the poor level (high moisture damage) show large decreases of strength and modulus magnitudes as compared to other levels of damage. Therefore, moisture damage determined by using these tests is best evaluated by calculating the change in test results between dry and saturated cores. Ratios can be used that are equal to the saturated property magnitude divided by the dry property magnitude. Two ratios are the tensile strength ratio (TSR) and the tensile E-modulus ratio (M_ER). For high moisture-damaged pavements, TSRs and M_ERs could be from 0.1 to 0.4. For low moisture-damaged pavements, the ratios could be from 0.7 to nearly 1.0.

When measuring relative changes, the test temperature of 55 F (285.9 K) is usually more advantageous than 73 F (295.9 K) because the tensile test data magnitudes are greater and thus tend to produce more reliable test results from conventional test machines.

After saturation and testing, all pavement cores opened at the fracture faces showed stripping or softening or both to the relative degree of the change in tensile strength and tensile E-modulus.

Test Results of Laboratory-Fabricated Specimens

Representative test results of a few sets of laboratory-fabricated specimens that duplicate pavement cores are shown in Figures 4 and 5. The data show tensile strengths and tensile E-moduli for laboratory specimens in conditions of dry, vacuum saturation and the thermal-cycle accelerated conditioning of vacuum saturation with 18 cycles of 0 to 120 to 0 F (255.4 to 322.0 to 255.4 K) temperatures. The 55 F (285.9 K) test results are shown; similar trends were obtained at 73 F (295.9 K).

The results in Figures 4 and 5 show the same general trends as were found in the cores. When the specimens became saturated, tensile strengths and E-moduli usually decreased. The accelerated thermal-cycle conditioning, representing the pavement's potential for moisture damage, produced lower strengths and lower E-moduli than did vacuum saturation only for moderate to highly damaged pavements.

Correct matching should show close test-result magnitude comparisons between cores and laboratory specimens in the dry condition, and between cores in the saturated condition and laboratory specimens in the saturated plus thermal cycle condition. Usually the test-result magnitudes for the pavement cores are higher because the asphalt in the cores (pavements) has undergone age-hardening over the years. A comparison for matching purposes is best done by using TSR or M_ER or both.

From the laboratory specimen test data, general estimate of rate of moisture damage can be obtained by observing the relative drop in test data from dry to vacuum-saturated conditions. For example (Fig. 4), the tensile strength drop for pavement A-2 was much greater than the drop for pavement M-1. This indicates that moisture damage built up quickly in A-2. In fact, 1 paving lift of A-2 had to be redone shortly after construction because of a rainstorm.

The laboratory specimens showed similar visual characteristics of moisture damage after thermal cycle conditioning. It is important to open up the cores to observe this damage, which is usually at the tensile-split fracture face. Moisture damage cannot be visually observed at the exterior of laboratory specimens.

The second type of accelerated conditioning, vacuum saturation followed by 0 F (255.4 K) freeze and 140 F (322.2 K) heating, also produced damage in test specimens, but it tended to be somewhat less than that from the thermal-cycle accelerated conditioning and test results appeared to be more scattered.

Predictability

Tensile strength ratios and E-modulus ratios for cores and laboratory specimens were compared at the test temperatures for the different accelerated conditionings to determine predictability. Comparisons for several of the pavements sampled are shown in Figures 6 and 7 for 55 F (285.9 K) test temperatures. In these figures the following should be pointed out:

Figure 4. Laboratory specimen tensile strengths.

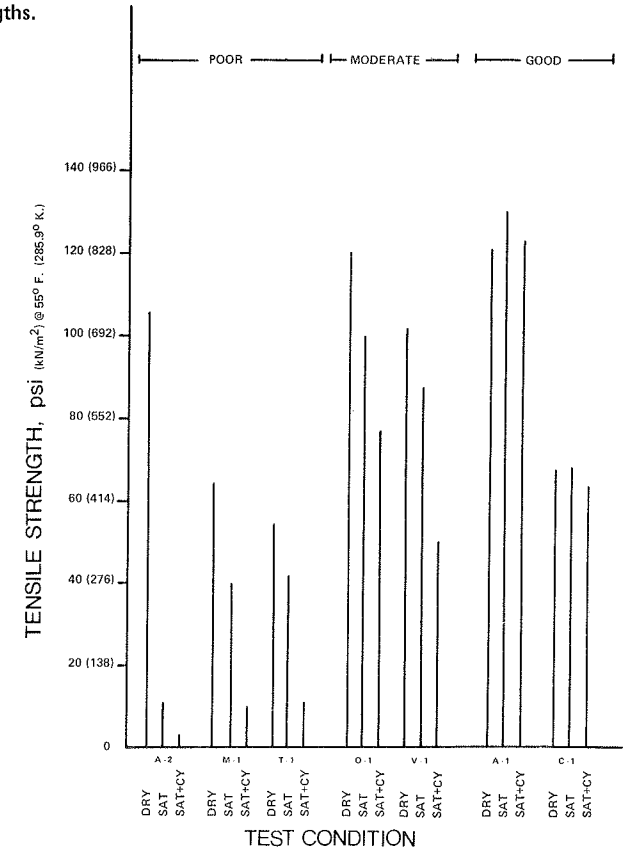

Figure 5. Laboratory specimen E-moduli.

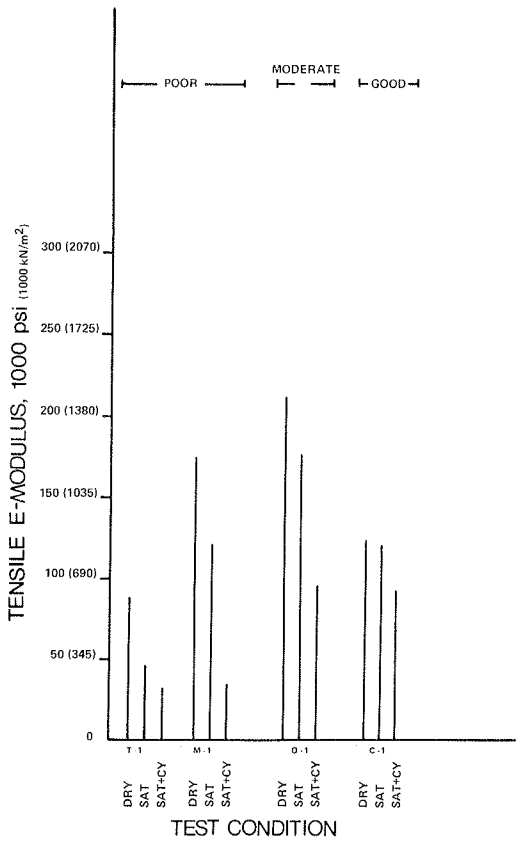

Figure 6. Comparison of core and laboratory tensile strength ratios.

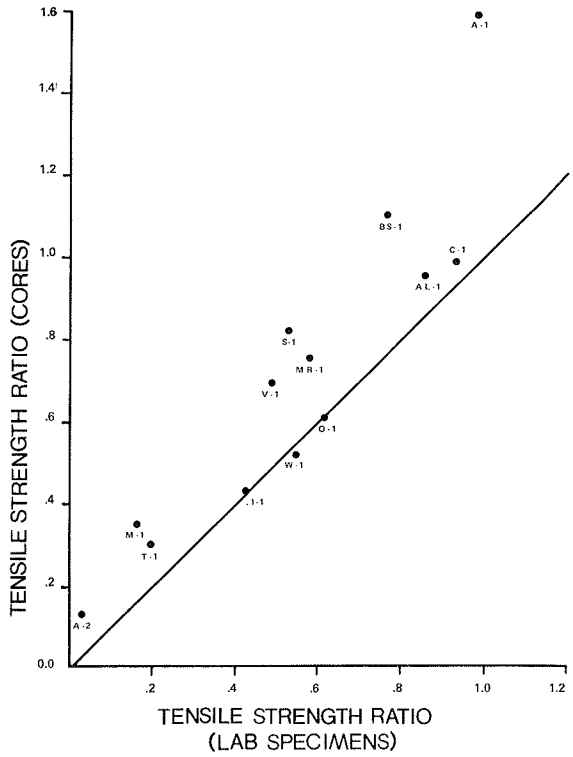

Figure 7. Comparison of core and laboratory E-moduli ratios.

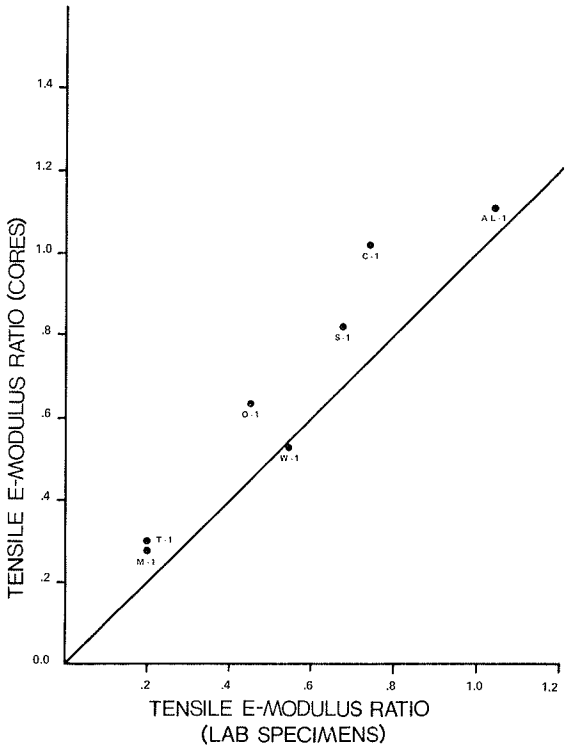

1. Data that plot on the 45-deg line of equality indicate equal matches of ratios for cores and laboratory specimens;
2. Data that plot to the left of the 45-deg line of equality represent overprediction of moisture damage (that is, laboratory specimens after accelerated moisture conditioning have lower ratios than pavement cores);
3. For cores, M_ERs and TSRs equal the vacuum-saturated modulus (strength) divided by the dry modulus (strength); and
4. For laboratory specimens, M_ERs and TSRs equal the vacuum-saturated plus the thermal-cycle conditioning modulus (strength) divided by the dry modulus (strength).

In general, there was overprediction. The laboratory specimen data predicted the moisture damage to cores in 2 or 3 categories. There were no significant underpredictions.

Similar types of ratio plots for test temperatures of 73 F (295.9 K) showed slightly more scatter. Plots of ratios for accelerated conditioning of vacuum saturation followed by a 0 F (255.4 K) freeze and a 140 F (333.2 K) heating underpredicted several of the cores.

Climate does not seem to have an effect on the laboratory conditioning results for moisture damage prediction. For example, when the accelerated moisture conditionings, which contain a freeze element, were applied, the effects were not severe for the cores from zero freezing climates (pavements T-1 and C-1 in Figs. 6 and 7), nor did they have inadequate severity for cores from high freezing climates (pavements M-1 and AL-1 in Figs. 6 and 7). Perhaps the differential thermal expansions (pore pressures and void space changes) and the warm "soak" elements of the accelerated laboratory conditionings combine to accelerate overall temperature change and traffic effects in all climatic locations where sampling was undertaken. It could be possible, however, that climate has an effect on rate of moisture damage along with moisture availability and basic aggregate-asphalt interactive characteristics.

Microphotographic comparison test data will determine which accelerated laboratory conditioning most closely matches cores.

More extensive field evaluations should include the continuous sampling and monitoring of pavements from time of construction. Better information about rate of moisture damage could then be obtained.

KINDS OF APPLICATIONS

Routine Mix Design

Obtaining design asphalt content could be accomplished by studying vacuum-saturated and accelerated-moisture-conditioned specimens having variable asphalt contents. Evaluations could be based on tensile E-modulus, tensile strength, and tensile strain obtained by using an indirect tension test.

Another approach could be to evaluate the moisture-damage resistance of the mix after one obtains the design asphalt content by conventional methods. This would entail making 8 to 12 additional standard-sized test specimens for design asphalt content and evaluating them in the indirect tension mode in dry, vacuum-saturated, and accelerated-moisture-conditioned states. After the results are evaluated, additives and changes in asphalt-aggregate combinations may be found to be needed.

Monitoring Pavements

Cores could be drilled from pavements soon after construction and be subjected to accelerated moisture-damage conditionings. The potential for moisture damage could then be predicted. Every year or 2 thereafter, additional cores could be drilled and tested in a dry, vacuum-saturated condition (without accelerated conditioning) to monitor the rate of moisture damage relative to the predicted potential (maximum) damage. This may help to provide schedule information for pavement maintenance or rehabilitation programs.

Additives and Remedies

Asphalt antistrip additives, filler additives, pavement surface penetrants, and mix variable changes such as voids could be evaluated for effectiveness by a predictive moisture-damage test system. Without an effective test system, predictability of benefits or disbenefits could not be obtained and every remedy used in a pavement could be evaluated only after the pavement was several years old.

ACKNOWLEDGMENT

The opinions and findings expressed or implied in this paper are those of the authors. They are not necessarily those of the Transportation Research Board, the National Academy of Sciences, the Federal Highway Administration, the American Association of State Highway and Transportation Officials, nor of the individual states participating in the National Cooperative Highway Research Program.

REFERENCES

1. Lottman, R. P. Predicting Moisture-Induced Damage to Asphaltic Concrete. NCHRP Project 4-8(3).
2. Schmidt, R. J., and Graf, P. E. The Effect of Water on the Resilient Modulus of Asphalt-Treated Mixes. Proc. AAPT, Vol. 41, Feb. 1972.

EFFECT OF TEMPERATURE, FREEZE-THAW, AND VARIOUS MOISTURE CONDITIONS ON THE RESILIENT MODULUS OF ASPHALT-TREATED MIXES

Robert J. Schmidt, Chevron Research Company, Richmond, California

Any material property, such as the resilient modulus (M_R), that can be used directly in the elastic layer calculation for pavement structural design should be determined under test conditions that simulate or reflect the actual conditions to be expected in the pavement. This study explored the effects of realistic variations of temperature, moisture, and freeze-thaw conditions on the M_R of a representative spectrum of asphalt-treated mixes, some of which contain lime or cement. A method is proposed that allows the M_R to be estimated at any temperature from -20 to 140 F from 2 M_R measurements. Suggestions are made on how the various findings can be used in pavement design procedures with a minimum of testing.

•THE THICKNESS required of each layer in the highway structure to limit fatigue failure or overstressing of the subbase can be estimated by using multiple elastic layer calculations if the effective elastic modulus of each layer of material is known. The resilient modulus (M_R) test gives a suitable elastic modulus for asphalt-treated materials. Any such test, however, must be determined under test conditions that simulate or reflect actual conditions. This study explored the effects of realistic variations of temperature and moisture conditions on the M_R of a representative spectrum of asphalt-treated mixes, some of which contained lime or cement.

The study considered M_R changes as the temperature varied from -20 to 140 F on both dry and water-saturated asphalt-treated mixes. Also considered were the effects of single and repeated freeze-thaw cycling on the M_R over the same temperature range. The M_R of asphalt-treated mixes in equilibrium with air at moderate and high humidities also was investigated.

SPECIMEN PREPARATION AND MEASUREMENT OF M_R

The effect of various environmental conditions on material performance can be studied most effectively with a nondestructive test that efficiently measures functional properties. These requirements are met by a diametral M_R test (1) on 4-in.-diameter, $2\frac{3}{4}$-in.-thick, asphalt-treated specimens made by a kneading compactor built to ASTM D 1561-65. These M_R measurements are made at $\frac{1}{10}$-second pulse durations repeated every 3 seconds.

Three aggregates were studied—crushed Bristol silica from Oregon; Apex calcite, which is a nearly pure limestone from Nevada; and Cache Creek gravel obtained from a pit near Sacramento, California, which was used most extensively. X-ray diffraction and emission spectrograph analysis of these aggregates are given in Tables 1 and 2. All aggregates were graded according to the I curve shown in Figure 1. This gradation was chosen because it has a high mineral surface area and because it gives specimens with voids contents that are high enough to permit both rapid water saturation and rapid drying. Both hot mixes and asphalt emulsion mixes contained 5 percent

Publication of this paper sponsored by Committee on Effects of Natural Elements and Chemicals on Bitumen-Aggregate Combinations.

Table 1. X-ray diffraction analysis of aggregates.

Aggregate	Silica (SiO_2)	Feldspar ($NaAlSi_3O_8$)	Calcite ($CaCO_3$)	Chlorite [$Mg_5Al_2Si_3O_{10}$, $(OH)_8$]	Mica [$KMg_3(Si_3AlO_{10})(OH)_2$]
Bristol silica	100				
Apex calcite limestone			100		
Cache Creek gravel	60	25		10	5

Table 2. Emission spectroscopy analysis of aggregates.

Aggregate	Component						
	SiO_2 (percent)	Al_2O_3 (percent)	Fe_2O_3 (percent)	MgO (percent)	CaO (percent)	Na_2O (percent)	K_2O (percent)
Bristol silica	98.0	0.2	<0.1	<0.6	0.8	<0.1	<0.1
Apex calcite limestone	2.0	0.6	0.2	0.9	>50.0	<0.1	0.3
Cache Creek gravel	74.0	8.0	5.0	2.0	1.0	2.0	0.8

Note: Values do not total to 100 percent because water and CO_2 are not included.

Figure 1. Gradation of aggregate.

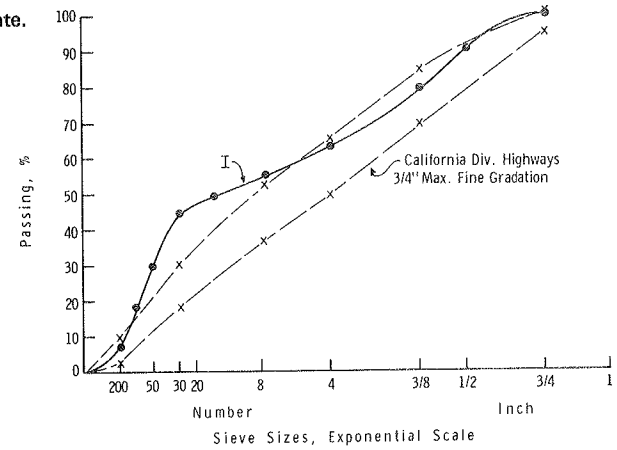

Table 3. Properties of asphalts used in tests.

Type	Boscan			Midway
	40-50	85-100	200-300	85-100
Original asphalt				
Penetration at 77 F	39	83	244	91
Viscosity at 140 F, kP	8.75	2.25	0.56	1.14
Viscosity at 275 F, cs	883	462	246	212
Glass transition temperature, deg F	-20	-27.5	-37	-17
Residue from rolling thin film oven exposure				
Penetration at 77 F	25	50	127	—
Viscosity at 140 F, kP	—	6.35	1.62	1.90
Viscosity at 275 F, cs	—	744	401	270
Residue recovered from specimens[a]				
Penetration at 77 F	24	48	108	52
Softening point temperature, deg F	149.5	131.5	115.5	132.2
Viscosity at 140 F, kP	28.2	6.1	1.7	5.2
Viscosity at 275 F, cs	1427	690	421	637

[a]Recovered from typical Cache Creek hot-mix specimens.

asphalt. Three of the asphalts used (40-50, 85-100, and 200-300 penetration grades) were made from Boscan (Venezuelan) crude oil. Also included in some tests was an 85-100 penetration grade Midway asphalt made from a California Central Valley crude oil. Boscan asphalts are low wax, high asphaltene asphalts that are not very temperature sensitive. The Midway asphalt is a low wax, low asphaltene asphalt that is highly temperature sensitive. ASTM SS-1 emulsions were made from the same 4 asphalts. Properties of these asphalts are given in Table 3.

Hot asphalt-treated mixes (ATM) containing lime (L-ATM) or cement (C-ATM) were prepared by adding the lime or type I cement as a slurry to the aggregate just before it was heated in an oven. One and three-tenths percent lime or cement was used. This amount previously was found to be effective in providing these mixes with excellent resistance to water damage (2).

All hot ATM, L-ATM, and C-ATM intended for temperature susceptibility for freeze-thaw studies were first vacuum saturated and then soaked at 73 F for 24 hours, air dried for 10 days, and finally vacuum desiccated at about 20 torr to constant weight. We followed this procedure to ensure that the lime or cement in the hot mixes had a reasonable chance to wet cure before testing and, accordingly, afford a more realistic comparison with the cement-modified asphalt emulsion-treated mixes (C-ETM). Asphalt emulsion-treated mixes (ETM) and C-ETM were allowed to air dry at 73 F and about 50 percent relative humidity (RH) until they reached constant weight (60 days).

TEMPERATURE SENSITIVITY OF M_R

Experimental Measurement

All of the dried specimens were allowed to equilibrate for approximately 24 hours in a chamber controlled at the test temperature. While they were in the temperature-controlled cabinet, their resilient moduli were determined diametrally (1). The M_R device was operated in the chamber through armholes equipped with long rubber gloves. An interior view of this device, installed in the cabinet, is shown in Figure 2. Also shown, in the lower part of the figure, is an electronic system that permits direct read-out of specimen deformation without use of recorders.

When wet or partially wet specimens were to be tested, they were kept in the chamber in double plastic bags. The specimens were removed from the bags for testing and then quickly returned to the bags. Little change in moisture content occurred during the short exposure.

Dry, Hot ATM

The M_Rs of dried, untreated ATM mixes made from Cache Creek aggregate containing 5 percent asphalt were tested over a temperature range of -20 to 140 F. As shown in Figure 3, at temperatures above 50 F the logarithm of M_R varied linearly with 1/K. This simple Arrhenius relationship also was found at these temperatures for plots of viscosity versus temperature.

The M_R of specimens made with the highly temperature-susceptible Midway asphalt, as expected, had a high temperature sensitivity. The 3 specimens made with the 3 different grades of Boscan asphalts generated parallel curves. These results, together with previous tests made on asphalts extracted from similar mixes after M_R testing (3), further illustrate the dependence of M_R on asphalt viscosity.

The resilient moduli of these mixes approached a limiting value of about 4 to 6 $\times 10^6$ psi as the temperature dropped to levels approaching the glass transition temperature (Table 3) of the asphalts used (4). Heukelom and Klomp's work (11), together with Van Draat and Sommer's modifications (12), suggests a limit of 2 to 9 $\times 10^6$ psi for wide differences in mix composition.

All of these dry mixes could be cycled from 0 to 73 F without apparent damage. No abrupt change in the M_R at any temperature was evident over the range from -20 to 140 F. That is, with dry mixes, no freeze-thaw damage was incurred.

Although the data are not given, lime- or cement-treated hot mixes were shown to have M_R versus temperature characteristics almost identical to those of untreated hot mixes. No freeze-thaw damage was evident in these treated mixes, either.

Figure 2. Resilient modulus test device.

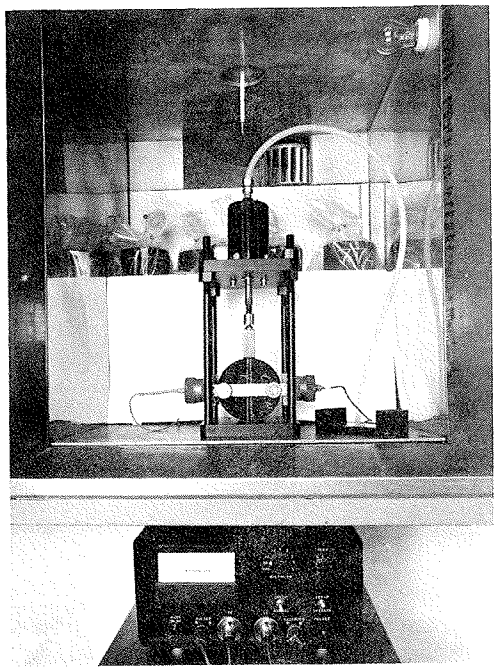

Figure 3. Temperature sensitivity of dry ATMs.

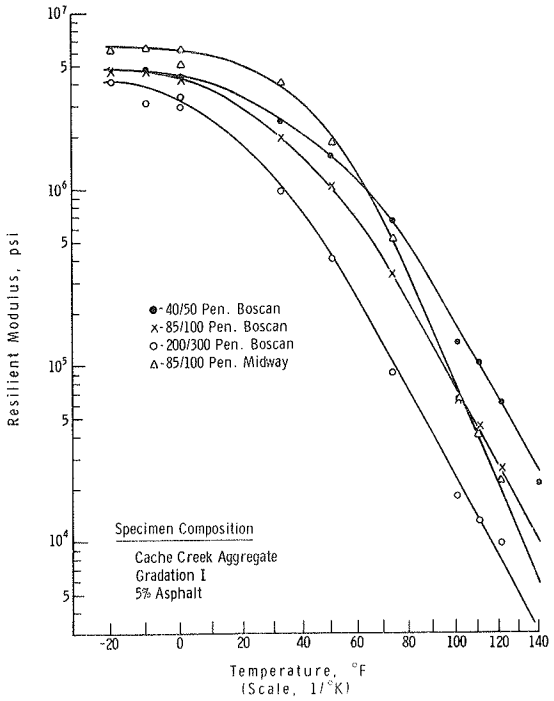

Figure 4. Comparison of temperature sensitivity of hot mix, ETM, and C-ETM.

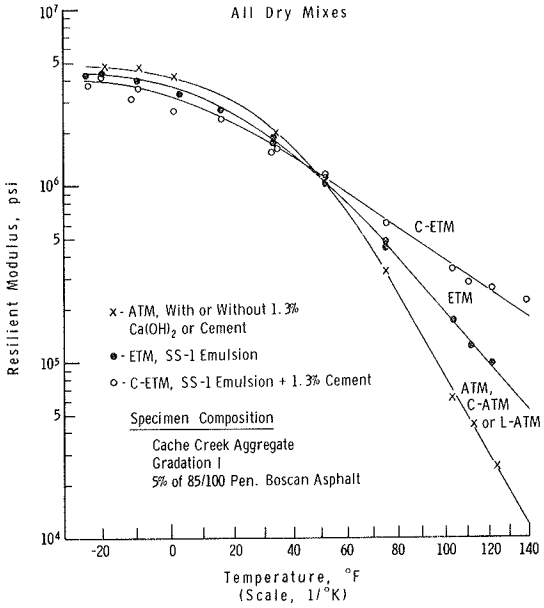

Figure 5. Freeze-thaw behavior of ATMs.

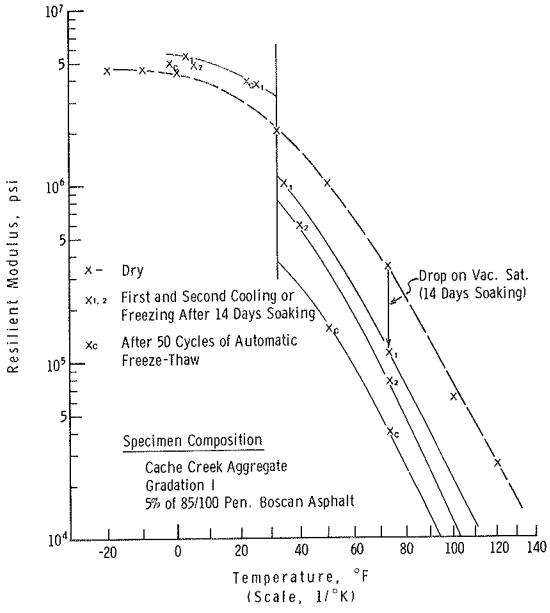

Dry ETM

An ETM made with the same aggregate and with an ASTM SS-1 asphalt emulsion containing the same 85-100 penetration Boscan asphalt had less temperature sensitivity than was found with the ATM as shown in Figure 4. The ATM made with the 85-100 penetration Boscan asphalt is also shown in Figure 4. At low temperatures, the M_R values for both mixes approached a similar limiting value of about 5×10^6 psi. However, at higher temperatures, the M_R value of this ETM was higher than that of the ATM. For example, at 140 F the ATM had an M_R value of 10,000 psi; the ETM made with the same asphalt had an M_R value of 50,000 psi. This 5 to 1 difference in M_R was obtained without an increase in the stiffness at low temperatures.

Other similar emulsion-treated mixes made with 40-50 or 200-300 penetration grade emulsified asphalt behaved in the same way except that the M_R level shifted to correspond with the hardness of asphalt used. All of the M_R values approached 5×10^6 psi as the temperature dropped below 0 F.

All of these dry ETMs could be cycled repeatedly through the freeze-thaw temperature range without apparent damage.

Dry C-ETM

A dried C-ETM (1.3 percent cement) made with the same aggregate and asphalt as the ATM and ETM discussed above is also shown in Figure 4. The C-ETM was less temperature sensitive than either ATM or ETM. The M_R values of the C-ETM at elevated temperatures were higher than those of the ETM and much higher than those of the ATM (with or without lime or cement). For example, the C-ETM had an M_R at 140 F of 250,000 psi; the ETM had an M_R of 50,000 psi.

Again, other similar C-ETMs made with 40-50 and 200-300 penetration asphalt behaved in the same way as the C-ETM made with the 85-100 penetration grade asphalt. The only apparent change was that the M_R levels were shifted by the asphalt hardness. These dry C-ETM's showed no change in M_R characteristics on repeated cycling through the freeze-thaw temperature range.

Wet ATM and Wet ETM

The response of M_R to freeze-thaw conditions, as shown in Figure 5, was quite different if the ATMs were thoroughly wet by vacuum saturation. Not only did water saturation lower the M_R at temperatures above freezing but there was also an abrupt increase in the M_R as the water in the specimen froze. The parallel nature of M_R versus temperature lines (dry and wet) indicates water soaking had not changed the temperature sensitivity of the M_R.

Below freezing, the M_R was significantly higher than it was in the dry specimen. As shown by Schmidt and Graf (3), the decrease in M_R of an ATM during water soaking is related to the length of time the saturated specimen is soaked before testing. When tested 13 days after saturation, the M_R had dropped from 346,000 to 105,000 psi. A repeat of the testing through the freeze-thaw range caused an additional drop in the M_R levels above freezing. Repeated automatic freeze-thaw cycles between 0 and 73 F reduced the M_R still further. The greatest decrease was noted above freezing. The automatic freeze-thaw sequence was 3 hours at 73 F, a 1½-hour transition to 0 F, 6 hours at 0 F, and a 1½-hour transition to 73 F.

These effects are even more clearly illustrated by the ETM behavior shown in Figure 6. Although the data for the ATM and ETM (Figs. 5 and 6) cannot be compared directly because they were soaked for different periods of time before the freeze-thaw cycles, the trends are similar. Not only was the initial drop in M_R on soaking distinct but also the added loss in M_R that resulted from each freeze-thaw cycle was clearly evident. The result of prolonged freeze-thaw cycles is also shown. The M_R drop, shown in Figure 5 for the ATM, was slightly less than is shown in Figure 6 for the ETM because the ATM was soaked for only 14 days compared to 42 days for the ETM.

Also shown in Figure 6 is the consequence of redrying the ETM. After it had been exposed to 50 freeze-thaw cycles, it had dropped to 6 percent of its original M_R. On

Figure 6. Freeze-thaw behavior of ETMs.

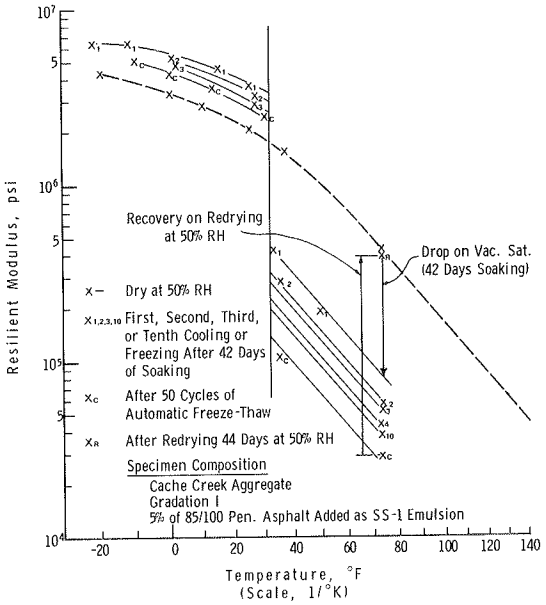

Figure 7. Freeze-thaw behavior of L-ATMs.

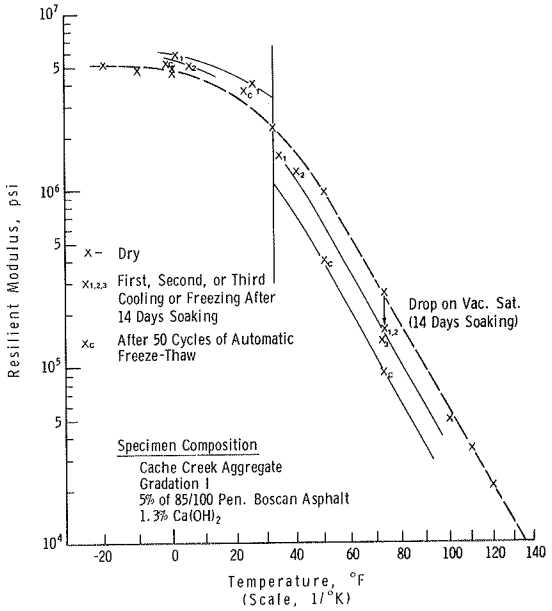

Figure 8. Freeze-thaw behavior of C-ATMs.

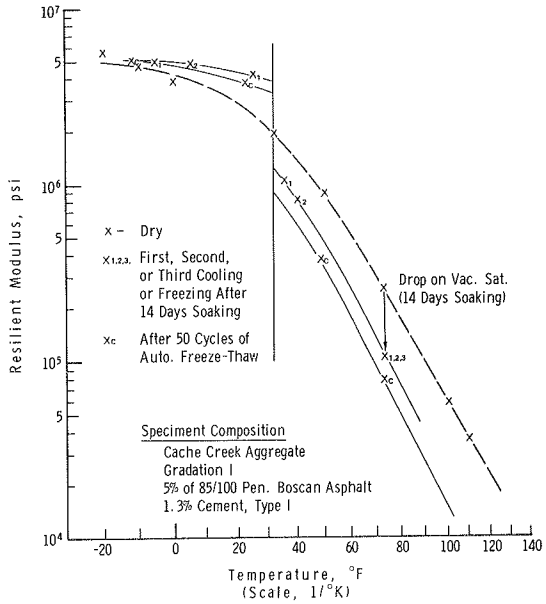

Figure 9. Freeze-thaw behavior of C-ETMs.

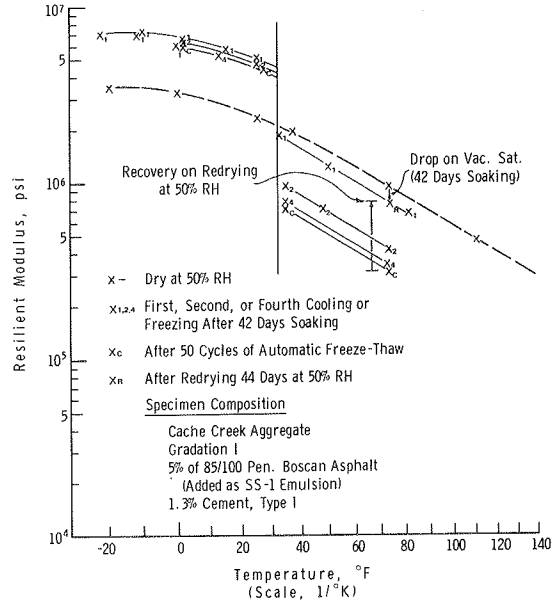

redrying at 73 F and 50 percent RH for 44 days, the specimen recovered to nearly the same M_R as was found on the original dry M_R.

The ability of ATMs to recover their strength on redrying is a most important characteristic. If it did not exist, the average life of asphalt pavements would be quite limited.

Wet Lime- or Cement-Treated Mixes

The behavior of water-saturated, hot L-ATM or C-ATM and water-saturated C-ETM is changed markedly from similar mixes not containing these modifiers. L-ATM and C-ATM as shown in Figures 7 and 8 were much less affected by 14 days of water saturation than the unmodified ATM. Subsequent repeated freeze-thaw cycles also were less damaging to these mixes than to the untreated ATM.

C-ETM as shown in Figure 9 changed only slightly on 42-day vacuum saturation. However, subsequent freeze-thaw cycles produced additional change. A comparison of Figure 9 with Figure 6 shows that the C-ETM was damaged much less than the unmodified ETM both by water saturation and by subsequent freeze-thaw cycles.

Also shown in Figure 9 is the consequence of drying the C-ETM specimen (73 F and 50 percent RH), which had been exposed to 50 cycles of freeze-thaw. This specimen recovered on redrying to 77 percent of the dry M_R value. Its actual recovered value was 730,000 psi; that of the ETM was 360,000 psi. Also, after the 50 cycles of freeze-thaw, the C-ETM only dropped to 310,000 psi compared to 29,000 for the ETM and 40,000 for ATM. Had the ATM been soaked 60 days instead of 14 days, its M_R value after freeze-thaw would have been lower.

EFFECT OF DRYING WET ATM AT DIFFERENT HUMIDITIES

Several investigators (3, 4, 5, 6, 7, 8, 9, 10) have used vacuum saturation to force water into asphalt-treated specimens. These investigators soaked or subjected the specimens to freeze-thaw cycles after saturation. These severe conditions were needed to simulate, in a short period of time, the most severe pavement deterioration likely to occur in the field.

This approach is useful principally to limit the extent of water sensitivity of acceptable materials. For example, Lottman's procedure (5, 6, 7, 8, 9, 10) reveals water-sensitive aggregates. Also, the moisture vapor sensitivity test (California Division of Highways Test Method 307-D) and the immersion compression test (ASTM D 1075-68, AASHO T 165-55) are used routinely to limit use of excessively moisture-sensitive aggregates. This section explores the extent of variation in M_R that the design engineer might expect under extreme as well as mild field conditions.

Although the exposure of water-saturated pavements to freeze-thaw cycles severely reduces the M_R, these extreme conditions seldom exist for long. Usually, intermediate moisture conditions prevail. The M_R on mixes when they are at equilibrium at about 50 percent and 95 percent RH should provide values that reflect relatively dry and near-saturated ground vapor conditions. These conditions are intermediate to the extreme dry conditions and those exposed to freeze-thaw cycles while saturated.

To investigate this, we vacuum saturated ATM specimens, soaked them for 7 days, and then air dried them at about 50 percent and 95 percent RH. We noted both the weight and M_R as they dried.

As expected, 2 specimens of a vacuum-saturated, soaked, Cache Creek, hot ATM as shown in Figure 10 lost water at 73 F and 50 percent RH at a faster rate than when they were dried at 73 F and 95 percent RH. Also, different equilibrium moisture contents (0.45 percent and 1.3 percent) were found in specimens dried under these conditions. No free water was present. If free water were present, even under an asphalt film, drying would have continued at both humidities until the free water disappeared.

As shown in Figure 11, the M_R increased more rapidly in the 50 percent RH than in the 95 percent RH. Although both specimens reached an equilibrium moisture content, the M_R of neither specimen stopped increasing. A comparison in Figure 11 of these 2 drying curves to a plot of M_R versus time of a dry ATM made with the same asphalt and aggregate suggests that at least some of the increase in M_R after moisture equilibrium

Figure 10. Equilibrium moisture content of ATM.

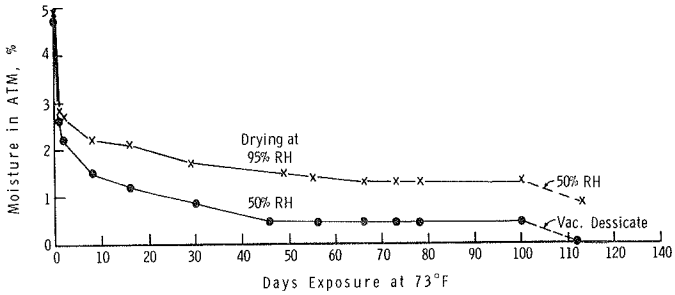

Figure 11. Level of ATM M_R.

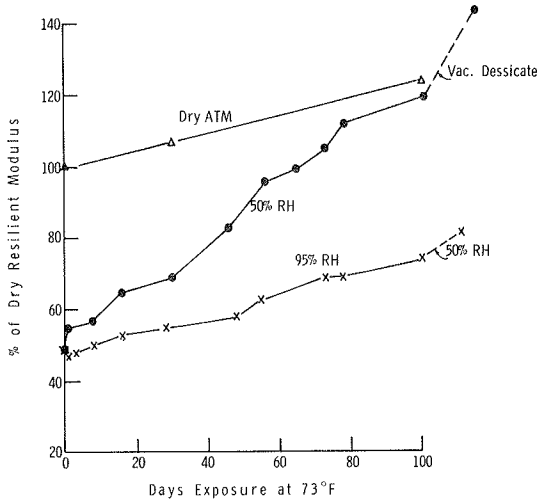

Figure 12. Effect of humidity during drying on water content and M_R of ATM.

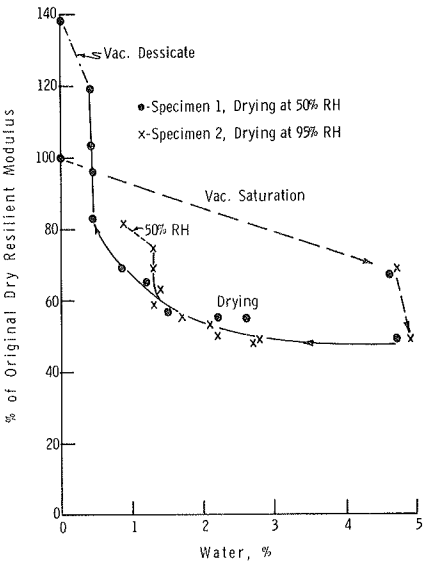

can be accounted for by the hardening of the asphalt in the specimen (that is, for the continued increase in M_R after 45 days and 65 days for the 50 percent and 95 percent RH cases).

Shown in Figure 12 are the M_R versus water content of specimens as they are first vacuum saturated and subsequently dried at 50 percent or 95 percent RH. As the specimens dried, the M_R changed very little until the moisture content dropped below about 2.5 percent, possibly until all free, unassociated, or excess water was lost. Between 2.5 percent and 1.4 percent water content, both curves are superimposed. However, at 1.3 percent the 2 curves diverge. The M_R of the specimen dried at 95 percent RH rose first and gradually continued to increase its M_R as long as it remained at 95 percent RH, whereas the specimen dried at 50 percent RH continued to dry to 0.45 percent water and gradually increased its M_R to a much higher value. A possible explanation for the divergence of these curves is that more oxidation of the asphalt took place in the specimen exposed to 95 percent RH during the longer period it took to dry to the same moisture content than did the specimen in the 50 percent RH atmosphere.

Results of similar experiments on ATM specimens made with the same gradation of Bristol silica or Apex calcite aggregates and with the same asphalt are given in Table 4. Also given are the consequences of pretreating these aggregates and the Cache Creek aggregate previously discussed. Pretreatments included 1.3 percent lime (as a slurry) or 0.1 percent solution of silane in benzene for an adhesion aid.

The general behavior of all of these aggregate systems, whether pretreated or not, was the same; they all dried more rapidly at 50 percent RH and reached a higher equilibrium moisture content at 95 percent RH than when they were dried at 50 percent RH. When the 95-percent-RH-equilibrated specimens were placed in air at 50 percent RH, they all approached the condition of the corresponding 50-percent-RH-cured specimens. All silane-treated specimens behaved very nearly the same as the untreated specimens except that, on vacuum saturation, the silane-treated silica and calcite specimens were more water resistant.

Lime treatment increased the equilibrium moisture content on all aggregate mixes about 0.2 percent to 0.3 percent. This extra residual water was likely combined chemically in the reaction product of the lime and aggregate. Also, lime-treated ATM dried at 95 percent RH attained the same or higher equilibrium M_R than it did when dried at 50 percent RH. These higher M_R values were evident even though the specimens contained about twice as much residual moisture when they were dried at the higher RH.

SIMPLIFIED METHOD FOR DEVELOPING TEMPERATURE VERSUS M_R CURVES

When the structural design (thickness of layer) is determined by the M_R value assigned to the pavement mixture, the most representative temperature under which the M_R of ATM is tested must be chosen.

M_R estimates can be made over the entire range of temperature from measurements made at 2 separate temperatures above 73 F. This greatly simplifies testing. Most conveniently, 1 measurement is made at room temperature and the other at about 100 F to 120 F. The appropriate M_Rs can then be taken from a plot constructed from these 2 points. M_R values of most ATMs at very low temperatures (below about 0 F) can be taken as about 5×10^6 psi. Between 0 and about 73 F, additional experimentally determined values should be obtained. However, a French curve laid tangentially to and touching at 73 F the line describing the M_R above 73 F and laid tangentially to and touching at 0 F a horizontal line made at 5×10^6 psi allows estimation of intermediate values. These intermediate values appear to be within a factor of 2 of the experimentally measured values. This method of estimation is certainly more convenient and possibly more accurate than the method of Heukelom and Klomp (11) as modified by Van Draat and Sommer (12).

Once the total M_R versus temperature curve is estimated, the M_R can be determined at various levels in the pavement structure in accordance with the yearly or, preferably, monthly average temperature existing at that level. These temperatures can be estimated from the climatic conditions by methods such as those of Christison and Anderson (13); Straub, Schenk, and Przybycien (14); Croney and Bulman (15); or Barber (16). The

Table 4. Drying of ATM at moderate and high humidities.

Aggregate and Treatment	Original Dry Specimen				7 Days' Soaking After Vacuum Saturation		Equilibrium After 100 Days		
	M_R (psi)		Density (pcf)						
	24 Hours at 73 F	Vacuum Dessication	24 Hours at 73 F	Vacuum Dessication	M_R (psi)	Dry M_R (percent)	M_R (psi)	Dry M_R (percent)	Water (percent)
50 Percent Relative Humidity									
Cache Creek gravel	224,000	321,000	142.2	142.0	110,000	49	267,000	119	0.44
Plus 1.3 percent $Ca(OH)_2$	199,000	308,000	142.4	142.5	157,000	79	285,000	143	0.87
Silane-treated	314,000	385,000	143.1	142.9	157,000	50	311,000	99	0.52
Bristol silica	77,000	108,000	137.7	—	71,000	92	115,000	150	0.28
Plus 1.3 percent $Ca(OH)_2$	179,000	200,000	140.1	—	204,000	113	268,000	149	0.47
Silane-treated	92,000	100,000	137.6	—	97,000	105	119,000	129	0.20
Apex calcite	342,000	302,000	143.6	—	263,000	77	389,000	114	0.36
Plus 1.3 percent $Ca(OH)_2$	275,000	388,000	146.6	—	286,000	104	410,000	148	0.55
Silane-treated	311,000	277,000	143.3	—	285,000	91	358,000	118	0.35
95 Percent Relative Humidity									
Cache Creek gravel	284,000	—	141.5	—	141,000	49	211,000	74	1.30
Plus 1.3 percent $Ca(OH)_2$	278,000	—	142.7	—	211,000	75	364,000	131	1.89
Silane-treated	323,000	—	142.0	—	152,000	47	243,000	76	1.19
Bristol silica	87,000	—	137.1	—	79,000	91	102,000	118	1.10
Plus 1.3 percent $Ca(OH)_2$	179,000	—	140.1	—	190,000	106	266,000	148	1.45
Silane-treated	104,000	—	138.0	—	98,000	94	118,000	113	1.27
Apex calcite	381,000	—	143.7	—	287,000	72	357,000	94	0.95
Plus 1.3 percent $Ca(OH)_2$	412,000	—	145.0	—	367,000	89	500,000	121	1.10
Silane-treated	386,000	—	145.0	—	306,000	79	386,000	100	0.75

Figure 13. Predicting M_R in equilibrium at 95 percent RH from M_R of 7-day vacuum-saturated ATMs.

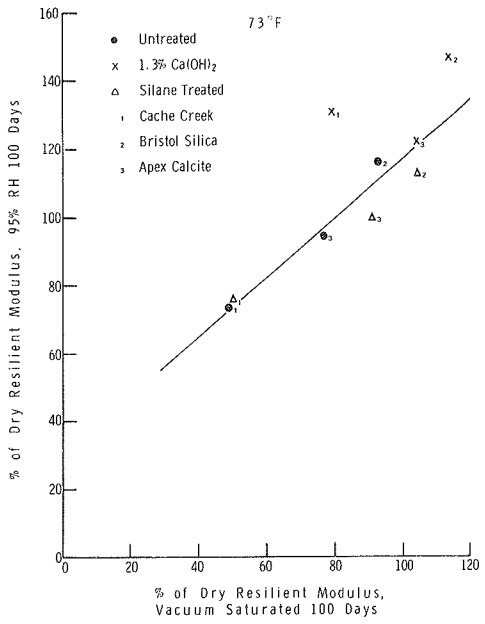

M_Rs estimated at these various levels are then used in the multilayer elastic design calculations by methods such as those described by Kasianchuk, Monismith, and Garrison (17) or by the Asphalt Institute (18).

METHOD FOR INCLUDING EFFECTS OF MOISTURE IN PAVEMENT DESIGN

Design of an efficient pavement structure depends, in part, on the use of realistic stiffness values for the composites. As seen herein, the stiffness, as measured by M_R, varies not only with temperature but also with moisture. This latter effect has been largely ignored except to the extent that material tests have been used that are designed to prevent use of those exceptionally water-sensitive materials (3, 5, 6, 7, 8, 9, 10) occasionally responsible for catastrophic pavement failures.

The extent of variation of M_R within the range of moderate moisture conditions is as significant as the effect of rather large changes in the average pavement temperature. For example, 4 percent water in an ATM made from a good aggregate can cause as much change in M_R as a 50 F change in the average pavement temperature (3). As shown earlier, the M_R of ATM drops nearly as much when in equilibrium with 95 percent RH vapor, a common condition under pavements. For example, the drop in M_R at 95 percent RH can be equal to about a 40 F rise in the average pavement temperature.

The actual drop in M_R observed at 95 percent RH on mixes made with a variety of aggregates as shown in Figure 13 was related to the M_R drop observed in the same mixes after vacuum saturation and soaking. Although this relationship was conservative for lime-treated mixes, the relationship showed that actually measuring the M_R of mixes in equilibrium at 95 percent RH is unnecessary. Measurement after vacuum saturation and soaking gave sufficient information to estimate the 95 percent RH M_R.

Also, measurement of M_R in equilibrium at 50 percent RH appears unnecessary. This value, given in Table 4, was at least as high as the original dry M_R (because of the asphalt hardening that takes place).

The total variation of M_R with field conditions can be assessed by using the following sequence:

1. Measure the M_R of the freshly made ATMs or ETMs as soon as they reach constant weight when dried at room temperature or when dessicated under vacuum;
2. Measure the M_R again after it has been vacuum saturated and allowed to stand under water at 73 F for at least 7 days; and
3. Measure the M_R after about 10 freeze-thaw cycles of 73 to 0 to 73 F. (This can be omitted when pavements are not frozen.)

If 95 percent RH is a condition similar to one prevailing in the pavement, the 95 percent RH M_R can be estimated by increasing the vacuum-saturated M_R by a factor of 1.25.

Although these tests allow the projected effective M_Rs to be estimated for the probable range of moisture conditions, there still remains to be estimated the proportion of time the projected pavement will be under each of these conditions. No such procedure is presently available so this judgment must still be made by the engineer.

CONCLUSIONS

Emulsion-treated mixes are less temperature susceptible than hot ATM made with the same asphalts and aggregates.

Cement-modified, asphalt emulsion-treated mixes have temperature susceptibilities substantially lower than ETM and greatly lower than ATM. Both improved high-temperature M_Rs are attained without an increase in the low-temperature M_R. Thus, the ETMs and, more particularly, the C-ETMs should have higher structural values at summer temperatures than do ATMs. They also should be more resistant to traffic consolidation and surface bleeding.

Dry ATM, which has been lime- or cement-pretreated, has almost the same M_R and M_R temperature susceptibility as dry, untreated ATM.

Although the M_R values of ATMs are lower when wet than when dry, the temperature susceptibilities of wet and dry ATM are nearly the same. This relationship is also true for ETMs.

No damage appears to occur on prolonged freeze-thaw cycling to dry, hot asphalt or treated or untreated asphalt emulsion-treated mixes.

Repeated cycling between a frozen and a thawed condition sharply drops the M_R of all water-saturated, hot asphalt or asphalt emulsion-treated mixes. After 50 freeze-thaw cycles, little further damage is apparent. Most of the damage occurs in the first 10 cycles. However, drying at room temperature reverses this freeze-thaw damage. Damage resulting from simple soaking after saturation is also reversible.

Damage occurring to water-saturated, cement- or lime-modified, hot ATMs as a result of freeze-thaw cycling is substantially less than that which occurs when similar unmodified ATMs are freeze-thaw cycled. Also, the damage sustained is largely reversed by drying.

Of particular importance is the greatly reduced freeze-thaw damage of water-saturated C-ETMs. Most of this damage is also temporary and is recovered after drying.

Saturated samples of ATMs made with Cache Creek, silica, or calcite aggregate dry to moisture contents in equilibrium with the humidity of the drying air. Moisture contents as high as 1.3 percent are found in equilibrium with 95 percent RH. Water contents in excess of about 2 percent exist as free or excess water. Pretreatment of either Cache Creek, silica, or calcite (pure limestone) aggregate with a silane had almost no effect on the equilibrium moisture contents. Pretreatment of these same aggregates with lime slurry increased the equilibrium moisture content but at the same time greatly increased the M_R at these equilibrium conditions.

The M_R of dry or wet mixes can be estimated from 73 to at least 140 F from a straight line constructed by plotting 2 experimentally determined points as the logarithm of M_R versus the reciprocal of the temperature in kelvins. At temperatures below 0 F, an M_R value of 5×10^6 psi for most mixes can be assumed to be without an error greater than ±50 percent.

Although they are easily determined directly by the diametral M_R device, values on dry mixes at intermediate temperatures (0 to 73 F) can be estimated by placing a smooth curve tangent to and touching the above limit at 0 F. The other end of the curve is tangent to and touching at about 73 F the line described by the logarithm of M_R versus 1/K. This method of estimation is more convenient and is possibly more accurate than other methods of estimating the M_R.

The M_R versus temperature curve on wet mixes above freezing can be estimated by drawing a curve through a measured point at room temperature parallel to the estimated dry curve. The curve below freezing intercepts the 32 F temperature at about 4×10^6 psi and extends to lower temperatures as a curve parallel to the dry curve.

M_R values determined dry, 7 days (or more, if convenient) after vacuum saturation of specimens, and, when necessary, after 10 cycles of freeze-thaw while specimens are saturated, are sufficient to give reasonable indications of the range of M_R that can be obtained in the actual pavements.

Methods still must be developed for estimating the proportion of the time the various layers of asphalt-treated mixes exist at the various moisture levels explored.

REFERENCES

1. Schmidt, R. J. A Practical Method for Measuring the Resilient Modulus of Asphalt-Treated Mixes. Highway Research Record 404, 1972, pp. 22-32.
2. Schmidt, R. J., Santucci, L. E., and Coyne, L. D. Performance Characteristics of Cement-Modified Asphalt Emulsion Mixes. Presented at Annual Meeting of AAPT, Houston, Texas, 1973.
3. Schmidt, R. J., and Graf, P. E. The Effect of Water on the Resilient Modulus of Asphalt-Treated Mixes. Proc. AAPT, Vol. 41, 1972, pp. 118-162.
4. Schmidt, R. J., and Santucci, L. E. A Practical Method for Determining the Glass Transition Temperature of Asphalts and Calculation of Their Low Temperature Viscosities. Proc. AAPT, Vol. 35, 1966, p. 61.
5. Lottman, R. P. Debonding Within Water-Saturated Asphalt Concrete Due to Cyclic Effects. Symposium on The Science of Asphalt in Construction, American Chemical Society, 1972.

6. The Moisture Mechanism That Causes Asphalt Stripping in Asphaltic Pavement Mixtures—Phase 1. First Annual Report, Eng. Exp. Station, Univ. of Idaho, Nov. 1968.
7. The Moisture Mechanism That Causes Asphalt Stripping in Asphaltic Pavement Mixtures—Phase 2. Second Annual Rept., Eng. Exp. Station, Univ. of Idaho, Dec. 1969.
8. The Moisture Mechanism That Causes Asphalt Stripping in Asphaltic Pavement Mixtures—Quarterly Progress Rept. Eng. Exp. Station, Univ. of Idaho, March 1970.
9. The Moisture Mechanism That Causes Asphalt Stripping in Asphaltic Pavement Mixtures—Quarterly Progress Rept. Eng. Exp. Station, Univ. of Idaho, June 1970.
10. The Moisture Mechanism That Causes Asphalt Stripping in Aspahltic Pavement Mixtures—Quarterly Progress Rept. Eng. Exp. Station, Univ. of Idaho, Sept. 1970.
11. Heukelom, W., and Klomp. A. J. G. Road Design and Dynamic Loading. Proc. AAPT, Vol. 33, 1964, pp. 92-115.
12. Van Draat, W. E. F., and Sommer, P. Ein Gerät zur Bestimmung der Dynamischen Elastizitätsmoduln von Asphalt. Strasse und Autobahn. Vol. 35, 1966.
13. Christison, J. T., and Anderson, K. O. The Response of Asphalt Pavements to Low Temperature Climatic Environments. Proc. Third Internat. Conf. on Structural Design of Asphalt Pavements, Vol. 1, 1972, p. 41.
14. Straub, A. L., Schenck, H. N., Jr., and Przybycien, F. E. Bituminous Pavement Temperature Related to Climate. Highway Research Record 256, 1968, pp. 53-77.
15. Croney, D., and Bulman, J. N. The Influence of Climatic Factors on the Structural Design of Flexible Pavements. Proc. Third Internat. Conf. on Structural Design of Asphalt Pavements, Vol. 1, 1972, p. 67.
16. Barber, E. S. Calculation of Maximum Pavement Temperatures From Weather Reports. Highway Research Bull. 168, 1957, pp. 1-8.
17. Kasianchuk, D. A., Monismith, C. L., and Garrison, W. A. Asphalt Concrete Pavement Design—A Subsystem to Consider the Fatigue Mode of Distress. Highway Research Record 291, 1969, pp. 159-172.
18. Full Depth Asphalt Pavements for Air Carrier Airports. In Construction Manual on Airports, The Asphalt Institute, MS-11, 1973.

QUANTITATIVE EVALUATION OF STRIPPING BY THE SURFACE REACTION TEST

Miller C. Ford, Jr., University of Arkansas;
Phillip G. Manke, Oklahoma State University; and
Charles E. O'Bannon, Arizona State University

In this study, an apparatus and a technique were developed to measure the amount of exposed surface area on asphalt-coated mineral aggregate particles after they had been subjected to the stripping effects of water. The test procedure is based on the principle that calcareous or siliciferous minerals will react with a suitable reagent and create a gas as part of the chemical reaction products. Within reasonable time limits in a sealed container, the generated gas creates a certain amount of pressure that can be considered proportional to the mineral surface area exposed to the reagent. With proper selection of reagents and reagent concentrations, asphalt, being a relatively inert substance, will not enter into the reaction and will not contribute to the created gas pressure. By using duplicate aggregate samples, one uncoated and the other asphalt-coated and partially stripped, the change in gas pressure of the respective samples can be compared to determine the amount of exposed surface area on the partially coated sample. This procedure was used to measure the amount of stripping evidenced by 11 aggregate-asphalt mixtures. The aggregates, obtained from various Oklahoma sources, included several different types of carbonate and siliceous materials. The quantitative results of the surface reaction test were compared with visual evaluations of similar mixtures that were subjected to static and dynamic immersion stripping procedures.

•MUCH of the limestone aggregate used in asphalt paving mixtures throughout the country has a tendency to polish or wear under traffic, and over a period of time the decrease in skid resistance of constructed pavements has become a serious highway performance problem. One approach to improving the skid resistance of the asphalt surfacing is to incorporate small quantities of siliceous aggregates in the mixture. The polishing tendency of these siliceous aggregates is generally much lower than that of carbonate aggregates. However, siliceous materials have been looked on with disfavor by the asphalt paving industry primarily because of their relatively poorer adherent properties with asphalt cement.

In addition to skid resistance, desirable properties of a bituminous paving mixture are stability and durability. Although several methods of mix design are available that ensure high stability, durability is more difficult to evaluate. Primarily, it is determined from field observations of in-place mixtures. One aspect of durability relates to pavement failures caused by stripping of asphalt cement from the aggregate in the mixture. Stripping occurs where there is loss of adhesion between the aggregate and the asphalt cement and is due primarily to water action. The resulting deterioration can be a serious problem causing a substantial reduction in total pavement performance.

Inherent factors that affect stripping in an asphalt paving mixture include absorption, surface texture and mineral composition of the aggregate, and chemical composition,

Publication of this paper sponsored by Committee on Effects of Natural Elements and Chemicals on Bitumen-Aggregate Combinations.

surface tension, and viscosity of the asphalt. External factors such as climate, traffic, and construction techniques also contribute to the stripping process. Thus, stripping is a complex phenomenon influenced by many variables, all of which have some effect on the adhesivity between the aggregate and binder used.

Because of the many factors that influence stripping and the various ways it can take place, a materials engineer should obtain quantitative information relative to the stripping propensities of the aggregates that will be used in the paving mixtures. Unfortunately, most stripping test procedures that are employed for this purpose yield qualitative results. Such tests force the engineer to make decisions based on less than adequate information that is primarily subjective in nature. A more objective approach to stripping measurement is needed to provide reliable quantitative information.

The purpose of this study was to develop such a test procedure whereby a relative measure of the exposed or uncoated surface area of an aggregate sample, partially stripped of its asphalt coating, could be determined. The test procedure was based on the principle that calcareous or siliciferous minerals will react with a suitable reagent and create a gas as part of the chemical reaction products. Within reasonable time limits in a sealed container, the generated gas will create a certain amount of pressure that can be considered proportional to the mineral surface area exposed to the reagent.

ADHESION AND STRIPPING THEORIES

Adhesion is defined as that physical property or molecular force by which one body sticks to another of a different nature (1). Four major theories on the cause of adhesion have been formulated and were summarized by Rice (2). These are the chemical reaction, mechanical adhesion, surface energy, and molecular orientation theories.

The chemical reaction theory states that the acidic components of the bituminous material react with basic minerals of the aggregate to form water-insoluble compounds at the interface. Because good adhesion has been reported between acidic (siliceous) aggregate and some asphalts, this theory does not hold true in all cases. Aggregate properties affecting mechanical adhesion include surface texture, absorption and porosity, surface coating and area, and particle shape. It has been observed that rough, irregular-surfaced aggregate has better retention of asphalt than smooth, glossy-surfaced aggregate. Some components of asphalt, primarily the oily constituents, enter the pores or capillaries of an aggregate particle where they are preferentially absorbed. The interlocking of the asphalt coating with these pores makes the asphalt adhere more strongly so that it is less readily stripped by water action.

The surface energy theory is related to surface tension of the asphalt and the interfacial tension between the asphalt and the aggregate. When asphalt spreads over and wets the aggregate surface, a change in energy takes place called adhesion tension (2). Adhesion tension is a surface phenomenon and depends on closeness of contact, mutual affinity of the 2 materials, and time of contact. An aggregate tends to become coated by the liquid for which it has the greatest adhesion tension. Test results indicated that the adhesion tension for water to aggregate was higher than for asphalt to aggregate in most cases (2). When molecules of asphalt come in contact with the aggregate surface they orient themselves to satisfy all energy demands of the aggregate. Water molecules are strong dipoles whereas asphalt molecules appear to possess nonpolar or weakly polar characteristics. Thus, water possesses an advantage over asphalt to rapidly satisfy energy demands of polar aggregate surfaces. However, given enough time without water, the asphalt dipoles may orient themselves to obtain good adhesion between the asphalt film and the aggregate surface.

Stripping, in which water, through some mechanism, causes the bond between aggregate and asphalt to be diminished, is the reverse of adhesion. Several mechanisms of stripping have been advanced. These mechanisms, summarized by Majidzadeh and Sanders (3), include detachment, displacement, film rupture, and pore pressure. Detachment results when the asphalt cement, with no obvious break in the continuity of the coating, is separated from the aggregate surface by a thin film of water. Displacement occurs where there is a discontinuity or break in the asphalt coating and the aggregate, asphalt, and free water are all in contact.

Film rupture may occur when adhesion of the asphalt cement is not uniform over the entire aggregate surface and the action of traffic causes the coating to break or rupture at points of weakest bond. When ruptured, the asphalt film takes the form of lowest potential energy by retracting to spherical globules. Pore pressure may cause hydraulic scouring to take place in a saturated pavement where the impact of a tire presses water into the pavement surface in front of it and then as the tire leaves the spot the water is sucked out. This water movement facilitates stripping the coated aggregate, and any dust or particulate matter mixed with the surface water assists by abrading the asphalt films.

It is obvious from the foregoing discussion that no single, simple explanation of the stripping process will suffice for all cases. Each of the mechanisms, individually or in combination, may be operating in a given instance of stripping.

STRIPPING TESTS

Stripping tests may be divided into 2 groups, depending on the type of bituminous mixture. The first group, related to appraising materials for layered systems of construction, comprises tests on uncompacted single-size aggregate particles coated with asphalt. The second group includes tests on compacted samples or specimens of a bituminous mixture, which represent a hot-mix, hot-laid, or road-mix type of paving material.

Coated-Aggregate Tests

Tests devised for layered system materials have a common procedure. The aggregate to be evaluated is usually 1 size; commonly, it passes a $\frac{3}{8}$-in. sieve and is retained on a $\frac{1}{4}$-in. or No. 4 sieve. The aggregate is coated with the asphalt material, subjected to the effects of distilled water, and then evaluated to ascertain the percentage of asphalt coating still adhering to the aggregate.

Various methods of subjecting the coated aggregate to the effects of water such as dynamic immersion, static immersion, and boil or chemical immersion techniques are used in these tests (4). The amount of stripping is determined by visually estimating the percentage of the total area that remains coated with asphalt. ASTM D 1664 specifies evaluation by visual examination, and the estimate is reported as either above or below the 95-percent-coated level (5).

In the past, considerable research effort has been expended to develop a more quantitative method to measure the amount of stripping that occurs (4). These procedures have used radioactive isotope tracers, lithium tracer-salt, dye adsorption, and leaching. Generally, these tests measured a change in some property of the coated aggregate material after stripping occurred. None of these tests has been widely accepted.

Compacted Mixture Tests

Tests on compacted mixtures measure change in a physical property of the mix that is caused by the effects of water. This change in physical property is then related to stripping effects of water on the bituminous mixture. Several test methods that have been developed include immersion-compression tests, laboratory test tracks, vertical swell tests, abrasion weight-loss tests, and sonic vibration tests (4). Although all of these tests have their merits, the immersion-compression test has been the only one standardized by ASTM (6).

The following are some advantages attributed to tests of compacted bituminous mixtures over stripping tests of coated aggregate particles:

1. Test results are in quantitative terms (that is, some change in a physical property of the mixture is measured),
2. Compacted test specimens represent the actual bituminous mixture that will be used in highway construction, and
3. Laboratory specimens are subjected to water action in a coherent mass, which more nearly simulates actual field conditions (7).

These advantages are offset somewhat by the necessity for more elaborate test equipment and by lengthy and laborious test procedures.

TEST DEVELOPMENT

Despite the large number of tests already devised to study the effects of water on coated aggregate particles and compacted mixtures, an examination of the technical literature revealed continuing research in this area (4). Presently, there is no "standard" test to directly evaluate in a quantitative manner the amount of stripping that occurs when asphalt-coated aggregates are subjected to the detrimental action of water. There appears to be a definite need for such a test.

Existing tests were either too complex for routine testing or had questionable accuracy because results were based on the operator's visual judgment. The general procedure proposed for this study was to obtain a measure of the surface area of an uncoated aggregate sample and then, by using a similar asphalt-coated sample, to obtain a measure of the surface area stripped after exposure to water action. The ratio of these measured quantities, that is, the stripped value divided by the uncoated value, was considered a quantitative criterion of the amount of stripping that occurred.

If an aggregate sample is contacted with a suitable reagent, the resulting chemical reaction between the acid and the exposed surface minerals of the aggregate will liberate a gas as well as a certain amount of heat. For example, when hydrochloric acid (HCl) is added to limestone, which is predominantly calcium carbonate ($CaCO_3$), the following reaction occurs:

$$CaCO_3 + 2HCl \rightarrow CaCl_2 + H_2O + CO_2 \uparrow + \text{heat}$$

If hydrofluoric acid (HF) is added to a predominantly siliceous aggregate, one that is predominantly silicon dioxide (SiO_2), a similar type of reaction occurs:

$$SiO_2 + 4HF \rightarrow 2H_2O + SiF_4 \uparrow + \text{heat}$$

It was reasoned that the amount of these reaction products should be proportional to the exposed aggregate surface area. If the reaction is confined, the generated gas creates a certain amount of pressure that is easily measured and can be used as a determinant for surface area. With proper selection of reagents and reagent concentrations, asphalt, because it is a relatively inert substance, will not enter into the reaction and will not contribute to the created gas pressure.

Reagents

Hydrochloric and hydrofluoric acids were found to be suitable for this investigation. A suitable reagent was considered to be one that, when placed in contact with an aggregate surface, would react to create a measurable gas pressure and would not react with asphalt cement. Reagent strength or concentration such that the chemical reaction would not deeply etch the aggregate surface was desired.

There was concern that a strong reagent, with sufficient time to react, would not only dissolve the exposed surface molecules of the aggregate, but also would continue to react and undermine adjacent asphalt-coated areas of the aggregate surfaces. If this occurred, the resultant increase in gas pressure would cause considerable error in determining the exposed aggregate surface area. This problem was minimized by using the weakest reagent solution that would create a measurable change in gas pressure. This change in pressure in a minimum amount of time was measured.

Preliminary laboratory work indicated that $CaCO_3$ in limestone would react in the desired manner when about 1.0 normal HCl was used. A 100-g sample of aggregate, when reacted with 200 ml of 1.0 normal HCl acid solution, created between 4 and 10 psi of gas pressure. The acid solution was depleted in about 10 min of reaction time at normal laboratory temperature.

For aggregate composed mainly of SiO_2, about 23.0 normal HF was required to obtain the desired reaction and a measurable gas pressure. This reaction creates

silicon tetrafluoride gas (SiF_4). Both the acid fumes and SiF_4 gas are highly toxic, so all work with the hydrofluoric acid was carried out in a well-ventilated fume hood with appropriate safety equipment.

Mixed composition aggregates are those containing appreciable amounts of both $CaCO_3$ and SiO_2 as well as other constituents. Preliminary work indicated that a mixture of HF and HCl would create a measurable gas pressure when reacted with aggregate of mixed composition. A 200-ml acid solution used with this type of aggregate was composed of 27 ml concentrated HF, 54 ml concentrated HCl, and 119 ml of distilled water.

Equipment

The proposed method of testing required the measurement of the gas pressure generated during a chemical reaction. Because the temperature of the reaction affects the volume of the gas, it was necessary to measure and record simultaneously the pressure and temperature generated during the reaction. The apparatus developed to contain the reaction and measure the reaction products was essentially a modified 6-quart stainless steel pressure cooker equipped with suitable instrumentation to monitor and record the desired quantities evolved.

A dual-arm recorder was used to record both temperature and pressure in the pressure container. A pressure transducer with a range of 0 to 30 psig and a thermistor (linked to a scanning telethermometer) were mounted on the lid of the container and connected to the recorder (Fig. 1). With this equipment, pressure in the container could be determined to the nearest 0.025 psig and temperature to the nearest 0.5 C. This sophisticated instrumentation for measuring and recording the pressure and temperature was not absolutely necessary. A simple manometer or pressure gauge and a thermometer, suitably graduated, could be used and observers could record the values at stipulated time intervals.

The pressure transducer was centrally mounted on the removable top of the pressure vessel. The temperature probe cavity extended through the top about 1 in. and was just large enough in diameter to contain the thermistor. A stainless steel pressure release valve also was mounted on the top. This valve was used in calibration of the pressure transducer and to release the pressure in the vessel at the completion of the test. Details of the pressure container are shown in Figure 2.

Because the pressure vessel was to be operated as a closed system, it was necessary to provide a means of adding the acid to the aggregate without changing the ambient pressure. A 250-ml stainless steel beaker was attached by a threaded joint to a rod extending through the body of the pressure vessel. The rod opening was sealed by using neoprene O-rings both inside and outside the wall of the pressure vessel. A handle was attached to the exterior end of the shaft. To inundate the aggregate specimen the beaker was positioned upright and filled with 200 ml of the acid solution, and the handle was turned until the contents of the beaker were poured into the plastic container holding the aggregate sample.

Because of the corrosive nature of the reagents being used, stainless steel was used for all the component parts of the pressure apparatus exposed to the acid solutions and gases generated during the tests. To reduce contact between the acid solutions and the pressure vessel, a small polyethylene container was placed inside the vessel to hold the aggregate-acid mixture during the reaction period. The size of this container was such that a 100-g aggregate sample would be completely inundated by the 200-ml acid solution.

INVESTIGATIVE PROCEDURES

To compare the surface reaction procedure with other methods of evaluating stripping, we conducted a series of stripping tests by using carbonate and siliceous aggregates from various Oklahoma sources. Static immersion and dynamic immersion stripping tests were performed and the results collated with those obtained from the surface reactions test.

Materials

The asphalt cement used in this study (penetration grade 85-100) was chosen because it is a common binder used in asphalt pavement construction in Oklahoma. Selection of the mineral aggregates was based on a research study conducted by the Oklahoma Department of Highways (8). This study indicated that the incorporation of small quantities of polish-resistant siliceous aggregates would improve the skid resistance properties of their standard paving mixtures. Eleven different sources were sampled and the aggregates included 3 types of limestone, 3 types of sandstone, 1 chert, and 4 types of gravel. These aggregates were named for the town adjacent to the source location. They are identified for insoluble residue, specific gravity and absorption, geologic unit and age (period), and general aggregate classification in Table 1.

Sample Preparation

We sieved the material from each of the respective sources to obtain approximately 2000 g of aggregate passing the $\frac{3}{8}$-in. sieve and retained on the $\frac{1}{4}$-in. sieve. We then washed, oven-dried, and quartered the aggregate to obtain representative samples of approximately 100 g each. The dry aggregate was weighed (100.0 ± 0.2 g) and placed in large aluminum moisture boxes for storage until required in testing. Ten samples of each of the various aggregates were prepared in this manner. Six of these samples, i.e., duplicate samples, were used in performing the static immersion and dynamic immersion stripping tests and the surface reaction test. The remaining samples were used for specific gravity and absorption tests and for checks on results of the other stripping tests.

Samples for the static immersion and dynamic immersion tests were coated in the following manner. The aggregate and asphalt cement were heated to 120 C before coating. To each of the 100-g samples of aggregate, 6 g of asphalt was added. The mixture was stirred and manipulated with a spatula until each rock was coated with asphalt. A hot plate was used to heat the mixture, as required to achieve 100 percent coating. About 3 min of hand-mixing time ordinarily was required. The individual particles of asphalt-coated rock were placed in a pan of cold distilled water after mixing. Cold water prevented the coated rocks from sticking together. This sample preparation and coating procedure is in accordance with ASTM D 1664 (5).

Static Immersion Stripping Test

After cooling in the chilled water, the coated sample was placed in a glass jar and covered with 600 ml of distilled water. The jar was capped and placed, partially submerged, in a 25 C water bath and left undisturbed for 18 hours. The amount of stripping was then visually estimated by using the ASTM standard procedure. To facilitate this evaluation, a comparison chart was prepared. This chart was made by tracing the outline of typical aggregate particles inside a circle the same diameter as the glass jar in which the samples were immersed. A series of these tracings were made and the cross-sectional areas of the aggregate particles in each were darkened to represent different amounts of coated surface (ranging from 50 to 100 percent coated).

The chart was placed flat on the table adjacent to the jar sample to be evaluated. The top was removed from the jar, and any film of asphalt on the surface of the water was removed by skimming with a paper towel. The chart was moved until, by visual observation of the sample from above and through the water, the sample matched 1 of the covered or darkened areas of the comparison chart. It was difficult to estimate the area covered with asphalt any closer than to the nearest 5 percent. Therefore, duplicate test results were averaged and then rounded to the nearest 5 percent.

No stripping of any of the various aggregates was observed when they were coated with asphalt cement and subjected to the static immersion stripping (SIS) test at 25 C. With a longer period of immersion or higher immersion temperatures, we anticipated that some stripping of the aggregates would occur. Therefore, the SIS (25 C) samples were then placed in a 60 C water bath and left undisturbed for 18 hours. The amount of stripping (which was considerable) was then visually estimated by using the comparison chart as before.

Figure 1. Surface reaction test equipment.

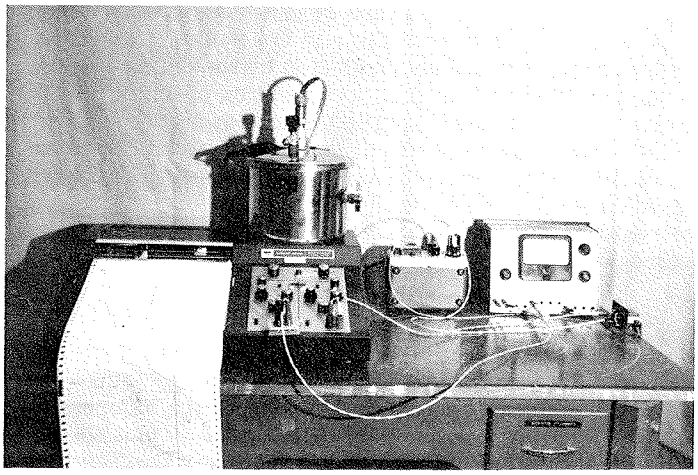

Figure 2. Details of pressure container device.

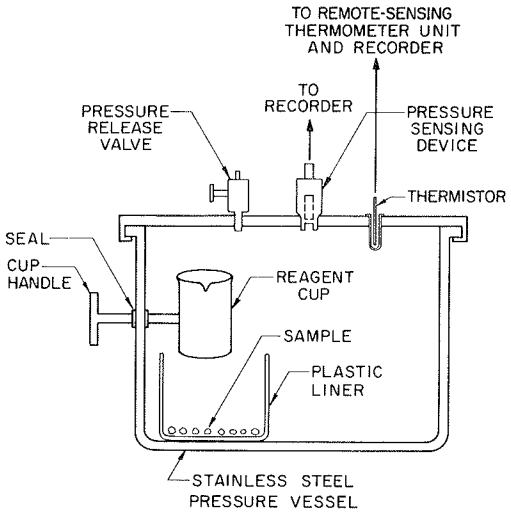

Table 1. Aggregate identification and properties.

Sample	Insoluble Residue (percent)	Bulk Specific Gravity	Absorption	Geologic Unit and Period	General Classification
Cooperton	1.2	2.67	0.8	Kindblade limestone, Ordovician	Limestone
Hartshorne	23.3	2.66	1.0	Wapanucka limestone, Pennsylvanian	Limestone (partly siliceous)
Stringtown	72.8	2.57	0.5	Wapanucka limestone, Pennsylvanian	Siliceous limestone
Cyril	59.2	2.64	0.9	Rush Springs, Permian	Calcareous sandstone
Keota	96.3	2.48	2.4	Bluejacket, Pennsylvanian	Siliceous sandstone
Onapa	92.1	2.47	4.1	Bluejacket, Pennsylvanian	Siliceous sandstone
Asher	99.8	2.46	3.2	Wellington-Admire, Permian	Chert gravel
Broken Bow	98.3	2.69	1.3	Alluvial Deposit, Quaternary	Siliceous gravel
Gore	97.9	2.68	0.6	Alluvial Deposit, Quaternary	Siliceous gravel
Hugo	99.0	2.52	1.8	Terrace Deposit, Quaternary	Chert gravel
Miami	95.4	2.56	1.2	Boone, Mississippian	Chert

Dynamic Immersion Stripping Test

To accelerate the stripping action of water on coated aggregate we constructed a dynamic stripping device. A literature review showed many previous investigators had used a dynamic immersion stripping (DIS) test to evaluate the effects of water on asphalt-coated aggregate. The method originally used by Nicholson (1) was followed in this study. Aggregate was coated with asphalt cement as in the SIS test and subjected to 4 hours of water agitation. A visual estimate of the amount of stripping was made at the end of 1, 2, and 4 hours. An apparatus was designed and built to hold 6 glass jars of approximately 1 quart capacity. The device was rotated about a horizontal axis at about 40 rpm. This caused the coated aggregate sample to fall from one end of the jar through the water to the other end during each revolution.

Preliminary tests using the DIS device revealed that the nonstripping aggregate (Cooperton limestone) would partially strip when the sample was tumbled continuously for 4 hours. The siliceous aggregate particles also retained more than 50 percent of their coating at the end of 4 hours of tumbling. Therefore, a 4-hour DIS test period was chosen, with the temperature maintained at about 20 C, which was the normal laboratory temperature.

The DIS test was intended to induce stripping by subjecting each aggregate sample to the same amount of agitation in a water medium, and then to compare the visually estimated retained coating with a measured amount as determined by the surface reaction test.

Surface Reaction Test

Half of the aggregate samples used in the surface reaction test (SRT) previously had been coated with asphalt cement and partially stripped in the DIS test. An uncoated duplicate sample of the aggregate was immersed in distilled water at the same time as the DIS specimen was immersed. At the end of the DIS test, the partially stripped and uncoated samples were dried by blotting with paper towels and spread out in pans to air dry for approximately 24 hours before the SRT.

We wanted to perform this test on oven-dried materials but when the partially stripped aggregate samples were oven dried at 100 C, the remaining asphalt cement diffused and completely recoated the stripped aggregate surfaces, so oven drying was eliminated and the samples were simply air dried before testing.

Each test required 200 ml of acid solution. Because duplicate samples (2 uncoated and 2 partially coated samples of each of the various aggregates) were tested, a litre of acid solution was prepared for each series of aggregate samples. The acid test solutions were prepared by using reagent grade acids and deaired distilled water. All proportions of these acid solutions were calculated on a weight basis.

The 200 ml of acid solution to be used in each test was measured with a graduated cylinder and placed in a 250-ml Nalgene jar. The weight of acid solution in each jar was determined and its density, in g/ml, was calculated. This density and weight determination was used as a check to obtain equal strengths of solution for each test. The balance of the litre of solution originally prepared was retained for titrations. The actual normality of the acid was determined by titration against a known weight of sodium carbonate by using methyl orange as an indicator (9). All work with the acid solutions containing HF was carried out with polyethylene or polystyrene containers.

Procedure—Before initiating a test, samples to be tested, acid solutions, and the pressure container were placed in a fume hood and brought to a constant temperature of 20 C. The recording equipment was placed adjacent to the fume hood. This test procedure was used.

1. The pressure release valve was opened and the lid of the pressure vessel removed.
2. The sample to be tested was placed in the plastic container and the container was positioned inside the pressure vessel.
3. The beaker was installed in the pressure vessel, leveled, and 200 ml of acid solution was poured into the beaker.

4. The lid was placed on the pressure vessel, the pressure recording pen was set to zero, and the chart drive of the recorder was started.
5. The pressure release valve was closed and the exterior handle turned to pour the acid from the beaker. A stopwatch was started at the instant the acid was poured onto the aggregate sample.
6. The reaction was monitored by observing the pressure and temperature traces on the recorder.
7. At the completion of the test, which ordinarily lasted 5 min, the pressure release valve was opened and the recorder chart drive stopped.
8. After the pressure was released, the top of the pressure vessel was removed and the acid beaker taken out. The sample was removed and the reaction of the acid solution and sample was terminated. For samples tested with HCl this was accomplished by flooding the mixture with tap water. For samples tested with HF the reaction was stopped by slowly adding a sufficient amount of calcium oxide slurry to deplete the HF in the mixture. Methyl orange indicator was used to determine when the solution was neutralized.
9. The acid beaker and plastic sample container were then washed and dried before starting another test.

Stripping Calculation—The pressure-temperature curves plotted on the recorder chart were analyzed. A horizontal line was drawn on the chart paper for each 15 sec of elapsed reaction time. The pressure and temperature readings were scaled from the chart paper and tabulated. Pressures were adjusted to 20 C for comparative stripping calculations. This adjustment of pressures was necessary because of the slightly different operating temperatures and the higher temperatures created by some of the reactions.

The surface area exposed was considered proportional to the change in pressure over a certain time interval. For limestone aggregates and aggregates of mixed composition, the change in pressure from 0.25 to 1.5 min of reaction time was used. The reaction between the siliceous aggregates and the HF solution was slower or less violent and required a longer reaction time (0.25 to 5.0 min) to obtain a significant pressure difference. The effect of inertia on the pressure transducer operation and the recorder chart pen response were the primary reasons for using the initial gas pressure value at 0.25 min of reaction time. The reaction time for the final pressure value was that required to obtain a measurable pressure without deeply etching the exposed aggregate surfaces.

A drawing typical of the strip-chart recorder tracing of the pressures obtained for an uncoated limestone aggregate sample and a partially coated limestone aggregate sample is shown in Figure 3. The initial pressure reading, taken at 15 sec of reaction time, is shown as P_1; the final pressure reading, taken at 90 sec of reaction time, is shown as P_2. The retained coating of asphalt was calculated as follows:

$$RC = 100 - \left(\frac{\Delta P_s}{\Delta P_u}\right) 100$$

where

RC = percent retained coating of stripped sample,
$\Delta P_s = P_{2_s} - P_{1_s}$ = change in pressure for stripped sample, and
$\Delta P_u = P_{2_u} - P_{1_u}$ = change in pressure for uncoated sample.

Relation Between Surface Area and Change in Gas Pressure—The hypothesis that generated gas pressure is proportional to exposed surface area was examined by using small disks cut from samples of the Cooperton limestone material. Large pieces of rock, weighing from 2 to 5 kg, were obtained at the quarry where this aggregate is produced. With a concrete saw, these rocks were sawed into slabs ranging from 5 to 10 mm in thickness. A diamond core drill with an inside diameter of 19.0 mm was used to cut uniform diameter disks from these slabs of limestone rock. Each disk was numbered and its average thickness determined by using a micrometer dial gauge. The

surface area of each disk was calculated and the disks were then divided into five different surface area groups. These groups had approximate surface areas of 6 000, 12 000, 18 000, 24 000, and 30 000 mm^2. Duplicate groups of approximately the same surface area also were prepared. Each group of disks was reacted with a HCl solution by using the test procedure previously outlined, and the resulting gas pressures were determined. A graph of the surface area of each disk sample with the corresponding increase in gas pressure for a reaction time of from 15 to 90 sec is shown in Figure 4.

Each plotted point on the figure is the average value for duplicate disk samples. A good linear relationship between disk surface area and change in gas pressure is noted. The increase in gas pressure was approximately 0.059 psi (0.041 g/mm^2) for each 1 000 mm^2 of disk surface area. Verification tests on other aggregates used in this study have not been completed, but a similar relationship of surface area to gas pressure increase is anticipated.

DISCUSSION OF RESULTS

The results of the various stripping tests on each of the respective aggregates are given in Table 2. Each of the tabulated values of the percent of retained coating is the average of the values obtained from duplicate test samples.

None of the aggregates exhibited any stripping when tested according to standard ASTM procedure at 25 C. When the SIS test was made more rigorous by increasing the immersion temperature to 60 C, considerable stripping was evidenced. The visually estimated retained coatings ranged from 95 percent for the Hugo chert gravel to 40 percent for the Gore siliceous gravel.

According to ASTM D 1664 (5), the static immersion stripping results at 25 C are reported as above or below the 95 percent retained coating level. On this basis, each of the 11 aggregates would be rated as having a retained coating above 95 percent. The limitation of this test method is that it does not provide for evaluation below this level. The limitation results from the poor reproducibility obtained when rating the same sample by visual observation. It would appear that little or no useful information regarding the relative stripping tendencies of various aggregates could be obtained from visual evaluation in accordance with the ASTM method.

The DIS test results are reported for the various periods of tumbling used in the investigation. At the end of 1 hour, all of the aggregate samples retained 90 percent or more of their original asphalt coating and, at the end of 2 hours, most of the samples had greater than 85 percent retained coating. After 4 hours of tumbling the estimated retained coatings ranged from 85 percent for the Cooperton limestone, Keota sandstone, and Onapa sandstone to 65 percent for the Gore siliceous gravel.

A comparison of the retained coating percentages of each aggregate for the SIS test at 60 C and the 4-hour DIS test shows little correlation. Mathews, Colwill, and Yuce (10) also reported little correlation of test results from SIS and DIS tests performed on 16 different types of aggregates.

It should be repeated that, in the SRT, both uncoated and partially coated or stripped samples of each aggregate were tested. The partially coated samples were those resulting from the 4-hour DIS test. The change in gas pressure (over the selected time interval) exhibited by duplicate coated and uncoated test samples agreed closely. In most cases, these corresponding differential pressure (ΔP) test values differed by less than 0.014 g/mm^2. The average ΔP values for the coated and uncoated samples of a given aggregate were used to calculate the percentage of asphalt cement coating retained, as has been previously discussed. The SRT retained coating percentage for each aggregate is given in Table 2.

The measured retained coatings varied from 93 to 54 percent. The limestone aggregates (Cooperton, Hartshorne, and Stringtown) with 89 percent retained coating had the highest group average. The sandstone aggregates (Cyril, Keota, and Onapa) averaged 63 percent; the gravels (Asher, Broken Bow, Gore, and Hugo) averaged 68 percent.

These results show the same trend of resistance to stripping as was obtained from a series of immersion-compression tests on compacted mixtures containing the same aggregates. These tests were performed on compacted specimens of a standard

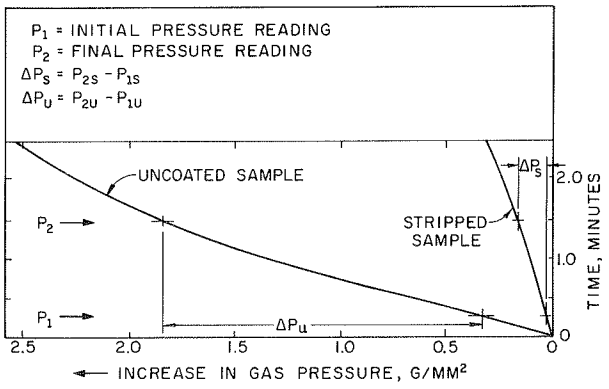

Figure 3. Typical SRT pressure-time curves for limestone aggregate.

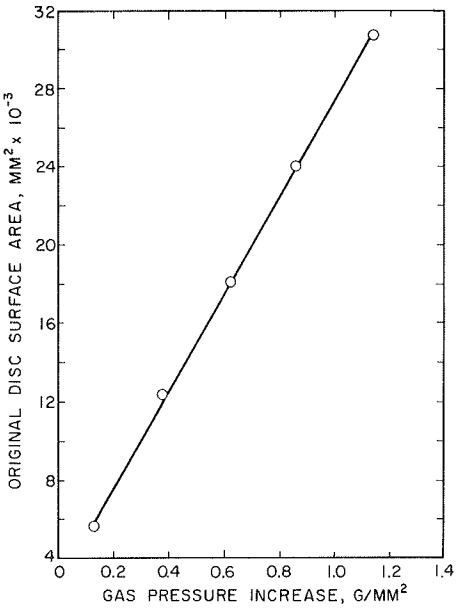

Figure 4. Original disk surface area versus gas pressure increase, Cooperton limestone.

Table 2. Results of SIS and DIS tests and SRT.

	Static Immersion Retained Coating (percent)		Dynamic Immersion Retained Coating (percent)			Surface Reaction Retained Coating	
Aggregate	77 F	140 F	1 Hour	2 Hours	4 Hours	Percent	Variation (percent)[a]
Cooperton	100	85	95	90	85	90	±0.5
Hartshorne	100	75	95	90	75	85	±0.5
Stringtown	100	65	95	90	85	93	±0.7
Cyril	100	60	90	80	75	64	±0.7
Keota	100	50	95	90	80	56	±0.0
Onapa	100	50	95	90	85	68	±0.8
Asher	100	90	95	90	80	74	±3.4
Broken Bow	100	90	95	90	70	54	±3.6
Gore	100	40	90	85	65	65	±2.2
Hugo	100	95	95	90	80	78	±0.5
Miami	100	70	95	85	75	60	±3.5

[a]Variation based on maximum and minimum values of duplicate tests.

Oklahoma Department of Highways surface course mixture in which these aggregates comprised the coarse aggregate fraction. The retained strength values from these immersion-compression tests also indicated that the limestones were better than the gravels, which were in turn better than the sandstones.

A measure of the reproducibility achieved with the SRT was obtained by using the results of the 4 tests performed on each type of aggregate. The smallest and largest of the individual ΔP values from each SRT series were used to calculate a maximum and minimum percent of retained coating. The difference between these maximum and minimum values is given in Table 2 as the variation in retained coating for each aggregate. A variation of less than 1 percent is noted for 7 of the aggregates, with the largest variation being only 3.6 percent (Broken Bow gravel).

There was low correlation between visually estimated retained coatings of the DIS tested samples and the SRT measured values for the same samples. This emphasizes some of the problems associated with the visual estimation procedure. Several factors affect the visual estimation of the amount of retained asphalt coating on the aggregate including color of the aggregate, visual perception limited to the plan or 2-dimensional view, undetectable microscopic breaks in the asphalt in a state of "detachment," and operator error or bias.

The color of the aggregate influences the operator's estimation of coating, with lighter colored aggregates being rated lower than darker colored aggregates when both may have the same amount of asphalt-coated surface. This is due to the greater contrast between the black asphalt cement coating and the light-colored aggregate, which causes the operator to assign a lower value of retained coating to the lighter colored material.

This color factor may be the reason that the light-colored Cooperton and Hartshorne limestones were visually rated about 5 to 10 percent lower than the SRT results indicated. Conversely, the dark-colored Keota and Onapa sandstones were visually rated about 20 percent higher in retained coating than the SRT results indicated.

The standard method of visual estimation considers only the exposed aggregate surfaces that appear in plan view and assumes that the stripping evident in a 2-dimensional scene is representative of that throughout the sample. This assumption may or may not be valid and depends, to a large extent, on the shape and orientation of the aggregate particles. In the SRT, however, the acid solution reacts with all exposed surfaces, and the results are indicative of the total aggregate surface area that has been stripped of its asphalt coating.

By unaided visual examination of stripped aggregate particles there appeared to be no disturbance in the asphalt surface where the coating remained in place. However, under a 30-power microscope, numerous pinholes or small breaks in the asphalt coating could be seen. After the SRT, there was evidence of etching or surface reaction at these small discontinuities.

Perhaps the most important factor in the visual estimation method is the operator. Repeatability of visual estimates of the aggregate surface area coating was examined by Brown, Sparks, and Marsh (11). In this work, 4 experienced operators were used to evaluate 36 different test samples of partially coated aggregates. Their average range in estimated retained coatings was 16 percent; their differences varied from 2 to 32 percent. Roediger (12) reported the results of a cooperative stripping test visual estimation project in which 10 laboratories estimated the amount of stripping evidenced by 22 different samples. Their visual estimates of percent of retained coating for the same test specimen ranged from 4 to 44 percent, with an average difference between laboratories of 24 percent. Different operators were noted to agree more closely when the amount of stripping was small.

All of these visual factors were eliminated when stripping was evaluated by SRT. The SRT results in a more precise and quantitative determination of exposed surface area. A high degree of reproducibility can be expected because the results of replicate surface reaction tests indicate less than 4 percent variation. Because the results are measurable rather than estimated quantities, they are more indicative of the relative stripping tendencies of various asphalt-aggregate mixtures and better correlation of these laboratory values with field performance of the materials should be possible.

CONCLUSIONS

The SRT provides a quantitative measure of total exposed surface area on a stripped mineral aggregate sample and eliminates the problems associated with visual estimation techniques.

The results of the SRT are reproducible with a minimum amount of variation between duplicate test sample values.

The SRT is simple and straightforward and usually can be performed in less than 10 min. The required equipment is neither expensive nor complicated.

The use of highly corrosive and toxic reagents is a disadvantage of this procedure. However, with proper laboratory equipment and safety precautions this drawback can be minimized.

With proper verification methods, the test procedure could be applied to surface area measurements of a variety of materials that have been crushed or broken down into irregularly shaped fragments.

The standard SIS test showed no stripping in the asphalt-aggregate combinations used and would be of little or no value in predicting the relative stripping tendencies of such mixtures.

Generally, the asphalt-aggregate mixtures containing the limestones were more resistant to stripping than those containing the gravel and sandstone type aggregates. Within the group of gravels, the aggregates with appreciable amounts of quartz (Broken Bow and Gore) were more susceptible to stripping than those composed predominantly of chert.

REFERENCES

1. Nicholson, V. Adhesion Tension in Asphalt Pavements, Its Significance and Methods Applicable in Its Determination. Proc. AAPT, Vol. 3, 1932, pp. 28-49.
2. Rice, J. M. Relationship of Aggregate Characteristics to the Effect of Water on Bituminous Paving Mixtures. ASTM STP 240, 1958, pp. 17-34.
3. Majidzadeh, K., and Sanders, R. R., Jr. Effect of Water on Behavior of Sand-Asphalt Mixtures Under Repeated Loading. Highway Research Record 273, 1969, pp. 99-109.
4. Majidzadeh, K., and Brovold, F. N. State of the Art: Effect of Water on Bitumen-Aggregate Mixtures. HRB Spec. Rept. 98, 1968.
5. Standard Method of Test for Coating and Stripping of Bitumen-Aggregate Mixtures. ASTM Designation: D 1664-69.
6. Standard Method of Test for Effect of Water on Cohesion of Compacted Bituminous Mixtures. ASTM Designation: D 1075-54 (R 1968).
7. Goetz, W. H. Methods of Testing for Water Resistance of Bituminous Mixtures. ASTM STP 240, 1958, pp. 84-96.
8. McCasland, W. Study of the Wearability and Polish Resistance of Oklahoma's Coarse Aggregates. Oklahoma Department of Highways, Dec. 1972.
9. Theroux, F. R., Eldridge, E. F., and Mallman, W. L. Laboratory Manual for Chemical and Bacterial Analysis of Water and Sewage. McGraw-Hill Book Co., New York, 1943.
10. Mathews, D. H., Colwill, D. M., and Yuce, R. Adhesion Tests for Bituminous Materials. Jour. Appl. Chem., Vol. 15, No. 9, 1965, pp. 423-431.
11. Brown, A. B., Sparks, J. W., and Marsh, G. F. Objective Appraisal of Stripping of Asphalt From Aggregate. ASTM STP 240, 1958, pp. 58-63.
12. Roediger, J. C. Stripping Test for Bitumen-Aggregate Mixtures. Proc. ASTM, Vol. 52, 1952, pp. 394-411.

DISCUSSION

M. J. Fernando, Highways Department, Ratmalana, Sri Lanka

I wish to congratulate the authors of this paper on their brilliant attempt to put

forward a new quantitative test to evaluate the stripping action of asphalt. It is well known that the standard stripping test, ASTM D 1664 (5), is highly qualitative in nature and subject to personal errors. Therefore, a better procedure is necessary to make this test quantitative and to eliminate personal judgment.

The test procedure outlined in this paper is based on the principle that a suitable reagent (such as an acid) reacts with the mineral aggregate and liberates a gas as part of the reaction. The gaseous pressure developed is considered to be proportional to the exposed surface area of the aggregate. Therefore, the chemical composition of the aggregate surface is an important factor. It appears to me that the authors do not take into consideration the presence of non-gas-producing reactions when acid comes in contact with aggregate surface. I think that the direct evaluation of amount of acid reacted with the aggregate surface, under a suitable set of experimental conditions, may be more fundamental, simpler, and a better approach to the problem. Therefore, I wish to share some observations made on evaluating stripping by an elementary acid-base titration.

THEORY

If

S_a = total surface area of uncoated aggregate,
V_a = volume of standard acid reacted for a certain time with S_a,
S_b = total surface area of the aggregate coated with asphalt, and
V_b = volume of the same standard acid reacted for the same interval of time with S_b,

and, if after stripping

S_a' = surface area of the uncoated aggregate,
S_b' = surface area of the aggregate coated with asphalt, and
V_b' = volume of the same standard acid reacted for the same interval of time,

then we know that

$$S_a' + S_b' = S_a \tag{1}$$

Dividing Eq. 1 by S_a gives

$$\frac{S_a'}{S_a} + \frac{S_b'}{S_a} = 1 \tag{2}$$

and

$$V_b' = \frac{S_a'}{S_a} \cdot V_a + \frac{S_b'}{S_b} \cdot V_b \tag{3}$$

Since $S_a \approx S_b$

$$V_a' = \frac{S_a'}{S_a} \cdot V_a + \frac{S_b'}{S_a} \cdot V_b \tag{4}$$

That is to say

$$V_b' = \frac{S_a'}{S_a} \cdot V_a + V_b \left[1 - \frac{S_a'}{S_a}\right] \tag{5}$$

Therefore,

$$\frac{S_a'}{S_a} = \frac{V_b' - V_b}{V_a - V_b}$$

or $\frac{S_a'}{S_a}$ = fraction of surface area stripped.

PROCEDURE

The limestone aggregate passing a ¾-in. sieve and retained on a ½-in. sieve was washed with distilled water and oven dried at 110 C for 2 hours. Then the aggregate was allowed to cool to room temperature. Two hundred grams of the oven-dried aggregate were heated to 150 C and coated with asphalt at 150 C. The asphalt content in all mixes was maintained at 4.5 percent by aggregate weight. The coated aggregate was allowed to cool to room temperature.

Test 1

Two hundred grams of uncoated aggregate was reacted with 200 ml of N/10 HCl for 5 min. By titrating the excess acid with N/10 sodium carbonate using methyl orange as indicator, the volume of the acid reacted was obtained (V_a ml).

Test 2

The same procedure used in test 1 was repeated with 200 g of aggregate coated with asphalt (V_b ml).

Test 3

The same aggregate used in test 2 was washed with distilled water 3 times to free it from acid and boiled for 15 min in 400 ml of distilled water. The water was drained off quickly and the material was allowed to cool for about half an hour and test 1 was repeated (V'_b ml). Because the reaction of HCl with limestone is fast, a weak acid such as oxalic acid is found to be more suitable. The reaction of 1N-oxalic acid with limestone reaches completion in about 15 min because of the formation of acidic nonsoluble calcium oxalate on the exposed surface. The oxalic acid used up may be determined with N/10 sodium hydroxide with phenolphthalein as an indicator.

This procedure does not require elaborate and expensive apparatus, although a mixture of HCl and HF acids should be used for siliceous or mixed aggregate.

AUTHORS' CLOSURE

We appreciate Fernando's discussion. He illustrates another approach to the quantitative evaluation of stripping. Lortscher, Snyder, and Filbert (13) reported a similar approach to evaluation of stripping of limestone aggregate by reacting the aggregate with dilute HCl and measuring the depletion rate of the acid by titration. We hope that Fernando also will publish test results to confirm the validity of the SRT.

REFERENCE

13. Lortscher, L. L., Snyder, M. J., and Filbert, R. B., Jr. Improved Methods of Estimating Stripped Area in Asphalt Stripping Tests. HRB Proc., Vol. 35, 1956, pp. 314-321.

CHANGES IN ASPHALT CONCRETE MIXTURE PROPERTIES AS AFFECTED BY ABSORPTION, HARDENING, AND TEMPERATURE

Byron E. Ruth, University of Florida; and
Charles F. Potts, Florida Department of Transportation

This paper provides information on the split cylinder testing of laboratory-compacted specimens and cores taken from in-service pavements. Tension test data were obtained for mixtures containing different aggregates, asphalt contents, types of asphalt, and temperatures. Relations between energy and vertical and horizontal deformations were developed from the test data. It was observed that energy decreased at lower temperatures. The horizontal and vertical deformations as measured in the split cylinder test were found to be related to the viscosity of the asphalts as influenced by hardening and temperature. This could be significant because it may provide a method to evaluate the composite effects of asphalt-aggregate interaction for use in quality control of asphalt paving mixtures. Further information is provided on penetration-viscosity relations and the properties of the materials used in the investigation.

•NUMEROUS factors can contribute to the fatigue cracking of flexible pavements. In Florida, the unexpected increase in traffic volume is considered a major contributor to early fatigue failure. The prevalence of pavement cracking in northern Florida has been of particular interest. Highly absorptive lime rock aggregates are used for pavement construction in this region. Preliminary studies of this paving material revealed that volume changes that are caused by the absorption of water or drying effects were very small and, undoubtedly, could not be a primary cause of pavement cracking.

Other investigations of pavement cracking on Interstate 10 in the northern part of Florida provided at least a partial insight into the factors affecting pavement performance (1). High air-void and low asphalt contents were generally synonymous with more extensive cracking than was observed on pavement sections with low air-void and high asphalt contents. Poor performance appeared to result from excessive hardening of the asphalt. It was observed that cracking was most prevalent when the extracted asphalt viscosity exceeded 10 megapoises (MP) at 25 C.

Further investigation of I-10 and several other pavements were directed toward the identification of the composite properties of paving materials (compacted asphalt-aggregate mixture). Laboratory-compacted specimens and cores from different pavement sections were split cylinder tested to separate good performing pavement sections from bad performing pavement sections by the tensile properties of the paving materials. The general approach to testing was similar to that of Breen and Stephens (2) in that work energy expended to failure was used as a definitive parameter.

MATERIALS

The aggregates used in this investigation were typical of those used in northern and southern Florida. Aggregate blends were selected to provide duplication of mixtures

Publication of this paper sponsored by Committee on Effects of Natural Elements and Chemicals on Bitumen-Aggregate Combinations.

used in actual paving projects. The gradation, specific gravity, and absorption values for each of the 4 aggregate blends used in the study are given in Tables 1 and 2. Mixtures 1 and 2 are almost identical except for slight differences in fine aggregate blending. These mixtures are representative of the surface course used in the construction of I-10 in northern Florida. Mixtures 3 and 4 are typical of asphalt surfacing materials used in the Miami area.

The absorptive character of Florida aggregates is quite variable. Natural silica sands have absorptions of usually less than 0.80 percent whereas the lime rocks and oolitic limestones range between approximately 2.0 percent to 5.0 percent. The screened shell used in mixture 3 had a water absorption of 2.25 percent. Visual observation of asphalt mixtures that contain absorptive aggregates indicated that selective absorption may exist.

Table 3 presents a summary of properties for each of the 5 asphalts used in the study. Asphalt A was an aromatic, temperature-susceptible asphalt with a high glass transition temperature. Asphalts B and E were highly asphaltic and similar in properties except for substantial differences in glass transition temperature and flash point. Asphalts C and D were both air-blown materials derived from naphthenic base crudes.

These asphalts gave similar penetration and viscosity values for the 25 C test temperature. However, considerable differences in glass transition temperatures, degree of hardening, and viscosities at other temperatures were obtained for the asphalts. These differences appeared to be significant because of their effect on the results of split tension testing of compacted mixtures containing these asphalts.

TESTING PROCEDURES

The laboratory testing procedures included the use of the following:

1. Marshall method (ASTM D1559-71) to determine design asphalt contents and preparing test specimens for each mixture;
2. Corps of Engineers procedure (ASTM D854-52) to evaluate the bulk-impregnated specific gravity of the aggregate blends;
3. Rice method (ASTM D2041-71) to obtain the virtual specific gravity and asphalt absorption of the mixtures prepared with the different asphalts;
4. Atlas weatherometer to accelerate the weathering of compacted asphalt mixture specimens; and
5. Split tension testing of unweathered (control) and weathered specimens.

In some instances it was necessary to modify the standard procedures. The specimens for processing in the weatherometer and split cylinder testing were mixed at temperatures corresponding to 1.5 P viscosity and compacted by using 6-blow Marshall compaction. This level of compaction provided densities that were slightly lower than actual pavement densities, but it was advantageous to obtain accelerated weathering of the specimens.

The standard sample size for the bulk-impregnated specific gravity test was reduced to 300 g of aggregate and 150 g of asphalt to minimize the difficulty in eliminating entrapped air and the time required for each specific gravity determination. Duplicate tests were conducted at preparation temperatures corresponding to viscosities of 10, 4, and 1.5 P for each aggregate blend and type of asphalt.

Accelerated weathering of test specimens was accomplished by using an Atlas weatherometer that contained carbon electrodes for arc light and a water spraying device. Temperatures up to 160 F were common during the heating cycle; an average temperature for each day was approximately 90 F. The 6-blow, Marshall-compacted specimens were arranged on a 2-level revolving rack in the weatherometer that continuously rotated around the light source and under the water spray bar. The specimens were revolved a quarter turn and rotated between top and bottom rack daily to obtain a uniform weathering exposure. The daily weathering schedule is given in Table 4. Specimens of mixtures 1 and 2 and mixtures 3 and 4 were exposed for a total of 864 hours and 672 hours respectively.

The tensile properties of unweathered and weathered laboratory specimens and pave-

Table 1. Aggregate gradation of test mixtures.

Sieve Size	Percent Passing			
	Mixture 1[a]	Mixture 2[b]	Mixture 3[c]	Mixture 4[d]
3/8 in.	100	100	100	100
4 in.	65.0	65.0	68.6	67.0
No. 10	42.1	42.0	45.3	41.8
No. 40	34.1	34.0	33.8	28.0
No. 80	14.9	18.9	11.6	15.7
No. 200	4.8	4.8	4.6	5.1

[a]58 percent No. 16 live oak crushed stone, 35 percent Oak Ridge silica sand, and 7 percent crushed stone screenings.
[b]58 percent No. 16 live oak crushed stone, 31.5 percent Oak Ridge silica sand, and 10.5 percent crushed stone screenings.
[c]56 percent No. 16 Dade County crushed stone, 8.1 percent crushed stone screenings, 32.4 percent Palm Beach screened shell, and 3.5 percent portland cement mineral filler.
[d]57 percent No. 16 Dade County crushed stone, 39.5 percent crushed stone screenings, and 3.5 percent portland cement mineral filler.

Table 2. Aggregate properties of test mixtures.

Asphalt	Bulk Specific Gravity	Apparent Specific Gravity	Water Absorption (percent)
Mixture 1	2.511	2.629	2.14
Mixture 2	2.506	2.630	2.27
Mixture 3	2.454	2.623	2.51
Mixture 4	2.461	2.615	2.40

Table 3. Asphalt properties.

Properties	Type of Asphalt				
	A	B	C	D	E
Penetration at 25 C	91	85	84	88	87
Specific gravity at 25 C	1.012	1.032	1.002	0.997	1.032
Flash point, deg C	257	215	324	313	294
Solubility in trichloroethylene, percent	99.96	99.95	99.95	99.96	99.59
Ductility at 25 C, cm	150+	150+	150+	150+	146
Viscosity					
V135 at 135 C, P	1.64	5.88	2.93	3.17	6.15
V60 at 60 C, kP	0.930	3.07	1.22	1.72	2.11
V25 at 25 C, MP[a]	0.875[b]	1.11[b]	1.25[b]	1.05[b]	0.99[b]
V25 complex flow, C	1.02[b]	0.80[b]	0.87[b]	0.78[b]	0.76[b]
V5 at 5 C, MP[a]	996[bc]	132[b]	275[b]	122[b]	134[b]
V5 complex flow, C	1.15[b]	0.80[b]	0.76[b]	0.66[b]	0.54[b]
Glass transition, isobaric method, 1 C/min					
1 atmosphere, deg C[d]	1.0	-4.5	-2.0	-7.0	-9.0
500 atmosphere, deg C[d]	16.5	12	12.5	8.0	7.0
Pressure sensitivity, m	0.033	0.031	0.028	0.029	0.030
Penetration method, deg C[e]	3.7	-0.2	4.8	1.2	-1.8
TFOT residues					
Penetration at 25 C	52	36	58	61	53
Penetration, percent of original	57	42	69	69	61
Loss, percent	0.26	1.53	—	—	0.34
Gain, percent	—	—	0.06	0.07	—
V60, kP	1.91	22.1	2.39	3.11	7.05
Viscosity ratio	2.05	7.20	1.96	0.98	3.34
V25, MP[a]	3.21	6.61	2.57	1.98	3.43
V25 complex flow, C	1.11	0.73	0.81	0.75	0.70
Ductility at 25 C, cm	150+	58	150+	150+	45

[a]Florida capillary method at constant shear rate for power input of 10^5 erg/cm^2 sec (4).
[b]Average of 2 tests.
[c]This material exhibits "glassy" phenomena at 5 C.
[d]By interpolation or extrapolation of data.
[e]Shoor, Majidzadeh, and Schweyer method (5).

Table 4. Daily weathering schedule.

Time	Water Spray	Arc Lamp
0700	Off	Off
0900	On	Off
1030	Off	On
1830	Off	Off
1900	On	Off
2300	Off	On

Note: Total water spray time: 5.5 hours. Total arc lamp time: 16 hours. Total time off: 2.5 hours.

ment cores were evaluated by using a split cylinder test. This test was selected because of its simplicity and potential to evaluate those physical properties of compacted asphalt mixtures that relate to flexibility, fatigue resistance, or resistance to cracking.

The test mechanism consisted of two 0.5-in.-wide parallel steel contact plates, one mounted on a load cell and the other mounted directly below the platen of the test machine. The screw-driven testing machine was limited to a single speed that provided a constant vertical deformation rate of 2.68 in./min. Instrumentation consisted of a 10,000-lb load cell and a linear variable differential transformer (LVDT) connected to a strip chart recorder. Horizontal deformation was measured across the 4-in.-wide specimens by using a LVDT.

Figure 1 shows typical data output from the split cylinder tests. Data curves for mixture 4 using asphalt A and asphalt D illustrate the extremes in response obtained for the different asphalt mixtures tested at 5 C. Energy and strain ratios were computed from the data in the following manner.

1. Initial deformation that was due to seating of the steel contact plates on the 4-in.-diameter asphalt concrete specimens was eliminated from the analysis by projecting the linear portion of the curve to the abscissa.
2. Vertical deformation corresponding to the point where the rate of horizontal deformation increased rapidly was used to calculate initial energy (E_I) as illustrated in the following computation for asphalt D shown in Figure 1:

$$E_I = \begin{pmatrix}\text{avg}\\ \text{load}\end{pmatrix} + \begin{pmatrix}\text{vertical}\\ \text{deformation}\end{pmatrix} = \left[\frac{3{,}000}{2}(0.1)\right] + \left[\frac{3{,}000 + 4{,}500}{2}(0.084)\right] = 465 \text{ in.-lb} \quad (1)$$

3. The horizontal/vertical strain ratio (ϵ_H/ϵ_V) was computed by using a horizontal deformation increment of 0.04 in. measured from the point at which the horizontal deformation rate increased. The vertical deformation increment was determined from the data plot by using the previously defined horizontal deformations. An example of this calculation using asphalt D data is

$$\frac{\epsilon_H}{\epsilon_V} = \frac{0.04}{0.0617} = 0.65 \quad (2)$$

4. Additional vertical energy was computed by using the vertical deformation as determined in Eq. 2. The following example illustrates this computation for asphalt D:

$$E_A = \begin{pmatrix}\text{avg}\\ \text{load}\end{pmatrix}\begin{pmatrix}\text{vertical deformation for}\\ \text{0.04-in. horizontal deformation}\end{pmatrix} = (3{,}800)(0.0617) = 234 \text{ in.-lb} \quad (3)$$

5. The computation for total energy is as follows:

$$E_T = E_I + E_A = 465 + 234 = 699 \text{ in.-lb} \quad (4)$$

The energy values presented in this report have been corrected for specimen diameter and thickness so that the energy corresponds to a standard specimen 4 in. in diameter and 2.5 in. in thickness.

Viscosity tests on asphalts recovered by the Abson method (ASTM D1856-69) from laboratory samples and field cores were obtained to evaluate hardening that had occurred in mixing and in weathering. Viscosity tests were performed at 25 C although it would have been desirable to have low temperature viscosity data.

RESULTS

The Marshall mixture design results for the different mixtures using asphalt E are given in Table 5. The air-void content for the mixtures at the design asphalt content may appear low, which is common for these mixtures because the density and stability values do not change appreciably at different asphalt contents. The optimum asphalt contents were used as a guide in selecting asphalt contents for preparation of the tension

Figure 1. Analysis of split cylinder test data.

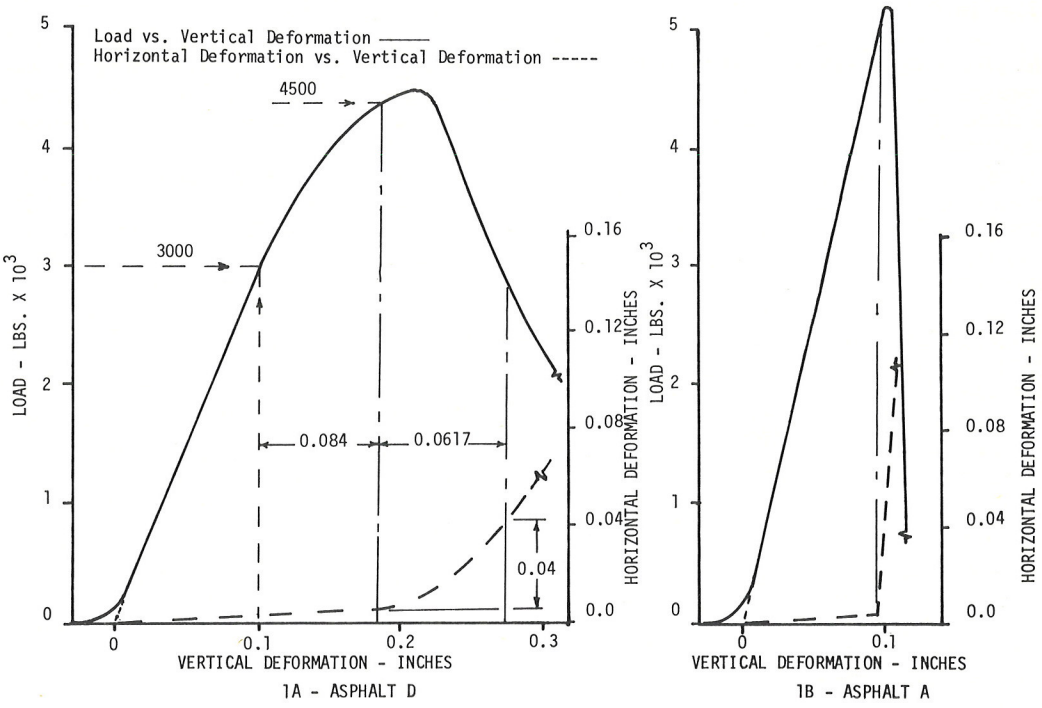

Table 5. Marshall mixture design results.

Mixture	Unit Weight (pcf)	Stability (lb)	Flow (0.01 in.)	VMA (percent)	Air Voids (percent)	Optimum AC (percent)
1	142.80	1,265	8.5	14.0	2.4	6.10
2	141.90	1,360	9.6	14.2	3.2	6.30
3	140.5	2,010	10.7	13.8	4.0	6.0
4	141.0	2,780	12.2	14.3	2.9	6.6

Note: 1 pcf = 16.01 kg/m^3. 1 lb = 4.45 N. 1 in. = 25.4 mm.

Table 6. Compaction data for tensile test specimens.

Mixture	AC (percent)	Compaction Blows per Side	Unit Weight (pcf)	Marshall Compaction (percent)
1	5	6	135.36	95
	6	6	137.50	96.5
2	5	6	134.71	95
	6	6	136.60	96.3
3	5	6	131.27	93.5
	6	6	132.51	94.4
4	5.5	6	130.16	92.4
	6.8	6	132.45	94.0

Note: 1 pcf = 16.01 kg/m^3.

test specimens. The compaction data for the 6-blow, split cylinder test specimens are given in Table 6.

The bulk-impregnated specific gravity test results are given in Table 7. Data for the 10.0 P test temperature have been deleted because it was found that removal of entrapped air was difficult to achieve at this higher viscosity. The test values for asphalt E were essentially the same as values obtained on mixtures tested by the Rice method as given in Table 8.

The results of the 5 C split cylinder tests on mixtures 1 and 2 and cores from I-10 are presented in Figures 2 and 3 respectively. Mixtures 3 and 4 are not presented because the data were essentially the same as those for mixtures 1 and 2. Variation in specimen and core thickness were taken into account by adjusting all test values to a standard thickness of 2.5 in. Because the effect of weathering was substantial for mixtures containing asphalt B, it was decided to shortcut the weatherometer process and to use asphalts from the thin film oven test (TFOT) for preparation of specimens. The data for this limited study are shown in Figure 4. The dashed lines representing the data trends are exactly the same in Figures 2, 3, and 4.

Viscosity data for the extracted asphalts from laboratory specimens and I-10 cores are given in Tables 9 and 10. Also, penetration data and asphalt contents for the different sections are presented in Table 9 for comparative purposes.

DISCUSSION OF RESULTS

Preliminary analysis of the viscosity data indicated that a considerable difference exists among asphalts in their hardening properties. The summary of laboratory viscosity data for the different asphalts, as given in Table 11, shows that some hardening occurs in the heating, mixing, and preparation of test specimens. Asphalt B was the most affected by the process whereas air-blown asphalts (asphalts C and D) showed negligible hardening. Good correlation was obtained between TFOT and weatherometer viscosities. The weatherometer produced greater hardening of asphalt A than did the TFOT. This hardening had a noticeable effect on the split tension test results; this can be readily identified in Figures 2 and 3 where the energy values decrease and the strain ratio increases for the weathered specimens containing asphalt B.

All viscosity and penetration data for original asphalts, TFOT residue, and extracted asphalts were compared to the viscosity prediction curve, which is based on the following equation developed by Schweyer (3):

$$N_p = 3{,}240\ P^{-2.32} \tag{5}$$

where

N_p = viscosity in MPa·s at a constant power input of 10^5 erg/cm^2·sec and
P = penetration at 25 C.

This comparison, as shown in Figure 5, indicates reasonably good correlation between the prediction equation and the experimental values.

The effect of asphalt content on the split cylinder tests was observed by Breen and Stephens (2). At low temperatures they concluded that work appeared to be independent of asphalt content. The test results presented in Figures 3 and 4 indicate a slight increase in energy as the asphalt content is increased. However, the initial energy from the test data is directly comparable to Breen and Stephens work values and appears to justify their conclusions.

Any change in energy values with changes in asphalt content may be a result of compacted density variations. However, comparison of tension test results for 50-blow and 6-blow compacted specimens gave essentially the same energy and strain ratio values.

Breen and Stephens (2) observed the effect of increasing viscosity by lowering the temperature for the split cylinder tests. They note that with decreasing temperature the fracture load increases slowly and the work required to fracture the specimen decreases. This phenomenon was observed in tests conducted on mixture 4 by using different asphalts and test temperatures of 2, -3.3, and -8 C. As shown in Figure 6, the

Table 7. Bulk-impregnated specific gravity values.

Type of Asphalt	Mixture 1	2	3	4
4.0 P test results				
A	2.556	2.583	2.566	2.574
B	2.547	2.561	2.548	2.557
C	2.545	2.563	2.544	2.554
D	2.556	2.555	2.536	2.541
E	2.558	2.568	2.555	2.564
1.5 P test results				
A	2.564	2.577	2.562	2.574
B	2.538	2.558	2.544	2.555
C	2.545	2.560	2.546	2.558
D	2.543	2.554	2.540	2.548
E	2.551	2.556	2.544	2.553
Mean of B, C, D, E	2.548	2.559	2.545	2.545
Standard deviation of B, C, D, E	0.0078	0.0071	0.0073	0.0083
Difference between asphalt A and mean	+0.016	+0.018	+0.017	+0.020

Table 8. Comparison of bulk-impregnated and Rice method specific gravity methods, 4.0 P test results.

Mixture	Bulk-Impregnated Method, Asphalt E	Rice Method, Asphalt E	Asphalt Absorption (percent)
1	2.558	2.572	1.12
2	2.568	2.570	1.38
3	2.555	2.549	1.65
4	2.564	2.558	1.67

Figure 2. Energy-strain ratio relationship for laboratory test specimens.

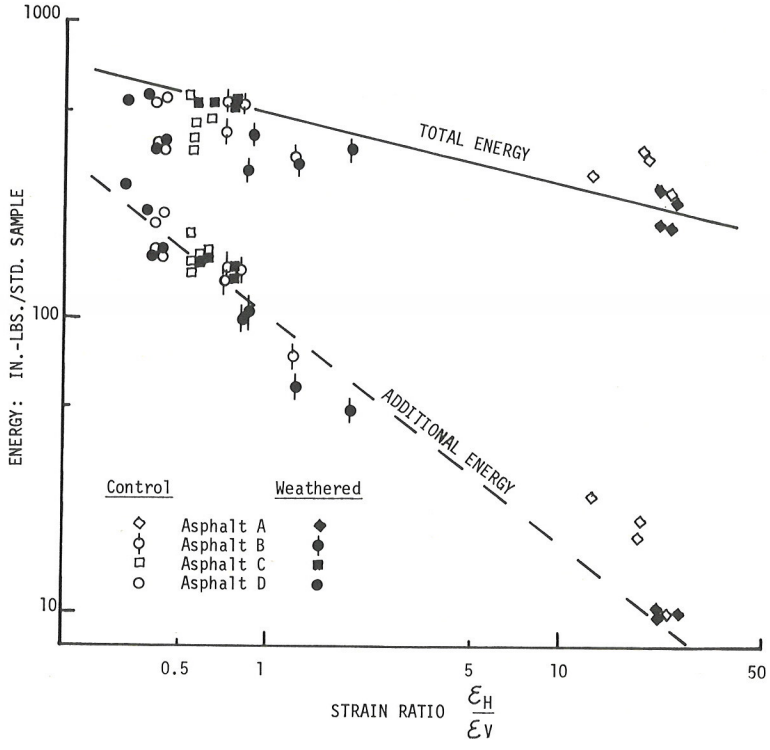

Figure 3. Energy-strain ratio relationship for I-10 cores.

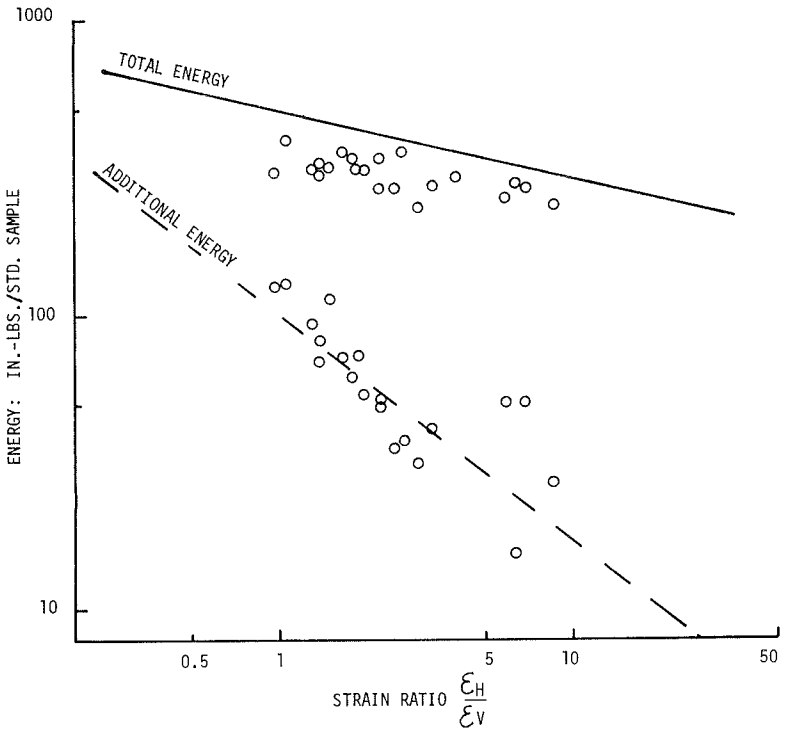

Figure 4. Energy-strain ratio relationship for laboratory test specimens containing TFOT asphalt residues.

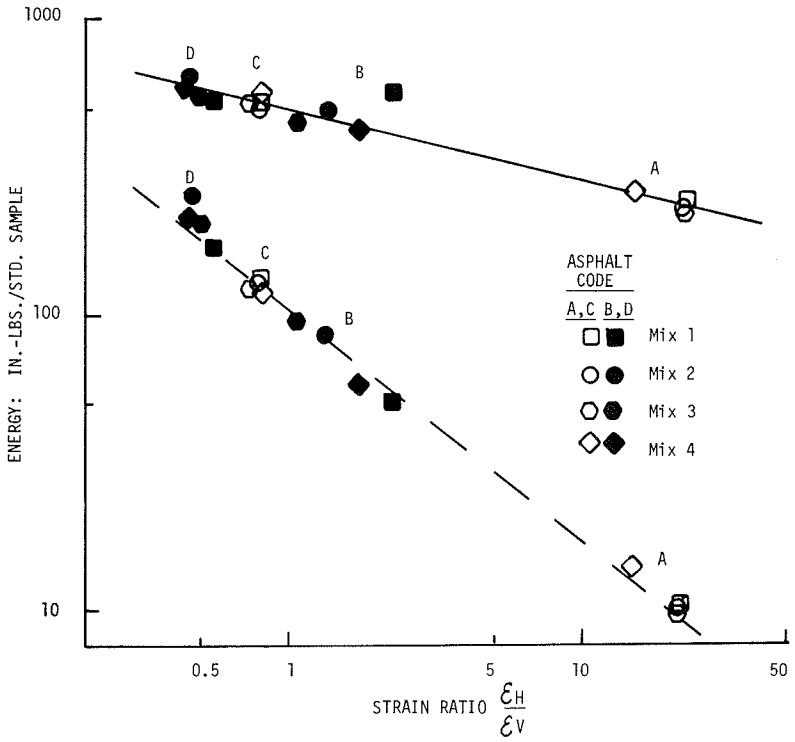

Table 9. Viscosity of asphalts extracted from test specimens.

Type	AC (percent)	Viscosity at 25 C (MP) Control Specimens	Viscosity at 25 C (MP) Weatherometer Specimens
Asphalt A			
Mix 1	5.0	1.30	4.90
	6.0	1.41	5.83
Mix 2	5.0	1.99	5.48
	6.0	1.71	5.03
Mix 3	5.0	1.35	4.48
	6.0	1.75	4.14
Mix 4	5.5	2.11	5.03
	6.8	1.71	4.96
Asphalt B			
Mix 1	5.0	2.24	10.3
	6.0	1.41	6.76
Mix 2	5.0	2.25	7.29
	6.0	3.97	4.67
Mix 3	5.0	1.83	6.58
	6.0	2.27	5.80
Mix 4	5.5	1.98	5.19
	6.8	2.19	5.02
Asphalt C			
Mix 1	5.0	1.57	2.17
	6.0	1.22	2.37
Mix 2	5.0	0.86	3.02
	6.0	1.49	3.47
Mix 3	5.0	1.37	2.21
	6.0	1.55	2.26
Mix 4	5.5	1.66	2.32
	6.8	1.53	2.12
Asphalt D			
Mix 1	5.0	1.46	1.88
	6.0	1.14	1.35
Mix 2	5.0	1.13	1.96
	6.0	0.93	1.91
Mix 3	5.0	1.12	1.72
	6.0	1.18	1.91
Mix 4	5.5	1.14	2.00
	6.8	1.24	2.18

Table 10. Penetration and viscosity data for recovered asphalts from I-10 cores.

Section Number	Penetration at 25 C	Viscosity at 25 C (MP)	AC (percent)
7	26	15.6	—
8, 9	18	42.0	—
10	25	18.0	—
11	25	20.8 to 23.0	—
15	22	31.1	—
16	24	25.4	5.3 to 5.6
21	41	—	6.2 to 6.5
21	37	—	6.5
22	43	13.9	—
23	37	8.09	6.3
25	23	21.0	—
26	25	19.1	5.4
27	25	—	5.5 to 5.9
28, 29	27	19.6	5.2 to 6.1
30	21	—	—

Table 11. Comparison of viscosity data.

Type of Asphalt	Original Asphalt	Average Viscosity Values at 25 C (MP) Extracted From Control Specimens	TFOT Residue	Extracted From Weatherometer Specimens
A	0.875	1.67	3.21	4.98
B	1.11	2.27	6.61	6.48
C	1.25	1.41	2.57	2.49
D	1.05	1.17	1.98	1.86
E	0.99	—	3.43	—

Figure 5. Penetration-viscosity relations.

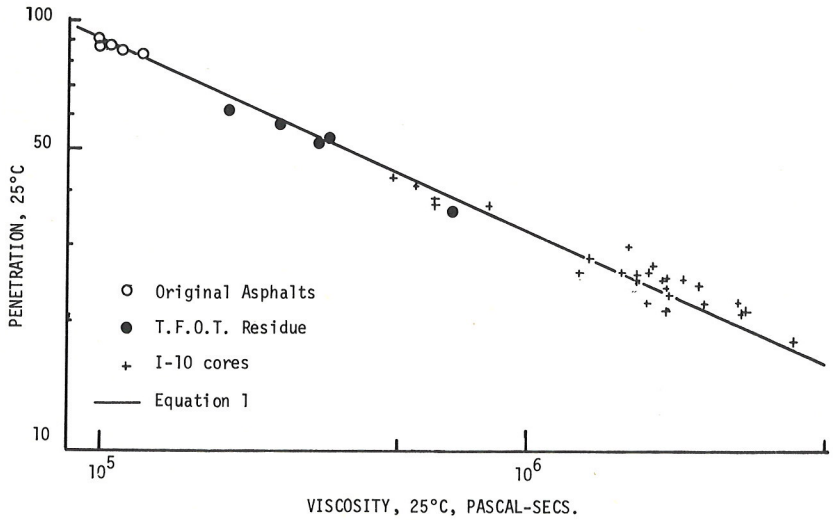

Figure 6. Energy-strain ratio relationship for certain asphalts at different temperatures.

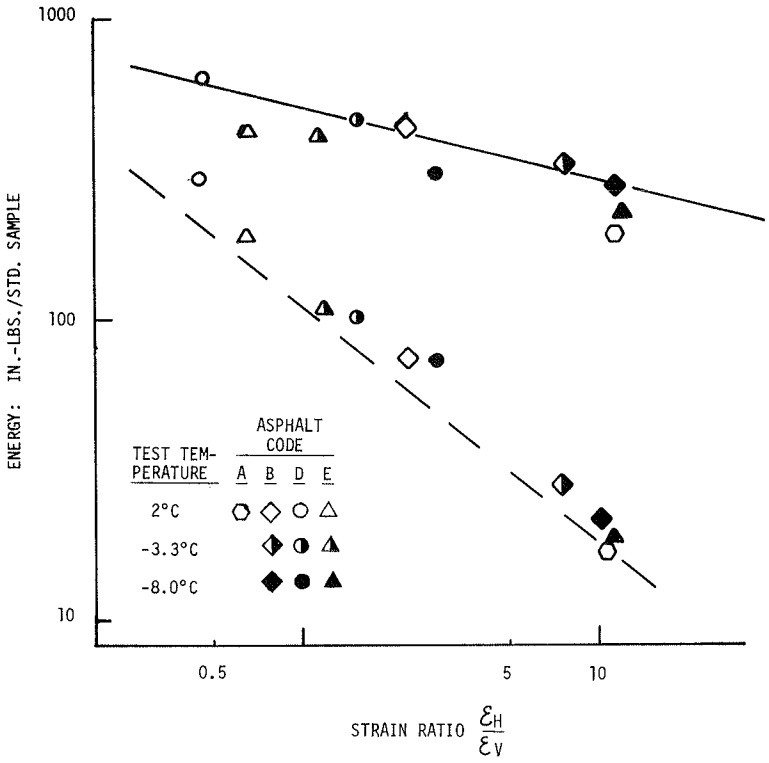

Figure 7. Deformation-energy-viscosity relations.

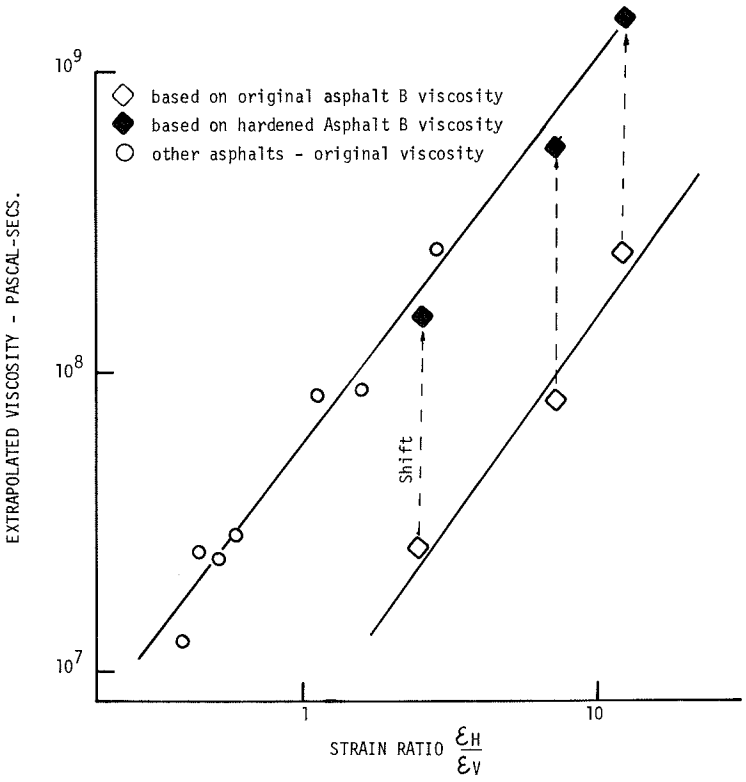

energy decreases and the strain ratio increases as the temperature is lowered. This effect was directly related to viscosity changes and brittle fracture as experienced with asphalt A mixtures, which occurred near or at the glass transition temperature.

The split cylinder test, in particular the strain ratio, evaluates the composite effects of selective absorption or surface tension and viscosity or glass transition temperature as influenced by asphalt hardening. The pressure exerted on asphalt films between aggregate particles by loads on a pavement conceivably could increase the glass transition temperature. The pressure sensitivity given in Table 3 implies that glass transition temperature would increase about 1 C for each pressure increase of 450 psi. The combined influence of pressure and the greater absorption of asphalt A, as given in Table 6, would justify the glassy, brittle fracture obtained in the split tension test at 5 C.

The relationship between asphalt viscosity and the strain ratio is illustrated in Figure 7. The viscosity data was based on extrapolation of the viscosity trend by using viscosity curves for the original asphalt that included 5 C data. Viscosity values for hardening that is caused by mixing or weatherometer processing were determined by shifting the original viscosity curve to the viscosity corresponding to the measured values at 25 C. Asphalts C, D, and E show the same general relationship for different test temperatures (viscosity). The curve depicting asphalt B was based on the original viscosity curve. However, if the hardening caused by mixing is taken into account by using the shifted viscosity curve, the data come close to superimposing over the viscosity-strain ratio curve for the other asphalts. This same technique appeared to be valid for asphalt A although it was difficult to evaluate because of the brittle nature and high viscosity of this asphalt at all test temperatures. A few test temperatures above 5 C would have improved the range in values and hopefully the accuracy of the relationship.

CONCLUSIONS

The ability of an asphalt concrete pavement to resist cracking depends on the strains induced by vehicular loading and the ability of the paving materials to accommodate cumulative tensile strains without fracture at low temperatures. Conventional specifications for bituminous materials cannot evaluate totally the adequacy of an asphalt as it interacts with different types of aggregates. The split cylinder test is relatively simple and provides a direct evaluation of the tensile properties for paving materials.

It is envisioned that tensile testing methods could be devised to either control the quality of asphalts as influenced by hardening and absorption by aggregates or use the test parameters in pavement design by testing the actual materials to be used in construction. Although additional research is needed, a pavement design approach may be developed that incorporates the ratio of pavement tensile strain to fracture tensile strain. In this approach the maximum pavement surface tensile strain is the sum of load-induced strain and thermal strains that occur at some critical temperature. This temperature depends on the pavement temperature gradient and the low temperature properties of the asphalt such as fracture strain and nonrelaxed thermal tensile strains.

These are the specific conclusions obtained from the research.

1. Strain energy of asphalt concrete subjected to tensile stress decreases as the temperature decreases or as the asphalt viscosity increases. Viscosity changes may be attributed to temperature, hardening, or absorption.
2. Asphalt viscosity appears to be an indirect measure of the strain ratio as obtained in the split cylinder test. At viscosities of 1,000 MP or more the material approaches a brittle condition or the glass transition temperature. At these higher viscosities a strain ratio in excess of 2.0 was obtained.
3. Asphalt content and density do not have any appreciable influence on the energy or strain ratio.

ACKNOWLEDGMENTS

This test program has been sponsored by the Florida Department of Transportation.

Asphalt extractions and conventional bituminous testing were performed by personnel of the Florida DOT and are gratefully acknowledged. The assistance of H. E. Schweyer in performing viscosity tests and providing technical assistance was a significant contribution to the research. His efforts are sincerely appreciated.

REFERENCES

1. Potts, C. F., Schweyer, H. E., and Smith, L. L. An Analysis of Certain Variables Related to Field Performance of Asphaltic Pavements. Res. Rept. 173, Office of Materials and Research, Florida Department of Transportation.
2. Breen, J. J., and Stephens, J. E. Split Cylinder Test Applied to Bituminous Mixtures at Low Temperatures. In Jour. Materials, ASTM, Vol. 1, No. 1, March 1966.
3. Schweyer, H. E. Asphalt Rheology in the Near-Transition Temperature Range. Highway Research Record 468, 1973, pp. 1-15.
4. Schweyer, H. E. Asphalt Cement Viscosities at Ambient Temperatures by a Rapid Method. Highway Research Record 404, 1972, pp. 86-96.
5. Shoor, S. K., Majidzadeh, K., and Schweyer, H. E. Temperature-Flow Functions for Certain Asphalt Cements. Highway Research Record 134, 1966, pp. 63-74.

MOLECULAR INTERACTIONS OF ASPHALT IN THE ASPHALT-AGGREGATE INTERFACE REGION

J. C. Petersen, E. K. Ensley, and F. A. Barbour, U.S. Bureau of Mines, Laramie, Wyoming

Evidence for molecular interactions in the asphalt-aggregate interface region was demonstrated by using 3 different approaches: a study of asphalt-aggregate interactions by inverse gas-liquid chromatography (IGLC), chemical analysis of strongly adsorbed species, and physical measurements of molecular adsorption. IGLC studies showed that polar asphalt molecules, initially present or formed on oxidation, interact strongly with aggregate surfaces. Asphalt fractions showed more interaction with limestone than with quartzite. The catalytic effect of a mineral surface on the oxidation of asphalt fractions was shown. Limited IGLC studies also showed a correlation between asphalt-aggregate interactions and water-stripping resistance. Ketones, dicarboxylic anhydrides, and carboxylic acids were found to be the major asphalt components strongly adsorbed to road aggregates; they were concentrated in the strongly adsorbed fraction by factors of 1.9, 9.5, and 14 respectively. Evidence for multilayer adsorption of asphalt molecules on mineral surfaces was obtained by heats of immersion, flow through porous media, and photomicroscopy studies. The results indicated that adsorption, or molecular orientation, of asphalt molecules in the asphalt-aggregate interface region is a slow process and often continues for many hours and even days at 150 C (423 K). The adsorbed layer appears immobile at 150 C (423 K), and its buildup rate, typically of the order of 20 Å/min with normal aggregates, is affected by both the nature of the mineral surface and the composition of the asphalt. Speculation about the possible significance of the reported studies to asphalt paving technology is presented.

•MINERALOGICAL composition of aggregates appears to be of primary importance to asphalt-aggregate adhesion and resistance of the adhesive bond to the stripping action of water. The chemical nature of the aggregate surface sometimes is altered intentionally by treatment with lime, metal salts, or other materials. Adhesion promotors, which are believed to affect the asphalt-aggregate interface, sometimes are added to the asphalt to improve the adhesive characteristics of the road mix. The voluminous literature in this area is summarized by Majidzadeh and Brovold (1).

In addition to the influence of the interactions between asphalt and aggregate at the aggregate surface, the chemical nature of the aggregate has long-range influences that extend deep into the asphalt-aggregate interface region. Mack (2) suggested that asphalt molecules are aligned on the aggregate surface causing a similar alignment of molecules within the liquid, which extends for a distance of thousands of molecules. Asphalt technologists know that mineral fillers have profound effects on the properties and performance of asphalt mixes that cannot be precisely predicted from the well-recognized properties of the fillers such as density and particle size. Watanabe and Abe (3) rationalized this unpredictability by assuming that a "solid asphalt" layer exists around

Publication of this paper sponsored by Committee on Effects of Natural Elements and Chemicals on Bitumen-Aggregate Combinations.

the filler particle. Asphalt technologists talk of "slow-setting" or "tender" mixes and the effects of additives and asphalt components such as asphaltenes on the "setting rate" of road mixes. These phenomena may well have their bases in long-range molecular interactions in the asphalt that are promoted by the aggregate surface. Recent work by Ensley (4) supports this.

In spite of the apparent importance of asphalt-aggregate interactions, little fundamental knowledge of the nature of the interactions exists. Chemical reactions between asphalt components and the aggregate surface have not been shown conclusively even though certain asphalt components apparently are strongly adsorbed and not readily extracted from the aggregate in road cores by commonly used solvents such as benzene. Alcohol often is added to the solvent to effect more complete recovery; however, methods for establishing the functional types strongly adsorbed on the aggregate surfaces have not been readily available. Reversible changes in the bulk properties of the asphalt sometimes referred to as "steric hardening," which may be promoted by the aggregate surface, have eluded direct study in the past because this hardening is destroyed during solvent recovery of the asphalt from road mixes.

Several years ago the Bureau of Mines's Laramie Energy Research Center began to study both the chemical and physical nature of asphalt-aggregate interactions. Several new experimental techniques have been developed and applied, and considerable progress has been made toward a more fundamental understanding of the asphalt-aggregate interaction. The purpose of this Bureau of Mines paper is to highlight the current findings of these studies and to suggest their implications for asphalt technology.

For convenience, the studies have been divided into 3 areas on the basis of the experimental approach.

First, the interactions between chemical functional groups in asphalt and the functional groups on the aggregate surface were studied by IGLC. The IGLC technique (5) was developed in our laboratory and applied originally to the study of asphalt composition (5, 6, 7, 8, 9). In the present work, asphalt was coated on sized aggregate particles that served as the gas chromatographic column packing (10), thus allowing study of the chemical interactions between asphalt and aggregate while they are in intimate contact.

Second, the chemical functional types strongly adsorbed on the aggregate surface were studied both qualitatively and quantitatively by an analytical technique using both selective chemical reactivity and differential infrared spectroscopy (11).

Finally, the interactions at the asphalt-aggregate interface and their long-range effects on reversible changes in the properties of the asphalt binder while in contact with the aggregate surface were studied by several physical methods. These included heats of immersion of aggregate in asphalt (4, 12), flow through a porous medium of aggregate particles (13), and photomicroscopy of the asphalt interface region previously in contact with a mineral surface (13).

EXPERIMENTAL WORK

Materials

Four study asphalts (B-2959, B-3036, B-3051, and B-3602) and 4 study aggregates (quartzite "15," "Hol" limestone, Riverton limestone, and granite "P-6") were supplied by the Federal Highway Administration (FHWA) (14, 15, 16). The FHWA also supplied 2 sets of 10 asphalts each that were recovered from duplicate 11- to 13-year-old pavement cores. One set of asphalts was extracted from the pavement cores by FHWA personnel with benzene only; the other set was extracted with a 4:1 mixture of benzene and 95 percent ethanol. Extractions in each case were continued until the extracting solvent issuing from the aggregate was colorless. The sample numbers of these asphalts correspond to those used in previous publications (17, 18, 19, 20). The Wilmington, California, asphalt and the preparation of the Wilmington asphalt fractions by pentane precipitation of the asphaltenes and by chromatography of the maltenes on basic alumina have been described previously (5, 10, 21, 22, 23, 24, 25).

The quartzite and limestone used in the IGLC study were obtained from the Laramie, Wyoming, area. Fluoropak 80 was the nonpolar fluorocarbon gas chromatograph solid support. Bauxite used in heat-of-immersion studies was regular grade Porocel.

Aggregate surface area measurements were made on -35+48-mesh particles by using the BET method with krypton as the adsorbate. The antistripping agent was Redicote 80S.

Procedures

Inverse Gas-Liquid Chromatography—IGLC characterization of the interactions between aggregates and asphalts or asphalt fractions was carried out by using a modification (10) of the original IGLC procedure (5) in which the inert solid column packing on which the asphalt was coated was replaced by -20+40-mesh aggregate. Oxidation of the asphalts in the laboratory was accomplished by replacing the inert column carrier gas with air (6). Both the oxidation and the test compound determinations were carried out at 130 C (403 K).

Analysis of Chemical Types—Ketones, carboxylic acids, and dicarboxylic anhydrides in oxidized asphalts generally have overlapping and indistinguishable absorption bands in the carbonyl region of the infrared spectrum. The amounts of these functional types were therefore determined by using a recently developed method that combines chemical reaction and differential infrared spectroscopy (11). In brief, the acids and anhydrides were reacted with sodium hydroxide and the acids were independently silylated and reacted with potassium bicarbonate; the resulting changes in the infrared absorption bands of the functional types were measured quantitatively by using selected sets of differential spectra from which concentration data were calculated (11). Ketone concentrations were obtained by difference.

Physical Measurements of Multilayer Adsorption—Heat-of-immersion studies of the asphalt-aggregate interaction energy were performed at 130 C (403 K) by using an extremely sensitive differential microcalorimeter designed and built by Ensley (4). This calorimeter is capable of measuring temperature changes of less than 5×10^{-6} K. The rate of association of asphalt molecules was also measured in the microcalorimeter (12). Flow-through-porous-media (FTPM) experiments were performed by flowing melted asphalt through a porous bed of aggregate under a nitrogen atmosphere and noting changes in the flow rate of the asphalt through the aggregate (13). Photomicroscopy using both optical and scanning electron microscopy were used in a conventional manner to examine striated fracture surfaces in asphalt samples (13).

Calculations

Calculation methods used to determine the interaction coefficient (I_g) from IGLC data, to determine the concentrations of functional compound types in asphalts, and to determine heats of immersion in the microcalorimetry have been reported previously (4, 5, 9, 11).

The asphalt fraction strongly adsorbed to the aggregate surface in the FHWA road cores was not isolated. It was therefore necessary to calculate the concentrations of functional types in this fraction from the differences in composition between the asphalts extracted from the road cores with benzene only and the corresponding asphalts extracted from the road cores with benzene-alcohol. By assuming that the asphalts have a specific gravity of unity, one can compare the concentration in moles per litre and the weight of asphalt. If one assumes 1 litre of the benzene-alcohol-recovered asphalt, then

$$X = BA - B(1 - W) \quad (1)$$

where

X = moles of functional type that was strongly adsorbed contained in 1 litre of benzene-alcohol-recovered asphalt;
BA = concentration of functional type as measured in benzene-alcohol-recovered asphalt, mol/l;
B = concentration of functional type as measured in benzene-only-recovered asphalt, mol/l; and
W = weight fraction strongly adsorbed.

BA and B were calculated from the infrared analysis (11), and W was obtained from the mass balance data obtained during the recovery of the asphalts from road cores. The term 1 - W corrects the term B for material lost on the aggregate in the benzene extraction.

Knowing X, then

$$\frac{X}{BA} \cdot 100 = \text{percent of functional type strongly adsorbed} \quad (2)$$

and

$$CF = \frac{X/BA}{W} \quad (3)$$

where CF = concentration factor representing the increase in concentration of the functional type in the strongly adsorbed layer over that in the whole asphalt recovered with benzene-alcohol. If one assumes that the molecules are monofunctional and have a molecular weight of 700, then

$$\frac{X \cdot 700}{10} = \text{strongly adsorbed functional type as percent by weight of total strongly adsorbed material} \quad (4)$$

RESULTS AND DISCUSSION

IGLC Studies of Chemical Interactions

Initial investigations in our laboratory of asphalt-aggregate interactions were carried out by using a modified IGLC technique. In brief, the technique involved preparing a gas chromatographic column consisting of a thin coating of asphalt or asphalt fraction on 20- to 40-mesh particles of aggregate. This asphalt-aggregate column was analyzed by passing known chemical compounds with carefully selected functional groups (test compounds) through the column and measuring the time required for them to emerge. Interactions between the functional group of the test compound and functionality on the column increased the emergence time. From the emergence times, the specific interaction coefficients, I_g, were calculated (9). The I_g is referenced to the behavior of a hypothetical nonpolar hydrocarbon of the same molecular weight as the test compound; therefore, the I_g is a measure of the interaction of the chemical functional group of the test compound with functionality on the column.

Interpreting the data was difficult because of the complexity of the interactions. Emergence times, and thus I_g values, can be increased by interactions of functional groups in asphalt with the test compound or by interactions between the test compound and chemical functionality on the aggregate surface. Of particular interest in the present study were the interactions between the asphalt and the aggregate; these interactions reduce the number of reactive asphalt and aggregate sites that are available for interaction with the test compound and thus reduce the I_g. Thus, IGLC data on an asphalt-aggregate column must be interpreted as the net result of all these interactions. In spite of the complexity of the system, qualitative meaning can be given to the results of the asphalt-aggregate data by comparing them with data obtained on the asphalt alone by using an inert solid support instead of aggregate and data obtained on columns of aggregate only.

Interaction data for 3 test compounds (propionic acid, phenol, and 2-methylpyridine) on 4 fractions from a Wilmington, California, asphalt coated on inert Fluoropak 80, quartzite, and limestone are given in Table 1. Data on 7 additional test compounds are reported elsewhere (10). The test compounds were selected to represent functional types known to be present in asphalt and capable of forming strong molecular complexes. Specific interaction coefficients on uncoated quartzite and limestone could not be calculated because emergence times for hydrocarbon references were too short for accurate measurement and test compounds did not emerge from uncoated limestone

after 150 min (5, 9). Interactions with bare quartzite were much less intense than with bare limestone, and all test compounds emerged from the quartzite column.

Data on the saturates fraction in Table 1 show that interactions on both quartzite and limestone were greater than on the inert Fluoropak. Test compounds permeated the nonpolar saturates fraction and interacted with sites on the aggregate surfaces. In fact, the data on unoxidized saturate-coated limestone were similar to data on bare limestone in that none of the test compounds emerged from the columns. The data show that the unoxidized saturates fraction does not contain significant amounts of strongly interacting functional groups that are capable of interacting with reactive sites on the aggregate surface. These sites are thus blocked from interaction with the test compounds.

After oxidation of the saturates on quartzite, the interaction of the test compounds with polar groups produced by oxidation is apparent from the increase in the I_g values in the oxidized column. On limestone, however, interaction of the oxidation products with the limestone surface, which blocks reactive sites on the aggregate, is evidenced by a decrease in the I_g for phenol and 2-methylpyridine. Of additional interest is the apparent absence of significant amounts of oxidation products in the saturates fraction oxidized on Fluoropak as indicated by the absence of significant changes in the I_g values on oxidation. The data on quartzite, when compared with the Fluoropak data, indicate that the quartzite surface catalyzed the oxidation of the saturates fraction. Examination of the infrared spectra of the recovered fractions showed the virtual absence of oxidation products in the saturates oxidized on Fluoropak, the presence of significant amounts of oxidation products in the saturates oxidized on limestone, and the presence of even greater amounts in saturates oxidized on quartzite.

The unoxidized aromatics fraction on Fluoropak showed greater interactions with the test compounds than did the saturates, suggesting more polar groups are in this fraction. The unoxidized aromatics apparently have sufficient polar groups to inactivate enough sites on the limestone surface to allow phenol and 2-methylpyridine to emerge from the column. Data for the oxidized aromatics on limestone show that the net effect of the interactions of the oxidation products with the limestone surface is greater than that of the interactions of the oxidation products with the test compounds. On the other hand, data for oxidized aromatics on quartzite show that the net effect of interactions of the oxidation products with test compounds is greater.

The polar aromatics and asphaltenes contain most of the highly polar functional groups initially present in the asphalt as evidenced by their large I_g values on Fluoropak and by their infrared spectra. The unoxidized polar aromatics and asphaltenes have sufficient polar groups to interact with and block many sites on the aggregate surfaces. This is shown by increases rather than decreases in the I_gs (except propionic acid) after oxidation of the fractions on limestone; increase results from interaction of the test compounds with oxidation products in excess of those interacting with the aggregate.

Evidence for the association of asphaltenes into molecular aggregates, or micelles, is found by comparing the I_gs for the polar aromatics and asphaltenes on both Fluoropak and limestone. Data on the inert Fluoropak show that interactions between the test compounds and the 2 fractions are very similar. Note, however, that I_gs on limestone are significantly greater for asphaltenes than for polar aromatics. This is interpreted as an increase in interaction between the test compounds and the limestone surface in the asphaltene-coated sample. Aggregation of the asphaltene molecules would reduce the number of functional groups in the asphaltenes that are physically able to interact with the aggregate surface. More sites on the aggregate surface would, therefore, be exposed to the test compounds.

IGLC data for 4 asphalts and 4 aggregates from the FHWA cooperative study are shown in Table 2. Also included in the table are surface areas of the aggregates and water-stripping data obtained by FHWA by using the ASTM D 1664 procedure modified by changing the immersion temperature to 100 F (311 K). In spite of the complexity of the IGLC data, some general differences between asphalts and aggregates are apparent.

Upon oxidation of the asphalts, interactions of oxidation products with the aggregates become apparent when data on Fluoropak are compared with data on aggregates; this is

Table 1. Specific interaction coefficients for unoxidized and oxidized Wilmington asphalt fractions on Fluoropak 80, quartzite, and limestone.

Asphalt Fraction	Percent of Total[a]	Specific Interaction Coefficient: Propionic Acid, Unoxidized	Propionic Acid, Oxidized	Phenol, Unoxidized	Phenol, Oxidized	2-Methylpyridine, Unoxidized	2-Methylpyridine, Oxidized
Saturates	23.3						
On Fluoropak 80		16	15	65	67	44	43
On quartzite		45	68	80	118	61	89
On limestone		—[b]	—[b]	—[b]	93	—[b]	62
Aromatics	31.0						
On Fluoropak 80		59	78	118	143	64	67
On quartzite		90	105	141	171	87	103
On limestone		—[b]	—[b]	183	147	79	77
Polar aromatics	25.0						
On Fluoropak 80		133	133	164	183	84	88
On quartzite		156	163	199	228	103	114
On limestone		—[b]	153	189	207	100	109
Asphaltenes	13.3						
On Fluoropak 80		138	146	166	197	90	95
On quartzite		173	190	193	230	109	123
On limestone		—[b]	—[b]	206	264	120	145

[a]7.4 percent loss during chromatographic separation. [b]Retention time greater than 150 min or emergence undetectable.

Table 2. Specific interaction coefficients and water-stripping data for FHWA study asphalts on mineral aggregates.

Aggregate-Asphalt System	Specific Interaction Coefficient: Propionic Acid, Unoxidized	Propionic Acid, Oxidized	Phenol, Unoxidized	Phenol, Oxidized	2-Methylpyridine, Unoxidized	2-Methylpyridine, Oxidized	Stripping Test (percent stripped)	Surface Area (m^2/g)
Fluoropak 80								—
Asphalt B-2959	61	95	107	158	63	91	—	
Asphalt B-3036	57	90	104	152	63	76	—	
Asphalt B-3051	85	108	129	170	68	90	—	
Asphalt B-3602	—[a]	148	137	146	69	72	—	
Quartzite "15"								0.515
Asphalt B-2959	92	104	144	171	82	97	40	
Asphalt B-3036	84	94	137	168	80	95	80	
Asphalt B-3051	108	113	147	185	88	102	40	
Asphalt B-3602	93	148	158	179	93	97	90	
"Hol" limestone								0.104
Asphalt B-2959	112	113	152	183	82	101	45	
Asphalt B-3036	101	105	143	172	79	84	40	
Asphalt B-3051	—[a]	128	155	192	86	101	20	
Asphalt B-3602	—[a]	164	169	175	87	92	75	
Riverton limestone								1.09
Asphalt B-2959	—[a]	—[a]	—[a]	178	77	85	5	
Asphalt B-3036	—[a]	139	—[a]	191	78	103	5	
Asphalt B-3051	—[a]	152	163	206	99	111	10	
Asphalt B-3602	—[a]	160	157	173	86	90	20	
Granite "P-6"								0.561
Asphalt B-2959	—[a]	113	140	178	90	120	1	
Asphalt B-3036	—[a]	106	134	176	88	99	8	
Asphalt B-3051	—[a]	110	144	187	86	106	0	
Asphalt B-3602	—[a]	123	151	172	89	94	5	

[a]Retention time greater than 150 min or emergence undetectable.

indicated by generally greater increases in I_gs for asphalts oxidized on Fluoropak than for asphalts oxidized on aggregates. In some cases, such as propionic acid on limestone columns, I_gs were actually lower on oxidized columns than on unoxidized columns, which indicates considerable interaction of the oxidation products with the aggregate surface thus reducing the interaction of the asphalt and aggregate functions with the test compounds.

A significant observation relating water-stripping resistance to asphalt-aggregate interactions can be made by comparing the changes in the I_gs for propionic acid to the stripping resistance of road mixes made from the corresponding materials. For example, the I_gs on all asphalts increase with oxidation on quartzite "15," indicating a minimum interaction of the oxidation products with the aggregate surface; the asphalts when coated on quartzite "15" are also readily stripped in the stripping test. On the other hand, propionic acid did not emerge from any unoxidized asphalt columns on granite "P-6" although after oxidation the propionic acid I_gs were as low as, or lower than, the corresponding I_gs on any other aggregate except for 2 asphalts on quartzite "15." This indicates considerable interaction of the oxidation products with the granite "P-6"; the asphalt-granite "P-6" mixes were also those most resistant to water stripping. Mixes made with "Hol" and Riverton limestones showed interactions of oxidation products with the aggregates and stripping resistances in between those for quartzite "15" and granite "P-6" mixes; the Riverton limestone was more resistant to stripping and showed greater interactions with the asphalts than did the "Hol" limestone.

Unlike the rest of the asphalts, asphalt B-3602 showed a decrease in the propionic acid I_g on oxidation on Fluoropak. Independent studies showed that this asphalt contained an excess of strong base (possibly alkali) and the carboxylic acids present were carboxylate ions. Oxidation either destroyed much of the base or produced functional types that consumed it, thus reducing interaction with the acidic test compound and restoring free acid in the asphalt. Whether the basic nature of the asphalt is related to its comparatively lower resistance to stripping is unknown.

Analyses of Chemical Types Strongly Adsorbed on Aggregate Surfaces

Chemical groups involved in the asphalt-aggregate interactions were identified and quantitatively determined in a study of 10 asphalts recovered from 11- to 13-year-old road pavements. Ketones, carboxylic acids, and dicarboxylic anhydrides were identified and quantitatively determined in material that was strongly adsorbed by the aggregates. The strongly adsorbed material (although not isolated) is defined as that not desorbed from the aggregate with benzene but desorbed with a 4:1 benzene-ethanol mixture. (All of the benzene-alcohol-recovered asphalts were soluble in benzene when separated from the aggregate.) Quantitative results were calculated by using data on independent sets of samples recovered with benzene and with benzene-alcohol; thus the data on the strongly adsorbed material were calculated from the differences in the 2 sets of samples.

The concentrations of the ketones, dicarboxylic anhydrides, and carboxylic acids in the recovered asphalts and estimates of the amounts of these chemical types in the strongly adsorbed material are given in Table 3. The amounts of these functional types present in the recovered samples vary from one asphalt to another. Except for small amounts of carboxylic acid initially present, this variation is primarily a result of the oxidation that took place in the asphalt during construction and service in the roads.

The amounts of functional types are determined with reasonable accuracy unless concentrations become unduly small. However, individual estimates of the amounts of ketones in the strongly adsorbed material may be subject to considerable error because of the compounding of several factors such as

1. Total ketones in the recovered samples are determined by difference after determination of acids and anhydrides;
2. Amounts of ketones strongly adsorbed are small relative to the total amount; and

3. Strongly adsorbed ketones are estimated by the difference between the asphalts recovered with benzene-alcohol and benzene only.

Although results for the individual road cores may vary, it is believed that the average value reported for the 10 road core extracts is typical. Even though the estimates of the strongly adsorbed anhydrides and acids are determined by difference, individual estimates are inherently more reliable because they are determined directly, and the relative amounts of the total functional type that is strongly adsorbed are much greater. The accuracy of the determinations could have been improved by multiple determinations or by direct analyses of the strongly adsorbed materials had they been available. The number of significant figures given in the table for the individual determinations does not necessarily represent accuracy but is carried for computation of averages.

Calculated data on the ketones, dicarboxylic anhydrides, and carboxylic acids strongly adsorbed from the asphalts by the aggregates are given in Table 4. The concentration factor, which represents the concentration of the functional type present in the strongly adsorbed material relative to its concentration in the benzene-alcohol-recovered asphalt, is a measure of the tendency of the functional type to be adsorbed by the aggregate. The average concentration factor for ketones, the most weakly adsorbed materials, was 1.9. Dicarboxylic anhydrides were next in their affinity for the aggregate surface. The average concentration factor in strongly adsorbed material was 9.5. Carboxylic acids, the most strongly adsorbed, had an average concentration factor of 14.

Data in Table 4 show that although ketones were the most weakly adsorbed, they represented an estimated 61 percent of the strongly adsorbed material because of their great abundance. Anhydrides and acids accounted for a total of 13 and 10 percent respectively of the strongly adsorbed materials. These estimates assume monofunctional compounds with an average molecular weight of 700 and are at best only approximate. Based on these assumptions, the last column in Table 4 shows that 84 percent of the strongly adsorbed material, on the average, was ketones, anhydrides, and acids. The 2 individual estimates that are greater than 100 percent probably reflect inaccuracies in the assumptions—most likely, that no more than 1 functional group is produced on an individual molecule on oxidation.

Physical Measurements of Multilayer Adsorption of Asphalt Molecules

Considerable evidence has been collected in our laboratory supporting the thesis that many thousands of molecular layers of asphalt molecules are adsorbed on mineral surfaces (4, 12, 13). Only a summary of the findings dealing with this phenomenon, known as multilayer adsorption, will be presented here.

We first studied multilayer adsorption of asphalt by immersing -35+48-mesh aggregate particles in melted asphalt in a specially built differential microcalorimeter (4) to measure the energy released from interactions between the asphalt and aggregate as a function of time. The data are collected as a curve on a strip-chart recorder. Immersion curves (4) characteristically have an initial peak believed to be largely representative of the initial interactions of asphalt with the aggregate surface, followed by a long tail that remains nearly constant for hours or days. This tail on the curve is believed to represent energy released from multilayer adsorption or molecular orientation of asphalt molecules in the asphalt-aggregate interface region. The amounts of energy released in the heat-of-immersion studies are orders of magnitude greater than normal heats of wetting and can only be explained by a chemical reaction or by a continuous adsorption process. Arguments leading to the conclusion that heats of immersion are primarily a manifestation of multilayer adsorption rather than chemical reaction have been considered previously (4, 11, 12).

Heats of immersion have been determined on a number of different asphalt-aggregate systems at 130 and 150 C (403 and 432 K). Peak heights of the immersion curves were typically in the range of 2 to 15 mcal/g·min. Tail heights after 3 hours were 0.2 to 1.5 mcal/g·min. Values obtained on differing asphalt-aggregate systems were quite different from each other. Immersion energy at 150 C (423 K) may be either higher or lower than that at 130 C (403 K), depending on the particular asphalt-aggregate

Table 3. Concentrations of ketones, dicarboxylic anhydrides, and carboxylic acids in asphalts recovered from 11- to 13-year-old FHWA study road cores.

Asphalt Number	Strongly Adsorbed Asphalt (weight percent of total)[a]	Concentration (mol · l^{-1} × 10^{-2})						Strongly Adsorbed Functional Type (percent of total)[d]		
		Nonacid Carbonyls as Ketones		Dicarboxylic Anhydrides		Carboxylic Acids				
		B[b]	BA[c]	B	BA	B	BA	Ketones	Anhydrides	Acids
19	2.0	51.9	52.5	1.6	1.8	2.1	2.5	3.12	12.9	17.7
25	3.9	50.8	52.5	1.8	2.2	0.9	1.6	7.0	21.3	46.0
30	3.5	63.3	64.2	2.9	3.8	0.9	1.6	4.86	26.3	45.7
61	1.4	45.3	44.1	0.8	2.0	0.4	0.7	-1.28	60.5	43.7
67	2.3	30.9	31.5	0.6	1.0	0.4	0.5	4.17	41.4	21.8
71	3.7	49.8	51.0	1.8	2.2	0.2	0.4	5.96	21.2	51.9
72	3.4	64.5	67.5	2.5	2.9	0.4	0.7	7.7	16.7	44.8
73	3.0	33.3	35.3	0.7	1.1	0.2	0.4	8.5	38.5	51.5
74	4.3	40.5	42.6	1.2	1.7	0.2	0.7	9.03	32.4	72.6
166	1.2	21.3	22.5	0.8	0.9	0.5	1.0	6.47	12.2	50.6
Average	2.87	45.16	46.37	1.47	1.96	0.62	1.01	5.40	27.1	40.5

[a]Calculated from differences between total amounts desorbed with benzene and with benzene-alcohol.
[b]Concentration (mol/litre) of functional type in benzene extract.
[c]Concentration (mol/litre) of functional type in benzene-alcohol extract.
[d]Not desorbed with benzene but with a 4:1 mixture of benzene, 95 percent ethanol.

Table 4. Calculated data on the ketones, dicarboxylic anhydrides, and carboxylic acids strongly adsorbed from asphalts by the aggregates in 11- to 13-year-old FHWA study road cores.

Asphalt Number	Estimated Concentration Factor of Strongly Adsorbed Material[a]			Strongly Adsorbed Material (percent of total adsorbed)[b]			Sum of Strongly Adsorbed Materials[bc]
	Ketones	Anhydrides	Acids	Ketones	Anhydrides	Acids	
19	1.56	6.45	8.85	57.5	8.1	6.5	72
25	1.79	5.47	11.8	66.2	8.4	13.2	88
30	1.39	7.52	13.1	62.3	20.0	14.6	97
61	-0.92	43.1	31.2	-28.6	60.5	15.3	47
67	1.81	18.0	9.5	40.0	12.6	33.3	86
71	1.61	5.73	14.0	57.3	8.8	3.9	70
72	2.26	4.91	13.2	107	10.0	6.5	123
73	2.83	12.8	17.2	70.0	9.8	4.8	85
74	2.10	7.55	16.9	62.5	9.0	8.3	80
166	5.38	10.1	42.2	85.0	6.4	29.5	121
Average[d]	1.88	9.46	14.1	61.0	13.0	9.9	84

[a]Percent of functional type in strongly adsorbed material divided by percent of total asphalt in same fraction (compare Table 3).
[b]Calculated by assuming monofunctional molecules and a molecular weight of 700.
[c]Values are presented as percent of total strongly adsorbed asphalt.
[d]Calculations based on averages of concentrations (compare Table 3).

system. This apparent contradiction can be explained by considering the processes involved in multilayer adsorption. The rate of migration of molecules to adsorption sites is diffusion- (viscosity-) controlled and increases with temperature; but, in a reversible adsorption process, the tendency of the molecules to be adsorbed after collision with the adsorption sites is reduced with increasing temperature. The temperature dependence of the total adsorption process is therefore a net result of these 2 opposing effects.

Adding 1 percent Redicote 80S (an antistripping agent) to the asphalt before determining the heat of immersion greatly increased the immersion energy of some asphalt-aggregate systems, particularly that represented by the tail of the immersion curve. Treatment of the aggregate surface with silylating reagents or with diazomethane apparently inhibited multilayer adsorption because it caused a complete loss of the tail of the immersion curve.

Of particular significance is the apparent slow rate of the proposed multilayer adsorption process. Heat-of-immersion data suggest that this goes on for several days at the test temperatures. The slow rate of the asphalt molecular association reactions also has been demonstrated in independent microcalorimetric studies without aggregate. Reversible interactions of the order of 1 to 2 cal/g have been shown to take place in asphalt (12); these interactions take hours to reach equilibrium at 150 C (423 K). The slow nature of the interactions is undoubtedly influenced by viscosity and the complexity of the system. Asphalt is a complex mixture of many structurally different molecules, and the concentration of any one is extremely low. Association reactions are specific for molecular type and orientation; therefore the probability of a molecular collision in asphalt resulting in an association reaction is low.

Additional evidence for multilayer adsorption was obtained from FTPM experiments (13). For example, when filtered asphalt B-3036 containing 1 percent of the antistripping agent Redicote 80S was flowed at constant static pressure through a bed of -100+150-mesh phosphate slag at 130 C (403 K) in a nitrogen atmosphere, the flow rate decreased in a regular fashion. After 9 days the flow rate decreased from 6.1×10^{-3} g/min to 0.33×10^{-3} g/min, indicating that the "free" volume through which the asphalt could flow was reduced from its initial 45 percent to 5 percent. Thus it appears that asphalt molecules gradually build up on the surface of the aggregate in an immobilized layer to restrict the normal flow through the plug. The calculated buildup rate was 17.5 ± 1.5 Å/min. Assuming molecular interactions in the adsorption process on the order of a fraction of a calorie per mole, the buildup rate is consistent with the energy released in heat-of-immersion studies.

The immobilized asphalt material in the plug from the FTPM experiment was dissolved from the aggregate with carbon tetrachloride. The recovered material was analyzed by infrared spectroscopy and found to be essentially identical to the original asphalt. No significant concentration of antistripping agent was found in the material from the plug. Molecular weight determinations by vapor pressure osmometry in benzene of the material from the plug and the original asphalt were 910 and 876 respectively. Thus it appears that although the asphalt was immobilized in the plug it was not significantly fractionated or altered chemically.

A general correlation exists between the data from the heat-of-immersion and FTPM studies. For example, in a number of different systems the heat-of-immersion energy and the decrease in flow rate in FTPM experiments were both greater when the antistripping agent was added to the asphalt. Also, in a model FTPM study, the flow of asphalt B-3036 through a laboratory adsorbent of bauxite ($Al_2O_3 \cdot 2H_2O$) nearly ceased in an unusually short time—5 hours at 130 C (403 K)—indicating that 95 percent of the void space had closed off; the calculated buildup rate of the immobilized layer was about 3000 Å/min. Heat-of-immersion experiments on this system showed peak and tail heights of 264 and 3.6 mcal/g·min respectively, much greater than for normal aggregates.

Recently, both optical and scanning-electron photomicroscopy provided evidence of molecular orientation of asphalt on mineral surfaces (13). Oriented layers were prepared by heating $\frac{1}{8}$ to $\frac{1}{4}$ in. of asphalt in an aluminum dish under nitrogen atmosphere for 10 to 14 days at 130 or 150 C (403 or 423 K). The aluminum surface may be replaced

by mica, calcite, or some other mineral by placing a smooth wafer of the mineral in the bottom of the dish before adding asphalt. After heating for the extended period, the samples were rapidly cooled and fractured perpendicular to the surface that was previously in contact with the bottom of the pan. Microscopy showed a striated region with sharply defined boundaries emanating from and perpendicular to the surface initially in contact with the mineral. A general correlation was found between the thickness of the striated regions and the buildup rate of the immobilized layers calculated from FTPM experiments. For example, when Asphalt B-3036 containing 1 percent Redicote 80S was heated on a mica surface for 2 weeks at 130 C (403 K), cooled, and fractured, a striated region 0.04 mm thick was observed. The calculated buildup rate was 24 Å/min, which is of the same order of magnitude as the buildup rate calculated from FTPM.

POSSIBLE SIGNIFICANCE TO ASPHALT PAVING TECHNOLOGY

One might speculate on the significance of the work reported in this paper to asphalt paving technology. The IGLC and chemical identification work showed that products of oxidation in asphalt interact with aggregate surfaces and that different aggregates have quite different responses. Because considerable oxidation of asphalt occurs in a hot-mix plant and while a road is being laid, amounts and nature of the oxidation products adsorbed on the aggregate surfaces must be important to adhesion and water-stripping resistance. Because these oxidation products and other interacting species must migrate to the aggregate surface, the viscosity of the asphalt at elevated temperatures may be quite important. Significant molecular migration is unlikely after the asphalt has cooled to ambient temperatures, except over long periods of time. Furthermore, multilayer adsorption to produce immobilized layers in the asphalt-aggregate interface region appears to take place very slowly—even near plant-mix temperatures, 130 to 150 C (403 to 423 K). A "solid" layer of asphalt on the aggregate surface might be of considerable benefit in preventing deterioration of the mix by water. Thus, the potential improvement of stripping resistance by hot storage before asphalt lay-down should be investigated.

Any immobilization of asphalt in the asphalt-aggregate interface region after the road has been compacted should increase the bonding strength or friction at the points of contact between aggregate particles, which would be reflected in the physical properties of the asphalt concrete. This reasoning suggests that the cooling rate of a freshly laid road mix may be important. The buildup of an immobilized asphalt layer may thus be related to such phenomena as "setting rate" and "tender mixes." The possible relationship between the data presented in this paper, which suggest that certain antistripping agents affect the rate of multilayer adsorption of asphalt molecules, and data reported from field observations, which suggest that antistripping agents often alter mix characteristics, might well be studied.

ACKNOWLEDGMENT

The authors gratefully acknowledge partial financial support of this work by the Federal Highway Administration in an interagency cooperative program with the U.S. Bureau of Mines. In particular the personal interest and assistance given by Woodrow J. Halstead, Edward Oglio, and others of the Office of Research, Materials Division, Federal Highway Administration, are greatly appreciated.

Mention of specific brand names or models of equipment has been made for information only; it does not imply endorsement by the U.S. Bureau of Mines.

REFERENCES

1. Majidzadeh, K., and Brovold, F. N. State of the Art: Effect of Water on Bitumen-Aggregate Mixtures. HRB Spec. Rept. 98, 1968, 77 pp.
2. Mack, C. Physical Properties of Asphalts in Thin Films. Ind. Eng. Chem., Vol. 49, 1957, pp. 422-427.

3. Watanabe, T., and Abe, Y. Special Characteristics of Thin Asphalt Films in Filler-Asphalt and Sand-Filler-Asphalt Mixes. Div. Petrol. Chem., Amer. Chem. Soc., Preprints, Vol. 16, No. 1, 1971, pp. D74-D88.
4. Ensley, E. K., and Scholz, H. A. A Study of Asphalt-Aggregate Interactions by Heat of Immersion. Jour. Inst. Petrol., Vol. 58, 1972, pp. 95-101.
5. Davis, T. C., Petersen, J. C., and Haines, W. E. Inverse Gas-Liquid Chromatography: A New Approach for Studying Petroleum Asphalts. Anal. Chem., Vol. 38, No. 2, 1966, pp. 241-243.
6. Davis, T. C., and Petersen, J. C. An Adaptation of Inverse Gas-Liquid Chromatography to Asphalt Oxidation Studies. Anal. Chem., Vol. 38, No. 13, 1966, pp. 1,938-1,940.
7. Davis, T. C., and Petersen, J. C. An Inverse GLC Study of Asphalts Used in the Zaca-Wigmore Experimental Road Test. Proc. AAPT, Vol. 36, 1967, pp. 1-15.
8. Davis, T. C., and Petersen, J. C. Inverse Gas-Liquid Chromatographic Studies of Asphalt: Comparison With Analyses by Fractionation. Anal. Chem., Vol. 39, No. 14, 1967, pp. 1,852-1,857.
9. Barbour, F. A., Dorrence, S. M., and Petersen, J. C. Inverse Gas-Liquid Chromatographic Studies of Asphalt: Variations in Experimental Parameters. Anal. Chem., Vol. 42, No. 6, 1970, pp. 668-670.
10. Barbour, F. A., Barbour, R. V., and Petersen, J. C. A Study of Asphalt-Aggregate Interactions Using Inverse Gas-Liquid Chromatography. Jour. Appl. Chem and Biotech., 1974.
11. Petersen, J. C. A Quantitative Method for the Determination of Compound Types in Asphalts Absorbing in the Carbonyl Region of the Infrared Spectra. Anal. Chem., 1974.
12. Ensley, E. K. A Study of Asphalt-Aggregate Interactions and Asphalt Molecular Interactions by Microcalorimetric Methods—A Proposed Reaction Mechanism. Jour. Inst. Petrol., Vol. 59, No. 570, 1973, pp. 279-289.
13. Ensley, E. K. Orientation of Asphalt Molecules Adsorbed on Mineral Aggregate Surfaces and Other Substrates. U.S. Bureau of Mines, Laramie, Wyoming.
14. Welborn, J. Y., Oglio, E. R., and Zenewitz, J. A. A Study of Viscosity-Graded Asphalt Cements. Proc. AAPT, Vol. 35, 1966, pp. 19-60.
15. Schmidt, R. J., and Santucci, L. E. A Practical Method for Determining the Glass Transition Temperature of Asphalts and Calculation of Their Low Temperature Viscosities. Proc. AAPT, Vol. 35, 1966, pp. 61-90.
16. Puzinauskas, V. P. Evaluation of Properties of Asphalt Cements With Emphasis on Consistencies at Low Temperatures. Proc. AAPT, Vol. 36, 1967, pp. 489-540.
17. Welborn, J. Y., and Halstead, W. J. Properties of Highway Asphalts, Part I: 85-100 Penetration Grade. Public Roads, Vol. 30, 1959, pp. 197-207.
18. Welborn, J. Y., Halstead, W. J., and Boone, J. G. Properties of Highway Asphalts, Part II: Various Grades. Public Roads, Vol. 31, 1960, pp. 73-85, 99.
19. Rostler, F. S., and White, R. M. Composition and Changes in Composition of Highway Asphalts—85-100 Penetration Grade. Proc. AAPT, Vol. 31, 1962, pp. 35-89.
20. Vallerga, B. A., and Halstead, W. J. Effects of Field Aging on Fundamental Properties of Paving Asphalts. Highway Research Record 361, 1971, pp. 71-92.
21. Petersen, J. C. An Infrared Study of Hydrogen Bonding in Asphalts. Fuel, Vol. 46, 1967, pp. 295-305.
22. Ramsey, J. W., McDonald, F. R., and Petersen, J. C. Structural Study of Asphalts by Nuclear Magnetic Resonance. Ind. Eng. Chem. Prod. Res. Develop., Vol. 6, 1967, pp. 231-236.
23. Helm, R. V., and Petersen, J. C. Compositional Studies of an Asphalt and Its Molecular Distillation Fractions by Nuclear Magnetic Resonance and Infrared Spectroscopy. Anal. Chem., Vol. 40, 1968, pp. 1,100-1,103.
24. Helm, R. V. Separation of Asphaltic Materials by Reversed Phase Partition and Adsorption Chromatography: Comparison of Fractions by Infrared Spectrometry. Anal. Chem., Vol. 41, 1969, pp. 1,342-1,344.
25. Barbour, R. V., and Petersen, J. C. Molecular Interactions of Asphalts: An Infrared Study of the Hydrogen-Bonding Basicity of Asphalt. Anal. Chem., Vol. 46, 1974, pp. 273-277.

STORAGE OF ASPHALT CONCRETE

Michael S. Zdeb and Ronald A. Brown, New York State Department of Transportation

The effect of asphalt concrete storage on asphalt cement properties and on the variability of gradation and asphalt content was determined. One mix stored in inert gas and 2 stored in normal atmospheres (all for 18 hours) were sampled before and after storage. In addition to these, 1 stored for 48 hours in an inert gas and another stored for 24 hours in a normal atmosphere were sampled solely to determine changes in asphalt cement properties. Four mixes were resampled from pavements after 1 year for further comparison of properties of asphalts from stored and control mixes. Properties of asphalt cement extracted from fine mixes were not altered by storage in either inert gas or normal atmospheres. Coarse mixes stored in normal atmospheres hardened significantly. For the 4 mixes resampled after 1 year in pavements, all initial similarities and differences were maintained. Gradation variability of all mixes, both fine and coarse, was increased by storage. Fine mix cores taken shortly after construction, however, show stored mix to be no more variable than mix directly from the pug mill.

•THE FLEXIBILITY of operation and economic benefits accorded by asphalt concrete storage bins have led to a marked increase in their use. With this have come numerous types of facilities manufactured for storing asphalt concrete. This combination of increased use and varying facilities has generated concern about the effects of storage on asphalt concrete gradation, asphalt content, and asphalt cement properties. Several studies have been initiated to determine the effects of storage on mix and asphalt characteristics.

Many factors may influence the effects of storage on asphalt concrete. Table 1 gives some and the mix component they might affect. A number of investigators have attempted to determine the significance of various combinations of these factors. However, because of the variety of possible combinations, no single study gave definitive answers to all questions.

The effects of storage fall into 2 main areas—asphalt cement and gradation (asphalt content included). Table 2 gives the correspondence between studies that have dealt with measurement of change in asphalt cement characteristics. Methods of sampling, sample sizes, and numbers of samples differed from study to study.

Tuttle (1) concluded that asphalt cement hardens significantly if asphalt concrete is stored in the temperature range of 250 to 350 F (121.1 to 162.8 C) for prolonged periods; neither segregation nor asphalt migration was investigated. Middleton, Goodknight, and Eaton (2) stored fine-graded asphalt concrete for 4 days, sampling the mix periodically to the point of final discharge from the storage bin. Although a marked change in the asphalt cement occurred during mixing in the pug mill, negligible change resulted from storage. Again, segregation and asphalt migration were not specifically studied, although past problems with asphalt migration were cited, which led to regular use of a silicone additive. Thus, silicone was incorporated into their work not to prevent oxidizing but to prevent nonuniform asphalt content. Pavements placed with mix from Middleton, Goodknight, and Eaton's study and with mix placed at the same time but not subjected to storage were cored after 1 year in service (3). No significant difference was found between asphalt cement penetrations from the 2 sets of cores; both pavements had hardened approximately 20 penetration points since the original sampling.

Publication of this paper sponsored by Committee on Characteristics of Bituminous Materials.

Table 1. Factors affecting hot-mix storage.

Factor	Mix Property Influenced		
	Gradation Variability	Asphalt Content Variability	Asphalt Cement Consistency
Storage system			
Type of loading device	✓	✓	
Bin shape	✓	✓	
Presence or absence of insulation and/or heating system			✓
Normal or inert atmosphere			✓
Asphalt concrete mix			
Gradation and asphalt content	✓	✓	✓
Composition and inherent properties of asphalt cement		✓	✓
Presence or absence of silicone or other antioxidant		✓	✓
Situation-specific variables			
Duration		✓	✓
Temperature		✓	✓

Table 2. Effect of storage on asphalt cement.

Reference	Bin Description	Atmosphere	Temperature (deg F)	Storage Duration (hours)	Additive	Gradation	Asphalt Content (percent)	Asphalt Penetration Grade[a]	Decrease in Asphalt Cement Penetration[b] (percent)
1	Fully insulated, hot-oil heated, cylindrical silo	Normal	300	17	None	Fine	6.5	85-100 (60)	38
				66				85-100 (57)	39
				19				85-100 (78)	22
				66				85-100 (60)	25
2	Fully insulated, lower third hot-oil heated (cone), cylindrical silo	Normal	≈300	22.5	Silicone	Fine	7.5	85-100 (69)	None
				71.5					16
				95.0					3
4	Not given	Normal	Not given	24	None	Fine	≈5.0	85-100 (68)	42
				24	Silicone	Fine	≈5.5	85-100 (74)	16
				72					49
5	Fully insulated, hot-oil heated, cylindrical silo	Normal	≈300	24	Silicone	Fine	4.9	85-100 (73)	23
				72					59
		Normal	≈300	24	None	Fine	4.9	85-100 (68)	46
		Normal	320	24	Proprietary	Fine	4.2	40-50 (29)	None
				72					None
		Normal	≈300	24	None	Fine	4.2	40-50 (32)	None
				72					47
6	Fully insulated, hot-oil heated, oval bin	Inert	≈300	24	Silicone	Coarse	4.9	— (48)	None
				72					None
		Normal		24			5.2	— (59)	24
				72					None
		Inert		24	None	Coarse	5.0	— (55)	7
				72					23
		Normal		24			5.0	— (54)	41
				72					30
7	Fully insulated, hot-oil heated, cylindrical silo	Inert	≈300	168	None	Coarse-fine	5.4	85-100 (79)	23
8	Fully insulated, hot-oil heated, cylindrical silo	Inert	≈315	24	None	Fine	—	AC-20 (42)	25
				72					21
		Inert	≈300	24		Coarse	3.6	AC-20 (48)	19
				72					21
9	Fully insulated, hot-oil heated, cylindrical silo	Normal	—	23	—	Fine	≈5.0	— (51)	10
				47					18

Note: 1°C = 5/9 (°F - 32).

[a]Numbers in parentheses are penetrations of asphalt at 77 F (25 C) extracted immediately before storage.
[b]Changes in penetration measured as percent decrease from penetration after pug mill mixing but before bin loading; all values are for penetrations at 77 F (25 C).

Table 3. Storage installations sampled.

Installation	Year	Bin Number	Bin Description	Capacity	Atmosphere	Temperature (deg F)	Loading Device	Gradation[a]	Asphalt Content (percent)	Asphalt Grade	Duration (hours)
1	1971	2	Fully insulated, hot-oil heated, cylindrical silo	160 tons 160 tons	Inert gas	300	Slat conveyor	Fine (1A top)	6.0	85-100	18
2	1972	2	Fully insulated, hot-oil heated, cylindrical silo	150 tons 150 tons	Inert gas	310	Slat conveyor	Fine (1A top)	6.4	AC-20	48
3	1973	2	Fully insulated, unheated, rectangular bin	200 tons 250 tons	Normal	300	Skip hoist	Fine (1A top)	6.2	AC-20	24
4[b]	1971	2	Fully insulated, unheated, rectangular bin	140 tons 180 tons	Normal	275	Skip hoist	Coarse (1A binder)	4.5	85-100	18
5[b]	1971	2	Fully insulated, unheated, rectangular bin	140 tons 180 tons	Normal	275	Skip hoist	Coarse (1A base)	3.7	85-100	18

Note: 1°C = 5/9 (°F - 32), 1 U.S. ton = 0.907 metric ton.

[a]No additives are used. New york State specifications are given in parentheses.
[b]Two mixes sampled at different times at the same location.

Vallerga and White (4) attempted to assess the merits of silicone as an antioxidant during storage. They reported that the hardening rate was significantly decreased by adding silicone. In cases with and without silicone there was no asphalt cement migration or mix segregation.

Foster (5) also found silicone to be a means of extending storage time. He stated nothing conclusive about segregation and migration; he found them to have occurred in some of his investigations but not in others. Another study by Foster (6) concerned the effects of an inert gas atmosphere on storage of coarse mixes. A combination of a silicone additive and inert gas resulted in no change in asphalt cement penetration after 3 days of storage. Even without silicone, however, inert gas provided a significant improvement over normal atmosphere in preventing asphalt hardening. Segregation and changes in asphalt content occurred, but asphalt content variations were shown to be related to variations in mix gradation and were attributed to segregation.

Two other studies involving inert gas systems were conducted by Parr and Brock (7) and Kandahl and Wenger (8). In neither case was silicone present. Parr and Brock found a statistically significant decrease in asphalt cement penetration after 7 days of storage. They stated, however, that the percent of retained penetration after storage still conformed to many thin-film-oven-loss test specifications. Segregation within trucks occurred as the mix was unloaded from the bin. Kandahl and Wenger found that both fine and coarse mixes hardened at similar rates. After 72 hours, each experienced a 21 percent increase in penetration. They also stated that only the normal variation inherent in asphalt concrete production was evident in mix gradation and asphalt content.

In a recent Louisiana study, Hearld and Lay (9) stored a fine-graded mix in a normal atmosphere and found 10 and 18 percent decreases in penetration after 1 and 2 days respectively.

Because of the large number of factors involved, no one study answered all questions involved with storage. However, several points are evident from past work. First, both inert gas and silicone can extend storage times for asphalt concrete beyond those possible with normal atmospheres and untreated asphalt cements. Second, the degree of hardening of asphalt cement is situation specific, that is, no all-encompassing statements can be made for different times and temperatures about how hard asphalts will become because of storage in various systems. Third, little work has been done to determine whether effects on asphalt cement consistency are transitory or lasting; only 1 study involved resampling a stored mix that had been in place for an extended period. Fourth, experience with mix segregation has differed from study to study; limited work has been directed toward determining whether asphalt concrete variability increased by storage is negated by the laydown process, that is, the remixing in the paver.

The objectives of the study reported here were to determine the following for each installation sampled:

1. Effect of storage on variability of aggregate gradation and asphalt content;
2. Whether increased variability that may be detected remains after stored mixes are placed and compacted;
3. Effect of storage on penetration, viscosity, and ductility of asphalt cement; and
4. Whether storage effects on asphalt cement are transitory or lasting.

The situation of storage systems available for study in New York State made choosing specific combinations of system and mix factors (the first 2 groups in Table 1) impossible. This investigation, which seeks to clarify the issue of the effects of storage on asphalt concrete, should be viewed as a replication and expansion of previous research of others.

SAMPLING AND TESTING

Storage systems were studied as they began operating on state contracts. In 1971, only 2 were available for sampling and testing. Although the number of installations in New York increased markedly beginning in 1972, only 2 more were sampled—1 in 1972, another in 1973. These installations were the only 2 both operating on state contracts and offering a combination of factors different from the 2 sampled in 1971.

All installations were studied for changes in asphalt cement properties, but only installations 1, 4, and 5 (Table 3) were studied for changes in gradation variability. For each of these 3, sampling was a 2-day operation. On the first day, mix going directly from the pug mill to the pavement was sampled from trucks immediately after discharge from the pug mill. Storage bins at each of these locations were loaded on the first day with mix sampled from the loading device before storage. On the second day the storage bin was emptied into trucks for hauling to the job site. Mix was sampled from each truck immediately after discharge from the bin; cores were taken once the mix was in place. Cores also were taken from a section of road containing mix directly from the pug mill that was placed the first day.

Installations tested only for asphalt cement properties were sampled by coring sections paved with mix that came directly from the pug mill and with mix that came out of storage bins. The numbers of samples taken from the 5 installations are given in Table 4.

All loose mix samples were of a 1-gal (3.8-dm^3) size; cores were 6 in. in diameter. Cores were not quenched or packed in dry ice, but they were stored at 20 F (-6.7 C) until testing. Asphalt was extracted from all samples according to ASTM D 2172-67 (Method B: trichlorethylene solvent). Asphalt cement was recovered by using the Abson method (ASTM D 1856-69). Recovered asphalts were tested by using the following procedures:

1. ASTM D 5-65 at 77 F (25 C) for penetration;
2. ASTM D 2171-66 at 140 F (60 C) with a Cannon-Manning vacuum viscometer and ASTM D 2170-67, 275 F (135 C) with a Zeitfuchs cross-arm viscometer for viscosity; and
3. ASTM D 113-69 at 60 F (15.6 C) for ductility.

Aggregate was sieved according to New York State Materials Method 5.

ASPHALT CEMENT PROPERTIES

Summaries of results of tests on recovered asphalt cements are given in Tables 5 and 6 and Figure 1. Ductility results are presented as histograms because of the impossibility of computing statistics from data often reported as 100+ cm rather than as discrete values. The following hypothesis was tested for all properties given in Tables 5 and 6:

$$H_0 : \mu \text{ stored} \leq \mu \text{ control}$$

$$H_1 : \mu \text{ stored} > \mu \text{ control}$$

where $\mu \equiv$ mean (asphalt cement property).

The t-distribution was used at the 0.01 significance level. Acceptance of the hypothesis H_0 indicates that there is no evidence showing asphalt cement to be harder after storage than from mix directly out of the pug mill. Rejection of H_0 indicates that a change has occurred—that a real difference was caused by storage.

Inert Gas

Storage of fine mixes in an inert gas atmosphere for periods of 18 and 48 hours did not significantly alter their asphalt cement properties (penetration and viscosity) when compared to a control mix placed directly from the pug mill. Although asphalt cements from both stored and control mixes increased in consistency from their original state, there is no experimental evidence to consider the stored asphalts harder. Figure 1 shows no change in ductility at 60 F (15.6 C) for the mix stored for 18 hours. After 1 year, asphalt cements can be seen to have hardened; both stored and control mixes harden at the same rate. Thus, a fine mix stored in inert gas appears to have suffered no detrimental effects. No data were generated on coarse mix storage.

Table 4. Sample size.

Installation	Loose Mix: After Pug Mill	Loose Mix: From Loading Device	Loose Mix: After Storage Bin	Cores From Road: At Construction	Cores From Road: After 1 Year
1	72	To bin 1: 25 To bin 2: 25	72	72 (36 stored, 36 control)	30 (18 stored, 12 control)
2	—	—	—	22 (13 stored, 9 control)	20 (14 stored, 6 control)
3	—	—	—	31 (22 stored, 9 control)	—
4	75	To bin 1: 22 To bin 2: 28	75	72 (36 stored, 36 control)	30 (18 stored, 12 control)
5	75	To bin 1: 22 To bin 2: 28	75	72 (36 stored, 36 control)	19 (10 stored, 9 control)

Table 5. Asphalt cement properties in mixes stored in normal atmosphere.

Mix	Number of Samples	Penetration at 77 F[a]: Mean	Penetration at 77 F[a]: Standard Deviation	Viscosity at 140 F: Mean (poises)	Viscosity at 140 F: Standard Deviation (poises)	Viscosity at 275 F: Mean (centistokes)	Viscosity at 275 F: Standard Deviation (centistokes)
Sampled at Construction							
Fine, top course, stored 24 hours							
Stored	22	40	3	6 110	1 100	625	113
Control	9	40	4	6 600	1 900	710	70
Coarse, binder course, stored 18 hours							
Stored	36	38	3	12 560	2 370	840	58
Control	34	59	6	3 830	940	520	48
Coarse, base course, stored 18 hours							
Stored	30	46	5	6 375	1 065	615	40
Control	32	63	6	2 970	770	445	45
Sampled After 1 Year in Place[b]							
Coarse, binder course, stored 18 hours							
Stored	18	35	5	17 600	5 160	970	105
Control	12	52	3	4 870	470	585	25
Coarse, base course, stored 18 hours							
Stored	10	50	5	5 250	1 475	555	75
Control	9	62	6	2 880	450	450	35

Note: 1°C = 5/9 (°F - 32).

[a]0.1 mm, 100 g, 5 s. [b]Top course placed in 1973; no data available.

Table 6. Asphalt cement properties in mixes stored in inert gas atmosphere.

Mix	Number of Samples	Penetration at 77 F[a]: Mean	Penetration at 77 F[a]: Standard Deviation	Viscosity at 140 F: Mean (poises)	Viscosity at 140 F: Standard Deviation (poises)	Viscosity at 275 F: Mean (centistokes)	Viscosity at 275 F: Standard Deviation (centistokes)
Sampled at Construction							
Fine, top course, stored 18 hours							
Stored	33	56	5	2 760	325	460	28
Control	35	55	6	2 835	580	455	27
Fine, top course, stored 48 hours							
Stored	13	54	6	3 990	910	590	50
Control	9	55	1	3 320	180	555	10
Sampled After 1 Year in Place							
Fine, top course, stored 18 hours							
Stored	—	36	4	5 280	1 070	590	40
Control	—	36	4	6 255	1 000	590	33
Fine, top course, stored 48 hours							
Stored	14	46	6	5 030	1 080	655	70
Control	6	41	6	5 355	110	640	7

Note: 1°C = 5/9 (°F - 32).

[a]0.1 mm, 100 g, 5 s.

Figure 1. Asphalt cement ductilities at 60 F at construction.

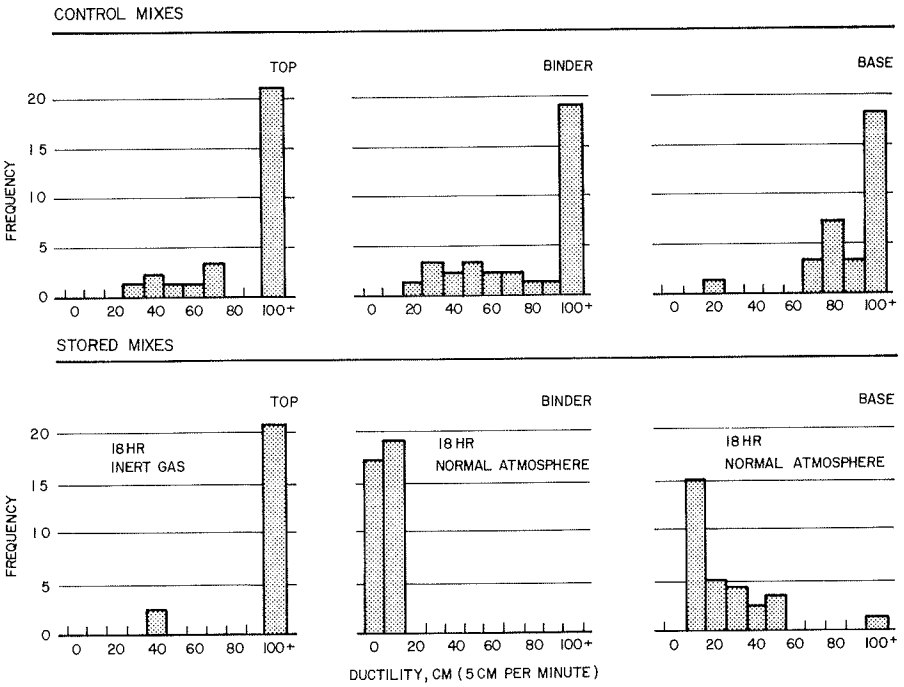

Table 7. Gradation variances on a sieve basis at different sampling locations.

Sieve	Pug Mill	Bin 1 In	Bin 1 Out	Bin 2 In	Bin 2 Out	In Place Pug Mill	In Place Stored	Specification
Fine Mix, Top Course, Cylindrical Bin								
½ in.	0.00	0.00	0.00	0.00	0.06	0.00	0.00	6.25
¼ in.	9.67	4.30	7.04	3.93	29.96	9.80	9.92	12.25
⅛ in.	4.59	0.94	5.60	1.99	12.03	7.90	5.95	12.25
No. 20	1.51	1.65	2.10	0.32	3.31	3.88	3.24	12.25
No. 40	0.83	0.45	0.45	0.22	0.63	3.28	0.48	12.25
No. 80	0.27	0.14	0.44	0.04	0.30	0.19	1.61	4.00
No. 200	0.10	0.11	0.14	0.04	0.18	0.10	0.20	1.00
Percent AC	0.04	0.07	0.03	0.02	0.05	0.41	0.36	0.04
Total samples	70	22	35	24	34	36	36	—
Coarse Mix, Binder Course, Rectangular Bin								
1 in.	0.04	0.00	0.00	0.06	0.00	—	—	6.25
½ in.	6.45	7.67	8.59	4.62	15.73	—	—	9.00
¼ in.	5.38	1.77	5.87	0.90	9.24	—	—	4.00
⅛ in.	2.56	0.32	1.34	0.45	2.94	—	—	2.25
Percent AC	0.20	0.04	0.08	0.02	0.05	—	—	0.04
Total samples	71	21	33	28	40	—	—	—
Coarse Mix, Base Course, Rectangular Bin								
1 to 2 in.	0.00	0.00	0.00	0.00	0.00	—	—	12.25
1 in.	43.96	31.93	49.41	16.82	23.16	—	—	16.00
½ in.	30.91	13.35	40.94	5.23	29.02	—	—	12.25
¼ in.	7.08	6.60	13.26	2.56	7.14	—	—	9.00
⅛ in.	2.50	1.65	2.47	5.28	1.82	—	—	4.00
Percent AC	0.16	0.03	0.14	0.13	0.75	—	—	0.04
Total samples	68	22	32	28	33	—	—	—

Note: 1 in. = 25.4 mm.

Normal Atmosphere

Results of storage of a fine mix in a normal atmosphere paralleled those for storage in inert gas. After 24 hours of storage, asphalt cement extracted from a fine mix was not significantly harder than a control mix. Because stored and control mixes were both placed in 1973, they have yet to be recored to determine asphalt hardening rate.

Both coarse mixes (binder and base) stored for 18 hours in normal atmospheres experienced significant changes in asphalt cement consistency and ductility. The consistency differences have been maintained for a 1-year period, but neither has hardened as much as the fine (top course) mixes stored in inert gas. The base course, covered by both binder and top course mixes, has been protected from the effects of exposure to air and sunlight. The binder course has benefited from the cover provided by the top course. The very slow hardening rate of subsurface courses indicates that although storage caused a significant change in asphalt cement consistency, the change possibly could be tolerated. Observations of pavement condition where these mixes are in place bear this out.

VARIABILITY OF GRADATION AND ASPHALT CONTENT

Gradation variances for each of the 3 mixes sampled are given in Table 7, which also gives specification variances for each sieve and for asphalt content. Specification tolerances are based on 2 standard deviations as determined in previous studies of mix variability in New York State. The tolerances were halved, then squared, to determine the specification variances given in Table 7.

Mean gradations can be found in Table 8. No inferences were attempted about the effect of storage through use of the mean values. If sampling of the storage process is done to characterize all material entering and leaving a bin, mean comparisons should always result in statistical equality. When statistically significant differences in mean values are found, either of the following has happened: The aggregate has undergone some physical change (degradation), or more likely, sampling at either the loading or discharge points (or both) was inadequate to characterize the material in question.

Mean comparisons, therefore, do have some value because they can indicate the adequacy of sampling procedures. However, if the purpose is to compare all material before storage to all after storage, variability should be considered.

A multivariate approach was used to compare gradation variability at different points (10). Covariance matrices were computed at each production point given in Table 7 (except the pug mill) and compared as follows:

$$H_0 : \Sigma \text{ into bin} \geq \Sigma \text{ out of bin}$$

$$H_1 : \Sigma \text{ into bin} < \Sigma \text{ out of bin}$$

where $\Sigma \equiv$ covariance matrix (overall gradation).

In addition, for top course mix, in-place comparisons were made between pug mill and stored mixes.

Asphalt content variability was compared using the univariate F-test as follows:

$$H_0 : \sigma^2 \text{ into bin} \geq \sigma^2 \text{ out of bin}$$

$$H_1 : \sigma^2 \text{ into bin} < \sigma^2 \text{ out of bin}$$

where $\sigma^2 \equiv$ variance (asphalt content). Both covariance and variance comparisons used the F-distribution at the 0.01 significance level.

All mixes—fine and coarse—changed in overall gradation variability because of the storage process. For the fine mix (top course) the greatest change was in $\frac{1}{4}$- and $\frac{1}{8}$-in. (6- and 3-mm) material leaving the bin. The 2 coarse mixes were most affected on the $\frac{1}{2}$- and $\frac{1}{4}$-in. (13- and 6-mm) materials. The 1 additional gradation comparison, between in-place fine mixes stored and direct from the pug mill, showed no difference in

Table 8. Gradation statistics.

Sieve	Pug Mill	Into Bin 1	Out of Bin 1	Into Bin 2	Out of Bin 2	Pug Mill in Place	Stored in Place
Top Course							
½ in.							
Mean	99.94	99.99	99.99	99.99	99.89	99.99	100.00
Standard deviation	0.08	0.02	0.02	0.01	0.25	0.00	0.00
¼ in.							
Mean	74.03	75.50	75.42	77.30	72.38	78.24	78.48
Standard deviation	3.11	2.07	2.65	1.98	5.47	3.13	3.15
⅛ in.							
Mean	49.15	50.67	50.62	51.24	48.08	51.96	53.12
Standard deviation	2.14	0.97	2.37	1.41	3.47	2.81	2.44
No. 20							
Mean	30.77	30.37	30.77	32.42	30.06	31.05	30.95
Standard deviation	1.23	1.28	1.45	0.57	1.82	1.97	1.80
No. 40							
Mean	14.73	14.75	14.25	15.32	14.48	15.90	16.56
Standard deviation	0.91	0.67	0.67	0.46	0.79	1.81	0.69
No. 80							
Mean	3.27	3.65	3.27	3.38	3.15	4.44	5.01
Standard deviation	0.52	0.37	0.67	0.21	0.55	0.44	1.27
No. 200							
Mean	1.93	2.26	1.93	2.00	2.18	2.62	2.91
Standard deviation	0.31	0.33	0.37	0.20	0.43	0.31	0.45
Percent AC							
Mean	6.17	6.16	6.10	6.12	5.93	6.53	6.40
Standard deviation	0.21	0.26	0.17	0.15	0.23	0.64	0.60
Total samples	70	22	35	24	34	36	36
Binder Course							
1 in.							
Mean	99.98	100.00	100.00	99.92	100.00	–	–
Standard deviation	0.19	0.00	0.00	0.25	0.00	–	–
½ in.							
Mean	61.30	65.12	60.69	62.42	63.32	–	–
Standard deviation	2.54	2.77	2.93	2.15	3.97	–	–
¼ in.							
Mean	25.11	24.19	28.23	24.04	24.24	–	–
Standard deviation	2.32	1.33	2.42	0.95	3.04	–	–
⅛ in.							
Mean	15.60	17.70	18.21	17.75	18.03	–	–
Standard deviation	1.60	0.57	1.16	0.67	1.71	–	–
Percent AC							
Mean	4.30	4.42	4.42	4.40	4.59	–	–
Standard deviation	0.14	0.21	0.28	0.14	0.23	–	–
Total samples	71	21	33	28	40	–	–
Base Course							
1 to ½ in.							
Mean	100.00	100.00	100.00	100.00	100.00	–	–
Standard deviation	0.00	0.00	0.00	0.00	0.00	–	–
1 in.							
Mean	59.68	66.56	64.18	64.21	63.77	–	–
Standard deviation	6.63	5.65	7.03	4.10	4.81	–	–
½ in.							
Mean	23.23	33.72	31.47	32.35	31.08	–	–
Standard deviation	5.56	3.65	6.40	2.29	5.39	–	–
¼ in.							
Mean	11.89	18.49	19.13	16.16	16.57	–	–
Standard deviation	2.66	2.57	3.64	1.60	2.67	–	–
⅛ in.							
Mean	9.93	11.92	12.68	8.79	8.30	–	–
Standard deviation	1.58	1.28	1.57	2.30	1.35	–	–
Percent AC							
Mean	3.13	3.46	3.63	3.44	3.80	–	–
Standard deviation	0.40	0.17	0.39	0.37	0.50	–	–
Total samples	68	22	32	28	33	–	–

Note: 1 in. = 25.4 mm.

overall variability. Apparently, the construction procedures produced enough remixing of material to counteract any variability increase caused by storage of the fine mix.

Asphalt content variability comparisons were of questionable value when the changes in gradation were found. Although changes in asphalt content variability occurred in 2 cases (binder from bin 2, base from bin 1), past research has shown that such changes may result from variations in gradation (6). Therefore, no conclusions were reached about the effect of storage on variations in asphalt content.

Gradation variability data were analyzed in 1 other manner. Comparisons were made to the variability allowed by New York specification tolerances rather than to overall variability between production points:

$$H_0 : \sigma^2 \text{ mix} \leq \sigma^2 \text{ specification}$$

$$H_1 : \sigma^2 \text{ mix} > \sigma^2 \text{ specification}$$

where $\sigma^2 \equiv$ variance (sieve).

All comparisons were done on a sieve-by-sieve basis by using the χ^2/degrees of freedom distribution at the 0.01 significance level. This test is commonly used when comparison to a standard (in this case, mix specification) is necessary (11).

This analysis showed only the following material to have been altered beyond variability that is normally allowed by specifications:

1. A ¼-in. (6-mm) top course out of bin 2;
2. A ½- and ¼-in. (13- and 6-mm) binder out of bin 2;
3. A ½-in. (13-mm) base out of bin 1; and
4. A ½-in. (13-mm) base out of bin 2.

The 1-in. (25-mm) base course coming out of bin 1 was also beyond the variability allowed as was the 1-in. (25-mm) material going into bin 1. Therefore, nonconformance of the 1-in. (25-mm) material out of the bin did not necessarily indicate a storage effect.

CONCLUSIONS

Storage of a fine asphalt concrete mix in an inert gas atmosphere for 18 and 48 hours had no significant effect on asphalt cement consistency.

Fine asphalt concrete mix stored in a normal atmosphere for 24 hours did not experience any significant change in asphalt cement consistency.

Storage of 2 coarse asphalt concrete mixes for 18 hours in a normal atmosphere resulted in significant increases in asphalt cement consistency.

For 4 mixes resampled after 1 year in place, all initial similarities or differences between asphalt cements from control mixes (direct from the pug mill) and stored mixes persisted.

Overall gradation variability was increased by storage for both fine and coarse mixes. However, on a sieve-by-sieve basis, most material for all mixes was still within the variability permitted by specifications.

ACKNOWLEDGMENTS

Work on this project was accomplished under the administrative and technical direction of William C. Burnett and William P. Chamberlin, Engineering Research and Development Bureau, New York State Department of Transportation, in cooperation with the Federal Highway Administration. Those playing a major role in sample collection and processing and the data summation include Harold P. Sloan and John W. Alvey. The authors also gratefully acknowledge the assistance of Harry H. McLean and James J. Murphy of the Materials Bureau. Special thanks are also given George Marra of the Materials Bureau Chemistry Laboratory for processing and testing samples. This paper's contents reflect the authors' opinions, findings, and conclusions and not necessarily those of the New York State Department of Transportation or the Federal Highway Administration.

REFERENCES

1. Tuttle, L. Investigation of the Effects of Holding Hot Bituminous Mixtures in Storage Hoppers for Short and Extended Periods of Time. Proc. Canadian Technical Asphalt Assoc., Vol. 11, 1966, pp. 237-248.
2. Middleton, S. C., Goodknight, J. C., and Eaton, J. S. The Effects of Hot Storage on an Asphaltic Concrete Mix. Proc. AAPT, Vol. 36, 1967, pp. 180-191.
3. Parr, W. K., and Foster, C. R. Discussion of paper by Middleton, S. C., Goodknight, J. C., and Eaton, J. S., The Effects of Hot Storage on an Asphaltic Concrete Mix. Proc. AAPT, Vol. 36, 1967, pp. 205-205b.
4. Vallerga, B. A., and White, R. M. Discussion of paper by Middleton, S. C., Goodknight, J. C., and Eaton, J. S., The Effects of Hot Storage on an Asphaltic Concrete Mix. Proc. AAPT, Vol. 36, 1967, pp. 195-201.
5. Foster, C. R. Hot-Storage of Asphalt Paving Mixtures. Presented at convention of National Asphalt Pavement Assoc., San Juan, Puerto Rico, Jan. 1967.
6. Foster, C. R. More on Hot-Storage of Asphalt Paving Mixtures. Presented at convention of National Asphalt Pavement Assoc., Los Angeles, Feb. 1968.
7. Parr, W. K., and Brock, J. D. Statistical Study of the Effect of Hot Storage on the Composition and Properties of Asphaltic Concrete. Proc. AAPT, Vol. 41, 1972, pp. 1-20.
8. Kandhal, P. S., and Wenger, M. E. Storage of Bituminous Concrete in Inert Gas. Highway Research Record 468, 1974, pp. 61-72.
9. Hearld, J. L., and Lay, L. D. Variation in Temperature and Physical Properties of Asphalt Concrete Due to Storage in Surge Bins. Louisiana Dept. of Highways, Res. Rept. 67, March 1973.
10. Cooley, W. W., and Lohnes, P. R. Multivariate Analysis. John Wiley and Sons, Inc., New York, 1971.
11. Dixon, W. J., and Massey, F. J., Jr. Introduction to Statistical Analysis, 2nd Ed. McGraw-Hill Book Co., New York, 1957.

SERVICE BEHAVIOR OF ASPHALT CONCRETE: A 10-YEAR STUDY

Gordon W. Beecroft, John C. Jenkins, and James E. Wilson,
Oregon Department of Transportation

The 10-year study of asphalt pavement behavior described herein was initiated to follow the changes that occur with time and traffic and to supplement existing information on material properties that contribute to more durable pavements. Measurement of surface characteristics and sampling of asphalt concrete and stone base were conducted twice yearly, during spring and fall, at 32 test points. Properties of the asphalt concrete and stone base important to performance were measured in the laboratory for each sampling period. Samples were taken both in wheel-track and shoulder areas to indicate the effect of traffic. A linear regression program was used to analyze the various interrelationships of properties that affect service behavior. The relative importance of the different properties to a given dependent property is indicated by the order in which the variables enter the regression equations. The correlation coefficients generally are low, but the equations provide a useful qualitative indication of the different relationships. A summary of the predominant indications provided by the equations is presented.

•DESIGN of asphalt concrete has developed from a rather uncertain art to a reasonably well-defined science during the last 20 to 30 years. Laboratory methods to evaluate design properties have become well established and reliable. Studies of in-place material have been less common. In an effort to refine the limits of the many properties known to influence the performance of asphalt concrete, the Oregon Highway Division has conducted several long-term studies of asphalt concrete pavements (1). This paper presents findings from a 10-year study of the service behavior of pavements at 32 test points on 8 different projects. Samples of asphalt concrete and base rock were obtained at 6-month intervals and analyzed for various aggregate, asphalt, and mix characteristics. In addition to the sampling, wheel-track depressions were measured and general pavement condition was observed. During the later years of the study, Benkelman beam deflections were obtained each spring. The in-place density, moisture content, and gradation were determined for the granular base at each sampling. Hveem stability, density, relative compaction, penetration of recovered asphalt, air-void, thin-film-oven-loss, asphalt content, and gradation of aggregate in mix tests were performed on the asphalt concrete throughout the project.

The pavements studied on the project were designed on the basis of a predicted 10-year life, although at the time of their design traffic was categorized as very heavy, heavy, moderate, or light; calculation of equivalent wheel loads (EWLs) as would be done at present was not done. During the study, normal maintenance practices were continued without regard to the test points. Most of the sections were sealed during the study, and some of the test-point areas were patched. Materials added to the surface in the form of seals or patches were removed from the samples before laboratory analysis so that testing would be done on the original pavement only. There would, of course, be some effect from the protection against weathering provided by the surface treatments.

Publication of this paper sponsored by Committee on Mechanical Properties of Bituminous Paving Mixtures.

PURPOSE

The project was initiated to evaluate the service performance of several asphalt concrete pavements and to distinguish the changes that occur with age and traffic. Principal physical characteristics were evaluated at construction to provide a base for measurements of progressive changes. The locations of the test-point projects were selected to provide a geographical distribution representing the state's different climatic characteristics. Each point used the design established for the section; no variations were made in the design or construction to intentionally create variations in performance. The purpose was to measure any changes that occurred in pavements designed and constructed according to the practices in effect at that time.

SCOPE AND PROCEDURE

Test-point locations were selected on the basis of not only different climatic conditions but also heavy traffic. Eight projects were selected, each of which had 4 test points. To represent the more severe climate, 3 projects—test points 1 to 12—were chosen in eastern Oregon in an area having significant snowfall and hard freezing. Two projects—points 13 to 20—were in the southern portion of the state having relatively high summer temperatures, intermediate precipitation [32 in. (0.81 m) per year], and only slight winter freezing. The other 3 projects—test points 21 to 32—were in western valley areas having moderate freezing and rainfall of about 40 in. (1.02 m) per year. No construction of heavy traffic highways was in progress in the arid portions of the state at the time the study was initiated. Identification of the projects and design information on the number of lanes, pavement structure thickness, and subgrade soil classifications are given in Table 1.

Samples were obtained in the spring and fall in the wheel track nearest the pavement edge and in the shoulder area away from concentrated traffic. Two samples were taken in each case at the same longitudinal position along the road to permit comparison of properties of pavements under the kneading action of traffic to those having little traffic. Care was taken to remove both the shoulder sample and the wheel-track sample from the same lay-down panel. Each wheel-track sample consisted of two 4-in. (100-mm) cores and one 16-in. (0.4-m) square cut with an impact chisel. The shoulder samples consisted of two 4-in. (100-m) and two 6-in. (150-mm) cores. Each set of samples was taken 4 ft upstream to traffic flow from the previous set to avoid roughness effects.

Sampling and testing determined properties of the base and top lifts of asphalt concrete and granular base rock. Wheel-track depressions were measured and, during the later portion of the study, Benkelman beam deflections were obtained once a year at 50-ft (15-m) intervals.

Tests on the granular base included those on density, moisture content, relative compaction, grain size analysis, liquid limit, and plastic limit. An air-degradation test was not included originally but was added about midway in the study. Density was determined by using sand of a known loose density to measure the hole volume.

The asphalt concrete studies included the properties not only of in-place material but also samples having undergone laboratory compaction and specimens having been remolded in the laboratory. The core analyses included those on in-place density, air voids, stabilometer S value, and cohesiometer value. In an effort to detect any changes in compactibility caused by changes in particle orientation or aggregate degradation caused by the traffic, we reheated the cores to 240 F (115 C) in molds and recompacted them by applying 160 blows at 450 psi (3 102 kPa) with the kneading compactor. Density and stability determinations were repeated for each core after the recompaction, and this density was used for calculation of relative compaction.

The square-cut sample and the 6-in. cores provided material for aggregate gradation analysis, asphalt content, and penetration of recovered asphalt. Asphalt recovered by the Abson method (ASTM D1856-69) was tested for penetration at 77 F (25 C) and 39.2 F (4 C); thin film loss and penetration after thin film loss were determined. For laboratory testing of the mix, any materials foreign to the original asphalt concrete such as a tack coat at the bottom or seals and patches at the top were removed from the sample by sawing. A portion of the cut sample was reheated and used to fabricate additional

Table 1. Pavement structure and subgrade details.

Highway Section	Test Point Numbers	Number of Lanes	Asphalt Concrete Thickness (in.)	Cushion Course Thickness[a] (in.)	Base Course (in.)		Subgrade Classification
					Size	Thickness	
Emigrant Hill, Deadman's Pass	1 to 4	4	4	1½	1½ to 0	10	A-1-b(0)
Meacham-Glover, Station 140	5 to 8	4	4	1½	2 to 0	9½	A-2-7(0)
Meacham-Glover, Station 369	9 to 12	4	4	1½	2 to 0	9½	A-2-7(0)
Jumpoff Joe Creek, Louse Creek	13 to 16	4	4	1½	2 to 0	9½	A-1-b(0)
Myrtle Creek, Ford's Bridge	17 to 20	4	4	2	1½ to 0	6	A-1-a(0)
Salem Bypass	21 to 24	4	4	2	2 to 0	18	A-4(8)
Valley Junction, Wallace Bridge	25 to 28	2	3½	2	1½ to 0	16	A-6(12)
Lebanon Road, Halsey Interchange	29 to 32	4	4	2	2 to 0	20½	A-7-6(18)

Note: 1 in. = 25.4 mm.
[a]Material: ¾ in. to 0.

Table 2. Approximate asphalt concrete properties.

Test Points	Asphalt Content (percent)	Penetration Grade	Specific Gravity of Mix	Air Voids (percent)	S Value		Cohesion	Material (percent)		Ratio ¼ to 10: ¼ to 0	P 200 (percent)
					In Place	Recompacted		¾ to ¼ in.	¼ in. to No. 10		
1 to 4	5.3	85-100	2.28	11.4	22	43	293	34.1	30.3	0.51	6.8
5 to 8	4.9	85-100	2.18	13.5	22	53	190	42.2	26.8	0.51	3.4
9 to 12	5.9	85-100	2.18	13.1	23	52	216	36.9	29.3	0.51	3.6
13 to 16	5.4	85-100	2.19	8.9	22	45	286	39.9	27.5	0.50	3.7
17 to 20	5.2	85-100	2.27	9.1	23	51	250	41.7	24.2	0.45	3.5
21 to 24	4.7	85-100	2.21	11.4	25	54	275	42.2	26.6	0.50	5.0
25 to 28	4.8	85-100	2.30	13.2	20	59	316	37.5	30.1	0.52	6.1
29 to 32	5.4	60-70	2.24	11.1	22	49	239	39.0	27.9	0.50	3.8

Note: 1 in. = 25.4 mm.

Table 3. Initial properties of stone base.

Test Points	Dry Density (pcf)	Relative Compaction (percent)	Moisture Content (percent)	Nominal Size	Material (percent)		Passing (percent)		Liquid Limit	Plasticity Index
					1½ to ¾ in.	2 to 1 in.	¼ in.	No. 200		
1 to 4	141	93.6	5.6	1½ in. to 0	17.2		41.8	7.9	22	1
5 to 8	129	93.6	6.6	2 in. to 0		14.5	43.3	4.5	26	1
9 to 12	122	89.7	7.9	2 in. to 0		17.1	38.9	4.7	35	9
13 to 16	136	98.3	5.9	2 in. to 0		19.5	42.7	5.5	25	2
17 to 20	141	97.1	5.2	1½ in. to 0	13.8		52.3	7.8	21	2
21 to 24	130	92.1	4.4	2 in. to 0		17.1	32.8	4.0	18	0
25 to 28	142	94.2	4.8	1½ in. to 0	22.9		41.0	8.9	22	2
29 to 32	126	90.5	6.6	2 in. to 0		22.1	32.5	5.4	30	9

Note: 1 pcf = 16.02 kg/m^3. 1 in. = 25.4 mm.

stabilometer specimens that were subsequently tested for stability, density, and cohesion and, after being reheated and subjected to a second compaction, the same properties were measured again. These tests were conducted to compare the in-place properties as well as to determine any discernible changes in compactibility, stability, or cohesion that accompany aging and traffic. Because the changes that occur in pavement components during service would be somewhat affected by the general characteristics at time of placement, the initial properties of the asphalt concrete are shown in Table 2 and the initial properties of the stone base are shown in Table 3.

Failure of asphalt pavements can be categorized broadly as rutting or shoving in mixes lacking stability, poor surface texture from too little or too much asphalt, and cracking from embrittlement or excessive flexing. Factors that contribute favorably to high flexibility and fatigue resistance generally reduce stability. As all designers know, asphalt concrete mix design involves compromise. One of the concerns that led to this long-term study was that stability might be overemphasized at the expense of flexibility. The various stabilometer measurements were made to provide information on in-place values and corresponding values for the same material subjected to different laboratory compactions. Observations made at the time of sampling concerning cracking, patches, seal coats, and other signs of distress were used to establish a pavement condition code ranging from 0 to 4 as follows:

0 No cracks, no seal, and no patches
1 Sealed only, no patches
2 Minor cracking or patching
3 Major cracking or patching
4 Multiple patching or severe cracking

This code is arbitrary and imprecise, but a numerical rating was desired for the analysis and no system of rating had been used during the study.

The other tests on the mixtures and components thereof were conducted with the hope that correlations would appear between given characteristics and properties associated with good service of long duration.

ANALYSIS

Although some periodic examination was made of the progressive changes in several of the factors under study, analysis during the study was limited. A preliminary report was prepared when the test points had been in service from 7.5 to 9.5 years (2). It presented trends in changes of density of the base rock, specific gravity of asphalt concrete, air voids in asphalt concrete, and hardening of the recovered asphalt for length of service. No analysis of the interactions between properties was attempted at that time.

At the conclusion of the 10-year period of sampling and testing, the values were tabulated for each property for each 6-month interval of time. Each property was assigned an arbitrary code number so that the many variables in a computer analysis of correlations and regression analyses could be handled. The properties and respective code numbers are given in Table 4. Tabulated values for the properties were punched on cards to provide flexibility in computer analysis so that the points could be handled individually or in various combinations. The code 99 values, cumulative 5,000-lb (2 268-kg) EWLs, were estimated by using traffic volumes recorded at locations near the test points, classification counts from the nearest permanent recorder station, and factors to convert truck counts by axle classification to 5,000-lb (2 268-kg) EWL. Information on the division of truck traffic between the outer and median lanes was not obtained during the study, and review of available literature provided little basis for an estimate. Ten percent of the outer lane EWL was used as an approximation for truck loads on the median lanes.

A stepwise regression analysis program, referred to as Biomed 2 or BMD02R, available through the Data Processing Unit of the Highway Division, was used for the project (3). In addition to the regression equations, this program provides a simple correlation

Table 4. Properties included in study.

Code	Property
Year	Length of time in service
51	Field density of stone base, pcf
52	Relative compaction of stone base, percent
53	Moisture content of stone base, percent
54	Stone base passing ¼-in. sieve, percent
55	Stone base passing No. 200 sieve, percent
56	Wheel-track depressions, inches
57	Specific gravity of asphalt concrete, in lane, base lift
58	Specific gravity of asphalt concrete, in lane, top lift
59	Specific gravity of asphalt concrete, shoulder, base lift
60	Specific gravity of asphalt concrete, shoulder, top lift
61	Air voids in asphalt concrete, percent, in lane, base lift
62	Air voids in asphalt concrete, percent, in lane, top lift
63	Air voids in asphalt concrete, percent, shoulder, base lift
64	Air voids in asphalt concrete, percent, shoulder, top lift
65	Stabilometer S value in-place, in lane, base lift
66	Stabilometer S value in-place, in lane, top lift
67	Stabilometer S value in-place, shoulder, base lift
68	Stabilometer S value in-place, shoulder, top lift
69	Relative compaction of asphalt concrete, in lane, base lift
70	Relative compaction of asphalt concrete, in lane, top lift
71	Relative compaction of asphalt concrete, shoulder, base lift
72	Relative compaction of asphalt concrete, shoulder, top lift
73	Stabilometer S value recompacted, in lane, base lift
74	Stabilometer S value recompacted, in lane, top lift
75	Stabilometer S value recompacted, shoulder, base lift
76	Stabilometer S value recompacted, shoulder, top lift
77	Cohesion value in-place, in lane, base lift
78	Cohesion value in-place, in lane, top lift
79	Cohesion value in-place, shoulder, base lift
80	Cohesion value in-place, shoulder, top lift
81	Penetration of recovered asphalt 77 F, in lane, base lift
82	Penetration of recovered asphalt 77 F, in lane, top lift
83	Penetration of recovered asphalt 77 F, shoulder, base lift
84	Penetration of recovered asphalt 77 F, shoulder, top lift
85	S value of remolded mix, second compaction, base lift
86	S value of remolded mix, second compaction, top lift
87	Asphalt content, percent by weight of mix, base lift
88	Asphalt content, percent by weight of mix, top lift
89	Benkelman beam deflections, 15-kip axle, inches
90	Pavement condition code
91	Mix aggregate retained on ¼-in. sieve, percent, base lift
92	Ratio of ¼ in. to No. 10: ¼ in. to 0 mix aggregate, base lift
93	Mix aggregate retained on ¼-in. sieve, percent, top lift
94	Ratio of ¼ in. to No. 10: ¼ in. to 0 mix aggregate, top lift
95	Mix aggregate passing ¼-in. sieve and retained on No. 10 sieve, percent, base lift
96	Mix aggregate passing ¼-in. sieve and retained on No. 10 sieve, percent, top lift
97	Mix aggregate passing No. 200 sieve, percent, base lift
98	Mix aggregate passing No. 200 sieve, percent, top lift
99	Cumulative 5,000-lb EWL's millions

Note: 1 in. = 25.4 mm. (1 F-32)/0.8 = 1 C. 1 kip = 444.8 N. 1 lb = 0.45 kg.

matrix comparing each variable with every other variable. Although many of these comparisons have no meaning, the data processing specialists considered it easier to include all the data rather than sort out those for which some correlation might be conceivable. In determining coefficients for linear multiple regression equations, the variables to be considered were limited to those items thought to have some logical chance of influencing the dependent variable. Primarily, the purpose was to exclude the irrelevant factors between shoulder and traveled lane, between granular base and base lift, and between base lift and top lift of pavement. Equations were generated for 38 different variables of the 49 coded items in Table 4. The regression equations are in the Appendix. The remaining variables were properties expected to influence other factors but not to be influenced by other factors.

A number of alternatives were tried in the analysis of data. Points were processed individually, all were averaged, regional groups were averaged, and, finally, the concatenate data for the regional groups and for the 32 test points were processed. The early computer runs were made with a high degree of significance required for a variable to be included in the equations (variance ratio, F = 4). It was found that the interrelationships of properties often were not indicated when this high degree of significance was required. Because the principal interest in the regression equations was to identify these interrelationships in a qualitative way, the requirement for inclusion in the equations was lowered appreciably (F = 1). With this change, the concatenate data for the 32 test points together were quite effective in bringing out the desired influence between properties.

Properties of Stone Base

The density of the stone base showed an increase during the study for all of the projects. The equations for the different regional groups of points and for the 32 points combined used years of service as the most significant correlation. Although the change in density should have been traffic-related, the cumulative wheel loads were found less significant than time. Correlation coefficients for density were low, so most of the variation remains unexplained. The trends indicated by the equations for all points combined showed an increase in density with years of service, an increase with higher percentages passing a No. 200 (75-μm) sieve, a decrease with higher percentages passing a ¼-in. (6.3-mm) sieve, and an increase with increased EWL (importance to the correlations as in the order listed). Only years of service and percent passing a No. 200 (75-μm) sieve showed up in the equations for regional groups of test points.

The relative compaction of the stone base had a higher correlation coefficient because properties such as particle shape, texture, and specific gravity were removed as variables. For the 32 points combined, the equation for relative compaction had an inverse relationship to moisture content as the most important variable, followed by direct relationships of years of service, percent passing a No. 200 (75-μm) sieve, EWLs, and percent passing a ¼-in. (6.3-mm) sieve.

Properties of Asphalt Concrete

The various properties of asphalt concrete will be discussed first by general trends and then by more specific comments on the regression equations.

The specific gravity of the asphalt concrete generally related first to the air-void content and then to the percent passing a No. 200 (75-μm) sieve, decreasing with higher air voids and increasing with higher amounts passing a No. 200 (75-μm) sieve. In some cases, the higher amount passing a No. 200 (75-μm) sieve was first and higher air voids second, but these were consistently the first 2 variables in the equations for the concatenate data. The third variable was usually the relative compaction followed by other gradation variables. Beyond the third term, though, there was little consistency.

The air-void percentage equations generally were most influenced by the relative compaction and then frequently by the stabilometer S values of the recompacted mix. Air voids increased with reduced relative compaction and increased S values. Frequently high in the order of influence was the ratio of ¼ in. to No. 10:¼ in. to 0 (6.3 mm to 2.0 mm:6.3 mm to 0); the higher the ratio, the greater the influence.

Effects of years of service and cumulative wheel loads were found to have little influence on the air voids.

The stabilometer S value of the in-place material had the strongest correlation with relative compaction, high S values being associated with high relative compaction. There was also a strong positive effect in the traveled lanes from the EWLs. Entering the equations with less regularity are cohesion, percent passing a No. 200 (75-μm) sieve, air-void content, and years of service.

After the in-place stabilometer values were determined, the cores were heated and recompacted to provide a basis for evaluation of relative compaction. The regression equations for relative compaction usually related first to the in-place S value and second to the air-void percentage, increasing with higher S values and decreasing with higher air voids. The next most frequent was a negative relationship to the percent passing a No. 200 (75-μm) sieve. Less consistent, but common, were entries of percent of asphalt (negative coefficients), ratio of ¼ in. to No. 10:¼ in. to 0 (6.3 mm to 2.0 mm: 6.3 mm to 0) (positive coefficients), and percent passing a ¼-in. (6.3-mm) sieve and retained on a No. 10 (2.0-mm) sieve (negative coefficients).

Stabilometer S values of the recompacted samples related first to percent of asphalt for the top lift; this variable, however, never entered the equations for the bottom lift. Apparently some top lift samples were close to the critical asphalt content and lost stability on recompaction, while this did not occur in the bottom lift samples. Other items important in the equations were air-void content, in-place S values, cohesion, and ratio of ¼ in. to No. 10:¼ in. to 0 (6.3 mm to 2.0 mm:6.3 mm to 0).

Cohesiometer values increased with years of service, which was the most important variable, followed generally by the percent passing a No. 200 (75-μm) sieve (positive coefficients). Then came as important variables in-place S values (positive coefficients) and the air-void percentage (negative coefficients). For the equations for concatenate data for all 32 test points, both percent of asphalt and penetration of recovered asphalt had negative coefficients although these variables entered equations for several regional groups with positive coefficients. In neither case did the variables contribute appreciably to the correlations.

Without exception, the equations for penetration of the recovered asphalt showed an inverse relationship with years of service being most important. The next 2 factors were percent of air voids (negative coefficient) and percent of asphalt (positive coefficient). Items that appeared irregularly were relative compaction, percent passing a No. 200 (75-μm) sieve, and cumulative wheel loads. The hardening of the asphalt as measured by loss in penetration occurred rapidly at first; the rate declined progressively with longer service.

None of the various aggregate properties of the mix were considered to be dependent variables except degradation with time and traffic. Inspection of the data did not indicate any change in gradation, so only the percentages passing a No. 200 (75-μm) sieve in base and top lifts were included in the computer analysis. The resulting equations confirmed that there was no significant degradation. When included, years of service generally had a negative coefficient and EWLs a positive coefficient, but neither was significant.

Performance Properties

Several factors involve the performance of the total pavement structure, asphalt concrete and granular base combined. These are wheel-track depressions, Benkelman beam deflections, and pavement condition code. All variables thought to have any conceivable effect on these items were included in the analysis. Twenty-six items for wheel-track depressions, 28 items for Benkelman beam deflections, and 28 items for pavement condition code were included.

The equation for wheel-track depressions, resulting from the data for all 32 test points, included the following variables, listed in the order of their importance to the correlation: EWLs, cohesiometer value for base lift, in-place S value of base lift, air-void percentage in base lift, percent of relative compaction of top lift, percent passing a No. 200 (75-μm) sieve in top lift, percent of asphalt in top lift, and the percent passing a ¼-in. (6.3-mm) sieve and retained on a No. 10 (2.0-mm) sieve in top

lift. Except for the last 2 variables, the coefficients had positive signs. Several of these signs were opposite to what might be expected if the given variable were viewed alone, but, considering the complex interaction between properties as affected by time and traffic, they seemed reasonable. The major influence on wheel-track depressions was the cumulative wheel loads, as would be expected.

Although the regression equations for wheel-track depressions were influenced mainly by loads and mix properties, the Benkelman beam deflections related heavily to properties of the stone base. The variables selected in the Benkelman beam regression for the concatenate data for all 32 test points were (the sign of the coefficient is in parentheses): wheel-track depression (+), percent passing a ¼-in. (6.3-mm) sieve in stone base (-), percent of asphalt in top lift (-), percent passing a No. 200 (75-μm) sieve in stone base (+), ratio of ¼ in. to No. 10:¼ in. to 0 (6.3 mm to 2.0 mm:6.3 mm to 0) in top lift (+), percent of air voids in base lift (-), cohesiometer value for base lift (+), and years of service (-). Of 28 variables to choose from, these provided the best correlation. Again, some of the signs for Benkelman beam deflections were opposite to anticipated relationships, but it is difficult to visualize the various subtle effects that one variable has on another.

The final regression equation for the project was for the pavement condition code. This code was established to express numerically the serviceability of the pavement in terms of the prevalence of cracking or patching that occurred during the study. The regression equation for the overall data included the following variables (in the order of importance to the correlation): years of service, in-place S value of top lift, percent of moisture content in stone base, wheel-track depressions, percent of air voids in base lift, EWLs, ratio of ¼ in. to No. 10:¼ in. to 0 (6.3 mm to 2.0 mm:6.3 mm to 0), and penetration of the asphalt in the top lift. Each coefficient had a positive sign. The fact that the equation related first to years of service instead of EWLs was probably caused by the fact that thin patches were often placed over both the median and outer lanes for smoothness and uniformity even though only the outer lane may have needed maintenance at the time. Records were not detailed enough to permit adjustment of the pavement condition code for this type of case. The variables selected in the regression analysis came from 28 possibilities, and it is interesting to note those of major importance. The second item, in-place S value of top lift, is logical in that high values result from dry or brittle mixes as does pavement cracking. Third in the correlation was the moisture content of the stone base, high moisture leading to early distress. The fifth item was the percent of air voids in the base lift. The high air-void content of these mixes would result in rapid embrittlement which, in turn, would lead to pavement cracking.

Multiple Regression Equations

Although the principal benefit of the regression equations in this study was to bring out the interrelationships of properties in a qualitative way, it may be useful to illustrate some of the actual coefficients. A tabulation of all the equations from the analysis of the concatenate data from the 32 test points is provided in the Appendix. The equations were all of the form:

$$Y = A_0 + A_1X_1 + A_2X_2 + A_3X_3 + \ldots A_nX_n$$

where

Y = desired relationship,
A_0 = constant,
A_1 to A_n = coefficients, and
X_1 to X_n = dependent variables measured in the study.

The number of variables included in the equations was controlled by an F level for inclusion of 1.0 with a maximum of 8 variables. The correlations resulting from the concatenate data from all 32 test points generally were not too precise. Deviations resulting from sampling and testing were high, and measures of the quality of construction were lacking. Also, climatic conditions and subgrade properties had no

input into the equations. Correlations for individual projects and regional groups were higher, but the combined data served to bring out the variables that were important to overall pavement performance.

To illustrate the equations, the percent of relative compaction of the top asphalt concrete in the traveled lanes can be estimated by:

Percent of relative compaction = 100.29 - 0.277 (percent of air voids) + 0.089 (in-place S value) - 0.0015 (in-place cohesion) - 0.0177 [penetration at 77 F (25 C)] - 0.446 (percent of asphalt) - 0.0796 [percent passing a ¼-in. (6.3-mm) sieve and retained on a No. 10 (2.0-mm) sieve] + 0.109 [percent passing a No. 200 (75-μm) sieve] + 0.0157 (EWL, millions)

Penetration of the recovered asphalt at 77 F (25 C) for the top lift pavement is approximately

Penetration = 99.63 - 3.244 (years of service) + 4.088 (percent of asphalt) + 0.457 [percent passing a No. 200 (75-μm) sieve] - 0.463 (percent of air voids) - 0.793 (percent of relative compaction)

The pavement condition code can be determined by

Condition code = -5.359 + 0.196 (years of service) + 0.062 (S value of top lift) + 0.177 (percent of moisture in stone base) + 0.659 (wheel-track depression) + 0.075 (percent of air voids in base lift) + 0.026 (EWL, millions) + 3.027 [ratio ¼ in. to No. 10:¼ in. to 0 (6.3 mm to 2.0 mm:6.3 mm to 0) in top lift] + 0.0094 [penetration at 77 F (25 C) in top lift]

Values near 0 indicate excellent service and values near 4 denote pavements requiring extensive maintenance. The variables in these examples are arranged in descending order with regard to their importance to correlation.

The equations illustrate the type of output obtained for 38 different variables for which some interdependence seemed likely. As mentioned, their principal value is in showing the general order of importance of the various properties. Equations similar to those illustrated were obtained for the various asphalt mix properties for top lift and base lift at locations in traveled lane and shoulders. Thus, 4 equations were available for many given properties. Generally, the first 2 or 3 variables important to a correlation were fairly consistent between equations, but the less important items were not consistent. Because regression coefficients depend on the particular variables included, numerical values differ appreciably between equations. However, the solutions obtained from substitution of typical values into the several equations for a given property are similar.

SUMMARY

Measurements made during the 10-year study were inspected to identify changes occurring with time. But, to determine the interdependence of individual properties on the overall service behavior, a multiple linear regression analysis was employed. This analysis confirmed in a qualitative way the known relationships between properties such as compaction, air voids, asphalt content, and penetration of recovered asphalt. In addition, some measure of the influence of time and traffic was obtained for many of the properties. The following summary statements are based on indications provided by the regression equations. In many cases, the order of importance of independent variables on a given dependent variable is not unanimous, but the statements represent predominant indications.

1. Densities of the stone base showed an increase for all projects; outer lanes had a greater increase than median lanes. Values during the final 4 years remained nearly constant; the early years showed most of the change. Time proved a better correlation than did equivalent wheel loads although both caused increased density. Stone base densities also increased; greater percentages passed a No. 200 (75-μm) sieve and smaller percentages passed a ¼-in. (6.3-mm) sieve.
2. No degradation of the stone base occurred.
3. Density of the asphalt concrete was increased primarily by reducing air voids and by increasing the percent passing a No. 200 (75-μm) sieve. The densities of mixes used on the test projects were increased only slightly by equivalent wheel loads and years of service.
4. The percent of air voids related inversely to relative compaction and directly to the Hveem stabilometer S value of the recompacted mix, which were the 2 most common variables. As the ratio of ¼ in. to No. 10:¼ in. to 0 (6.3 mm to 2.0 mm:6.3 mm to 0) increased, the mix became more "open" and air voids increased. The cumulative EWLs term indicated an average reduction in air-void percentage of about 1 percent in the base lift and 2.5 percent in the top lift that was caused by 10 years of freeway traffic.
5. Stabilometer S values for in-place materials increased with higher relative compaction, higher traffic volumes, higher percentages passing a No. 200 (75-μm) sieve, and higher cohesion. Although the in-place S values were generally low, no pavement instability existed on the test projects. S values of the in-place material were predominately between 15 to 25. Additional compaction of the cores in the laboratory increased the stability values to the range of 50 to 70 for most pavements. In a few instances, the additional compaction caused a reduction of stability on samples having high asphalt content.
6. For correlation, cohesiometer values increased in this order—years of service, percent passing a No. 200 (75-μm) sieve, and in-place S values. Also, cohesion increased with a reduction in penetration of the recovered asphalt.
7. Penetration of the recovered asphalt had inverse relationships to years of service and air-void content and a direct relationship to asphalt content as the 3 most important variables.
8. Wheel-track depressions increased with EWLs as the most important factor in the correlation. Following this are various materials properties, several of which have signs opposite to expected values. The depressions correlate directly with cohesion of base lift, S value of base lift, air voids in base lift, and relative compaction of top lift, in that order. No properties of the stone base enter into the regression equation.
9. The Benkelman beam deflections related first to the wheel-track depressions and then, by inverse correlations, percent passing a ¼-in. (6.3-mm) sieve in stone base and percent of asphalt in top lift, and, by a positive relationship, percent passing a No. 200 (75-μm) sieve in stone base. It is interesting to note that these tests indicate Benkelman beam deflections are reduced by having more passing a ¼-in. (6.3-mm) sieve and less passing a No. 200 (75-μm) sieve in the stone base. Although no properties of the stone base affected the wheel-track depressions, the stone base had a major influence on the Benkelman deflections.
10. An arbitrary numerical pavement condition code was devised to enable a correlation with the other properties in the multiple regression analysis. The regression equation for condition related first to years of service instead of EWLs probably because maintenance was extended over both the outer and median lanes to provide a smooth surface. Second in importance was the stabilometer S value for the top lift; higher S values corresponded to pavements having more cracking and needing more maintenance. Third was the moisture content in the stone base; higher moisture resulted in poorer service. These were followed by wheel-track depressions, percent of air in base lift, EWLs, ratio of ¼ in. to No. 10:¼ in. to 0 (6.3 mm to 2.0 mm:6.3 mm to 0) in top lift, and penetration of asphalt in top lift. In each case, higher values correspond to pavements needing more maintenance. The last item contributes very little to the correlation, but its effect is opposite to that expected. The correlation is probably

coincidental. The other factors affected performance as would be expected, with more maintenance being needed for more brittle mixes.

IMPLEMENTATION

In a long-duration study of this type, implementation of findings takes place as the study progresses. Many changes in pavement structure and asphalt concrete mix design have been made since the 10-year study was initiated. A number of these changes were influenced by results and observations of the service behavior study.

1. To achieve optimum moisture for compaction of aggregate bases and to prevent segregation of the material during processing, all base materials are plant-mixed to uniform moisture and then placed with a spreader.
2. Specifications were introduced to more closely control the gradation of aggregate bases by requiring that the ratio of ¼ in. to No. 10:¼ in. to 0 (6.3 mm to 2.0 mm: 6.3 mm to 0) be between 40 and 60 percent. This provides a gradation that gives high density without loss of strength from oversanding.
3. The Oregon air-degradation test was developed during the study to identify troublesome aggregates. Values obtained during the 10-year study helped to fix permissible limits. Also, the study indicated that no significant change in air degradation values occurs in service.
4. Recognition that better control of stone base properties was important to good service led to adoption of the sand equivalent test for aggregates. Although they were not a part of the service behavior study, observations made during the study contributed to an understanding of aggregate properties.
5. Specifications to require 95 percent relative compaction of aggregate bases were introduced during the study, and again there was some influence from observation of the test points. Previous specifications had been based on weight of roller and coverages.
6. Evidence that even though the in-place stabilometer S values were low there was no problem with pavement stability led to several changes in mix design. One of these was to increase the asphalt content to provide a more dense and more flexible pavement. Control of the ratio of ¼ in. to No. 10:¼ in. to 0 (6.3 mm to 2.0 mm: 6.3 mm to 0) between 42.5 and 57.5 percent provides a relatively open gradation that permits thick asphalt films without flushing. More fatigue-resistant pavements have resulted.
7. Emphasis in design has centered on control of air-void content and on the index of retained strength on immersion-compression specimens since it was established that stability is not a problem with normal gradation and crushing requirements.
8. The low densities and high air-void contents found so frequently in the 10-year study influenced putting greater emphasis on construction control. Compaction requirements were changed, and a greater effort was placed on obtaining adequate compaction. Data from the test points demonstrated a very rapid loss in penetration of the recovered asphalt in mixes having high air voids and a much less severe loss in mixes having lower air voids. Mixes having the higher retained penetration exhibited better fatigue resistance, as one would expect.
9. The drying of aggregates for asphalt concrete received additional attention as a result of the eastern Oregon projects. Residual moisture in the aggregate caused the mix to have the appearance and consistency associated with excess asphalt although it actually had a low asphalt content. Although specifications limiting moisture to 0.5 percent existed, more careful testing for compliance resulted from observing these projects.

The regression equations generally confirm relationships between variables known to exist, but occasionally unexpected correlations appeared. Also, the order of importance and the nature of the effect sometimes differed from that anticipated. Further study will be made of these equations to determine if other design changes are suggested by them. For instance, the ratio of ¼ in. to No. 10:¼ in. to 0 (6.3 mm to 2.0 mm: 6.3 mm to 0) in the asphalt concrete enters many equations and in a majority of cases

the effect of increasing the ratio is to worsen the dependent variable. This suggests that the limits for the ratio may be higher than they should be, a possibility that will be investigated. Other things that indicate that improved performance may be obtained by modifying proportions or procedures also will be investigated to continue implementing the research results.

CONCLUSIONS

This systematic evaluation of pavement performance has provided a measure of the interrelationships of variables over a long period of time. Frequently, this merely confirmed known factors, but the study did show the relative importance of various items. The study has had an influence on improvements in asphalt concrete design and construction control, and, as a result, better service is expected from pavements placed today.

ACKNOWLEDGMENTS

During the period of this study, many persons in the Materials Section of the Oregon Department of Transportation had a part in the field sampling and laboratory testing. To all of those involved, the conscientious work is sincerely appreciated. Also, the assistance of the Data Processing Unit in conducting the regression analyses is gratefully acknowledged. In particular, the help of George LeTourneux and Jay Paulus in adapting the regression program for the test-point data was vital. The project was conducted in cooperation with the Federal Highway Administration. The opinions, findings, and conclusions are those of the authors and are not necessarily those of the Federal Highway Administration or the Oregon State Highway Division.

REFERENCES

1. White, O. A. Service Behavior of Asphaltic Concrete. HRB Bull. 300, 1961, pp. 18-31.
2. White, O. A., Wilson, J. E., and Beecroft, G. W. Study of Service Behavior of Asphalt Concrete: Purpose Description and Trends. Proc. AAPT, Vol. 38, 1969, pp. 328-339.
3. BMD: Biomedical Computer Programs (Dixon, W. J., ed.). University of California Press, Berkeley.

APPENDIX

REGRESSION EQUATIONS

The following tabulation provides linear regression equations for the concatenate data from the 32 test points. To conserve space the variables are represented by their respective code numbers. The independent variables are listed in declining order with regard to the contribution they make to the correlation. The property represented by a given code number is given in Table 4.

$$Cd51 = 102.16 + 3.230\ (year) + 3.551\ (Cd55) - 0.416\ (Cd54) + 0.224\ (Cd99)$$

$$Cd52 = 92.45 - 1.542\ (Cd53) + 0.540\ (year) + 0.825\ (Cd55) + 0.107\ (Cd99) + 0.088\ (Cd54)$$

$$Cd53 = 16.48 - 0.114\ (Cd52) + 0.048\ (Cd55)$$

Cd54 = -2.505 - 0.190 (Cd99) + 0.391 (Cd52) + 1.179 (Cd53) - 0.216 (year)

Cd55 = -5.453 + 0.122 (Cd52) - 0.0604 (year) - 0.0142 (Cd99) + 0.0704 (Cd53)

Cd56 = -0.940 + 0.0181 (Cd99) + 0.00017 (Cd77) + 0.00409 (Cd55) + 0.0126 (Cd61) + 0.0113 (Cd70) + 0.0262 (Cd98) - 0.0422 (Cd88) - 0.00082 (Cd96)

Cd57 = 1.331 - 0.016 (Cd61) + 0.0271 (Cd97) + 0.00686 (Cd69) + 0.00417 (Cd91) + 0.0048 (Cd95) + 0.00108 (Cd99) + 0.00037 (Cd81) + 0.00107 (year)

Cd58 = 1.451 - 0.0015 (Cd62) + 0.0231 (Cd98) + 0.0109 (Cd70) - 0.0253 (Cd88) - 0.4976 (Cd94) + 0.00484 (Cd96) + 0.00138 (Cd99) + 0.00056 (Cd82)

Cd59 = 0.943 - 0.0195 (Cd63) + 0.0279 (Cd97) + 0.01196 (Cd71) + 0.00338 (Cd91) + 0.00467 (Cd95) + 0.00118 (year)

Cd60 = 2.565 + 0.0313 (Cd98) - 0.0189 (Cd64) + 0.00233 (Cd84) - 0.0464 (Cd88) - 0.2193 (Cd94)

Cd61 = 69.853 - 0.6913 (Cd69) + 0.0848 (Cd73) + 18.382 (Cd92) - 0.0579 (Cd81) - 0.00396 (Cd77) - 0.0691 (Cd91) - 0.0404 (Cd99) - 0.1394 (Cd87)

Cd62 = 76.111 - 0.7937 (Cd70) + 0.0709 (Cd74) - 0.0978 (Cd99) + 0.3438 (year) - 0.00471 (Cd78) + 15.389 (Cd94) + 0.0623 (Cd66) - 0.4241 (Cd88)

Cd63 = 53.575 + 0.0951 (Cd95) - 0.5671 (Cd71) + 0.0793 (Cd75) - 0.00698 (Cd79) - 0.0278 (Cd83) + 17.387 (Cd92) + 0.1651 (year) - 0.1608 (Cd87)

Cd64 = 59.008 + 0.0627 (Cd76) - 0.5712 (Cd72) + 15.981 (Cd94) - 0.1852 (Cd98) - 0.00436 (Cd80) + 0.1966 (year) - 0.1852 (Cd93) - 0.2499 (Cd88)

Cd65 = -167.356 + 1.923 (Cd69) + 0.2537 (Cd97) + 0.1818 (Cd99) - 0.607 (year) + 0.00876 (Cd77) + 0.4241 (Cd61) + 0.1715 (Cd91)- 11.579 (Cd92)

Cd66 = -88.893 + 0.2216 (Cd99) + 1.0288 (Cd70) + 0.0149 (Cd78) + 0.0943 (Cd93) + 0.4144 (Cd62) + 0.0497 (Cd82) - 0.5509 (Cd98) - 0.2951 (year)

Cd67 = -130.913 + 1.668 (Cd71) + 0.209 (Cd97) + 0.00766 (Cd79) - 0.3814 (year) - 18.131 (Cd92) + 0.2526 (Cd63) - 0.0211 (Cd83)

Cd68 = -130.597 + 1.519 (Cd72) + 0.00908 (Cd80) + 0.0939 (Cd93) + 0.0262 (Cd84) + 0.2456 (Cd64) - 0.1004 (year) - 4.403 (Cd94)

Cd69 = 93.213 + 0.1122 (Cd65) - 0.2019 (Cd61) + 0.0397 (Cd99) - 0.1859 (Cd97) - 0.0059 (Cd81) + 5.391 (Cd92) - 0.0537 (Cd95) + 0.0053 (Cd73)

Cd70 = 100.293 - 0.2769 (Cd62) + 0.0891 (Cd66) - 0.4456 (Cd88) - 0.0177 (Cd82) - 0.0796 (Cd96) - 0.00152 (Cd78) + 0.1080 (Cd98) + 0.0157 (Cd99)

Cd71 = 88.364 + 0.1553 (Cd67) - 0.2113 (Cd63) - 0.1939 (Cd97) + 0.0298 (Cd75) + 10.957 (Cd92) + 0.0580 (year) - 0.0655 (Cd95) - 0.0475 (Cd87)

Cd72 = 91.358 + 0.1470 (Cd68) - 0.0249 (Cd64) + 0.0116 (Cd76) + 0.0224 (Cd93) + 3.089 (Cd94) + 0.0386 (year) - 0.1348 (Cd88) - 0.00051 (Cd80)

Cd73 = -10.830 + 2.263 (Cd61) + 0.792 (Cd65) + 0.0153 (Cd77) - 43.779 (Cd92) - 1.212 (year) - 0.1372 (Cd81) + 0.188 (Cd99) + 0.466 (Cd69)

Cd74 = 45.019 - 7.216 (Cd88) + 1.391 (Cd62) + 0.698 (Cd66) - 0.318 (Cd82) - 1.147 (year) + 55.008 (Cd94) + 0.155 (Cd99) - 0.432 (Cd98)

Cd75 = -167.912 - 0.530 (Cd67) + 1.962 (Cd63) + 0.0188 (Cd79) - 0.693 (year) + 2.175 (Cd71) - 81.476 (Cd92) + 0.562 (Cd95) + 0.522 (Cd97)

Cd76 = -34.80 - 8.049 (Cd88) + 1.592 (Cd64) + 0.765 (Cd68) - 0.214 (Cd84) - 0.592 (year) + 0.977 (Cd72) - 1.109 (Cd98) + 0.498 (Cd96)

Cd77 = -226.942 + 23.819 (year) + 30.336 (Cd97) + 5.441 (Cd65) - 3.278 (Cd99) - 10.427 (Cd61) - 1.517 (Cd81) + 9.599 (Cd95) + 2.997 (Cd91)

Cd78 = 1191.29 + 29.977 (year) + 31.328 (Cd98) + 10.280 (Cd66) - 11.902 (Cd62) - 27.991 (Cd88) - 12.852 (Cd70) + 363.78 (Cd94) - 0.932 (Cd82)

Cd79 -93.261 + 19.804 (year) + 7.802 (Cd67) + 27.764 (Cd97) - 19.179 (Cd63) + 667.14 (Cd92) - 1.796 (Cd83) - 4.252 (Cd87) + 0.981 (Cd91)

Cd80 = 187.80 + 24.945 (year) + 28.375 (Cd98) + 8.666 (Cd68) - 15.350 (Cd64) - 21.541 (Cd88) - 1.432 (Cd84) + 136.93 (Cd94)

Cd81 = 152.91 - 3.475 (year) - 1.982 (Cd61) - 0.939 (Cd97) - 0.864 (Cd69) + 0.573 (Cd87)

Cd82 = 99.635 - 3.244 (year) + 4.088 (Cd88) + 0.457 (Cd98) - 0.463 (Cd62) - 0.792 (Cd70)

Cd83 = 48.447 - 3.148 (year) - 0.615 (Cd63) + 0.537 (Cd87)

Cd84 = 31.974 - 2.974 (year) + 2.846 (Cd88) - 0.432 (Cd64)

Cd89 = 0.0258 + 0.00868 (Cd56) - 0.00028 (Cd54) - 0.00220 (Cd88) + 0.00060 (Cd55) + 0.0240 (Cd94) - 0.00030 (Cd61) + 0.00001 (Cd77) - 0.00036 (year)

Cd90 = -5.359 + 0.196 (year) + 0.0622 (Cd66) + 0.177 (Cd53) + 0.659 (Cd56) + 0.0751 (Cd61) + 0.0260 (Cd99) + 3.027 (Cd94) + 0.0094 (Cd82)

Cd97 = 36.142 - 0.00455 (Cd77) - 0.347 (Cd69) - 0.148 (year) + 0.0279 (Cd99) + 0.0192 (Cd65) - 0.00599 (Cd81)

Cd98 = 2.324 + 0.00627 (Cd78) - 0.0823 (Cd66) + 0.0153 (Cd82) + 0.392 (Cd88) - 0.119 (year) + 0.0159 (Cd99)

LABORATORY EVALUATION OF RHEOLOGICAL BEHAVIOR OF AN ASPHALT CONCRETE CONTAINING AN SBR ELASTOMER

C. Verga, G. Battiato, and C. La Bella, SNAM PROGETTI, S.p.A., Milan, Italy

The subject of this paper is the influence of synthetic rubber [an elastomer styrene-butadiene rubber (SBR)] on the rheological behavior of asphalt concrete. The viscoelastic functions of a wearing course asphalt concrete with and without rubber have been evaluated with unconfined tensile creep tests and tensile-compressive stress dynamic tests at various frequencies and temperatures. The tests were carried out with an electrohydraulic system. The results obtained in the creep tests were perfectly comparable to those obtained in the dynamic tests, confirming the validity of the linear viscoelastic approach. The addition of rubber to concrete increases stiffness at high temperatures, long stress times (in creep tests), and low frequencies (in dynamic tests). Moreover, a general improvement in the elastic characteristics is found when phase angle between stress and deformation is reduced. Rubber contribution to asphalt concrete has also been evaluated in terms of fatigue behavior in a series of tests carried out in the laboratory under different loads.

•DURING recent years the increase in heavy traffic on Italian highways has necessitated research into the rheological behavior of pavement materials, with particular reference to the wearing course, both for the construction of new highways and the reinforcement of existing ones. It seemed indispensable to direct the research toward the improvement of asphalt concretes considering the effects of both aggregates and asphalt cement. The Italian National Hydrocarbons Authority (ENI) research laboratories, responsible for the study of petroleum products, directed their work toward the improvement of the elastic properties of asphalt concrete. The contribution of latex of SBR elastomers toward improving the elasticity, deformation resistance, and fatigue life of asphalt concrete was investigated.

EXPERIMENTAL EQUIPMENT AND TEST METHODS

Research was carried out with an electrohydraulic system on specimens of wearing course asphalt concrete, which were subjected to static and dynamic tests at temperatures of 32 F (0 C) and 68 F (20 C) (1).

Static tests under unconfined axial tensile stress were carried out to define creep compliance for times from 10^{-1} to 10^{3} sec. Stress was 1.5 bar at 32 F (0 C) and 0.3 bar at 68 F (20 C). Dynamic tests under tensile and compressive stress (a short period of tensile stress followed by one of compression) on specimens of the same kind to evaluate the complex modulus at frequencies of 0.03, 0.3, 3, and 30 Hz at the same temperatures were carried out. Stress levels were selected to remain in the field of linear viscoelasticity.

The last investigation was the definition of fatigue behavior of the concrete under examination. Tests were carried out only at 68 F (20 C) by applying to the specimens a sinusoidal axial stress (tensile amplitude equal to compressive) at a frequency of 10 Hz.

Publication of this paper sponsored by Committee on Mechanical Properties of Bituminous Paving Mixtures.

The experimental equipment included a MTS servo-controlled electrohydraulic testing machine by which dynamic stress functions were imposed and which could be programmed to different frequencies (Fig. 1). The specimens were lodged in a thermostatic cell with an accuracy of ±1 F (±0.5 C); the temperature was checked by 2 thermoresistors, one free in the environment and the other immersed in a reference specimen. Axial strains were measured by 2 strain gauges cemented at the middle of the specimen on diametrically opposed sides and inserted in a Wheatstone bridge circuit, which included 2 strain gauges belonging to the unstressed reference specimen used to compensate for temperature effects. A carrier frequency amplifier and a photographic galvanometer recorder were used for strain output measurement. The phase angle between stress and strain was directly measured by a frequency response analyzer.

COMPOSITION AND PREPARATION OF TEST SPECIMENS

Figure 2 shows the gradations of aggregates and the volume characteristics of the concrete mix used.

The experimental tests were carried out on cylindrical specimens (ϕ = 6 cm; h = 12 cm) compacted into molds of the required bulk density by applying at the same time the necessary load at 2 ends of the cylindrical molds by 2 opposed and free plungers.

The concrete was obtained from totally crushed stones composed according to specifications for the building of national highways from an 80-100 penetration grade asphalt produced by the Italian National Petroleum Agency (AGIP) and optimized in concentration by the Marshall method (ASTM D 1559-71). Both pure asphalt and that with 5 percent SBR latex (produced by ANIC of the ENI Group) added in dry weight were used for the production of concrete. This was carried out with mechanical mixers under strict temperature checks. The preparation of the specimens was carried out with systems that guaranteed the best uniformity of the bulk densities and the best repeatability.

For fatigue-test specimens, the same concrete was used, but the specimens were planned differently, because the creation of a weaker section where failure could occur was necessary. They were therefore produced in the shape and size shown in Figure 3 by using the above-mentioned methods. The concrete was compacted into molds that consisted of 2 specular parts firmly bound together that were easily separable after compaction.

Before testing, all the specimens were left for 3 weeks at room temperature to allow a suitable weathering of the concrete. They were then capped with steel caps as shown in Figure 4.

CREEP AND DYNAMIC TESTS

In Figure 5 the experimental creep compliance function is shown at 68 F (20 C) for concretes with and without rubber. The creep compliance reported on double log scale as shown in Figure 6 can be represented by the function

$$J(t) = J_e + J_v t^{\alpha} \qquad (1)$$

which fits the experimental data well for times up to 10^3 sec at 32 F (0 C) and up to 30 sec at 68 F (20 C) (2). J_e and α are practically temperature independent. J_e is the elastic component of the creep compliance ($1/J_e$ represents the upper limit of the absolute value of the complex modulus at low temperatures); its value was determined experimentally during the tests at 0 C. The values of J_e, α, and J_v obtained at 20 C are as follows:

Specimen	J_e	J_v	α
Concrete with rubber	5.5×10^{-6} bar^{-1}	7.8×10^{-5} bar$^{-1} \times$ sec$^{-\alpha}$	0.32
Concrete without rubber	5.0×10^{-6} bar^{-1}	12.7×10^{-5} bar$^{-1} \times$ sec$^{-\alpha}$	0.37

Concrete with rubber shows less tendency to strain during prolonged stress periods. Its resistance to permanent strain can therefore be seen.

Figure 1. General view of the experimental apparatus.

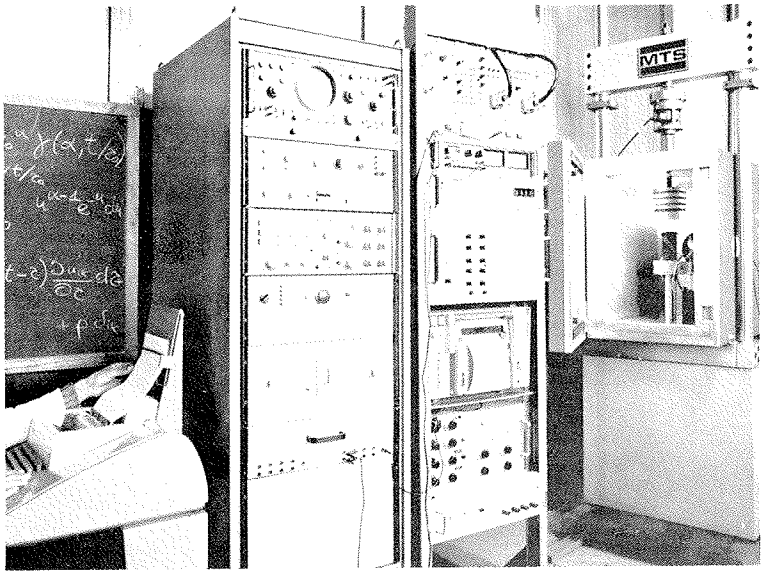

Figure 2. Asphalt concrete characteristics.

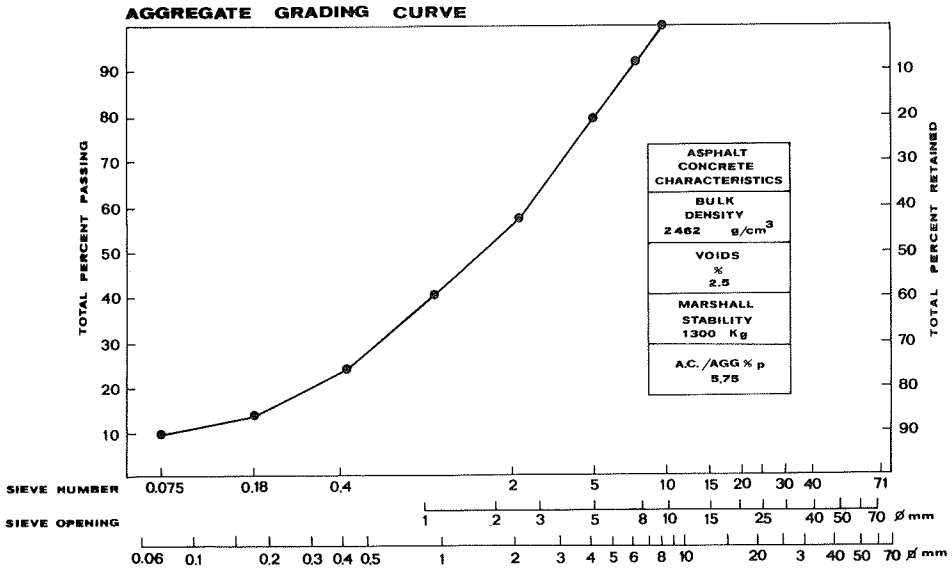

Figure 3. Dimensional view of specimen used in fatigue tests.

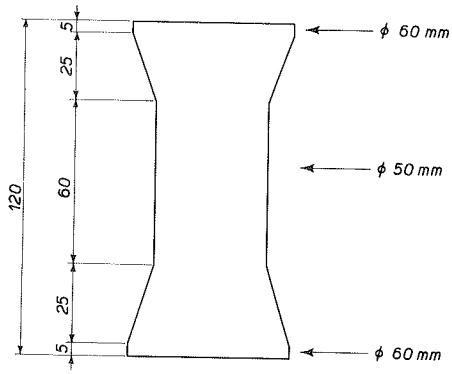

Figure 4. View of specimen used in creep and dynamic tests.

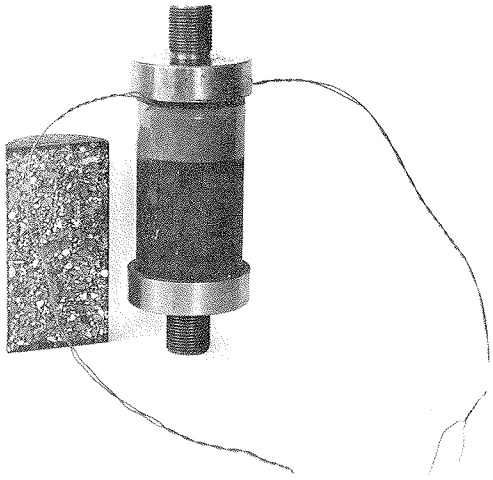

Figure 5. Creep compliance, experimental values at 20 C.

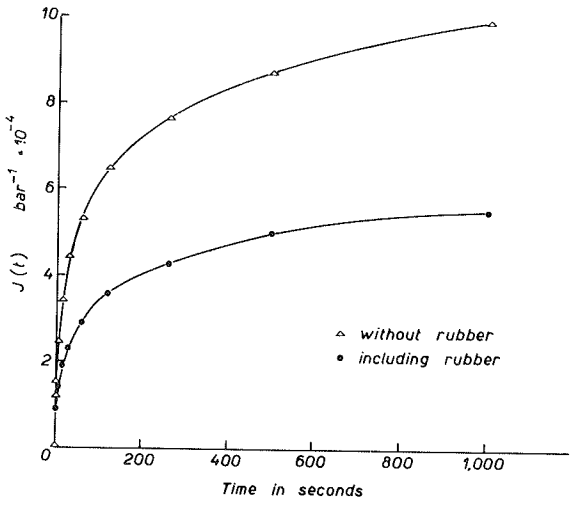

Figure 6. Creep compliance, experimental values at 0 and 20 C.

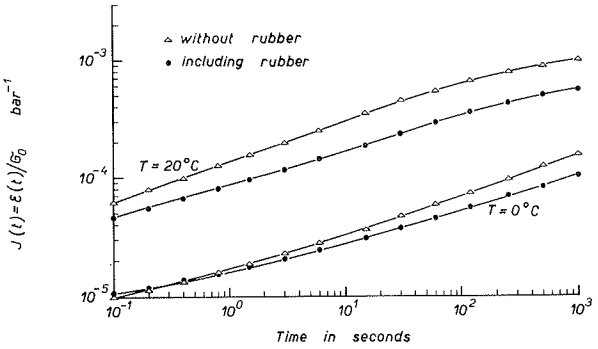

Figure 7. Absolute value of complex modulus, calculated from creep compliance.

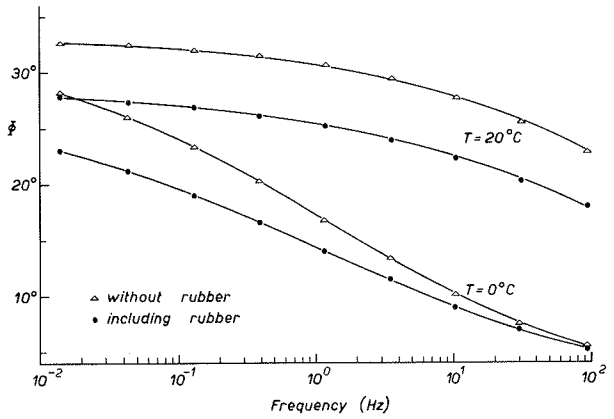

Figure 8. Phase angle between stress and strain, calculated from creep compliance.

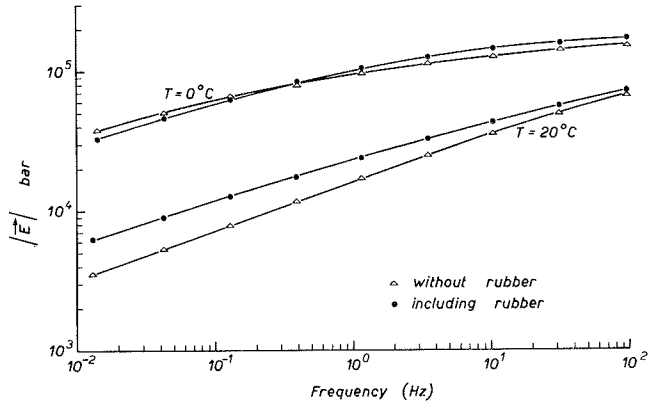

Based on the linear viscoelastic theory, an analytical expression of complex modulus from Eq. 1 can be obtained (3). The relationships of phase angle and absolute value of the complex modulus to the frequency calculated by creep compliance are shown in Figures 7 and 8 respectively. These values can be correlated to those measured directly with dynamic tensile-compressive tests at the same temperatures and in a frequency range from 3×10^{-2} to 30 Hz.

The experimental values of E and ϕ are shown in Figures 9 and 10. The good correlation confirms the validity of the phenomenological approach.

In terms of stiffness, rubber proved to be essential with increase of temperature and reduction of frequency in dynamic testing.

FATIGUE TESTS—GENERAL CONSIDERATIONS

The fatigue behavior of the asphalt concrete was the subject of various laboratory studies with stress or strain imposed, which often produced contradictory results (4, 5). Analysis of the fatigue phenomena of asphalt concrete under real traffic conditions shows that fatigue behavior with strain imposed is correlated to the phenomena to which the intermediate layers of flexible pavement were subjected because these layers have to follow the subbase strains. Otherwise, wearing course fatigue behavior is better representable in the laboratory through stress tests (6). It was decided to carry out dynamic tensile-compressive tests with constant stress amplitude until failure without intermediate rest periods.

This program justified the need both to observe the behavior of an asphalt wearing course and to evaluate the rubber contribution.

RESULTS

As is well-known, fatigue behavior studies in asphalt concrete are made difficult by considerable data dispersion. The statistical interpretation of these phenomena was done by the law of normal distribution of the failure cycle logarithm. In our case, the standard deviation of this distribution varied from a minimum of $\pm$ log 1.3 to a maximum of $\pm$ log 1.7 (15 specimens were used for each type of concrete and level of stress applied).

The axial strain versus time encountered during a fatigue test is shown in Figure 11. The specimen failure was observed to occur generally when the strain became twice the initial one. In the case of a concrete with rubber added, a failure strain was observed at about 3 times the initial value.

This behavior is consistent with the best ductility characteristics of asphalt cement at 68 F (20 C). The curve of the failure cycle numbers is shown in Figure 12 (mean values of log N) with respect to the stress applied, $\pm\sigma_o$ (tensile stress is indicated by +, and compressive stress by -). The experimental data were correlated with the function

$$\log N = \alpha \log \sigma_o + \beta \qquad (2)$$

where the α and β values were calculated with a linear regression. As shown in Figure 12, the elastomer contribution is clear, especially for the lowest values of applied stress. Compared with nonrubberized concrete, there was an increase in life from 2 to 5 times in the stress range considered.

The failure cycles and the initial strain values are given in Table 1 together with correlation results and strain standard deviations. The α value varied from -4.5 for the concrete without rubber to -6.0 for the concrete with rubber. This is in accordance with the fact that the angular factor α is generally greater (in absolute value) for stiffer concretes (2).

In Figure 13 failure cycles are shown with the mean values of initial strains obtained at 3 stress levels where ϵ_o represents the peak amplitude of the dynamic strain. The behavior of log N with respect to log ϵ_o can be represented in this case by a relation analogous to Eq. 2

Figure 9. Absolute value of complex modulus, experimental values.

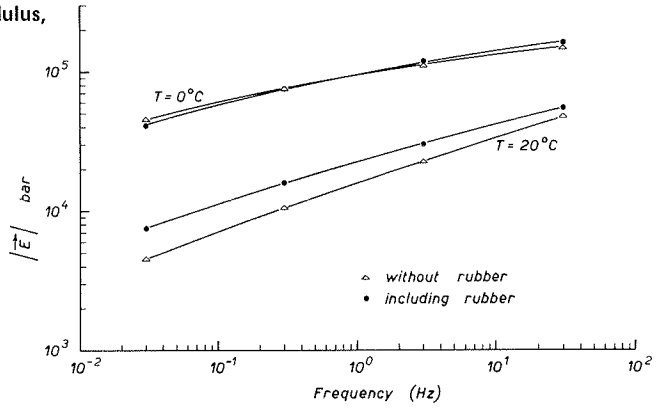

Figure 10. Phase angle between stress and strain, experimental values.

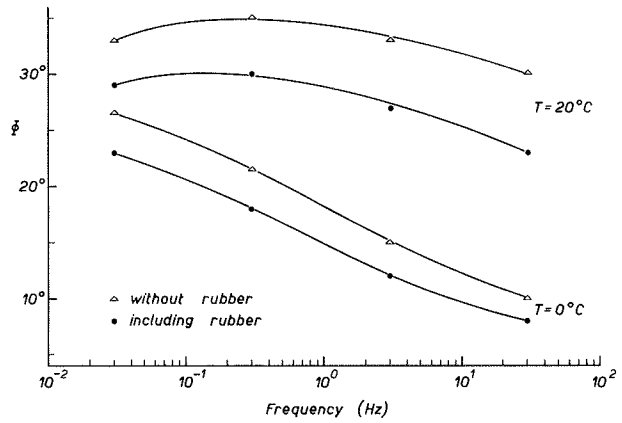

Figure 11. Axial strain versus time during a fatigue test.

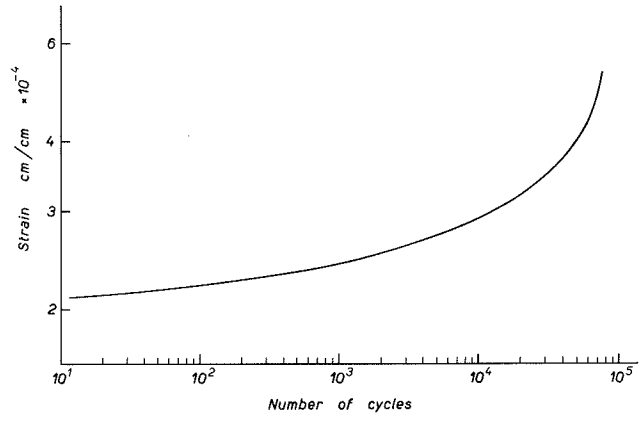

Figure 12. Tension compression fatigue test, failure cycle number versus stress applied.

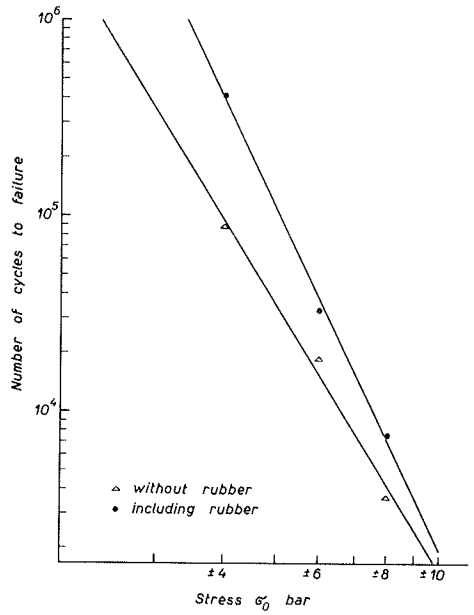

Table 1. Results of fatigue tests of sinusoidal stress of constant amplitude.

Stress, σ_0 (bar)	Number of Cycles to Failure	Initial Strain, $\epsilon_0 \times 10^6$	Log N = α log σ_0 + β	Log N = α log ϵ_0 + γ
Without Rubber				
±8	3,650	418 ± 22		
±6	18,700	304 ± 16	α = -4.5	α = -4.5
±4	88,000	208 ± 12	β = 7.7	γ = -11.8
With Rubber				
±8	7,500	324 ± 16		
±6	32,500	264 ± 14	α = -5.8	α = -6.1
±4	410,000	170 ± 10	β = 9.1	γ = -17.5

Figure 13. Tension compression fatigue test, failure cycle number versus initial strain.

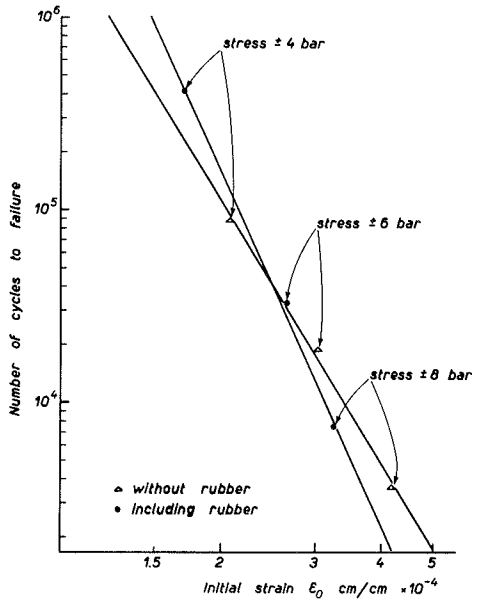

$$\log N = \alpha \log \epsilon_o + y \quad (3)$$

The best fatigue behavior observed in the rubberized concrete seemed to be a consequence of its greater stiffness. The curves in Figure 13 (log N versus log ϵ_o) show in fact that the initial strain is the parameter that principally affects the number of failure cycles; the 2 curves differentiate in their slope, intersecting at $\epsilon_o \approx 2.5$ cm/cm $\times 10^{-4}$. This may partially explain the apparent contradiction between the results obtained in the fatigue tests with applied strain and stress. For the latter, a better behavior for the stiffer concrete was found particularly in a limited field of values of applied stress; in the constant strain tests, a longer life for those with a lower modulus was generally noted.

For the high initial strains, the faster the fatigue process, the higher the modulus of the material was according to the hypothesis that the length of cracks appearing in material increases in time proportionally to σ^4.

CONCLUSIONS

The laboratory tests showed the validity of employing a latex of SBR because of the mechanical characteristics observed, in terms of both deformation resistance and fatigue behavior.

This improved performance is assuming particular importance in Italy because of the continuous increase of heavy traffic and loads over 10 tons/axle.

ACKNOWLEDGMENT

Permission to present this paper was given by the AGIP and ANIC of ENI Group.

REFERENCES

1. Verga, C., Battiato, G., and La Bella, C. Laboratory Evaluation of Rheological Behaviour of Wearing Course, Binder and Base Asphalt Concrete. Autostrade, Rome, Italy, Sept. 1972.
2. Verga, C., Battiato, G., La Bella, C., and Ronca, G. Viscoelastic Analysis of the Deformation Behaviour for Flexible Pavements Models. Acts of the 2nd Meeting of Italian Society of Rheology, Siena, Italy, May 1973.
3. Ferry, J. Viscoelastic Properties of Polymers, 2nd Ed. John Wiley and Sons, Inc., New York, 1970.
4. Pell, P. S. Fatigue of Asphalt Pavement Mixes. 2nd Internat. Conf. on Structural Design, Univ. of Michigan, Aug. 1967.
5. Kennel, M. Etude de la résistance à la fatigue des bétons bitumineux. Révue général des routes et aerodromes, Paris, Jan. 1973.
6. Doan, M. Contribution à l'étude du comportement à la fatigue des bétons bitumineux. Faculté des Sciences de Paris, Thèse de Docteur-Ingénieur, Paris, May 1970.

METHODS FOR PREDICTING MODULI AND FATIGUE LAWS OF BITUMINOUS ROAD MIXES UNDER REPEATED BENDING

Louis Francken and Jean Verstraeten, Centre de Recherches Routieres, Belgium

The use of modern pavement design methods to prevent cracking necessitates, among other things, determining the moduli and fatigue laws in bending of the bituminous road mixes (base courses and wearing courses). These determinations are now possible, but they involve sophisticated experiments that are not well adapted to practical purposes. The objective of this paper is to present an original contribution to the prediction of moduli and fatigue laws in sinusoidal bending (controlled stress tests) of bituminous mixes. The results obtained with a large variety of mixes having different bitumen, composition, and size distribution of the aggregates show that this prediction requires only the knowledge of the volumetric composition of the mix (aggregate volume content, bitumen volume content, and void content) and the knowledge of some characteristics of the bitumen used (asphaltene content and penetration). On the basis of the experimental results obtained, general formulas are presented to permit the prediction of the moduli and the fatigue law of a mix. Practical criteria for the selection of the bitumen are also proposed.

•WORK on predicting moduli and fatigue laws of bituminous road mixes (under repeated bending) is part of a more general research project on pavement design in progress at Belgium's Centre de Recherches Routières. This project covers design criteria, vehicles and traffic, multilayer theory, mechanical properties of road materials, influence of climatic effects, and experimental roads (1).

MIXES AND BITUMEN

The particulars of the mixes investigated are given in Table 1. Mixes cut out of experimental roads are designated with an "r" (2, 3). The other mixes were manufactured in the laboratory by static compaction. The maximum size of the coarse aggregates varied from 12 mm to 32 mm. The sand, which varied from 74 μm to 2 mm, was a mixture of natural sands except for the mixes P1r to P6r, P20 to P23, and S12 to S19r, where it was a mixture of ⅔ natural sand and ⅓ crushed sand. The filler (<74 μm) was a limestone filler except for mixes P15, P16, and 017 where it was a mixture of limestone and clay; limestone and chalk; and limestone, clay, and chalk respectively. The letter symbol under weight percentage of a mix refers to the kind of stones in the mix (P = porphyry, G = rounded gravel, S = hard sandstone, L = limestone, and PV = Voutre porphyry).

The characteristics of the bitumen used are given in Table 2. The meanings of the symbols are as follows: penetration at 25 C/100 g/5 s = Pen; softening point ring and ball = T_{AB}; penetration index = IP; asphaltene content defined as the percentage of the insoluble phase of the bitumen in normal heptane at the ambient temperature = α; specific gravity = γ_L; (d log pen)/(d log t) = derivative B; viscosity at 25 C for low shear stresses = η_o; and the ratio between viscosities at 25 C for low and high shear stresses = η_o/η_∞.

Publication of this paper sponsored by Committee on Mechanical Properties of Bituminous Paving Mixtures.

Table 1. Particulars of the mixes.

Mix	Weight Percentages				Volume Percentages			
	Stones (P)	Sand (S)	Filler (F)	Bitumen (L)	Voids	Aggregates	Bitumen	Bitumen[a]
P0	58	35	7	5.8	4.8	82.3	12.9	DU 60
P1r	53.8	36.2	10	6.1	3.5	83.2	13.3	T3 50-70
P2r	53.8	36.2	10	5.9	3.5	83.5	13.0	T2 50-70
P3r	53.8	36.2	10	6	3.5	83.5	13.0	T1 50-70
P4r	53.8	36.2	10	5.8	3.5	83.7	12.8	T3 80-100
P5r	53.8	36.2	10	5.7	3.5	83.9	12.6	T2 80-100
P6r	53.8	36.2	10	5.9	3.5	83.6	12.9	T1 80-100
P7	58	35	7	5.8	4.9	82.5	12.6	DT 40
P8	80	18	2	4.9	12.5	77.4	10.1	DT 180
P9	58	35	7	5.8	4.7	82.6	12.7	DT 180
P10	80	18	2	4.4	14.2	76.8	9	DT 80
P11	50	40	10	6.7	3.9	81.7	14.3	DU 80
P12	55	37.7	7.3	6.2	6.2	80.3	13.5	L 80
P13	55	37.7	7.3	6.2	6.1	80.9	13.1	D 80
P14	55	36	9	6	4.7	82.3	13	DU 60
P15	55	36	7+2	6	3.5	83.3	13.2	DU 60
P16	55	36	8.5+0.5	6	4.9	82.1	13	DU 60
P17	55	36	6.5+2+0.5	6	3.7	83.2	13.1	DU 60
P18	35	52.8	12.2	8	6.9	76.9	16.2	DU 40
P19	55	36	9	5.8	4.8	82.6	12.6	DU 60
P20	55	38	7	6.1	5.3	81.5	13.2	DU 60
P21	65	35	—	6.4	6.3	80.2	13.5	DU 40
P22	80	18	2	6.25	10.2	76.9	12.9	DU 60
P23	55	37	8	6.3	4.4	82.0	13.7	HN 80
P24	55	36.4	8.6	5	8.3	81.0	10.7	DU 60
P25	53	38.4	8.6	4.75	8.7	81.2	10.1	DU 60
P26	55	36.4	8.6	5.4	6.9	81.5	11.6	DU 60
P27	53	38.4	8.6	5.2	8.1	80.8	11.1	DU 60
P28	55	37	8	5.6	5	82.5	12.5	DT 80
L1	55	37.7	7.3	6.2	6.1	80.8	13.1	DU 40
L2	55	37.7	7.3	6.2	6.2	80.7	13.1	DU 80
L3	55	37.7	7.3	6.2	6.2	80.8	13.0	D 80
G1	55	37	8	5.8	5.1	82.3	12.6	DT 80
S1	55	37.7	7.3	6.2	5.1	81.3	13.6	L 80
S2	55	37.7	7.3	6.2	5.5	81.4	13.1	D 80
S3	55	37.7	7.3	6.2	5.7	81.3	13.0	H 50
S4	55	37.7	7.3	6.2	6.6	80.4	13.0	B 80
S5	55	37.7	7.3	6.2	6.6	80.4	13.0	E 50
S6	55	37.7	7.3	6.2	6	80.8	13.2	SG 80
S7	55	37.7	7.3	6.2	6.4	80.5	13.1	SK 80
S8	55	37.7	7.3	6.2	6.8	80.1	13.1	E 80
S9	55	37.7	7.3	6.2	5.1	81.6	13.3	SK 50
S10	35	52.8	12.2	8	7.3	76.7	16.0	DU 40
S11	55	37.7	7.3	6.2	6.1	80.8	13.1	LA 80
S12r	55	37.7	7.3	6.2	2.7	83.9	13.4	SK 80
S13r	55	37.7	7.3	6.2	1.9	84.5	13.6	SK 50
S14r	55	37.7	7.3	6.2	1.7	84.9	13.4	LA 80
S15r	55	37.7	7.3	6.2	1.8	84.9	13.3	H 50
S16r	55	37.7	7.3	6.2	1.9	84.7	13.4	E 50
S17r	55	37.7	7.3	6.2	2	84.4	13.6	SG 80
S18r	55	37.7	7.3	6.2	2.4	84.4	13.2	B 80
S19r	55	37.7	7.3	6.2	2.1	84.4	13.5	E 80

[a]From Table 2.

Table 2. Characteristics of the bitumen.

Type of Bitumen	Pen	T_{AS}	IP	α	γ_L	B	$\eta_o \times 10^{-5}$ N/m^2	η_o/η_∞
L 80	107	45.6	-2.04	0.9	0.995	0.495	0.56	1.33
D 80	83	46.6	-1.00	9.7	1.031	0.471	0.79	1.36
H 50	39	60.1	+0.89	29.3	1.046	0.312	30.0	7.50
B 80	81	49.1	-0.31	22.4	1.033	0.404	1.57	2.28
E 50	42	55.1	-0.02	24.1	1.028	0.345	14.40	4.74
SG 80	83	46.4	-0.23	16.4	1.020	0.440	1.10	1.72
SK 80	81	48.4	-0.18	19.8	1.022	0.384	1.45	1.71
E 80	79	49.7	-0.61	23.4	1.021	0.429	1.86	2.70
SK 50	49	55.7	+0.75	23.4	1.025	0.332	2.32	4.48
LA 80	70	49.5	-0.02	25.4	1.056	0.386	2.20	2.00
H 50[a]	33	—	—	32.9	1.056	—	70.40	8.66
B 80[a]	74	—	—	26.7	1.054	—	3.41	2.34
E 50[a]	29	—	—	29.2	1.044	—	54.10	4.92
SG 80[a]	114	—	—	18.6	1.025	—	1.37	2.40
SK 80[a]	76	—	—	23.1	1.033	—	2.79	2.07
E 80[a]	39	—	—	27.4	1.040	—	25.30	4.36
SK 50[a]	43	—	—	27.9	1.040	—	21.00	4.43
LA 80[a]	76	—	—	27.2	1.056	—	2.42	1.79
T1 50-70	60	50.0	-0.49	14.7	1.038	0.438	2.56	1.20
T2 50-70	64	53.5	+0.31	25.8	1.028	0.360	6.76	3.30
T3 50-70	57	55.5	+1.01	27.9	1.030	0.336	5.46	4.70
T1 80-100	84	47.0	-1.07	15.3	1.032	0.458	2.31	2.40
T2 80-100	80	49.0	-0.23	22.8	1.027	0.400	2.91	1.80
T3 80-100	92	49.0	+0.27	26.4	1.027	0.407	2.99	3.40
DT 40	46	57.9	+0.40	24.3	1.028	0.317	5.65	2.60
DT 80	93	48.5	+0.03	18.0	1.024	—	0.73	2.00
DT 180	208	37.3	-1.12	12.7	1.019	0.500	0.21	1.30
DU 40	42	59.0	+2.01	24.7	1.028	0.321	22.30	7.20
DU 60	57	54.5	+0.42	22.9	1.023	0.349	4.46	2.90
DU 80	97	47.5	-0.13	19.6	1.029	0.429	0.93	1.80
HN 80	73	48.5	-0.48	18.2	1.032	0.400	—	—

[a]Bitumen recovered from cores cut out of wearing course.

EXPERIMENTAL CONDITIONS

The tests were performed on specimens having trapezoidal shapes (bases were 9 cm and 3 cm; height was 35 cm; thickness was 3 cm) that were fixed at their larger base and detached at the other base in sinusoidal bending (controlled stress tests).

Frequencies ranged from 3 to 100 Hz; temperatures ranged from -20 to +30 C. Moduli were determined for a stress level such that fatigue failure would not occur for fewer than 10^7 repetitions. In fatigue tests, the number of cycles (N) before failure varied between 5.10^3 and 10^6.

Manufacture of the specimens and the description of the equipment are presented in a detailed research report (4).

METHOD FOR PREDICTING STIFFNESS MODULI

Experimental Results

Table 3 identifies the moduli that have been determined on 52 of the mixes given in Table 1. Each mix is characterized by the stiffness modulus, $|E^*|$, and the loss tangent, tg φ, both of which are functions of temperature, T, and frequency, f:

$$|E^*| = \sqrt{E_1^2 + E_2^2}$$

and

$$\text{tg } \varphi = E_2/E_1$$

where

E_1 = storage modulus and
E_2 = loss modulus.

The values of E_1, E_2, $|E^*|$, and tg φ were determined for 5 frequencies (3, 10, 30, 54, and 97 Hz) and 4 temperatures (-20, -5, +15, and +30 C). The numerical values of $|E^*|$ and tg φ obtained for the 52 mixes given in Table 3 are for 3 frequencies (3, 30, and 97 Hz) and the 4 temperatures mentioned. The interpretation of these values confirmed previously obtained results:

1. The $|E^*|$ moduli of bituminous mixes obey the frequency-temperature superposition principle—for every temperature, T, a factor α_T can be found, such that the curve ($|E^*|$ versus $\alpha_T \times f$) at temperature T coincides with the curve ($|E^*|$ versus f) at a chosen reference temperature T_s. The shifting factor α_T is given by an equation of the Arrhenius form

$$\alpha_T = \exp \frac{\Delta H}{R}\left(\frac{1}{T} - \frac{1}{T_s}\right) \qquad (1)$$

T and T_s are in kelvins, R is the universal gas constant, and ΔH (apparent activation energy) is practically a constant (5). For all the mixes investigated here, $\Delta H \approx 2.09 \times 10^5$ J/mol and $T_s = 288$ K (15 C).

2. The complex moduli $E^*(i\omega) = E_1 + iE_2$ can be written as the analytical formulation of a rheological model made of springs with 2 so-called parabolic cells (i.e., cells with a power-law creep function).

$$E^*(i\omega)/E_\infty = 1/[1 + \delta(i\omega\tau)^{-k} + (i\omega\tau)^{-h}](*) \qquad (2)$$

where

E_∞ = purely elastic modulus characterizing the mix at very low temperatures or at very high frequencies or both,
ω = angular frequency,
τ = parameter with the dimensions of a time, and
h, k, and δ = empirical factors (6).

The values of h, k, δ, and E_∞ obtained for the 52 mixes are given in Table 4.

Table 3. Numerical values of $|E^*|$ and tg φ.

	3 Hz								30 Hz								97 Hz							
	30 C		15 C		-5 C		-20 C		30 C		15 C		-5 C		-20 C		30 C		15 C		-5 C		-20 C	
Mix	$\|E^*\|^a$	tg φ^b	$\|E^*\|^a$	tg φ^b	$\|E^*\|^a$	tg φ^b	$\|E^*\|^a$	tg φ^b	$\|E^*\|^a$	tg φ^b	$\|E^*\|^a$	tg φ^b	$\|E^*\|^a$	tg φ^b	$\|E^*\|^a$	tg φ^b	$\|E^*\|^a$	tg φ^b	$\|E^*\|^a$	tg φ^b	$\|E^*\|^a$	tg φ^b	$\|E^*\|^a$	tg φ^b
P0	13	55	53	39	181	12	255	4	33	51	92	29	221	9	283	3	50	44	119	24	246	6	298	<1
P1r	11	78	50	42	165	13	246	6	27	66	87	32	202	9	273	4	42	57	109	26	222	8	287	3
P2r	8.3	83	45	51	174	15	262	7	23	71	83	36	215	10	289	3	38	63	110	30	238	9	303	1
P3r	10	128	82	56	245	9	311	3	40	93	144	32	280	5	331	1	66	69	177	25	300	—	343	—
P4r	5.8	82	36	55	162	19	259	7	17	78	72	40	206	11	291	5	31	65	98	36	232	10	307	3
P5r	6.8	88	46	57	180	15	266	5	21	82	87	37	221	10	291	2	37	74	114	31	243	8	305	2
P6r	9.6	128	70	48	217	9	283	3	36	84	125	28	250	5	303	—	61	74	153	22	266	4	312	<1
P7	12	78	56	45	190	13	261	6	32	64	96	31	227	9	287	4	48	56	119	27	245	8	301	2
P8	3.8[c]	111[c]	17	81	127	20	202	6	14[c]	101[c]	46	60	163	13	223	3	26[c]	87[c]	65	48	181	10	233	2
P9	4.3[c]	106[c]	20	86	137	22	240	7	16[c]	99[c]	52	59	181	13	264	3	32[c]	71[c]	76	48	203	10	277	2
P10	5.2	80	28	53	118	15	183	5	15	73	55	39	147	11	199	3	26	60	72	33	162	9	208	2
P11	4.8	88	29	62	149	19	236	6	15	81	63	45	190	13	265	4	28	61	84	37	220	9	278	3
P12	7	110	71	46	203	6	252	2	28	98	121	27	226	6	264	1	53	58	146	19	238	2	270	1
P13	6.5	104	49	53	182	8	236	2	24	90	93	33	205	5	248	1	45	54	117	22	219	3	255	<1
P14	10	71	48	45	179	14	248	5	26	70	88	37	210	9	274	3	42	53	112	28	233	8	282	3
P15	19	109	66	56	187	18	269	8	35	80	105	43	228	13	295	5	53	63	133	30	251	8	315	2
P16	9	68	43	52	172	17	255	8	24	71	81	37	208	11	277	4	39	52	105	28	227	8	290	2
P17	14	73	56	45	185	16	263	6	31	77	98	36	224	11	287	5	48	58	125	27	245	8	300	3
P18	8	59	35	41	126	16	204	10	19	65	61	35	156	12	223	7	30	45	76	25	175	8	224	2
P19	22	51	76	23	175	9	224	4	44	44	108	20	198	8	239	3	59	35	124	16	209	5	239	<1
P20	11	69	44	45	151	13	226	4	27	62	79	32	185	9	249	3	42	51	103	26	209	6	267	1
P21	14	60	48	38	151	12	222	5	31	53	80	30	184	9	247	2	45	44	101	24	201	7	267	2
P22	8.1	75	33	51	127	15	187	7	21	62	61	37	160	10	212	5	32	61	78	30	176	9	225	4
P23	10	97	49	56	190	14	265	4	32	78	95	35	225	8	286	2	47	68	120	30	245	7	298	0
P24	11	78	42	48	140	14	203	7	27	62	76	33	172	9.5	227	5	41	61	94	30	187	9	228	4
P25	10	72	42	48	153	16	207	7	27	65	76	33	186	12	230	4	41	58	97	29	204	9.6	242	4
P26	10	69	43	47	151	14	221	6	27	63	78	33	184	10	246	3	41	62	98	28	203	8	253	2
P27	10	71	41	50	144	14	217	6	27	63	75	34	177	9	239	3	41	58	97	28	195	8	249	2
P28	10	77	45	50	183	14	248	5	28	69	85	35	226	10	275	4	45	55	110	26	253	6	295	1
L1	15	67	56	38	156	12	214	5	32	56	87	27	184	9	230	3	46	42	107	21	203	5	238	1
L2	4	70	26	56	130	19	209	6	11	93	55	49	168	13	229	4	28	42	74	33	188	8	237	2
L3	9.2	100	64	51	194	9	219	2	31	85	109	32	220	5	252	2	53	55	135	21	231	3	260	<1
G1	5.7	85	33	57	142	17	234	7	17	80	66	41	176	11	250	3	29	72	89	34	197	9	259	2
S1	6.6	141	76	57	221	8	300	3	29	117	128	30	248	5	315	2	53	87	156	22	264	3	317	3
S2	8.6	111	70	51	206	8	258	2	33	97	119	30	230	5	271	<1	53	75	144	24	245	3	280	<1
S3	19	69	73	33	187	11	252	5	40	52	107	25	212	9	268	3	56	48	138	22	231	6	276	<1
S4	10	82	56	44	170	10	238	3	28	73	93	32	200	9	256	3	44	53	115	23	216	5	262	<1
S5	22	51	76	23	175	9	224	4	44	46	107	20	197	8	238	4	59	35	124	16	209	5	239	<1
S6	7.7	91	47	53	166	12	243	6	24	78	87	37	196	9	261	4	41	52	109	24	211	5	261	1
S7	7.1	86	37	46	141	12	210	4	18	73	70	36	172	10	230	3	32	45	87	31	189	7	239	<1
S8	13	63	58	32	164	9	229	4	29	56	91	26	192	7	245	2	43	41	110	20	205	4	253	<1
S9	14	61	54	34	160	11	227	5	32	56	86	27	188	9	245	3	47	43	106	20	202	4	250	<1
S10	8.3	54	38	37	125	15	190	6	20	61	66	31	155	9	211	4	30	45	81	24	168	9	217	5
S11	8	83	45	54	157	15	231	6	24	81	81	40	190	11	250	4	36	63	100	30	208	7	255	2
S12r	7	89	43	50	168	14	248	6	21	77	80	37	203	10	277	4	36	66	106	31	226	8	292	3
S13r	21	62	82	30	196	10	267	5	45	48	121	23	233	7	296	3	65	41	147	19	255	6	313	4
S14r	12	74	63	42	192	13	275	5	33	65	107	29	230	8	300	4	51	56	135	25	254	7	314	2
S15r	30	54	97	26	219	8	285	4	60	42	138	19	253	6	308	2	81	36	162	17	275	5	326	<1
S16r	36	51	115	22	236	9	298	4	66	37	153	16	265	5	318	3	87	33	177	14	285	5	335	<1
S17r	9	102	58	57	206	9	295	<1	30	85	111	36	250	8	322	2	49	72	140	29	274	6	336	2
S18r	11	92	61	46	199	13	277	5	30	77	106	31	236	8	300	2	49	62	134	25	258	7	315	1
S19r	20	62	91	29	222	10	290	6	46	51	133	22	254	7	314	3	65	43	159	18	275	5	329	<1

[a] $|E^*| \times 10^{-8}$ in N/m^2. [b] tg $\varphi \times 10^2$ in N/m^2. [c] Temperature = 25 C.

In view of these 2 conclusions,

$$|E^*| = E_\infty \times |R^*(f_R)| \quad (3)$$

where

$|R^*(f_R)|$ = a reduced modulus varying between 0 and 1 and
f_R = a reduced frequency equal to $\alpha_T \times f$.

Relation Between E_∞ and Mix Composition

On the basis of the numerical values of E_∞ as given in Table 4 for the 52 mixes and for 20 other mixes investigated by Van der Poel (7), Bazin and Saunier (8), Harlin and Uge (personal communication), and Huet (6), it was possible to establish that E_∞ depends only on the composition of the mix and is given by

$$E_\infty(N/m^2) = 1.436 \times 10^{10} \times R^{0.55} \times \exp(-5.84 \times 10^{-2} \times v) \quad (4)$$

where

$R = V_A/V_L$, the ratio between the aggregates percentage volume (V_A) and the bitumen percentage volume (V_L) (range of variation for the 72 mixes: 0.12 to 12) and
v = void contents (range of variation for the 72 mixes: 1.5 to 32 percent).

Figure 1 shows the comparison between the observed values of E_∞ and the values calculated on the basis of Eq. 4.

Relation Between $|R^*(f_R)|$ and Bitumen Characteristics

The analysis of the numerical values of $|R^*(f_R)| = |E^*|/E_\infty$ gives rise to the conclusion that $|R^*(f_R)|$ is dependent only on the bitumen characteristics Pen, B, or α.

Fitting a satisfactory formula on the basis of the empirical correlation to predict R^* from f_R could only be achieved piecemeal. The best formulas derived for 3 ranges of values of f_R are shown in Figure 2. A complete derivation of these formulas is presented in a detailed research report (9).

Predicting $|E^*|$

On the basis of the results presented by the Federal Highway Administration (1), Huet (3), and Verstraeten (4) and those in Figure 2, $|E^*|$, for different temperatures and frequencies, can be predicted solely by knowledge of the volumetric composition of the mix (V_A, V_L, and v) and the characteristics of the bitumen (Pen, B, or α). A computer program has been written to facilitate use of the formulas. Figure 3 shows the result of the comparison between the measured values and the calculated values of $|E^*|$ for mix P17.

Knowledge of $|E^*|$ is sufficient to apply pavement design methods based on the theory of elasticity (multilayer theory). For methods based on the theory of viscoelasticity, knowledge of the storage moduli (E_1) and the loss moduli (E_2) would be necessary. A method for predicting these moduli based on Eq. 2 is presented in detail in a research report (9).

METHOD FOR PREDICTING FATIGUE LAWS

Experimental Results

Table 5 identifies fatigue laws for 42 of the mixes that were given in Table 1. The results presented here complement the precise results presented by Verstraeten (5).

For the mixes investigated, the fatigue law in sinusoidal bending may be written

$$\sigma/|E^*| = \epsilon_r(N) = K \times N^{-a} \quad (5)$$

where

Table 4. Numerical values of k, h, σ, and E_∞.

Mix	k	h	δ	$E_\infty \times 10^{-8}$ N/m^2
P0	0.182	0.480	1.91	303.1
P1r	0.146	0.493	1.74	325.6
P2r	0.186	0.511	1.75	320.2
P3r	0.184	0.675	1.58	351.8
P4r	0.180	0.501	1.69	338.9
P5r	0.193	0.576	1.76	319.3
P6r	0.183	0.665	1.81	309.6
P7	0.182	0.512	1.88	325.5
P8	0.223	0.621	1.95	246.3
P9	0.205	0.598	1.78	294.9
P10	0.200	0.510	1.72	219.2
P11	0.197	0.532	2.11	303.7
P12	0.238	0.666	2.18	264.7
P13	0.167	0.587	1.34	253.8
P14	0.186	0.495	1.59	300.4
P15	0.212	0.633	1.61	334.7
P16	0.185	0.495	2.07	314.1
P17	0.193	0.546	1.88	331.5
P18	0.141	0.446	2.16	290.0
P19	0.205	0.525	2.65	298.1
P20	0.165	0.463	1.54	272.5
P21	0.152	0.419	1.42	269.7
P22	0.161	0.471	1.69	253.9
P23	0.200	0.580	1.60	298.7
P24	0.148	0.480	1.31	275.6
P25	0.225	0.545	2.41	261.4
P26	0.184	0.477	1.57	267.6
P27	0.151	0.467	1.38	277.8
P28	0.203	0.536	2.23	303.4
L1	0.178	0.485	1.84	252.3
L2	0.215	0.516	2.55	250.0
L3	0.208	0.612	1.37	258.1
G1	0.177	0.513	1.55	284.0
S1	0.103	0.681	1.78	335.6
S2	0.191	0.669	1.52	275.5
S3	0.180	0.475	1.50	294.4
S4	0.154	0.524	1.42	273.6
S5	0.193	0.497	2.86	251.6
S6	0.116	0.519	1.36	309.2
S7	0.178	0.528	1.81	247.1
S8	0.145	0.440	1.43	261.0
S9	0.157	0.461	1.72	262.2
S10	0.133	0.410	1.62	259.7
S11	0.179	0.538	1.52	289.9
S12r	0.164	0.525	1.65	322.6
S13r	0.107	0.415	1.46	365.5
S14r	0.159	0.487	1.46	342.9
S15r	0.144	0.414	1.78	343.0
S16r	0.130	0.383	1.39	358.6
S17r	0.172	0.582	1.35	336.5
S18r	0.195	0.571	1.93	325.0
S19r	0.147	0.444	1.62	350.1

Figure 1. Comparison of observed and calculated values of E_∞.

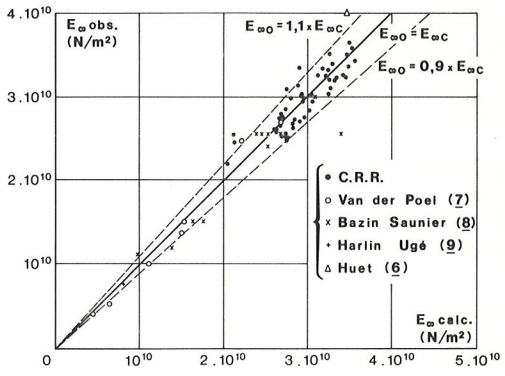

Figure 2. Formulas for predicting $|R^*(f_R)|$.

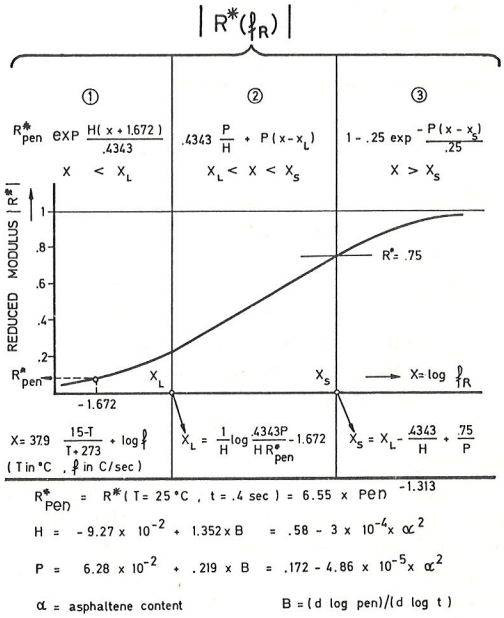

Figure 3. Comparison of observed and calculated values of $|E^*|$.

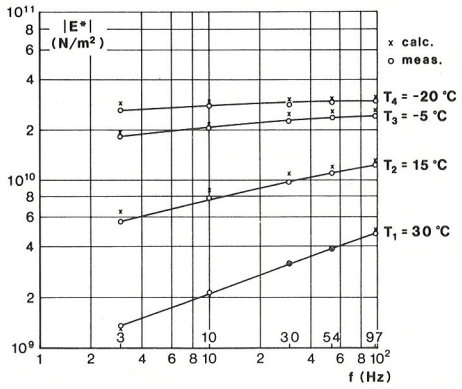

σ = assigned stress,
$|E^*|$ = initial modulus,
$\epsilon_r(N)$ = initial strain,
N = number of cycles to produce failure,
K = a factor depending on the mix considered but practically independent of the temperature and frequency, and
a = an empirical factor.

Values of log K and a for the 42 mixes are also given in Table 5. For the mixes considered, the a slopes of the straight lines [log $\epsilon_r(N)$ and log N] are nearly the same ($\bar{a}$ = 0.21; standard deviation = 0.02). On the basis of this, the fatigue law presented by Verstraeten (5) may thus be replaced by the approximation

$$\epsilon_r(N) = K' \times N^{-0.21} \tag{6}$$

K′ was chosen so that Eqs. 5 and 6 would yield the same ϵ_r value for $N = 10^6$.

Predicting Fatigue Laws

The results given in Table 5 suggest that the factor K′ in Eq. 6 depends on the composition of the mix and bitumen. Explicitly, the fatigue laws of bituminous mixes in repeated bending (controlled tests) may be written independently of frequency and temperature in the general form

$$\epsilon_r(N) = \bar{\Lambda} \times G \times [V_L/(V_L + v)] \times (N/10^6)^{-0.21} \tag{7}$$

where

$\bar{\Lambda}$ = a coefficient given by Figure 4 depending on the asphaltene content of the bitumen and
G = an empirical factor equal to unity when the following conditions are fulfilled: (a) aggregate volume content is between 78 percent and 85 percent; (b) bitumen content, without having an excessive value is such that the aggregates are fully coated; (c) aggregates are made up of fine aggregates and at least 50 percent coarse aggregates; and (d) $0.5 \times 10^{-4} \leq \epsilon_r\ (N = 10^6) \leq 1.3 \times 10^{-4}$.

This is the case for most mixes used in road construction; therefore, the case $G \neq 1$ is only of academic interest and is not further discussed.

Figure 5 shows the comparison between the experimental values of $\epsilon_r(N)$ derived from Table 5, Pell and Taylor (10), and Taylor (11) for 40-50 bitumen mixes ($\alpha \geq 20$ percent) with a calculated value of $\epsilon_r(N)$ derived from Eq. 7 for $N = 10^5$, 10^6, and 10^7.

Equation 7 thus permits prediction of the fatigue law in bending of a bituminous mix when the V_A, V_L, v, and α in the bitumen are known. The influence of factors such as grading, nature and shape of aggregates, and mode of compaction on the critical strain $\epsilon_r(N)$ is taken into consideration through the factor $V_L/(V_L + v)$.

Criteria for Selecting the Bitumen

The factor $\bar{\Lambda}$ of the fatigue law—Eq. 7—can also be related to other characteristics of the bitumen besides α, for example, T_{AB}, η_o at 25 C, and η_o at 25 C/η_∞ at 25 C. Consideration of the values of these characteristics given in Table 2 and of the coefficient Λ given in Table 5 shows that a high and fairly constant value of Λ generally is obtained. Therefore, the following may be taken as criteria for the selection of the bitumens:

1. $\alpha \geq 18$ percent,
2. $T_B \geq 48$ C,
3. η_o at 25 C $\geq 1.3 \times 10^5$ Ns/m^2, and
4. η_o at 25 C/$\eta_\infty \geq 1.75$.

Furthermore, observations made on experimental wearing courses (3) give rise to the following criteria, which complement the preceding ones:

Figure 4. Variation of Λ by α.

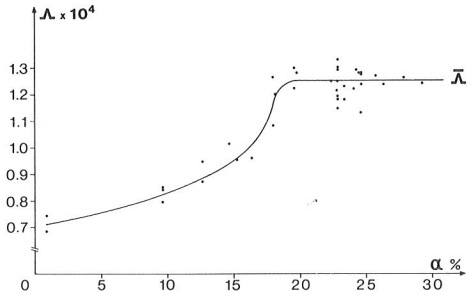

Figure 5. Comparison of measured and calculated values of $\epsilon_r(N)$.

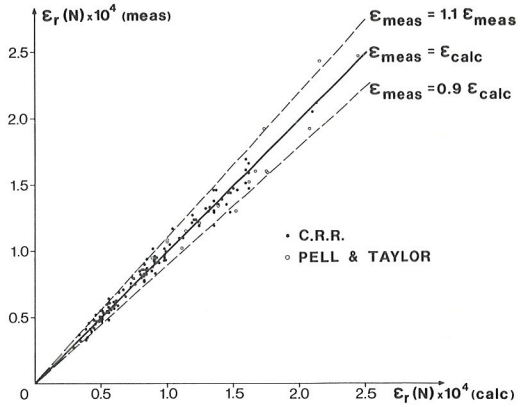

Table 5. Fatigue laws.

Mix	log K	a	$\epsilon_r(N = 10^6) \times 10^4$	$\Lambda \times 10^4$	$\bar{\Lambda} \times 10^4$	$\frac{\Lambda}{\bar{\Lambda}}$	G
P1r	2.800	0.20	1.00	1.263	1.250	1.010	1.0
P2r	2.680	0.22	1.00	1.269	1.250	1.015	1.0
P3r	2.957	0.19	0.80	1.015	0.935	1.086	1.0
P4r	2.693	0.22	0.97	1.235	1.250	0.988	1.0
P5r	2.822	0.20	0.95	1.214	1.250	0.971	1.0
P6r	2.925	0.20	0.75	0.953	0.960	0.993	1.0
P7	2.892	0.19	0.93	1.292	1.250	1.034	1.0
P8	2.640	0.27	0.55	0.876	0.880	0.996	1.4
P9	2.781	0.23	0.69	0.945	0.880	1.074	1.0
P10	2.729	0.25	0.59	1.082	1.160	0.933	1.4
P11	2.671	0.22	1.02	1.298	1.250	1.038	1.0
P12	2.888	0.24	0.47	0.686	0.710	0.966	1.0
P13	2.917	0.22	0.58	0.850	0.825	1.030	1.0
P14	2.882	0.19	0.95	1.293	1.250	1.034	1.0
P15	2.832	0.20	0.93	1.177	1.250	0.942	1.0
P16	2.887	0.19	0.94	1.294	1.250	1.035	1.0
P17	2.772	0.21	0.93	1.193	1.250	0.954	1.0
P18	2.626	0.21	1.30	1.235	1.250	0.988	1.5
P19	2.641	0.24	0.83	1.146	1.250	0.917	1.0
P20	2.871	0.20	0.85	1.191	1.250	0.953	1.0
P21	2.974	0.19	0.77	1.129	1.250	0.903	1.0
P22	2.697	0.24	0.73	1.250	1.250	1.000	1.0
P23	3.141	0.15	0.91	1.240	1.250	0.992	1.0
P24	2.919	0.20	0.76	1.299	1.250	1.039	1.0
P25	3.009	0.19	0.71	1.330	1.250	1.064	1.0
P26	2.926	0.19	0.86	1.334	1.250	1.067	1.0
P27	2.957	0.19	0.80	1.336	1.250	1.069	1.0
G1	2.786	0.21	0.90	1.264	1.160	1.090	1.0
S1	2.828	0.24	0.54	0.742	0.710	1.045	1.0
S2	2.992	0.21	0.56	0.795	0.825	0.964	1.0
S3	2.806	0.21	0.86	1.237	1.250	0.990	1.0
S4	2.941	0.19	0.83	1.251	1.250	1.000	1.0
S5	2.712	0.23	0.81	1.221	1.250	0.977	1.0
S6	2.860	0.22	0.66	0.960	1.010	0.951	1.0
S7	2.866	0.20	0.86	1.280	1.250	1.024	1.0
S8	2.788	0.22	0.78	1.179	1.250	0.943	1.0
S9	2.736	0.22	0.88	1.231	1.250	0.985	1.0
S10	2.739	0.19	1.32	1.281	1.250	1.025	1.5
L1	2.920	0.19	0.87	1.275	1.250	1.020	1.0
L2	2.821	0.21	0.83	1.223	1.250	0.978	1.0
L3	2.888	0.23	0.54	0.842	0.825	1.021	1.0
PV1	2.686	0.23	0.86	1.283	1.250	1.026	1.0

1. $\alpha \leq 27$ percent and
2. Pen > 40.

These 2 criteria aim at limiting the unfavorable effects of aging and effects caused by an increase of the rigidity of the mixes and excessive brittleness.

CONCLUSIONS

The research results presented in this paper give rise to several conclusions.

1. The $|E^*|$ moduli = $E_\infty \times R^*(f_R)$ of a bituminous mix can be predicted, for different temperatures and frequencies, on the basis of knowledge of the volumetric composition of the mix, which influences the value of the modulus of elasticity, and characteristics of the bitumen (B or α and Pen), which influence the value of the reduced modulus. On the basis of the formulas presented for this prediction and to facilitate their use, a computer program giving the components $|E^*|$ and φ of the complex modulus for any temperature or frequency has been written.
2. The fatigue law in sinusoidal bending (controlled stress tests) of a bituminous mix can be predicted on the basis of knowledge of the volumetric composition and asphaltene content of the bitumen.
3. From the point of view of fatigue strength, the following criteria for the selection of the bitumen are brought out: α from 18 to 27 percent, $T_{AB} > 48$ C, η_o at 25 C $\geq 1.3 \times 10^5$ N/m^2, η_o at 25 C/η_∞ at 25 C ≥ 1.75, Pen > 40.
4. Experiments are now in progress to complement the results obtained in repeated bending (cracking) with results in repeated compression (rutting). For this purpose a special apparatus was developed at the Centre de Recherches Routières (12, 13).

ACKNOWLEDGMENTS

We are grateful to J. Reichert, J. Romain, V. Veverka, and J. Huet, of the Centre de Recherches Routières for their help and interest.

We wish to express our thanks to J. De Bast, Institut National du Verre, to A. Fagnoul and K. Gamski, University of Liège, and to Professor R. Van Geen, University of Brussels, for their fruitful discussions.

We express particular appreciation to W. Sandra, P. Coignoul, and C. Lesoil for their care and efficiency in performing the experimental work.

We also wish to acknowledge the financial support of the Belgian Institut pour l'Encouragement de la Recherche Scientifique dans l'Industrie et l'Agriculture.

REFERENCES

1. World Survey of Current Research and Development on Roads and Road Transport. Federal Highway Administration, 1972, p. 31.
2. Huet, J., Reichert, J., and Outer, P. Tronçons Expérimentaux en Bétons Asphaltiques. La Technique Routière, Brussels, Vol. 14, No. 2, 1969, pp. 37-40.
3. Huet, J. Enseignements Tirés des Routes Expérimentales en Béton Asphaltique. La Technique Routière, Brussels, Vol. 17, No. 1, 1972, pp. 3-26.
4. Verstraeten, J. Loi de Fatigue des Mélanges Bitumineux: Influence des Caractéristiques des Bitumes et de la Composition des Mélanges (detailed English abstract). Centre de Recherches Routières, Brussels, Res. Rept. 161/JV/1973.
5. Verstraeten, J. Moduli and Critical Strains in Repeated Bending of Bituminous Mixes. Proc. 3rd Internat. Conf. on Structural Design of Asphalt Pavements, London 1972, pp. 729-738.
6. Huet, C. Etude par une Méthode d'Impédance du Comportement Viscoélastique des Matériaux Hydrocarbonés. Thesis presented at la Faculté des Sciences de l'Université de Paris, 1963.
7. Van der Poel, C. Building Materials (Reiner, M., ed.). North Holland Publishing Co., Amsterdam, 1954, Ch. 9, pp. 361-413.
8. Bazin, P., and Saunier, J. B. Deformability, Fatigue and Healing Properties of Asphalt Mixes. Proc. 2nd Internat. Conf. on Structural Design of Asphalt Pavements, Ann Arbor, 1967, pp. 553-569.

9. Francken, L. Module Complexe des Mélanges Bitumineux: Influence des Caractéristiques des Bitumes et de la Composition des Mélanges (detailed English abstract). Centre de Recherches Routières, Brussels, Res. Rept. 164/FL/1973.
10. Pell, P. S., and Taylor, J. F. Asphaltic Road Materials in Fatigue. Proc. AAPT, Los Angeles, Feb. 1969.
11. Taylor, J. F. Asphaltic Road Materials in Fatigue. Thesis submitted to Dept. Civil Engineering, Univ. of Nottingham, England, Oct. 1968.
12. Francken, L., and Hampson, A. H. Appareillage de Compression Sous Charges Répétées. La Technique Routière, Vol. 17, No. 1, 1972, pp. 1-19.
13. Francken, L. Properties of Materials. Proc. 3rd Internat. Conf. on Structural Design of Asphalt Pavements, Vol. 2, London, 1972.

HIGHWAY MATERIALS AS AGGREGATE-BINDER COMPOSITES

Robert L. Alexander, California State University, Long Beach

For many years engineers and scientists in geology, soil mechanics, and paving technology have contributed their efforts to improve the quality and economy of materials used in highway construction. Yet there has been a tendency to neglect the fact that the materials these specialists study possess a common denominator: All are aggregate-matrix composites. This paper provides a tentative classification of the materials involved in these 3 fields to support the claim that they can be organized by the systems approach. Unfilled binders, such as clay and asphalt cement, occur at one extreme of the composite spectrum; unbound fillers, such as clean sand and rock base, occur at the other. Examples are cited from particulate, viscoelastic, and graphic models that have interdisciplinary acceptance in displaying the rheological behavior of highway materials. In education, it is not enough that the student be taught how much different one conventional paving material is from another. More use should be made of those phenomenological tools and physical testing procedures that will enable the student to use the diverse combinations of fillers and binders being created to meet pressing economic and ecological needs.

BEFORE an engineer can understand and intelligently apply the principles of the design of highway pavement structures, he or she must be fully aware of the mechanical properties of the materials with which pavement systems are constructed. It is common knowledge that these systems consist of 1 or more layers of materials called courses supported on a foundation material called the subgrade. These materials belong to a category called composites; composite materials are classified as particle-reinforced, fiber-reinforced, and sandwich-reinforced. In pavement technology, the particulate system can be called an aggregate-binder composite.

In the past, highway aggregates have usually consisted of natural gravel, crushed rock, slag, or 1 of a variety of recycled products used on an experimental basis. The binder has consisted of a material such as portland cement paste, tar, cohesive soil, lime paste, or asphalt cement and may have contained a property-modifying admixture. It seems reasonable to expect that those involved with research, design, or construction of pavement systems possess adequate training in geology, soils, and concrete technology. Traditionally, there has been a tendency to compartmentalize the efforts of the specialists in these fields. Standard American textbooks on highway engineering have tended to emphasize the differences, for example, between portland cement and asphalt concretes rather than present a comprehensive approach to the understanding of both. The absence of such an approach to the mechanics of roadway materials reflects the past state of an industry content with such unqualified terms as "blacktop" and "cement pavement" in its technical vocabulary. The present annual investment of billions of dollars for research, development, and manufacture of highway pavements justifies a more rational attitude toward this important subject. A unified approach to pavement systems would facilitate education and design and, ultimately, make a more economical use of various highway materials.

This paper covers viscoelastic behavior of pavement joint fillers, expansion device materials, and elastomeric bridge bearings.

Publication of this paper sponsored by Committee on General Asphalt Problems.

AGGREGATE-BINDER SYSTEMS

How well do geology, soil mechanics, and concrete technology fit into a unified classification system? Table 1 gives a classification of the materials in these systems. The engineering geology column should apply only to sedimentary rocks and geologically unconsolidated sediments, but because these sediments sometimes contain igneous and metamorphic rock particles, they also are included. The soil mechanics column indicates that clean sand and remolded, fully saturated clays form the extremities of behavioral response in soil mechanics; usually, a little less than one-third of these by volume of cohesive soil are required to give a mixed soil rheological characteristics. Only the more commonly used concrete composite materials are included in the fourth column.

The highway cross section shown in Figure 1 is an example of a layered system that contains a variety of aggregates and binders including, remarkably, a strain-relieving interlayer that contains a binder almost as rigid as its filler. The shortage of economical sources of natural aggregates in some parts of the world has led to an exploration for suitable synthetics, and the technical literature is replete with a bewildering variety of binder admixtures, modifiers, patented cements, joint compounds, and bridge bearing materials. The conventional "they're either rigid or flexible" approach to highway materials has been abandoned because in layered-systems technology the number of mathematical combinations of compatible aggregates and binders spans the rigidity spectrum (1).

A study of Highway Research in Progress reveals the extent to which research in geology, soils, and paving materials is now going on (2, 3). Bituminous binders are being modified by rubber latex, asbestos fillers, chopped fiberglass, colored synthetic resins, tar-asphalt blends, powdered glass, and synthetic textiles. Portland cement is being used with polystyrene, silicones, polymer latex emulsions, synthetic polyester systems, alumina filaments, and in self-stressing, expansive applications. Cement-stabilized chalk, spent oil shale, gypsum, formed plastics, synthetic and organic polymers, bamboo fibers, and lignosol are some of the materials being used here and abroad to remedy structural deficiencies in base course and shoulder materials. Dramatic, ecology-promoted innovations are taking place in aggregate technology. Among the new materials being researched are ceramics, porous particles, cement-stabilized soil nodules, crushed moraine, sideritic concretions, anthracite mine waste, steel fibers, calcined bauxite, recycled plastic chips, cement clinker, building rubble, boiler slag, marine deposits, burned garbage, crushed glass, cast iron, vulcanized rubber particles, and reclaimed pavement surfacings. It seems reasonable to expect that as the use of more of these materials becomes economically feasible, the classical distinctions between portland cement and asphalt-bound materials will become increasingly blurred.

PHENOMENOLOGICAL MODELS OF AGGREGATE-BINDER MATERIALS

Particulate Models

During the years when the art of soil mechanics was becoming a science, particulate models were used as a research and teaching aid by such outstanding engineers as Casagrande, Taylor, and Terzaghi. Figure 2a shows a model of the honeycomb structure found in fine silts and clays and represents, therefore, the binder fraction of soil or material passing the No. 200 sieve (4). Figure 2b is taken from Gilboy (5) and clearly indicates that the flexural response of the mica platelets in a sand-mica soil causes excessive compressibility in this material. A model referred to by Holmes (6) is shown in Figure 2c as an example from physical geology. Sandstones can be thought of as natural concretes in which the aggregate frequently consists of fragments of disintegrated older rocks. This model shows graded graywacke; such layers often extend over large areas and are surprisingly uniform in thickness.

Figures 2d, e, and f are examples of particulate models on a larger microscopic scale than the preceding 3. To emphasize to students the importance of a rough aggregate surface texture to the stability of an asphalt concrete mixture, Monismith (7)

Table 1. Aggregate-binder systems used in highway engineering.

Category	Engineering Geology	Soil Mechanics	Concrete Technology
Unbound aggregate subsystem	Marine shells, mica flakes, silts, quartz sands, gravels, boulders, talus, volcanic ash, and fragments of detritus	Clean sand, river-run gravel, boulders, rubble, riprap, and other cohesionless construction materials	Clean granular base course materials, unbound macadam, crushed rock, and selected imported granular fills
Unfilled binder subsystem	Silica, carbonate, dolomite, clay, gypsum, haematite, limonite, clay shales, and other cementing minerals	Remolded clay, fine silts, water binders, lime, chemical additives, and other soil stabilizers	Portland cement paste, road tar asphalt cement, cutbacks, emulsions, elastomeric bearings, and joint fillers
Aggregate-binder system	Loess, alluvium, moraine, muddy grits, limestone, sandstone, siltstone, breccias, conglomerates, porphyrys, and grouts	Glacial till, manmade compacted mixed-soil roadway embankments, soil cement, and asphalt mixtures	Portland cement and asphalt concretes, grout, sand asphalt, bituminous macadam, filled elastomers, and bridge bearings

Figure 1. Cross section of a complex layered system of composite highway materials.

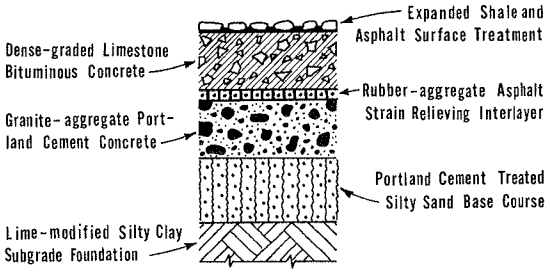

Figure 2. Particulate models from geology, soil, concrete, and composite materials technology.

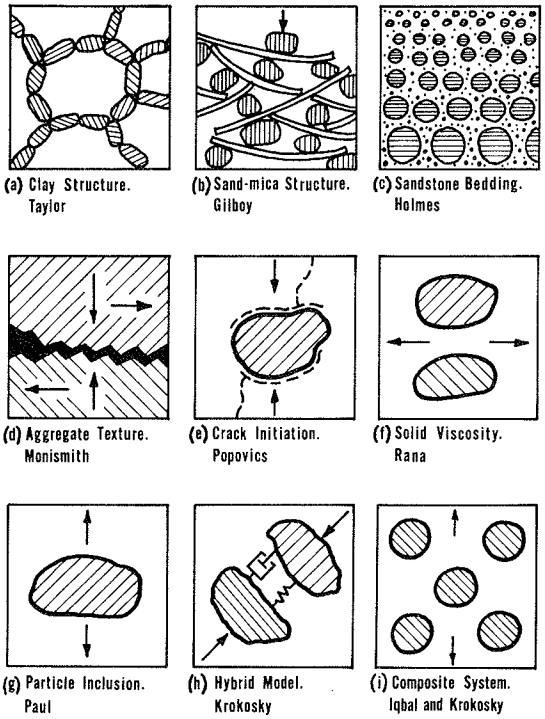

Figure 3. Clay subgrade, early Terzaghi rheological model.

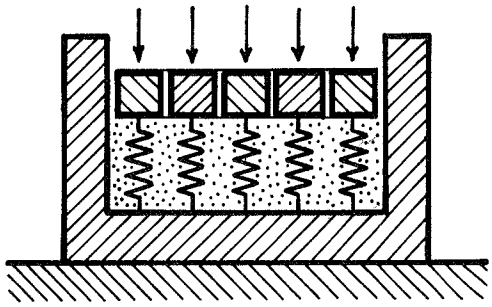

used the model of Figure 2d. The exaggeration of the roughness at the rock interfaces with the asphalt film is intentional. In a paper on the fracture mechanism of portland cement concrete, Popovics (8) used the model of Figure 2e to illustrate crack initiation and propagation in the mortar. At about 70 to 90 percent of the ultimate load, cracks (shown as broken lines in the model) through the mortar begin to increase appreciably; because of bridging between nearby bond cracks, a continuous network of cracks is formed. Figure 2f was used by Rana (9) in a paper on the viscosity of rocks. Rana stated that design criteria in rock technology, until quite recently, were based on the classical theory of elasticity, and he found that there were very few experimental data on solid viscosity of geological materials.

The model of Figure 2g was used by Paul (10) in his general solution to the problem of an elastic particle in an elastic matrix. The modulus of this system is a function of the modular ratio and the volume ratio of particles to matrix. Paul's analogy of a particle within a cubic matrix is restricted in usefulness to composites with a low volume ratio and no particle interlock. These limitations are critical for highway materials where volume ratios are relatively high and aggregate interlock may be very significant. Counto (11) used a cylindrical particle within a cylindrical matrix as his model to determine the effect of the modulus of the aggregate on the elastic modulus, creep, and creep recovery of portland cement concrete. To compare his model response with actual test results, he prepared concrete specimens that contained steel, flint, cast iron, and polythene coarse aggregates in order that the particles possess a wide range of elastic moduli and low water absorption.

Figure 2h was used by Krokosky (12) in illustrating the effect of temperature on the mechanical properties of an asphalt concrete. The asphalt film separating the particles of aggregate is depicted as a Kelvin material; this hybrid model was suggested by Krokosky as a rough approximation of the response of an asphalt concrete tested at temperatures between glass transition and about 100 F. Although conventional portland cement and asphalt concretes are sometimes described as 2-phase composites, the mixing operation usually creates an air-void phase even when air entrainment is not intentional. Figure 2i is from a paper by Iqbal and Krokosky (13) on their analysis of an idealized elastic composite system using the finite-element method. Each circle in the model can be used to represent either a cylindrical particle or an air void. They selected a particle to binder modular ratio of 100 and treated the voids as particles possessing a very small but finite dummy modulus. Hackett (14) used a model similar to Figure 2i and conducted a stress analysis for the case of an elastic particle in a viscoelastic binder, a solution that could fit those construction materials with marked rheological properties.

Viscoelastic Models

The use of viscoelastic or rheological models in analyzing the physical properties of aggregate-binder materials in geology, soil mechanics, and concrete pavement technology is well established. In 1927, Terzaghi (15) presented a paper on the importance of sound foundation engineering in the construction of portland cement concrete roads. He used the rheological model in Figure 3 to approximate the response to load of a layer of fully saturated clay. A rheological model can be used for highway composites in 3 different ways. It can model an unfilled binder such as a paving asphalt or a bridge-bearing elastomer; an unbound filler such as crushed rock or clean sand; and a complete system such as portland cement concrete, a mixed soil, or a consolidated sedimentary rock. To conserve space, alphabetical symbols have been used for the models and their elements in Figures 4 and 5. The conventional spring and dashpot element symbols are shown at the left of Figure 4a (16).

In Figure 4b, block M represents a spring and dashpot series configuration with each element equally stressed; block K represents them in parallel with each equally strained; the former model has been used by Emery (17) in the field of rock mechanics. Dennis (18) has suggested that the firmo-viscous deformation of some unconsolidated geological materials under stress can be approximated by a Kelvin model. A Maxwell and a Kelvin model connected in series are indicated in Figure 4c as block B; George (19) used this

Figure 4. Some commonly used viscoelastic models and symbols.

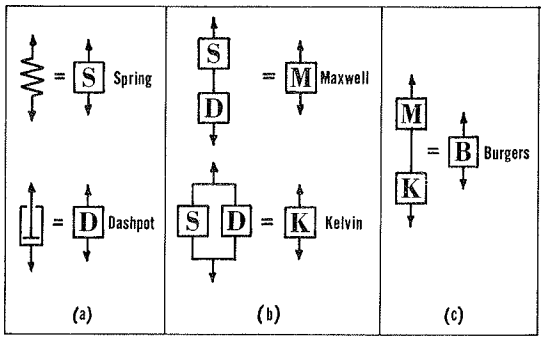

Figure 5. Additional viscoelastic models using elements from Figure 4.

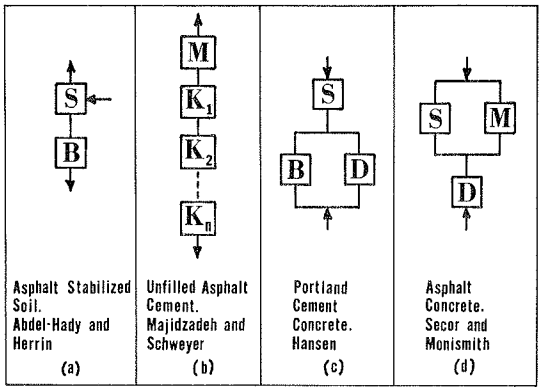

Figure 6. Unspecified load on a hypothetical material.

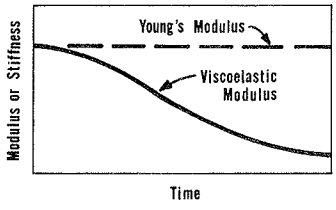

Figure 7. Graphic models, modulus dependency functions.

(a) Sand-asphalt in Stress Relaxation. Moavenzadeh and Soussou

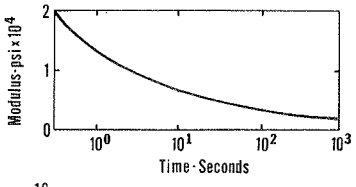

(b) Clayey-sand in Creep Loading. Pagen and Jagannath

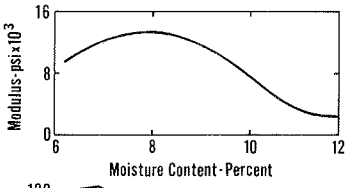

(c) Portland Cement Concrete in Dynamic Loading. Patterson

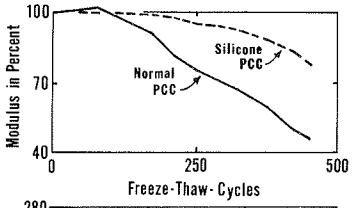

(d) Asphalt Concrete in Flexural Fatigue Loading. Deacon

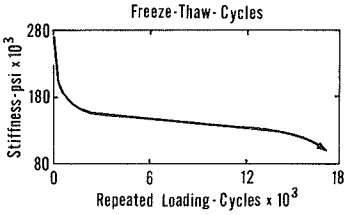

mechanical model in his analysis of shrinkage stresses in a sand-clay base course stabilized with portland cement. Using the model of Figure 5a, Abdel-Hady and Herrin (20) applied the theory of rate process and fairly accurately approximated the nonlinear viscoelastic response of an asphalt-stabilized soil. In their model, the free spring is modified by use of a stop (horizontal arrow) to represent the initial plastic deformation of this material under creep loading. Majidzadeh and Schweyer (21) subjected aged and unaged specimens of asphalt cement to creep tests at 32 F to better understand aging phenomena. The model they used to fit their data is shown in Figure 5b and consists of a Maxwell part in series with a selected number of multiple-parameter Kelvin parts that are, in turn, in series with each other. The Hansen model (22) for creep in portland cement concrete is shown in Figure 5c. The free spring represents the relatively elastic response of the aggregate phase; the dashpot represents the water and voids; and the Burgers part incorporates the effects of the gel, unhydrated cement, and crystalline products of hydration. The model of Figure 5d consists of a spring and a Maxwell part parallel to each other and collectively in series with a free dashpot; Secor and Monismith (23) used this model to predict the response to constant rate of compression loading of a particular asphalt concrete mixture.

The rheological models presented in Figures 3, 4, and 5 are deterministic because they represent ideal materials; that is, they predict response to load with a probability of unity. Gabrielson (24) used the concept of random spring and dashpot components in stochastic Maxwell and Kelvin models. This stochastic approach to viscoelastic behavior is particularly relevant to highway engineering materials because scatter of test data for particulate composites is more pronounced than for more homogeneous materials.

Graphic Models

In the context of this paper, a graphic model is defined as a plot of a theoretically or empirically derived modulus dependency function. Such a function has modulus or stiffness of a material as the dependent variable and time, temperature, or other significant factor as the independent variable or argument (16). The time-dependent modulus is a common example of a modulus dependency function. Figure 6 shows a schematic time-dependent modulus for an unspecified mode of loading (25); it incorporates both the viscous and elastic responses of a rheological material and could logically be called a viscoelastic modulus. Could the viscous parameter of this hypothetical material be made to approach infinity, its viscoelastic modulus would degenerate to Young's modulus as indicated on the figure; and at very short times, of course, all rheological materials tend to perform elastically.

A stress relaxation modulus is a time-dependent modular function for a material loaded in a specified environment under a constant-strain model. Figure 7a is the stress relaxation modulus in unconfined compression for a sand-asphalt mixture tested by Moavenzadeh and Soussou (26) at 35 C. Values of the argument of a modulus dependency function can be continuous or discrete; the plot of Figure 7a is an example of the continuous case and that of Figure 7b is discrete. Figure 7b is from a Pagen and Jagannath study (27) in which linear viscoelastic theory was used to provide a more rational method of determining the optimum moisture content in highway subgrade compaction operations. The ordinate represents the elastic part of the unconfined compressive creep modulus at 30 sec and the abscissa represents the molding water content of specimens compacted at 25 blows. The curve was fitted to data points plotted at discrete values of water content for specimens of clayey sand, a classical aggregate-binder material. In portland cement concrete technology, the dynamic modulus of elasticity has been used to measure the effectiveness of a silicone admixture in improving the resistance of a concrete bridge deck to repeated cycles of freeze-thaw. In Figure 7c, from Patterson (28), the upper plot contains dynamic modular data for silicone deck concrete and the lower one for normal concrete. This modulus is freeze-thaw-cycle dependent.

The moduli of bituminous materials and bearing elastomers are highly susceptible to temperature change; those of soils and other geological deposits may be sensitive to

moisture content or confining pressure, but fatigue-damage susceptibility is a property of all pavement and subgrade materials. Because major highways are subjected to millions of repetitions of a variety of axle loads during their service lives, the effect of cumulative fatigue damage on the moduli of highway materials is of interest to researchers and students in all areas of pavement materials technology. Figure 7d is from a thesis by Deacon (29) in which he provided dynamic deflection data from stress-controlled fatigue tests on an asphalt concrete mixture. He plotted the stiffness modulus of the mixture as a function of the number of load applications under a 113.5-psi flexural stress at 75 F.

This author has found that the behavioral response of a wide variety of highway materials can rapidly be demonstrated by plotting the appropriate modulus dependency functions.

CONCLUSIONS

An interdisciplinary approach to understanding the response of paving materials must begin in our educational system. I am not suggesting that courses in engineering geology, soil mechanics, and highway materials be replaced by a catch-all course in composite materials technology or aggregate-binder systems but that the first course in highway engineering or pavement materials be designed to devote a few lectures to a holistic approach to the behavior of stone-matrix materials. Table 1 presents a tentative classification of geological, soil mechanics, and concrete materials in an attempt to support the belief that they can be conceived in terms of aggregate-binder systems.

It is important that every available teaching aid be used to impress on students that predicting the behavior of complex rheological composites demands exacting interpretations of their loading histories. I recommend using 3 time-tested phenomenological models to achieve this end: particulate models, viscoelastic models, and graphic models. Particulate models develop a feeling for material response at the largest macroscopic scale; viscoelastic models give physical analogy to linear theory; and graphic models (modulus dependency functions) provide a ready tool for displaying empirical data. Some of the models presented in this paper are taken from the writings of eminent engineering educators and others from technical papers expounding important advances in the field of paving technology. Because these phenomenological aids were used to communicate new theoretical and empirical concepts to experienced researchers in the field, it seems reasonable to conclude that their use is even more vital in presenting a unified system of highway materials to students headed for careers in highway engineering.

REFERENCES

1. Alexander, R. L., and Spielman, N. K. Rigid Versus Flexible Pavements. American City, Vol. 38, No. 11, Nov. 1968.
2. Highway Research in Progress No. 5, TRB, Part 1, 1972.
3. Highway Research in Progress No. 5, TRB, Part 2, 1972.
4. Taylor, D. W. Fundamentals of Soil Mechanics. John Wiley and Sons, Inc., New York.
5. Gilboy, G. The Compressibility of Sand-Mica Mixtures. Proc. ASCE, Vol. 14, No. 2, Feb. 1928.
6. Holmes, A. H. Principles of Physical Geology. Ronald Press Co., New York, 1965.
7. Monismith, C. L. Asphalt Paving Mixtures—Properties, Design, and Performance. Syllabus Series, Univ. of California, Berkeley, 1961.
8. Popovics, S. Fracture Mechanics in Concrete: How Much Do We Know? Jour. of Engineering Mechanics Div., ASCE, Vol. 95, No. EM3, June 1969.
9. Rana, M. H. Experimental Determination of Viscosity of Rocks. Experimental Mechanics, Vol. 9, No. 12, Dec. 1969.
10. Paul, B. Prediction of Elastic Constants of Multiphase Materials. Transactions, ASME, Vol. 218, No. 36, Feb. 1960.

11. Counto, U. J. The Effect of the Elastic Modulus of the Aggregate on the Elastic Modulus, Creep, and Creep Recovery of Concrete. Magazine of Concrete Research, Vol. 16, No. 48, Sept. 1964.
12. Krokosky, E. M. The Rheological Properties of Asphalt Aggregate Compositions. Massachusetts Institute of Technology, PhD dissertation, 1962.
13. Iqbal, M. A., and Krokosky, E. M. Interaction Stresses in Composite Systems. Jour. of Engineering Mechanics Div., ASCE, Vol. 96, No. EM6, Dec. 1970.
14. Hackett, R. M. Viscoelastic Stresses in a Composite System. Polymer Engineering and Science, Vol. 11, No. 3, May 1971.
15. Terzaghi, C. Concrete Roads—A Problem in Foundation Engineering. Jour. of Boston Society of Civil Engineers, Vol. 14, No. 5, May 1927.
16. Monismith, C. L., Alexander, R. L., and Secor, K. E. Rheological Behavior of Asphalt Concrete. Proc. AAPT, Vol. 35, 1966.
17. Emery, C. L. The Strain in Rocks in Relation to Highway Design. Highway Research Record 135, 1966, pp. 1-9.
18. Dennis, J. G. Structural Geology. Ronald Press Co., New York, 1972.
19. George, K. P. Shrinkage Cracking of Soil-Cement Base: Theoretical and Model Studies. Highway Research Record 351, 1971, pp. 115-133.
20. Abdel-Hady, M., and Herrin, M. Characteristics of Soil-Asphalt as a Rate Process. Jour. of Highway Div., ASCE, Vol. 92, No. HW1, March 1966.
21. Majidzadeh, K., and Schweyer, H. E. Viscoelastic Response of Aged Asphalt Cements. Highway Research Record 231, 1968, pp. 50-61.
22. Hansen, T. C. Creep of Concrete—A Discussion of Some Fundamental Problems. Swedish Cement and Concrete Research Institute, Bulletin No. 33, Sept. 1958.
23. Secor, K. E., and Monismith, C. L. Viscoelastic Properties of Asphalt Concrete. Proc. Highway Research Board, Vol. 41, 1962, pp. 299-320.
24. Gabrielson, B. L. Stochastic Models for Viscoelastic Materials. Materials and Structures, Vol. 1, No. 4, July 1968.
25. Alexander, R. L. Testing Elastomers in Creep and Relaxation. Plastics Design and Processing, Vol. 9, No. 6, June 1969.
26. Moavenzadeh, F., and Soussou, J. Viscoelastic Constitutive Equation for Sand-Asphalt Mixtures. Highway Research Record 256, 1968, pp. 36-52.
27. Pagen, C. A., and Jagannath, B. N. Mechanical Properties of Compacted Soils. Highway Research Record 235, 1968, pp. 13-26.
28. Patterson, H. L. Use of Silicone Admixture in Bridge Deck Concrete. Highway Research Record 370, 1971, pp. 61-74.
29. Deacon, J. A. Fatigue of Asphalt Concrete. Univ. of California, Berkeley, PhD dissertation, 1965.

TENTATIVE MIX-DESIGN CRITERIA FOR GAP-GRADED BITUMINOUS SURFACES

C. P. Marais, National Institute for Road Research, Pretoria, South Africa

Since the turn of this century, extensive use has been made of gap-graded bituminous surfacing mixtures in the United Kingdom. The design of these mixtures has largely been empirical, and specifications have been of the recipe type. The excellent performance given by these mixtures, even under the most severe traffic conditions, has prompted engineers in other parts of the world to use these surfaces. Experience has shown that under some climatic conditions the United Kingdom specifications did not always produce the most satisfactory mixtures, and a national method of design was urgently required. This paper covers a research study into factors that affect the performance of gap-graded surfaces and isolates those that are of particular importance. It is shown that the Marshall test method, when used in combination with air permeability and indirect tensile tests, can be used to design gap-graded mixtures. Tentative criteria are established for the mix design of gap-graded bituminous surfaces; they will satisfy normally accepted standards with respect to distortion, fracture strength (toughness), fatigue, imperviousness, and durability.

•THE AMERICAN chemist and highway paving technologist, Clifford Richardson, introduced stone-filled, sand-sheet asphalt surfacing mixtures that could withstand heavy traffic and cold , wet climatic conditions to the London authorities at the turn of this century (1, 2). These mixtures have been modified over the years to meet changing traffic conditions in the United Kingdom and are covered by British Standard 594, which is updated from time to time to keep pace with advances in asphalt technology. This type of mix is characterized by the fact that its stability or distortion resistance is derived almost wholly from the stiffness of the mortar, that is, the bitumen-sand-filler mixture. For this reason the correct selection of the aforementioned components is important. Experience has shown that low stone content mixtures specified in BS 594 are more durable than those with high stone contents and are therefore favored for important highways. A disadvantage of the low stone content mix is its sandpaper texture, which is not suitable for high-speed traffic in wet weather. This problem has largely been overcome by introducing during construction carefully selected coated chippings to give a rugose surface texture.

The good performance of experimental gap-graded mixtures of low and high stone content on a heavily trafficked urban street in South Africa led South African road authorities to take a keen interest in gap-graded surfacing mixtures (3). During the past decade, gap-graded surfaces have, generally speaking, replaced the more critical continuously graded asphalt concrete; their use has become standard practice on urban and rural freeways. Because of the warm climate in South Africa, mixtures conforming strictly to BS 594 did not always perform well, so modifications to this specification were necessary. Varying natural materials such as sand and filler also resulted in varying performance. A need therefore arose for a design method whereby the properties of the mixture could be determined for the selection of an acceptable mixture composition by applying suitable design criteria. Research to meet this need has been in progress in South Africa and the United Kingdom (4, 5).

Publication of this paper sponsored by Committee on Mechanical Properties of Bituminous Paving Mixtures.

This paper describes a laboratory study and field data aimed at establishing the factors that control the performance of gap-graded surfaces and suggests design criteria to ensure adequate distortion resistance, fracture strength, fatigue resistance, imperviousness and durability of these mixtures.

LABORATORY STUDY

Mixture Composition

To cover a wide spectrum of practical gap-graded compositions, we selected a number of stone contents between 30 and 50 percent. Crushed coarse stone of 2 maximum sizes was used in combination with 2 different types of sand. The binder used was a 40-50 penetration grade bitumen vacuum distilled from Middle East crude oil. The bitumen content of each mixture was varied over a wide range. The typed filler and content, 7 percent by mass of aggregate (stone + sand), were not varied in this study. Combined aggregate gradings used in the study are shown in Figure 1. Physical tests carried out on the 2 sands used in this study are given in Table 1.

Mechanical Tests

From performance records of gap-graded surfacing mixtures laid in the United Kingdom it is clear that distortion is far more serious than fatigue cracking. Therefore, this study emphasized the deformation characteristics of the selected mixtures by using an apparatus similar to that used in the British Transport and Road Research Laboratory wheel-tracking test in which a 300- by 300- by 50-mm-thick compacted specimen of surfacing mix was subjected to to-and-fro motion, at 50 passes per min, of a 200- by 50-mm-solid rubber-tired wheel having a contact pressure of 780 kPa (Fig. 2) (6). In addition, Marshall tests (ASTM D 1559-71) were carried out on specimens compacted with 75 blows on each face at test temperatures of 40 and 60 C.

Studies carried out at the National Institute for Road Research (NIRR) have shown that gap-graded mixtures have a superior fatigue life to asphalt concrete and that, for thin surfaces, low rather than high stiffness is desirable for high fatigue resistance (7). A study by Maupin (8) showed that indirect tensile strength is a useful indicator of the fatigue susceptibility of asphalt mixtures, and for this reason the indirect tensile strength of the mixtures was measured at 30 and 40 C. Twenty-five-mm-wide curved loading strips were used to apply the load to the specimens at a rate of loading to 50 mm/min (9). The apparatus used in these tests is shown in Figure 3.

Physical Tests

An important function of a surface is to protect the base layer of the pavement from the entrance of surface water. To accomplish this the surface should be reasonably impervious without being too dense because this would cause fatting up and instability during periods of hot weather and heavy traffic. To study these characteristics we determined the air permeability in fundamental units at a pressure difference of 25 mm water on Marshall, 2 × 75-blow-compacted specimens by using the apparatus shown in Figure 4.

The durability of a surface can be controlled by the air permeability of the mix, which limits the transfer rate of oxygen, water, and microorganisms from the surface to the interior and that of volatile constituents from the interior to the surface (10). The film thickness of the bitumen also plays an important role in the durability of bituminous mixtures. Film thicknesses were calculated for the various gradings and bitumen contents by using the surface area factors recommended by the Asphalt Institute (11).

PERFORMANCE OF IN-SERVICE SURFACES

It has not been possible to observe the in-service performance of all the mixtures investigated in the laboratory. However, a gap-graded mixture containing mine sand, 30 percent stone, and 6 percent 40-50 penetration grade bitumen was laid on an experimental pavement on route S12 early in 1969 (12, 13). The dynamic properties and

Figure 1. Gap-gradings used in laboratory study.

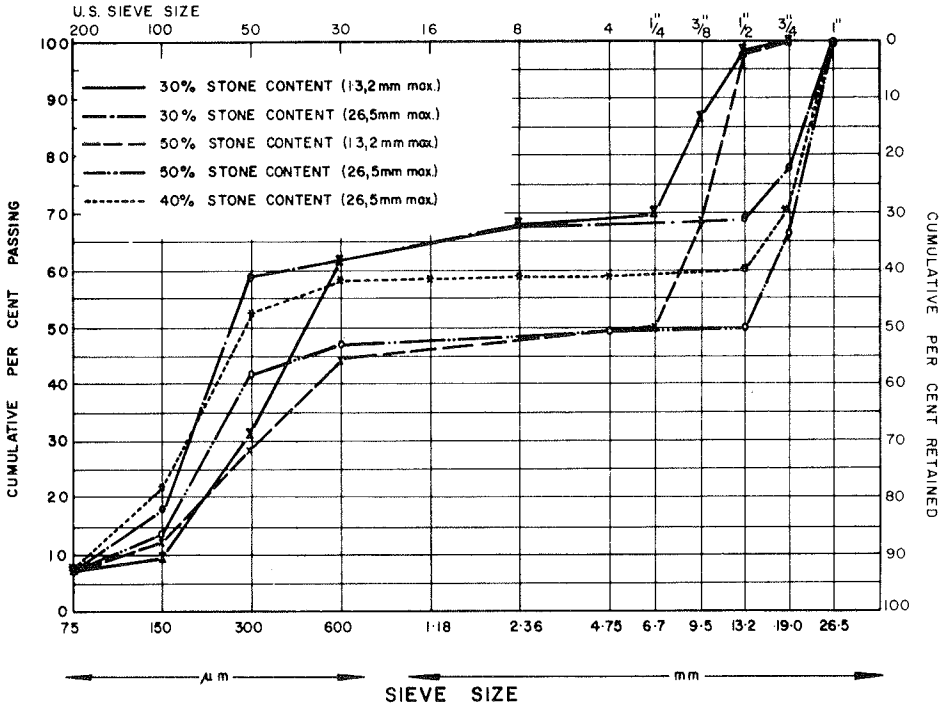

Table 1. Results of physical tests on sands used in this study.

Property	Pit Sand	Mine Sand
Fineness modulus[a]	1.35	0.99
Plasticity index	Nonplastic	Nonplastic
Bulk density, kg/m^3		
Compacted	1 596	1 487
Loose	1 494	1 330
Voids in compacted sand, percent	40	44
Sand equivalent value, percent	28	75
Dry viscosity, sec/100 g[b]	15.2	17.4

[a]Fineness modulus = $\frac{\Sigma \text{ percent retained on 4.75; 2.36; 1.18; 0.60; and 0.15 mm sieves}}{100}$ on a wet grading analysis.

[b]Flow time of 100 g of oven-dried mix: 297 μm + 149 μm sand fraction through a circular orifice 6.30 mm diameter.

Figure 2. Apparatus used for wheel-tracking tests (wheel ballast removed).

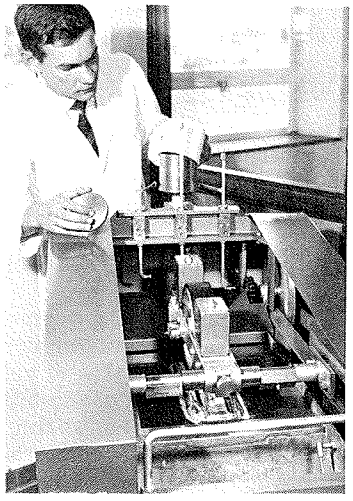

fatigue life of this mixture were studied in detail at the NIRR. In situ deformation observations were taken periodically with a precise level on the various pavement design sections. This information has been most valuable in assessing the applicability of some of the laboratory data and will be discussed under the section dealing with the results obtained from the study as a whole.

COMPACTABILITY OF GAP-GRADED MIXTURES

A detailed study has been made of densification after construction on gap-graded and asphalt concrete mixtures (3). Cores were removed from the surface in the wheel tracks of vehicles, and their bulk specific gravity was compared with the Marshall 2 × 75-blow laboratory density of these mixtures. In Figure 5, sections 5 and 34 are continuously graded asphalt surfacing mixtures and sections 83 and 84 are gap-graded with 30 per cent stone content. The rates of increase in bulk specific gravity of the 2 types of surfaces were significantly different; the asphalt concrete densified progressively under the traffic for a period of 3 years after which it reached an asymptotic value close to the Marshall 2 × 75-blow density. The gap-graded mixtures, however, showed hardly any traffic compaction and were, at the time of laying, close to the Marshall 2 × 75-blow density. The same construction compactions were used on both types of mixtures except that a pneumatic-tired roller (intermediate) was not used for gap-graded mixtures. The same traffic passed over the 2 groups of surfacing mixtures. The ease with which gap-graded mixtures reach their final density signifies their excellent in-service performance and their compaction control required during construction. In practice, then, control of compaction of gap-graded mixtures should be at a level of not less than 98 percent of 2 × 75-blow Marshall density.

DISCUSSION OF RESULTS

With regard to the deformation properties of gap-graded mixtures attention was directed to a possible relationship between the results obtained from the wheel-tracking test and the Marshall test.

Wheel-Tracking Test

Tracking tests were continued for approximately 100 min in cases where excessive distortion of the mix did not take place before this time. Measurements of rutting were taken every 10 min throughout the test period. Rut depth-time curves all followed a typical pattern in which a rapid increase in rut depth occurred during the initial period of 10 to 20 min and thereafter stabilized to a reasonably constant rate of tracking. After 45 min of tracking, the rut depth and rate of tracking were determined and used as parameters to characterize the distortion properties of the surfaces under dynamic wheel loads. Tests were carried out at 40 and 60 C. Results have been tabulated by the Asphalt Institute (11).

Marshall Test

Complete Marshall stability, flow, and voids analyses were completed on all mixtures studied. The bearing capacity and angle of internal friction of the mixtures were determined according to the procedures put forward by Metcalf (14). The stability index was calculated by using the stress-strain relationship applicable to the Marshall briquette, that is

$$\text{Stability Index} = S/F \times 15.7 \text{ MPa}$$

where

S = stability value in kilonewtons (corrected) and
F = flow in millimeters.

A detailed examination of the data from both the wheel-tracking and Marshall tests revealed that there were significant relationships among rate of tracking, bearing

Figure 3. Automatic load-deformation recorder in use during indirect tensile test.

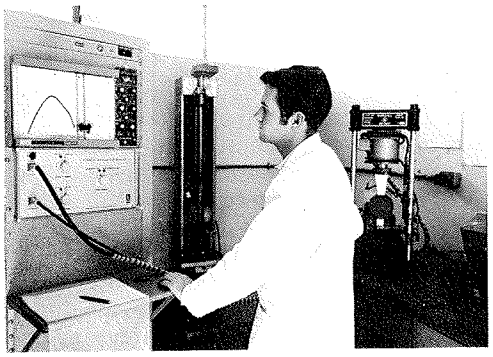

Figure 4. Apparatus for air permeability measurements on compacted Marshall specimens.

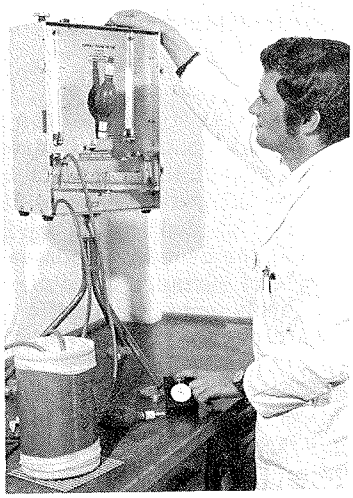

Figure 5. Rate of increase in bulk specific gravity of some typical bituminous mixtures caused by traffic compaction.

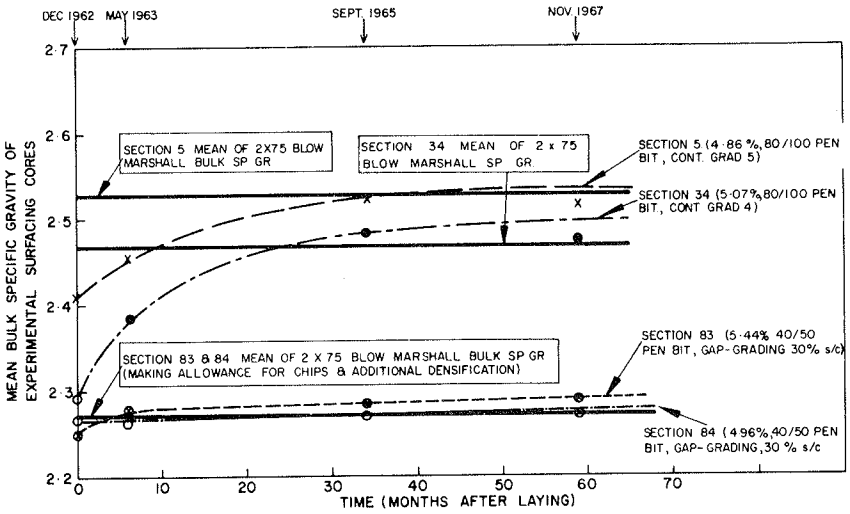

capacity, stability index, and the ratio of stability to flow at both test temperatures. Rut depth did not present as clear a trend as in the case of rate of tracking. However, because both rate of tracking and rut depth are important parameters with respect to permanent deformation of a surface, we decided that their product, the "tracking index," would be used. This index, at 40 C, was compared to the stability-flow ratio at 60 C of the various mixtures studied. There were 2 reasons for choosing 40 C for the tracking data. First, it was considered to be a reasonable average road surface temperature for hot climates like those in South Africa, and, second, at 60 C information was more limited because of the deep rut depths obtained in the tracking apparatus after only a few passes with the less stable mixtures (11). The relationship found is shown in Figure 6. On analysis, these data were found to fit a mathematical equation of the form

$$\log_{10}TI = 3.2353 - 1.2196 \log_{10}\left(\frac{10_S}{F}\right) \quad (1)$$

where

TI = tracking index (rate of tracking × rut depth at 40 C) in square millimeters × minutes^{-1},
S = Marshall stability at 60 C in kilonewtons, and
F = Marshall flow at 60 C in millimeters.

An examination of Eq. 1 reveals a large increase in the tracking index for stability-flow ratios above 1.5 kN/mm; it was concluded that this would be a limiting criterion to control excessive permanent deformation under traffic. Data feedback from practice have indicated that mixtures with stability-flow ratios below 1.5 kN/mm give rise to compaction problems and early traffic rutting.

A closer examination of the tracking data shows that the mixture containing mine sand, 30 percent stone content (maximum stone size: 26.5 mm), and 6 percent bitumen content falls on the acceptable side of the suggested limit of 1.5 kN/mm for the stability-flow ratio (Fig. 6) (11). This mixture is virtually identical with that laid on the experimental pavement on route S12. Measurements of pavement deformation (75-mm-thick, gap-graded surface supported on a 150-mm, cement-treated base) from 1969 until 1971 have been analyzed. This section was chosen especially because any measurable deformation was considered to result largely from distortion of the surface and not from the stabilized underlying layers. Deformation data was available only for 23 months under heavy traffic and showed the average permanent deformation over a 2.7-m-wide area in the center of the traffic lane to be 1.89 mm. The cumulative equivalent 80-kN axle load was approximately 7.4×10^5 in this lane for the 23-month period.

If a 25-mm rut depth is considered the limit value for retiring a pavement because of poor ridability, then this pavement had reached approximately 7.5 percent of the allowable deformation. However, on the basis of a 20-year life, the pavement had reached 10.5 percent of its life. Possibly this mixture would not deform excessively during the life of the pavement. These field performance data to a limited extent confirm the laboratory results and permit some confidence in the suggested laboratory criterion.

The limit value of 1.5 kN/mm for the stability-flow ratio determined from this study was also confirmed by Brien (4) who suggested stability-flow ratios for conditions in the United Kingdom of 0.98 kN/mm and 1.96 kN/mm for the most extreme climatic conditions (high temperatures). South Africa certainly does not have the most extreme climatic conditions in the world; therefore, a value of 1.5 kN/mm seemed appropriate.

To comply with this criterion, the surface-design engineer should have an understanding of the effect of binder content, stone content, maximum size of stone, and type of sand on the stability-flow ratio. From this study it appears that the sensitivity of this ratio to different bitumen contents depends on the type of sand in the mixture (Fig. 7). In the case of mixtures with mine sand, the bitumen content was not a critical factor with respect to the stability-flow ratio but was very critical in the case of mixtures with pit sand. At the same bitumen content, the mine sand had a lower stability-flow ratio at the lower stone content mixtures; the opposite was generally true for pit

Figure 6. Ratio of stability to flow at 60 C versus tracking index at 40 C for gap-graded mixtures.

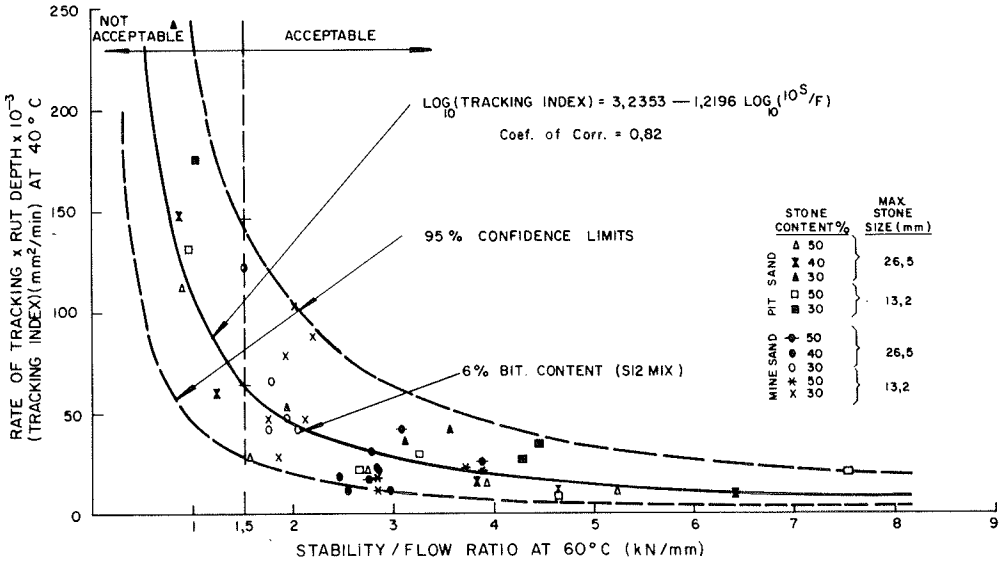

Figure 7. Relationship between permeability and air voids content for various gap-graded mixtures.

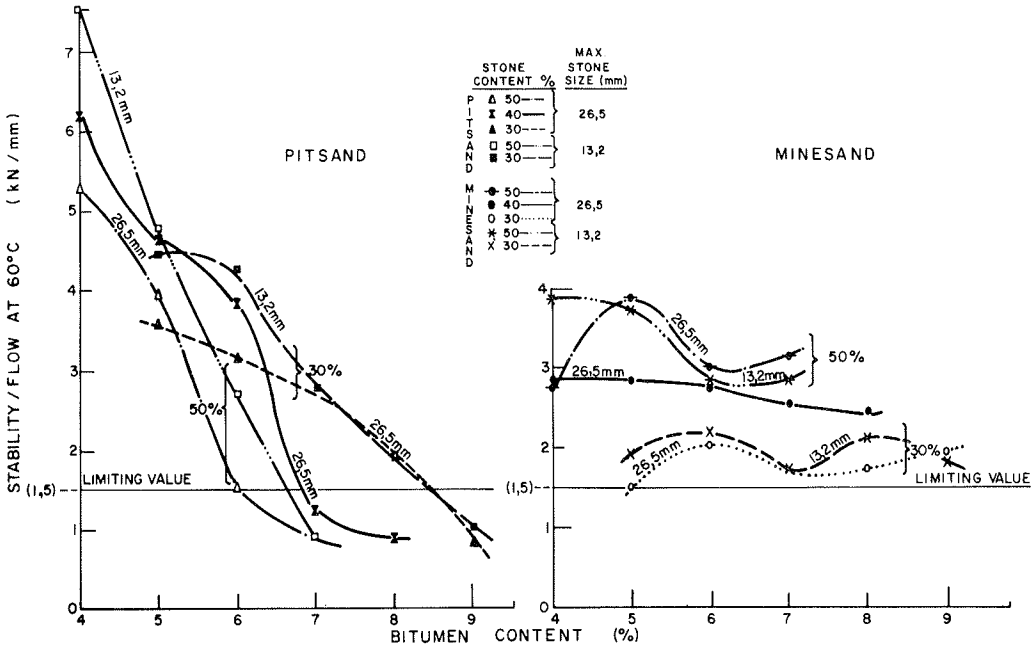

sand. There was no significant effect of maximum stone size on the stability-flow ratio for the 2 sizes tested. From this it is clear that type of sand is of paramount importance when one designs gap-graded mixtures.

Indirect Tensile Tests

The purpose of introducing the indirect tensile (split cylinder) test was to use the indirect tensile strength of the mixtures as an index to ensure that they are not designed with too high a stiffness, as defined by Van der Poel (15), or poor fatigue resistance (7). Published data on the relationship between indirect tensile strength, or for that matter direct tensile strength, and fatigue life are limited, and for this reason controlled-strain fatigue tests at 20 C at a strain level of 600 $\mu\epsilon$ were carried out on a range of gap-graded mixtures used in practice. Results are given in Table 2 where they are compared with the indirect tensile strength of these mixtures at 40 C. A linear regression analysis of all the data with respect to indirect tensile strength and Marshall stability showed the best relationship between these 2 parameters to be as follows (11):

$$x = 0.014y + 1.246 \quad (2)$$

where

y = indirect tensile strength at 40 C in kilopascals and
x = Marshall stability at 60 C in kilonewtons.

The coefficient of correlation of these data is 0.86, which indicates that the relationship could be used with reasonable confidence.

A similar analysis of the data in Table 2 indicates a strong linear relationship between direct tensile strength and log of service life of the form

$$y = 2989 - 588 \log N(x) \quad (3)$$

where N(x) = service life (Table 2). The coefficient of correlation of these data is 0.8. The relationship is of great significance; it enables a reliable estimate to be made of any desirable level of service life from the indirect tensile strength at 40 C of a particular gap-graded mixture. Indirectly from Eq. 2, Marshall stability may be used to determine the fatigue service life; however, this obviously would not give as good an estimate as would the indirect tensile strength.

From a previous fatigue study it is recommended that surfacing mixtures of a thickness not greater than 75 mm should have a minimum fatigue service life of 5×10^3 repetitions of load at 20 C and a strain level of 600 $\mu\epsilon$. From Eq. 3 this gives a maximum indirect tensile strength at 40 C of 810 kPa or, by using Eq. 2, a maximum Marshall stability of approximately 12.5 kN.

Air Permeability Test

A search of the literature dealing with the fundamental measure of permeability of bituminous surfacing mixtures failed to produce any criterion that could be applied directly. Most workers have adopted limits suggested by researchers dealing with drainage problems related to soils. However, the 2 problems are not related directly because, in the case of soils, water is permanently available in a draining situation at substantial pressure heads whereas, in the case of bituminous surfaces, water is available only when it rains and the pressure head is low (except possibly under the vehicle tire). It would seem that the limits of permeability of 1×10^{-11} to 1×10^{-14} cm^2 set for soils are overrestrictive with respect to surfaces (16). A reasonable limit of permeability of 1×10^{-8} cm^2 is suggested for gap-graded mixtures to ensure that surface water would not enter readily into the surface and thereafter into the base of the pavement. An investigation by McLaughlin and Goetz (17) of gap-graded surfacing mixtures used in Indiana showed that a limit of 1×10^{-8} cm^2 was applied to these mixtures, which presumably gave good in-service performance, thus corroborating the limit of permeability suggested.

The pore structure of a gap-graded mix is controlled largely by the type of sand used and the filler and bitumen content, which in turn control the voids content. The relationships between air permeability and voids content of the mixtures used in this study are shown in Figure 8. As can be seen, at a constant voids content, the mixtures with pit sand were more permeable than those with mine sand and, for both types of mixture, the higher the stone content the more permeable was the mixture. This finding confirms the experience in the United Kingdom that low stone content mixtures are more durable than high stone content mixtures. Because bitumen film thickness and permeability are probably the dominating factors that control the durability of a mixture, a limit on both bitumen film thickness and permeability would guarantee the long-term durability of a surfacing mixture. A tentative value of not less than 6 μm is suggested for bitumen film thickness in practice, which agrees with the limit suggested by Campen et al. (18).

Voids in Mix

The air voids in the various gap-graded mixtures were calculated by taking into account all the factors recommended by the Asphalt Institute (11). Experience has shown that a minimum of 2 percent voids content is necessary in the traffic-compacted surfacing mixture to ensure that there are sufficient voids in the mix to prevent flushing due to expansion of the bitumen during hot weather. Because the laboratory density of gap-graded mixtures is very similar to ultimate in-service density, a limiting voids content for laboratory-compacted Marshall specimens of 2 percent is recommended.

The relationship between stone content and voids content of mixtures containing the 2 types of sand and a range of bitumen contents is shown in Figure 9. It is clear from this figure that, at the same bitumen content, the voids content for both types of sand decreases when the stone content increases. However, in the case of the pit sand, the decrease was less significant at stone contents in excess of 40 percent. At the same bitumen content, mixtures with mine sand had significantly higher voids than those manufactured with pit sand. This difference probably was due to the distribution of voids and their shape within each mixture, which, in turn, was dependent on the particle shape and grading of the sand.

It is interesting that the mine sand that had a higher compacted voids content also yielded mixtures with higher voids than did the pit sand at the same level of bitumen content although this difference was much more exaggerated in the case of the mixtures (Table 1 and Fig. 9). This effect probably was due to the finer grading of the mine sand, which led to reduced bitumen film thickness and a consequent increase in air voids.

Angularity of sand can be determined indirectly by the dry viscosity test, the results of which show mine sand to be more angular than pit sand (Table 1).

Because of the large variation in voids for gap-graded mixtures using different sands, voids content is not a reliable parameter to ensure impermeability of the mixtures (Fig. 8).

A comparison of mixtures made with mine sand and pit sand at the same bitumen content shows the mixtures with pit sand to be generally more resistant to deformation (11). This at first seems illogical because mine sand had a greater inherent stability by virtue of its more angular particle shape; however, deformation of a bituminous mixture depends on a number of interrelated factors such as the angularity and grading of the aggregate, the properties of the filler, the type and grade of the binder, the average film thickness of the binder, and the voids content of the mixture. In addition, the rate of loading and temperature are important variables. A correlation between deformation of a mixture and the properties of the sand is remote. However, because of the importance of the sand fraction, particularly in the case of low stone content, gap-graded mixtures, a more detailed study is in progress at the NIRR where various sands are being investigated with a view to establish more realistic sand specifications for gap-graded mixtures.

Filler

The type of filler (-75 μm) material used in a gap-graded bituminous mixture plays

Table 2. Results of indirect tensile strength and fatigue service life of gap-graded surfacing mixtures.

Mixture Composition	Peak Stiffness at 20 C (GPa)	Indirect Tensile Strength at 40 C (kPa)	Average Service Life N(x) at Strain of 600 $\mu\epsilon$ (load repetitions)[a]
40 percent stone, 5.0 percent 60-70 penetration grade bitumen (7.4 μm film thickness)	6.0	604[b]	9.71×10^3
44 percent stone, 6.7 percent 60-70 penetration grade bitumen (8.6 μm film thickness)	4.1	316[b]	1.95×10^4
30 percent stone, 6.0 percent 40-50 penetration grade bitumen (4.9 μm film thickness)	2.8	186	5.94×10^4
44 percent stone, 5.0 percent 60-70 penetration grade bitumen (6.9 μm film thickness)	6.4	434[b]	1.40×10^4
50 percent stone, 5.3 percent 40-50 penetration grade bitumen (6.0 μm film thickness)	5.4	825	1.04×10^4
40 percent stone, 5.8 percent 40-50 penetration grade bitumen (6.0 μm film thickness)	3.5	500	2.87×10^4
30 percent stone, 6.1 percent 40-50 penetration grade bitumen (6.0 μm film thickness)	3.3	455	1.83×10^4

[a]From Freeme and Marais (7). [b]Calculated from Marshall stability value.

Figure 8. Relationship between permeability and air voids content for various gap-graded mixtures.

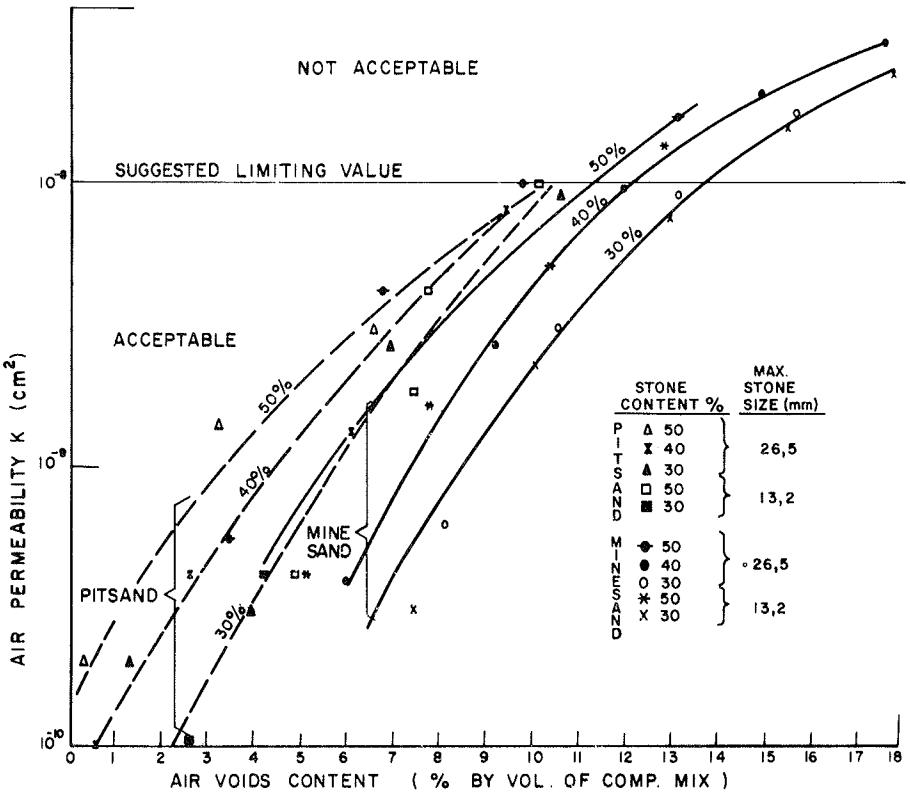

Figure 9. Relationship between stone content and voids content for various gap-graded mixtures.

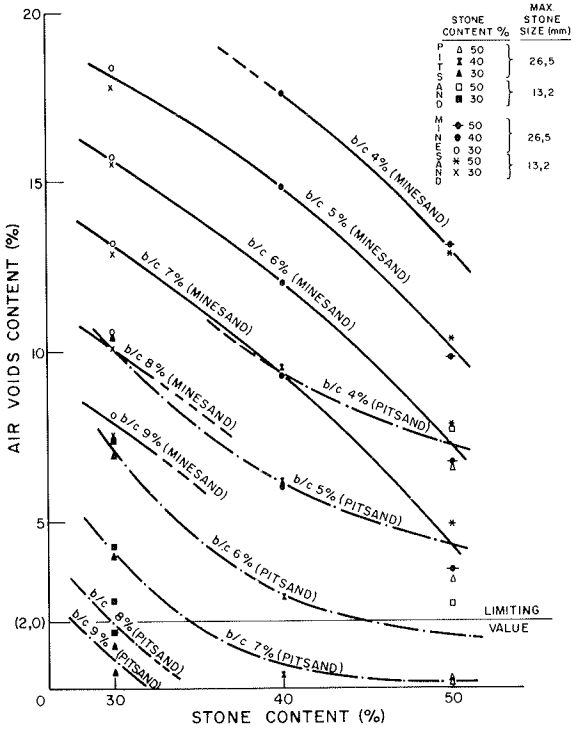

Table 3. Design criteria for gap-graded surfacing mixtures.

Test Property	Surfacing Property	Max	Min
Marshall stability-flow ratio at 60 C, kN/mm	Deformation or distortion	—	1.5
Indirect tensile strength at 40 C, kPa	Toughness, fatigue resistance, and fracture strength	810	—
Marshall stability at 60 C, kN	Toughness, fatigue resistance, and fracture strength	12.5	—
Immersion index	Stripping by water	—	0.75
Air permeability, cm^2	Imperviousness, durability	1×10^{-8}	—
Voids in mix, percent	Balance in design	—	2.0
Film thickness of bitumen[a], μm	Durability	—	6.0
Filler-bitumen ratio	Balance in design	—	1.0

[a]Calculated by using factors recommended by the Asphalt Institute (11).

an important role with respect to its stability, voids content, permeability, and bitumen demand, by which it affects the deformation and durability characteristics of the mixture. Studies made by Lee and Rigden (19) have shown that the fineness of the filler as determined by its bulk density in benzene is an excellent index to the deformation characteristics of the binder-filler mixture. For this reason BS 594 requires the filler to comply with a bulk density in benzene value of between 0.50 and 0.95 g/ml. The filler-bitumen ratio is also important to obtain a balanced composition and a mixture with adequate resistance to distortion. A study by Kraemer (20) recommends that this ratio should not be less than 1.0.

Effect of Moisture on Mix Properties

To ensure that moisture does not affect the stability of the surface adversely, specimens of mix compacted under 2 × 75-blow Marshall compaction should be soaked in clear potable water for a period of 24 hours at 60 C and thereafter tested for Marshall stability. The ratio of the soaked stability divided by the stability obtained under the standard Marshall test conditions is the immersion index, which should not be less than 0.75 for acceptable surfacing mixtures.

CONCLUSIONS AND TENTATIVE MIX-DESIGN CRITERIA

Several conclusions may be made as a result of this study.

1. An acceptable correlation exists between the Marshall stability-flow ratio and the rate of tracking at 40 C for gap-graded mixtures when tested with a wheel-tracking machine.
2. Fatigue service life of thin surfaces of gap-graded mixtures can be established and controlled within acceptable bounds by using the indirect tensile strength of the mixture at 40 C.
3. A reasonably good correlation between Marshall stability and indirect tensile strength exists to enable engineers in practice to control the fatigue resistance of gap-graded mixtures by specifying an upper limit to the Marshall stability value.
4. The sand used in the manufacture of gap-graded mixtures has a predominant effect on the properties of the mixture.
5. Maximum size of coarse stone used in a gap-graded mixture within the limits of 26.5 mm and 13.2 mm does not have a significant effect on the properties of the mixture.
6. Stone content of gap-graded mixtures is an important variable. The higher stone contents result in mixtures having greater resistance to distortion in the case of mine sand and lower resistance in the case of pit sand. Optimum stone content therefore depends on the type of sand.
7. Higher stone content mixtures result in surfaces with lower fatigue service lives and greater permeability at a given voids content.

The results of this study, combined with information from the literature, have permitted tentative limiting criteria to be established to control the following properties of a gap-graded bituminous surface:

1. Deformation or distortion,
2. Fracture strength,
3. Fatigue resistance,
4. Durability,
5. Imperviousness, and
6. Balanced composition.

These properties are governed by various laboratory tests that enable asphalt engineers to design suitable gap-graded mixtures in practice. Obviously, the intensity and type of traffic using a pavement as well as pavement geometrics and microclimate do influence surface performance. For example, a mixture that just complies with the deformation criteria would not be suitable for hot summer conditions under heavy truck traffic on a pavement with sharp bends and extreme sideway stresses.

This study has not investigated the influence of grade of bitumen because it is usual

in gap-graded mixtures to use a hard penetration grade such as a 40-50. However, cases exist in South Africa where 60-70 penetration grade bitumens have been used with success. Design criteria should take account of the grade of bitumen used.

Tentative mix-design criteria for gap-graded bituminous surfaces with stone contents within the range of 30 to 50 percent are given in Table 3. Some of these criteria require verification by controlled road experiments; such a program has been instituted at the NIRR.

Although the design criteria given in Table 3 do not, as is the case with many design methods, indicate the optimum binder content that should be used for a particular aggregate composition, the designer should always aim at introducing as much bitumen into the mix as it will tolerate without exceeding the bounds of the criteria established. This will, in effect, result in the most durable mixture that will satisfy all the necessary requirements of a good surfacing mixture.

This study has enabled mechanical test properties to be reduced to a minimum because the Marshall test fulfills all the necessary requirements of the mixture for design purposes. This results in a great saving in testing time and in the cost of additional testing equipment.

ACKNOWLEDGMENTS

This paper forms part of the research program of the National Institute for Road Research and is published by permission of the director. Special acknowledgment is made to Colin Broadbent, who carried out the bulk of the laboratory tests with care and precision.

REFERENCES

1. Richardson, C. The Modern Asphalt Pavement. John Wiley and Sons, Inc., New York, 1905.
2. Richardson, C. Asphalt Construction for Pavements and Highways. McGraw-Hill Book Co., New York, 1913.
3. Marais, C. P. Report on the Laying and Results of the First Inspection of a Premix Surfacing Road Experiment on a Heavily Trafficked Urban Street, Laid on Umbilo Road, Natal, in November/December 1962. National Institute for Road Research, Pretoria, South Africa, Unpublished Rept. RB/3/63, May 1963.
4. Brien, D. A Design Method for Gap-Graded Asphalt Mixes. Roads and Road Construction, May 1972.
5. Hugo, F. A Critical Review of Asphalt Mixes in Current Use With Proposals for a New Mix. Proc. 1st Conf. on Asphalt Pavements for South Africa, Durban, South Africa, 1969.
6. Broome, D. C., and Please, A. The Use of Mechanical Test in the Design of Bituminous Road Surfacing Mixtures II: Stability Tests on Rolled Asphalt. Jour. Appl. Chem., Vol. 8, Feb. 1958.
7. Freeme, C. R., and Marais, C. P. Thin Bituminous Surfaces: Their Fatigue Behavior and Prediction. HRB Spec. Rept. 140, 1973, pp. 158-182.
8. Maupin, G. W., Jr. Results of Indirect Tensile Tests Related to Asphalt Fatigue. Highway Research Record 404, 1972, pp. 1-7.
9. Hadley, W. O., Hudson, W. R., and Kennedy, T. W. An Evaluation of Factors Affecting the Tensile Properties of Asphalt Treated Materials. Center for Highway Research, Univ. of Texas Research Rept. 98-2, March 1969.
10. Hein, T. C., and Schmidt, R. J. Air Permeability of Asphalt Concrete. ASTM Spec. Tech. Pub. 309, June 1961.
11. Mix Design Methods for Asphalt Concrete and Other Hot-Mix Types. Asphalt Institute, Manual Series No. 2, May 1963.
12. Freeme, C. R., and Marais, C. P. The Structural Behaviour of Bituminous Surfacings in an Experimental Asphalt Pavement. 3rd Internat. Conf. on Structural Design of Asphalt Pavements, London, 1972.
13. Van Vuuren, D. J. Pavement Performance in the S12 Road Experiment; An AASHO Satellite Test Road in South Africa. 3rd Internat. Conf. on Structural Design of Asphalt Pavements, London, 1972.

14. Metcalf, C. T. Use of Marshall Stability Test in Asphalt Paving Mix Design. Highway Research Bulletin 234, 1959, pp. 12-22.
15. Van der Poel, C. A General System Describing the Viscoelastic Properties of Bitumens and Its Relationship to Routine Test Data. Jour. Appl. Chem., May 1954.
16. Terzaghi, K., and Peck, R. B. Soil Mechanics in Engineering Practice. John Wiley and Sons, Inc., New York, 1948.
17. McLaughlin, J. F., and Goetz, W. H. Permeability, Void Content, and Durability of Bituminous Concrete. HRB Proc., Vol. 34, 1955.
18. Campen, W. H., Smith, J. R., Erickson, L. G., and Mertz, L. R. The Relationship Between Voids, Surface Area, Film Thickness and Stability of Bituminous Paving Mixtures. Proc. AAPT, Vol. 28, 1959.
19. Lee, A. R., and Rigden, P. J. The Use of Mechanical Tests in the Design of Bituminous Road Surfacing Mixtures, Part I: Dense Tar Surfacings. Jour. Society Chem. Industry, June 1945.
20. Kraemer, P. Über die Bedentung der Gesteinsmehle als Füller für Bituminöse Mineralmassen. Bitumen-Teere-Asphalte-Peche und Verwandte Stoffe, Vol. 1, Jan. 1965, pp. 3-12.

MECHANICAL PROPERTIES OF GAP-GRADED ASPHALT CONCRETES

Dah-yinn Lee, Iowa State University

ABRIDGMENT

•THIS report presents the results of a laboratory study that compared well-graded and gap-graded aggregates used in asphalt concrete paving mixtures. There was a total of 424 batches of asphalt concrete mixtures involving 3,960 Marshall and Hveem specimens and 33 gradations of which 27 were gapped.

MATERIALS

Two crushed limestones, 1 natural gravel, and 1 crushed gravel were included in this study. The Ferguson aggregate (L_1), a dolomitic limestone, was used in series B and C. The Moscow aggregate (L_2), a lithographic limestone, was used in series D. The crushed and pit-run gravels were used in series F. To improve workability, a concrete sand was added to the major aggregates in all series for fractions retained on a No. 30 sieve and a No. 50 sieve at a 50-50 ratio.

Seventeen aggregate gradings were examined for $\frac{3}{4}$-in. (19.1-mm) maximum-size aggregates, including a gradation following Fuller's maximum density curve (A-F); a Federal Highway Administration (FHWA) curve, $P = 100(d/D)^{0.45}$ (A-P)(1); a midpoint Iowa type A grading (A-1)(2); and 14 gap gradings as shown in Figure 1. Eight aggregate gradings were examined for $\frac{1}{2}$-in. (12.7-mm) maximum-size aggregates: a FHWA maximum density grading (B-P), a British Standard 594 grading (B-B), and 6 gap gradings as shown in Figure 2. Eight aggregate gradings were studied for $\frac{3}{8}$-in. (9.5-mm) maximum-size aggregates for all crushed limestones, including a FHWA grading (C-P), 6 gap gradings, and a midpoint Iowa type A grading (C-I) as shown in Figure 3.

Three asphalt cements of 2 penetration grades were studied in conjunction with the aforementioned aggregate gradings. Asphalt A (65 penetration grade) was used in series C and D; asphalt B (94 penetration grade) was used in series B; and asphalt C (91 penetration grade) was used in series F.

METHODS AND PROCEDURES

Oven-dried crushed aggregates were first separated by $\frac{3}{4}$-in. (19.1-mm), $\frac{1}{2}$-in. (12.7-mm), $\frac{3}{8}$-in. (9.5-mm), No. 4, No. 8, No. 30, No. 50, No. 100, and No. 200 sieves. Concrete sand was separated and added to retain No. 30 and No. 50 fractions at a 50-50 ratio. Required weights of each fraction were then combined to produce the gradation curves shown in Figures 1 through 3. Asphalt concrete mixtures were made in a 50-lb (22.7-kg) laboratory pugmill mixer at asphalt contents from 3 to 7 percent. Nine specimens were prepared from each batch. Six specimens were compacted by the 50-blow Marshall method and 3 specimens by the Hveem method. Of the 6 Marshall specimens, 3 were tested by the standard Marshall method, 2 were tested by the Marshall immersion compression method (3), and 1 was tested for indirect tensile strength (4).

Publication of this paper sponsored by Committee on Mechanical Properties of Bituminous Paving Mixtures.

Figure 1. Grading curves for $^{3}/_{4}$-in. maximum-size aggregates (0.45 power).

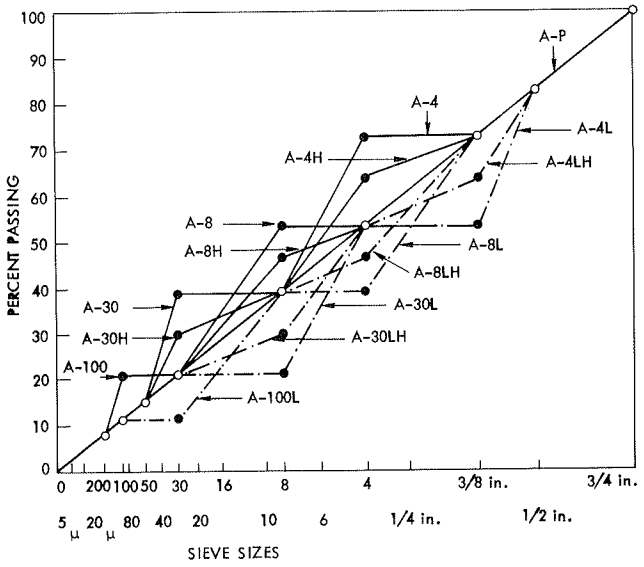

Figure 2. Grading curves for $^{1}/_{2}$-in. maximum-size aggregates (0.45 power).

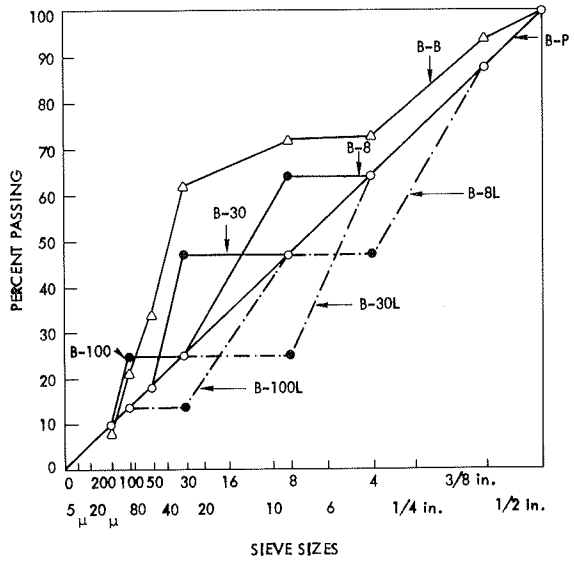

Figure 3. Grading curves for $^{3}/_{8}$-in. maximum-size aggregates (0.45 power).

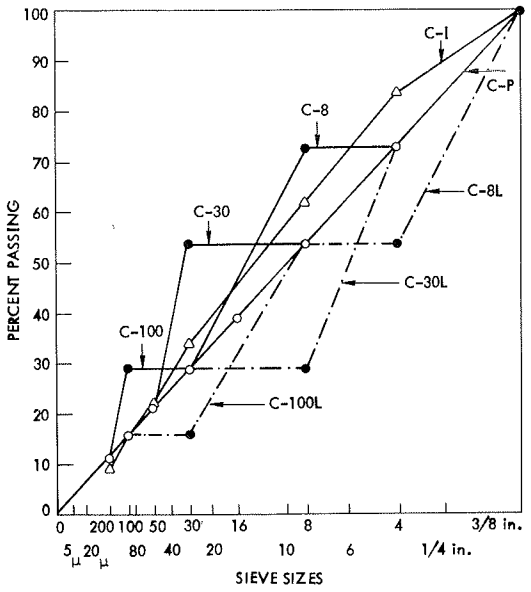

Figure 4. High and low Marshall unit weights, Series B, $^{3}/_{4}$-in.

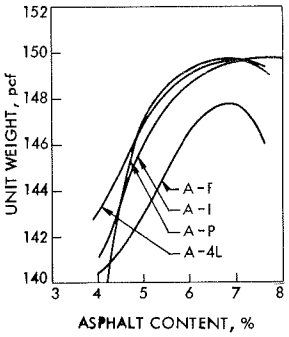

Figure 5. High and low Marshall unit weights, Series B, $^{1}/_{2}$-in.

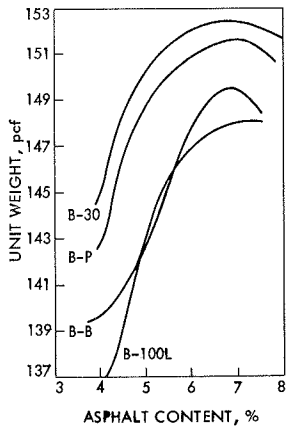

Figure 6. High and low Marshall unit weights, Series B, $^{3}/_{8}$-in.

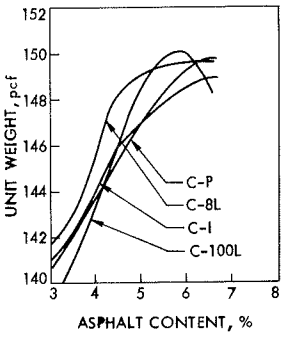

Figure 7. Comparison of Marshall unit weights among B-30, B-30H, and B-30L.

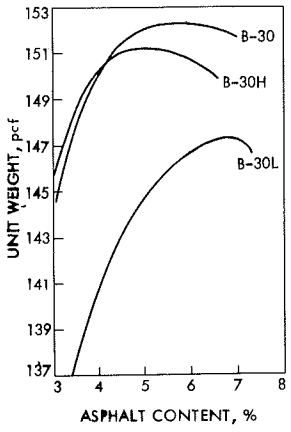

RESULTS AND DISCUSSION

Density and Gradation

By comparing the maximum densities for each gradation determined from unit weight-asphalt content plots within each series we noted the following:

1. In general, softer asphalt and harder limestone resulted in higher compacted density;
2. In most series, the well-graded gradings (F) were not among the gradings that give the highest maximum density; and
3. Gradings that consistently yielded mixtures of higher maximum density were A-4L, A-8L, B-30, and C-8L; gradings that consistently yielded lower maximum density were A-100L, B-30L, B-100L, C-I, C-30, and C-100L.

Some of these features are shown in Figures 4, 5, 6, and 7 for Marshall mixes in series B ($L_1 \times 94$ penetration grade).

Stability and Gradation

When the maximum Marshall stability (determined from stability versus percentage of asphalt plots) of various gradings was compared within each series and between series, we observed the following:

1. All mixes studied (gap or well-graded) yielded mixtures with maximum Marshall stability far exceeding the minimum of 750 pounds (3.34 kN) required of mixes designed for heavy traffic.
2. The best gaps for high-stability mixes appeared to be different for different maximum aggregate sizes and aggregate-asphalt combinations. The well-graded Iowa type A and FHWA gradings (I and P) were usually among the gradings that yielded high Marshall stability. The best gap gradings for Marshall stability were A-I, A-P, A-8, A-30, B-30, B-B, and C-100.

The Hveem stability at 3 percent air void content was determined for each grading within each series and was used as a basis for comparison. It was observed that

1. More than 50 percent of the gap-graded mixtures yielded stability at 3 percent air void content exceeding the minimum required stability of 35 as recommended by the Asphalt Institute method; and
2. The best gap gradings by this criterion were A-F, A-I, A-8, A-4H, A-4L, A-100L, B-100L, B-8L, C-I, and C-30.

Voids in Mineral Aggregate and Gradation

The purpose of minimum voids in mineral aggregate (VMA) requirements is to ensure sufficient air voids to prevent flushing and sufficient intergranular void space for enough asphalt for durability. As had been expected by many as one of the disadvantages of well-graded aggregates, the well-graded mixtures in this study produced mixtures of low VMA. However, data also indicated that gapping the grading may or may not increase the VMA values. For example, although all gap-graded mixtures gave VMA values higher than that of I or P gradings, gap-graded A-100, A-8, and C-100 mixtures had VMA values lower than corresponding well-graded mixtures. Further, the effects on VMA of the location of the gap and method of gapping were also different for different maximum sizes.

CONCLUSIONS

With proper combinations of type of aggregate, aggregate size, type of asphalt, and asphalt content, numerous gap-graded aggregates can be made into satisfactory paving mixtures. Therefore, it appears that rigid requirements of grading conforming to a certain constant mathematical relationship such as Fuller's curve, $P = 100(d/D)^n$, are not justified.

Because of the attractiveness of the cost (in certain areas), fatigue resistance, durability,

compactibility, and skid and wear resistance of gap-graded asphalt concrete, more research and experiments, especially in the field, should be conducted.

ACKNOWLEDGMENTS

The study presented in this report was sponsored by the Iowa Highway Research Board, the Iowa State Highway Commission, and the Federal Highway Administration. Sincere appreciation is extended to these organizations and to the engineers of the Iowa State Highway Commission for their support, cooperation, and counseling. This work was also partly supported by the Engineering Research Institute at Iowa State University.

REFERENCES

1. Goode, J. F., and Lufesy, L. A. A New Graphical Chart for Evaluating Aggregate Gradations. Proc. AAPT, Vol. 31, No. 176, 1962.
2. Standard Specifications. Iowa State Highway Commission, Ames, 1964.
3. Test Method MIL-STD-620 (CE). U.S. Army Corps of Engineers.
4. Kennedy, A. W., and Hudson, W. R. Application of the Indirect Tensile Test to Stabilized Materials. Highway Research Record 235, 1968, pp. 36-48.

CONSIDERATION OF PARTICLE ORIENTATION IN THE COMPACTION OF ASPHALT CONCRETE

William D. O. Paterson, National Institute for Road Research, Pretoria, South Africa

ABRIDGMENT

•WHEN a bituminous mixture deforms under load, as during compaction, changes occur in its internal structure. The initial structure of irregularly shaped solid particles randomly oriented and distributed is shaped into a structure with definite characteristics of packing and orientation. Analysis of the system of stresses and the transfer of energies shows that the particles are likely to be moved into a generally parallel orientation perpendicular to the principal imposed stress (1). This ultimate structure will be in a stable energy state and will be able to sustain the imposed traffic stresses without permanent deformation.

The 2 components of changes in internal structure are translation and rotation. The rotation or reorientation component has a significant effect on mixture strength. It is much smaller than the translation component in mixtures of near-spherical or cubical particles and in some uniform or 1-size mixtures, such as a sand-asphalt. But, in a dense-graded mixture, it is highly significant. Few quantitative studies have been reported of this topic (2), and thus an attempt is made here to assess the significance and contribution of particle orientation in dense-graded mixtures. A more detailed report is also available (1).

INVESTIGATION

During an investigation of traffic compaction in dense-graded mixtures we made measurements of particle orientation to determine the changes occurring during trafficking. Trafficking was full-scale and controlled in 2 levels of tire contact pressure (280.620 kPa) and 2 of mixture temperature (25 and 40 C) (3). The mixes were of 1 dense gradation of an aggregate with low flakiness and nominal maximum size of 16 mm. Binder viscosity, binder content, and initial density were varied. The thickness was 50 mm. Compaction was done by pneumatic rollers.

The orientation of individual particles was measured graphically from photographs made of thin strips cut from a block taken from the pavement as shown in Figure 1. Coordinate measurements of the end points of each particle were recorded. Orientation was the direction of the longest dimension on the projection. The data were subjected to the Tukey chi-square (χ^2) statistical analysis (4) in groups by particle length, depth, and region and in toto for each sample.

DISCUSSION OF RESULTS

Analysis of the data typically yielded distributions as shown in Figure 2 for the before and after trafficking states. The distributions are shown in the polar form common in geological applications with discrete ranges of 10 deg as used in the statistical analysis. Visual comparison with a random distribution indicates a high degree of preferred orientation.

The results of the statistical analyses are summarized in Table 1. These show that the aggregate particles did exhibit a preferred orientation in the range of 3 to 8 deg from the horizontal rather than in a random manner. This was demonstrated by the chi-square test, which indicated that there was less than 0.5 percent significance

Publication of this paper sponsored by Committee on Mechanical Properties of Bituminous Paving Mixtures.

Figure 1. Typical specimen for orientation analysis.

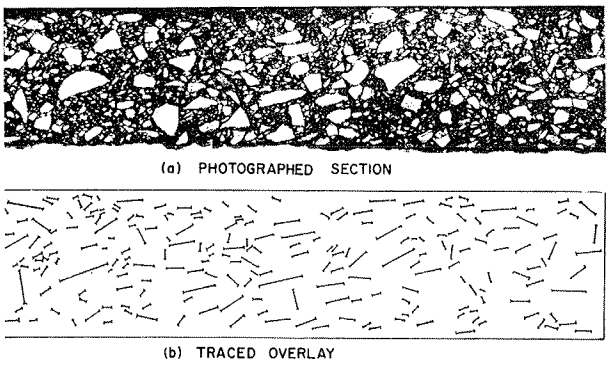

Figure 2. Typical polar distributions of orientation.

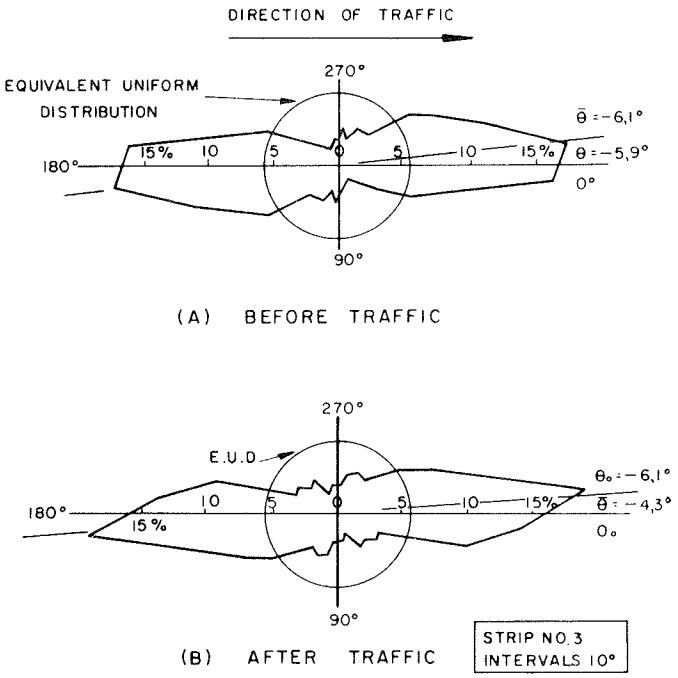

Table 1. Summary of particle orientation analysis.

Strip Number	Bitumen Content (percent)	Bitumen Viscosity (m^2/s at 40 C)	Initial Density (percent 2 × 75-blow)	Traffic	Orientation (degrees) Mean	Orientation (degrees) Preferred	Probability of Being Within 10 Deg of Mean	χ^2	Sample Size
1	6.1 (optimum)	2.0	98	Before	-3.6	-5.1	0.326	553	920
				After	-3.1	-4.4	0.298	334	786
2	6.1 (optimum)	2.0	95	Before	-7.3	-8.1	0.321	356	586
				After	-3.1	-7.2	0.274	46	494
3	6.8 (excess)[a]	2.0	98	Before	-6.1	-5.9	0.341	594	986
				After	-4.3	-6.1	0.354	420	822
4	6.1 (optimum)	0.50	98	Before	-2.8	-6.4	0.288	432	1,118
				After	-5.5	-8.6	0.291	553	1,268
5	5.2 (deficient)	0.50	98	Before	-5.1	-7.4	0.328	744	1,549
				After	-5.4	-7.5	0.298	543	1,311

Note: For particles with a projection >2 mm only.

[a]With respect to design.

Table 2. Subanalysis of orientation by size, depth, and region for strip 1.

Item	Massed Data	By Particle Size[a] 1 to 3 mm	3 to 6 mm	6 to 12 mm	>12 mm	By Depth in Pavement[b] 0 to 13 mm	13 to 25 mm	25 to 38 mm	38 to 50 mm	By Regions Along Block[c] 0 to 100 mm	100 to 200 mm	200 to 300 mm	300 to 400 mm
Before Traffic													
Preferred orientation, degrees	-5.1	-6.0	-5.3	-4.2	-4.8	-10.3	-4.6	-5.3	-2.5	-2.5	-4.1	-6.9	-8.7
Sample size	920	257	480	211	25	203	226	237	208	257	245	230	188
χ^2	553	130	258	161	16	124	130	128	130	153	128	164	93
Probability of occurrence, degrees	0.326	0.327	0.308	0.379	0.320	0.281	0.301	0.312	0.313	0.327	0.355	0.309	0.261
After Traffic													
Preferred orientation, degrees	-4.4	-2.8	-3.6	-5.0	-9.9	-10.4	-5.0	-5.4	-3.2	-6.0	-5.9	+1.6	-5.2
Sample size	786	334	347	196	27	150	154	176	190	194	209	190	198
χ^2	334	99	172	77	10	46	66	69	104	65	95	94	120
Probability of occurrence, degrees	0.298	0.269	0.343	0.240	0.370	0.254	0.326	0.270	0.250	0.280	0.325	0.303	0.308

[a]Range of exposed length. [b]From the surface. [c]From leading edge.

of random orientation, that is, the particles had a preferential orientation. The slight differences that could be noticed between the arithmetical mean orientations and the preferred orientations occurred when the distributions exhibited a smaller ill-defined peak in addition to the dominant peak. The dispersion of the distribution is given as the probability, P, of the orientation of a particle being within 10 deg of the mean, the probability of occurrence.

A comparison of the results of strips 1 and 2 indicates the effect of construction density for a normally designed mix with 80-100 penetration grade bitumen. Before trafficking, the highly compacted mix had a lower mean orientation (3.6 deg) than the lightly compacted mix (7.3 deg); after trafficking these were both reduced to 3.1 deg. Higher compactive effort seems to result in flattening the particles to a more horizontal position.

The effect of excess binder in a mix may be assessed by comparing the rich mix on strip 3 to the normal mix on strip 1. Although the mean orientation was slightly higher for the rich mix, the probability of occurrence was higher than that for the normal mix (0.341 versus 0.326) and increased further under traffic (0.354). This illustrates the more fluid nature of the rich mix, which allows easier manipulation of individual particles into their stable positions.

The effect of binder viscosity may be assessed by comparing the soft mix on strip 4 and the hard mix on strip 1. In the soft mix contrary characteristics are evident with the mean orientation increasing slightly and the probability of occurrence being low at 0.29.

The size, depth, and regional location of particles had the effects on orientation given in Table 2 for strip 1. Size appears to have negligible influence because there is no consistent trend in most parameters except a slight maximum for 3- to 6-mm length in the χ^2 value. Depth within the layer does appear to have an influence on orientation but its extent is masked in the most critical regions, such as near interfaces, because there the orientation is dictated by the nearest particle face rather than by the longest dimension adopted by definition. The analysis by regional location is a measure of the variation to be expected between similar subgroups and is thus an indication of the significance of the overall result. From the final panel of Table 2 it can be seen that the mean and preferred orientations vary by ±3 deg and the probabilities of occurrence by ±0.02 deg.

In the light of these naturally occurring variations it is apparent that the changes in orientation under traffic compaction and the differences due to subsidiary factors of mix design and construction conditions have a very low significance.

PRACTICAL IMPLICATIONS OF RESULTS

The significant degree of preferred orientation achieved under rolling compaction has important implications. The stability of a field core cut from a pavement was generally much lower than that of a block of the same mix molded in the laboratory by impact compaction to the same density conditions as shown in Figure 3. Little of the difference was attributable to mixing variations and most of it was due to differences in particle orientation. The rolling compaction in the field produced a preferentially horizontal orientation that was weak in the horizontal plane but strong in the vertical. Impact compaction however causes more wedging than alignment and in addition there is the perpendicular alignment due to the sidewall effects of the mold, which increase the strength in the diametral plane.

Another phenomenon is the effect that the constructed density had on the final density of a bituminous surfacing. Figure 4 shows the data for several mixes. If the initial structure had no influence on the final structure the curves would have zero gradient but the gradient is generally positive. In other words, normal traffic alone is insufficient to develop the same internal structure as developed by construction rollers, that is, the same arrangement of orientation and packing. At high mix temperatures this phenomenon becomes much less significant.

Figure 3. Influence of compaction mode on Marshall stability.

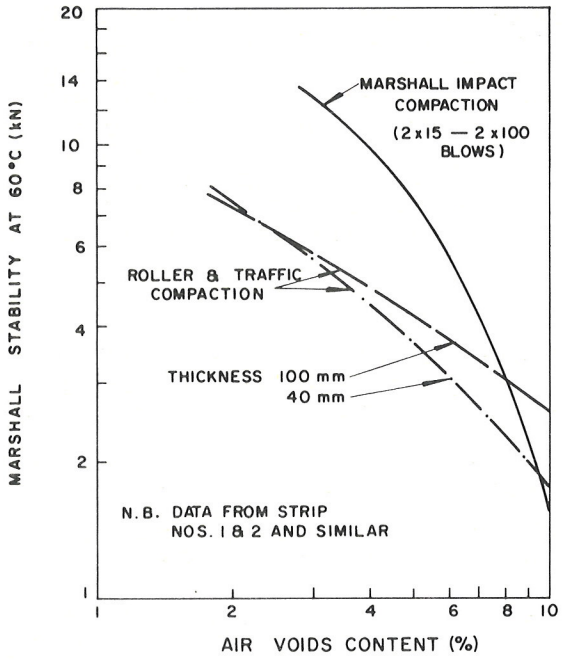

Figure 4. Influence of constructed density on final stable state density.

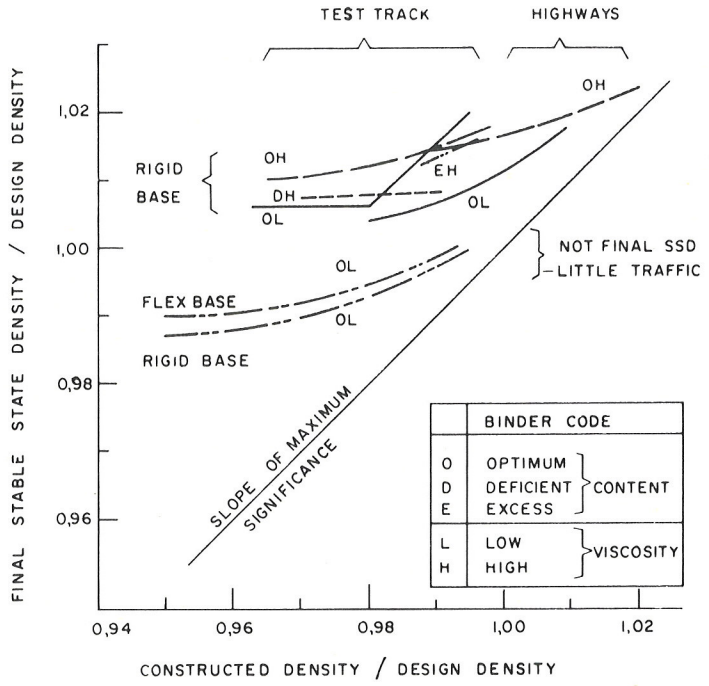

CONCLUSIONS

Measurements on dense-graded asphalt concrete samples cut from a pavement showed that approximately 30 percent of the particles were oriented at angles within 10 deg of the preferred orientation and that the preferred orientation was generally in the range 4 to 8 deg above the horizontal in the direction of trafficking. Small changes were apparent under the compacting effect of simulated traffic but these were barely significant statistically. Low viscosity and high binder content appeared to promote preferential orientation but, again, the differences were not statistically significant. Particle size had negligible influence. The structural properties of a mix are very sensitive to orientation characteristics. Reorientation appears to be a function primarily of viscous resistance in the binder; changes in packing density are more a function of aggregate characteristics.

ACKNOWLEDGMENT

The study was performed at the University of Canterbury, New Zealand, with assistance from the National Roads Board. Permission to publish was granted by the Director, National Institute for Road Research, Council for Scientific and Industrial Research, South Africa.

REFERENCES

1. Paterson, W. D. O. Consideration of Particle Orientation in the Compaction of Asphalt Concrete. Internal Rept. RP/13/73, Natl. Inst. Road Res., Pretoria, South Africa, 1973, 28 pp.
2. Lees, G., and Salehi, M. Orientation of Particles With Special Reference to Bituminous Paving Materials. Highway Research Record No. 273, 1969, pp. 63-75.
3. Paterson, W. D. O. Traffic Compaction of Asphalt Concrete Surface Courses. Univ. of Canterbury, New Zealand, PhD dissertation, 1972.
4. Harrison, P. W. New Technique for 3-Dimensional Analysis of Till and Englacial Debris Containing Particles From 3 to 40 mm Size. Jour. Geology, Vol. 65, 1957, pp. 98-105.

SPONSORSHIP OF THIS RECORD

GROUP 2—DESIGN AND CONSTRUCTION OF TRANSPORTATION FACILITIES
W. B. Drake, Kentucky Department of Transportation, chairman

BITUMINOUS SECTION
Moreland Herrin, University of Illinois, chairman

Committee on Characteristics of Bituminous Materials
Frank M. Williams, Ohio Department of Transportation, chairman
Stephen H. Alexander, C. J. Andres, Philip J. Arena, Jr., L. W. Corbett, James R. Couper, William H. Gotolski, Felix C. Gzemski, A. J. Hoiberg, George M. Jones, Larry L. Kole, Dah-Yinn Lee, John J. Lyons, Kamran Majidzadeh, Fred Moavenzadeh, Charles A. Pagen, J. Claine Petersen, Charles F. Potts, Vytautas P. Puzinauskas, F. S. Rostler, R. J. Schmidt, Herbert E. Schweyer, R. N. Traxler, J. York Welborn, Leonard E. Wood

Committee on Effects of Natural Elements and Chemicals on Bitumen-Aggregate Combinations
Herbert E. Schweyer, University of Florida, chairman
Jack N. Dybalski, E. Keith Ensley, William H. Gotolski, Felix C. Gzemski, Willis C. Keith, L. C. Krchma, Dah-Yinn Lee, Robert P. Lottman, Gene R. Morris, Robert E. Olsen, J. Claine Petersen, Charles F. Potts, R. J. Schmidt

Committee on Mechanical Properties of Bituminous Paving Mixtures
Rudolf A. Jimenez, University of Arizona, chairman
Grant J. Allen, David A. Anderson, H. W. Bushing, James A. Cechetini, Jon A. Epps, William J. Harper, R. G. Hicks, Yang Hsien Huang, Ignat V. Kalcheff, Bernard F. Kallas, Mohamed Osama Khalifa, Dah-Yinn Lee, Kamran Majidzadeh, Carl L. Monismith, Charles A. Pagen, Charles F. Potts, Byron E. Ruth, Lowell H. Shifley, Jr., Jack E. Stephens, Ronald L. Terrel, B. A. Vallerga, Thomas D. White, Leonard E. Wood

Committee on General Asphalt Problems
William H. Goetz, Purdue University, chairman
Verdi Adam, R. W. Beaty, Fay O. Bloomfield, Bud A. Brakey, Frank M. Drake, Charles R. Foster, John M. Griffith, Moreland Herrin, W. J. Kari, Philip E. McIntyre, Ora McKenzie, Jr., Donald J. McNutt, Thomas D. Moreland, Charles L. Perkins, Elmer V. Peterson, James M. Rice, John J. Shelly, Eugene L. Skok, Jr.

William G. Gunderman, Transportation Research Board staff

Sponsorship is indicated by a footnote on the first page of each report. The organizational units and the chairmen and members are as of December 31, 1973.